The control of Schwann cell myelination during development and after nerve injury

Sheridan L. Roberts

Submitted for Doctor of Philosophy

November 2015

Copyright statement.

AUTHOR'S DECLARATION

The control of Schwann cell myelination during development and after nerve injury submitted by Sheridan Leona Roberts of the Peninsula Schools of Medicine and Dentistry to Plymouth University as a thesis for the degree of Doctor of Philosophy in November 2015

This thesis, printed or electronic format, is available for Library use on the understanding that it is copyright material and that no quotation from the thesis may be published without proper acknowledgement.

I certify that all material in this thesis which is not my own work has been identified and that no unchanged or acknowledged material has previously been submitted and approved for the award of a degree by this or any other University.

At no time during the registration for the degree of Doctor of Philosophy has the author been registered for any other University award without prior agreement of the Graduate Sub-Committee.

Word count of main body of thesis: 62,767 words

Signed:

Date:

Acknowledgements

Firstly I would like to thank David Parkinson for all the support and encouragement you have given me throughout my PhD study. David, you have enabled me to see the light at the end of the tunnel when I have found it difficult, your enthusiasm has inspired me and I couldn't have wished for a better supervisor throughout this journey.

It has been a pleasure to work alongside Xin-Peng, Thomas and Lauren in the laboratory; I would like to thank you all for making this experience enjoyable. I appreciate both the advice and support you have all given me, along with your patience and understanding when I've been running around the lab like a crazy person and have desperately needed your help. I would also like to thank Kayleigh for always being there to lend a helping hand, it has been great to have shared this rollercoaster ride with you, through times of woe and happiness, from start to finish. You have been a great friend.

I would finally like to thank Simon, my Mum, Dad, Sister, Nan and Uncle Carl, who have done nothing but shower me with love and support, been there to listen to me, pointed me in the right direction and have always been there to make me smile. I truly couldn't have gotten to the end without your constant support.

Sheridan Leona Roberts

Title: The control of Schwann cell myelination during development and after nerve injury

Abstract

Schwann cells are the principal glial cell of the peripheral nervous system and are responsible for axon maintenance, regeneration and increasing saltatory conduction of neurons. Schwann cell differentiation and myelination is mediated by a core network of transcription factors and signalling pathways, which have been divided into two groups; positive and negative regulators. Sox10, NFATc4, Oct6, Krox20 and the ERK 1/2 signalling pathway have been characterised as positive regulators of Schwann cell differentiation and myelination; with Sox10 and Krox20 also playing critical roles in myelin maintenance. On the other hand, transcription factors cJun, Pax3, Id2 and signalling pathways Notch and p38 mitogen activated protein (MAP) kinases (MAPK) have been identified as negative regulators of Schwann cell differentiation and myelin formation. Recently, the HMG transcription factor Sox2 was identified as a negative regulator of Schwann cell myelination *in vitro,* however its role in Schwann cell myelination *in vivo* has not yet been studied. This study therefore aimed to examine the role of Sox2 overexpression in Schwann cells and how it effects Schwann cell differentiation and myelination during development and after injury. In addition, we aimed to investigate for the first time the specific role of p38α (the major isoform of p38 MAPK) in Schwann cell myelination *in vivo,* by generating Schwann cell specific p38α conditional knockout mice.

Sox2 is highly expressed in immature Schwann cells, but is downregulated as Schwann cells being to mature and differentiate. This study shows that continued expression of Sox2 during development and after injury, impairs Schwann cell differentiation and myelination by directly downregulating the expression of two core transcription factors; Sox10 and Krox20, as well as myelin proteins, P_0 and MBP. In addition, we observe that continued Sox2 expression significantly increases Schwann cell proliferation and maintains Schwann cells in an immature state. Unexpectedly, we also observed that continued Sox2 expression significantly increases the number of macrophages present in the nerves of Sox2 overexpressing mice at both P60 and 21 days post injury. Phenotypically, Sox2 overexpressing mice

show signs of a peripheral neuropathy and animals have impaired motor and sensory function. These findings confirm that Sox2 is a negative regulator of Schwann cell myelination and suggests that continued Sox2 expression is sufficient to drive the progressive development of a peripheral nerve disorder which may resemble Charcot-Marie-Tooth type 1 demyelinating neuropathy and congenital hypomyelinating neuropathy.

As a negative regulator of Schwann cell myelination, activity of the p38 MAPK pathway has been shown to inhibit myelin formation *in vitro* and to also induce the Schwann cell injury response; by driving Schwann cell dedifferentiation and demyelination following injury. Here we show that specific removal of the p38α isoform in Schwann cells leads to an increase in myelin thickness at early developmental time-points, along with an elevated expression of myelin proteins, P_0 and MBP. Further analysis following nerve injury revealed that removal of p38α results in an initial decrease in Schwann cell demyelination, yet improves axon remyelination at 21 days post injury. These results demonstrate the specific role of p38α in regulating Schwann cell myelination, and how it could be a direct therapeutic target for improving nerve repair after injury.

Table of Contents

Table of Figures

Table of Tables

Abbreviations

ADAM17	A disintegrin and metalloproteases 17
ADS	Antibody diluting solution
ADST	antibody diluting solution with Triton X-100
AP2α	activating enhancer-binding protein 2α
Ara C	cytosine arabinoside
Artn	artemin
BACE	β-secretase
BDNF	brain derived neurotrophic factor
Brn-2	brain 2
BSA	bovine serum albumin
CAG	cytomegalovirus (CMV) early enhancer element and chicken beta-actin promoter
cAMP	cyclic adenosine monophosphate
Caspr	contactin associated protein
cDNA	complementary deoxyribonucleic acid
ChIP	Chromatin immunoprecipitation
CMT	Charcot Marie Tooth
CMV	cytomegalovirus
c-Myc	myelocytomatosis oncogene
CNS	central nervous system
CoA	Coenzyme A
Cre	Cre recombinase
CREB	cAMP response element binding protein
db cAMP	dibutyryl cyclic adenosine monophosphate
Dhh	desert hedgehog
DM	Defined medium
DMEM	Dulbecco's Modified Eagle Medium
DNA	deoxyribonucleic acid
DPI	days post crush injury
DPC	days post cut injury
DRG	dorsal root ganglion
E?	Embryonic day ?
ECM	extracellular matrix
EDTA	ethylenediaminetetraacetic acid
EGF	epidermal growth factor
EGFR/ErbB	epidermal growth factor receptor
Egr	early growth response
Eph	Ephrin receptor
ER	estrogen receptor
ERK	extracellular signal-regulated kinase

FCS	foetal calf serum
FENIB	familial encephalopathy with neuroserpin inclusion bodies
FERM	4.1 protein, ezrin, radixin and moesin
GDNF	glial cell line-derived neurotrophic factor
GFAP	glial fibrillary acidic protein
GFP	green fluorescent protein
Gpr	G-protein coupled receptor
Hes	Hairy and enhancer of split 1
HMG	High mobility group
HRP	Horse-radish peroxidase
Id-2	inhibitor of DNA binding 2
IGF	insulin-like growth factor
IFNγ	interferon gamma
IL	interleukin
IRES	internal ribosome entry site
JNK	c-Jun N-terminal kinase
Klf-4	Krüpple-like factor 4
Krox	Krüppel box
L1	L1 cell adhesion molecule
LIF	leukemia inhibitory factor
MAG	myelin associated glycoprotein
MAI	myelin-associated inhibitor
MAM	mastermind
MAPK	mitogen activated protein kinase
MBP	myelin basic protein
MCP-1	monocyte chemotactic protein 1
Med12	Mediator complex subunit 12
MEK	MAPK/ERK kinase
Merlin	moesin, ezrin and radixin like protein
miR	microRNA
MKK7	mitogen activated protein kinase kinase 7
mRNA	messenger ribonucleic acid
MSE	myelinating Schwann cell enhancer
Myrf	myelin gene regulatory factor
Nab	NGFI A binding protein
NCAM	neural cell adhesion molecule
Necl	nectin-like
Nefl	Neurofilament light chain
NF1	Neurofibromatosis type 1
NF2	Neurofibromatosis type 2 or Merlin
NFAT	nuclear factor of activated T-cells
NICD	Notch intracellular domain

NRG	neuregulin
Oct	octamer
Olig2	oligodendrocyte transcription factor 2
oligo	oligonucleotide
OPCs	oligodendrocyte precursors
P?	Postnatal day ?
P_0	myelin protein zero
p75NTR	p75 neurotrophin receptor
PAGE	PAGE polyacrylamide gel electrophoresis
Pax-3	paired box 3
PBS	phosphate buffered saline
PC12	pheochromocytoma 12
PCR	polymerase chain reaction
PDGF	platelet-derived growth factor
PDGFR	platelet-derived growth factor receptor
PDL	poly-D-lysine
PFA	paraformaldehyde
PI3K	phosphatidylinositol 3 kinase
PKA	protein kinase A
PLL	poly-L-lysine
PMP22	peripheral myelin protein 22
PNS	peripheral nervous system
POU	Pituitary, Octamer and Unc
P/S	penicillin/streptomycin
PTEN	phosphate and tensin homologue
PVDF	polyvinylidene fluoride
RBPJ1	recombination signal binding protein for immunoglobulin κJ
Rho GDI	Rho GDP dissociation inhibitor
RIPA	Radio-Immunoprecipitation Assay
RT-PCR	reverse transcription polymerase chain reaction
SCE	Schwann cell enhancer
SCP	Schwann cell precursor
SDS	sodium dodecyl sulphate
SEM	scanning electron microscopy
siRNA	silencing RNA
Sox	sex determining Y-like box domain
TA	transactivation domain
TAE	tris-acetate-EDTA
TBS	tris buffered saline
TBST	tris buffered saline containing Tween-20
TGFβ	transforming growth factor β
tPA	tissue plasminogen activator

TBS	tris buffered saline
TBST	tris buffered saline containing Tween-20
uPA	urokinase plasminogen activator
VEGF	vascular endothelial growth factor
WPI	weeks post nerve crush injury
YAP	yes-associated protein
YY1	Yin Yang 1

Chapter 1 Introduction

The nervous system consists of two parts, the central nervous system and peripheral nervous system, both of which are broadly composed of two major cell types, neurons and glia. Neuronal cells conduct action potentials (electrical signals) and are thus responsible for cellular communication. Glial cells on the other hand are essential for neuronal support; this includes neuronal survival, guidance, synaptic formation and function, homeostatic regulation of neurotransmitter and potassium ion concentrations, as well as regulating the speed of action potentials (Jessen, 2004). In the central nervous system there are three main types of glia: microglia, astrocytes and oligodendrocytes. In the peripheral nervous system there are also three main types of glia: satellite glial cells (SGC), enteric glia and Schwann cells. In this introduction we focus on the myelinating cells of the nervous system; oligodendrocytes (OG) and Schwann cells (SC) [Figure 1.1] (Jessen, 2004).

Oligodendrocytes are the myelinating cell of the central nervous system which originate from oligodendrocyte precursors. During myelin assembly oligodendrocytes send out between 20-60 processes, and selectively myelinate axons which have a diameter >0.2µm (Simons and Nave, 2015, Simons and Trajkovic, 2006). The myelin sheath formed by oligodendrocytes differs slightly in protein composition compared to that formed by Schwann cells [see Section 1.2]; the major myelin proteins are proteolipid protein (PLP) and myelin basic protein (MBP), which make up 60-80% of the total myelin proteins (Quarles et al., 2005).

Schwann cells are subdivided into three main types; myelinating Schwann cells, non-myelinating Schwann cells and terminal/presynaptic Schwann cells. Myelinating Schwann cells enwrap all large calibre (>1µm) axons in the peripheral nervous system. In contrast to oligodendrocytes, myelinating Schwann cells form a 1:1 ratio with axons, they then generate a myelin sheath that insulates the axon, allowing for saltatory conduction. Non-myelinating Schwann cells ensheath groups of small calibre (<1µm) sensory axons, where they form structures known as Remak bundles and provide trophic support to axons (Meier et al., 1999, Monk et al., 2015). Terminal/presynaptic Schwann cells, are non-myelinating cells located at the neuromuscular junction (NMJ), and cover entire synapses (Monk et al., 2015). Terminal/presynaptic Schwann cells express neurotransmitter receptors and help to

regulate synaptic transmission. In addition these cells providing trophic support to axons at the NMJ and have been suggested to be important for developmental synaptic rearrangement (Monk et al., 2015, Feng and Ko, 2008).

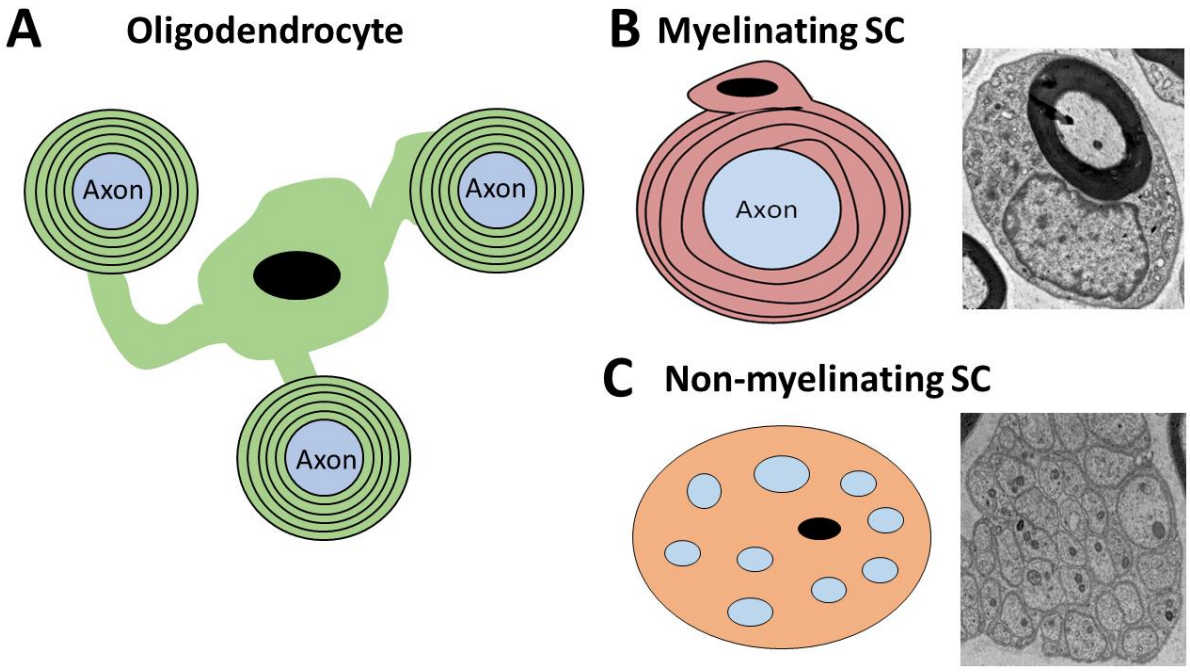

Figure 1. 1: Myelinating glia in the nervous system. (A) Oligodendrocytes (green) are the myelinating glial cell of the CNS, and wrap multiple axons (blue). (B) Myelinating Schwann cells (pink) are the myelinating glial of the PNS, and wrap only one large calibre (motor or sensory) axon. (C) Non-myelinating Schwann cells (orange) are present in the PNS, and are responsible for ensheathing multiple small calibre sensory axons, forming Remak bundles.

1.1 Structure of the myelin sheath

The Schwann cell myelin sheath is a lipid rich plasma membrane that forms numerous wraps around the axon, enabling rapid saltatory conduction of action potentials. Schwann cells are suggested to wrap the axon by undergoing a series of polymerisation and de-polymerisation steps, resulting in an actin network at the leading edge of the Schwann cells inner membrane, enabling it to spread and extend around the axon until a multilayer, compacted membrane is formed (Samanta and Salzer, 2015).

Schwann cell polarisation and wrapping of the axons results in the formation of distinct domains in the underlying axolemma; these include the internode, the juxtaparanode, the paranode, and the nodes of Ranvier [See Figure 1.2].

The internodal region is the area directly beneath the compact myelin, and is the largest region of the myelinated axon reaching up to 1mm in length. The Schwann cell inner membrane and axonal membrane are separated at this point by the periaxonal space which is about 15 nm wide (Salzer et al., 2008). However, Schwann cell and axon interaction along the internode is mediated by a distinct subset of cell adhesion molecules which include Nectin-like (Necl) proteins [See section 1.4]

The jutaxparanode is situated in-between the internode and the paranode, and lies just beneath the compact myelin. The juxtaparanode is enriched with potassium channels i.e. Kv 1. 1 and 1.2 which are thought to regulate the polarisation of action potentials. The Juxtaparanode is also composed of the adhesion molecules contactin associated protein 2 (caspr2) and the GPI-anchored adhesion molecule transient axonal glycoprotein 1 (TAB1); TAB1 which is expressed on the axon forming homophilic interactions with the Schwann cell expressed TAB1 on the glial paranodal loop, mediating axonal-Schwann cell contact (Salzer et al., 2008).

Paranodes are specialised axon-glial junctions which are located either side of the nodes of Ranvier. At this region the Schwann cells and axonal membrane are at their closest point of contact at just 3-5nm apart. The paranodal junctions promote axonal-Schwann cell adhesion and also provide a barrier that prevents ion diffusion between the internode and the nodes of Ranvier during action potential conduction (Salzer et al., 2008).

The nodes of Ranvier are regions of the axons which are unmyelinated. They are densely composed of voltage gated ion channels, predominantly sodium channels and are directly responsible for mediating the propagation of action potentials along the axon (Salzer et al., 2008).

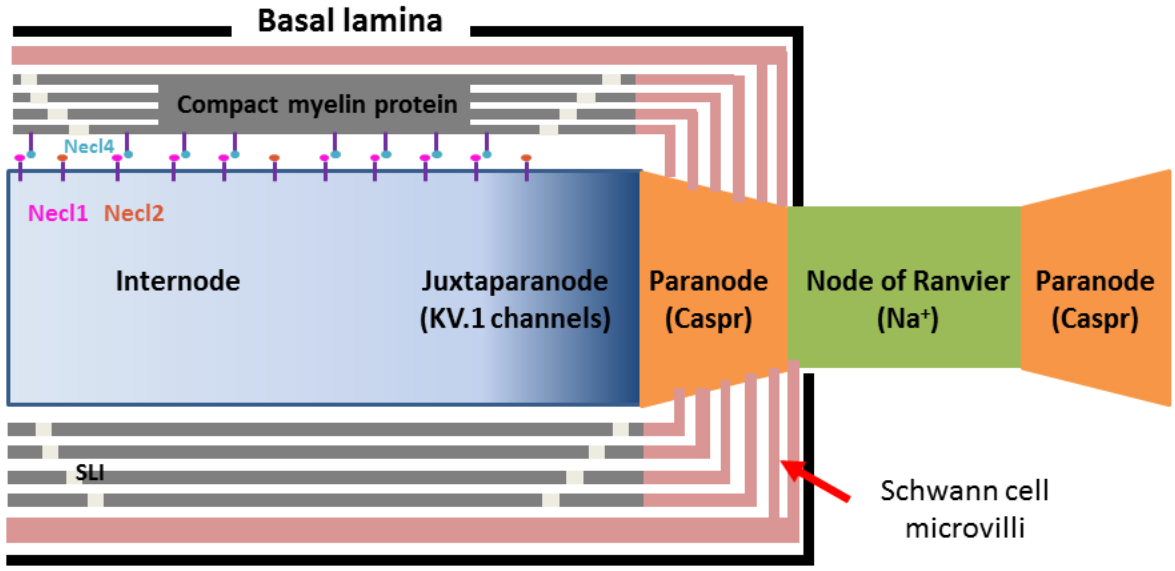

Figure 1. 2: Structure of the Schwann cell myelin & axonal membrane: Myelinating Schwann cells organise the axonal membrane into polarised compartmental structures. Schwann cells cover a segment of the axon, termed the internode and organise the axon subcellular domains (Schafer and Rasband, 2006). The juxtaxparanodal region branches from the internodal region and contains numerous Kv1 channels. The paranodal junction separates the juxtaxparanodal region and the nodes of Ranvier and functions as an attachment site for myelin as a paracellular and membrane protein diffusion barrier. The paranodal junction is composed of axonal cell adhesion molecules; caspr and contactin which form cis-interactions with neurofascin-155 on the Schwann cell membrane forming a protein binding complex (Charles et al., 2002). Nodes of Ranvier are formed between the gaps of myelin sheath, voltage gated Na^+ and K^+ channels cluster at the nodes of Ranvier mediating the transmembrane currents necessary for saltatory nerve conduction (Rasband and Trimmer, 2001). Transmembrane cell adhesion molecules Nectin like (Necl) 1 and 2 are present along the internode and juxtaparanode, while Necl4 is expressed along the Schwann cell adaxonal membrane. Necl-1 and Necl-4 form heterophilic interactions at the axon-glial interface, which is critical for normal myelin formation (Maurel et al., 2007, Spiegel et al., 2007). The Schwann cell binding partner for Necl2 expressed on the axon remains unknown. The abaxonal domain (the outermost wrap of the myelin sheath) is in close contact with the basal lamina; a thin layer of highly organised extracellular matrix components synthesised by the Schwann cells. The adaxonal domain (the innermost wrap of the myelin sheath) is in close contact with the axolemma (axonal cell membrane). Cytoplasm-filled channels known as Schmidt Lantermann incisures (SLI), which occur

through the compact myelin, connect the adaxonal and abaxonal cytoplasm (Schafer and Rasband, 2006, Pereira et al., 2012).

1.2 Composition of myelin

The myelin sheath is an extended plasma membrane that originates from the Schwann cell, and wraps around axons. Unlike other membranes which have a high protein: lipid ratio, the Schwann cell myelin sheath is composed of a high proportion of lipids (70-80%), and a lower proportion of proteins (20%-30%). This high lipid content is essential for the provision of electrical insulation (Garbay et al., 2000). It is widely accepted that myelin lipids form the lipid bilayer, while the myelin proteins are integrated into the lipid bilayers; where they can form homophilic interactions with apposing bilayers, linking them together to form compact layers of myelin (Quarles et al., 2005).

In the peripheral nervous system, the myelin sheath contains a variety of different lipids, these include cholesterol (20-30% of total lipids), ethanolamine phospoglycerides (28-39% of total lipids), Sphingomyelin (10-35% of total lipids), cerebrosides (Gal-C) (14-26% of total lipids) and sulfatides (SGal-C) (2-7% of total lipids) (Garbay et al., 2000). The myelin sheath also comprises oleic acid (C18:1), which is the major fatty acid present in the myelin sheath, accounting for 30-40% of the fatty acid in the sciatic nerve (Garbay et al., 2000).

The myelin sheath also contains a variety of proteins, these include structural and signalling compact myelin proteins; myelin protein zero (P_0), myelin basic protein (MBP) and peripheral myelin protein 22 (PMP22), as well as non-compact myelin proteins; myelin-associated glycoprotein (MAG), periaxin (Prx) and connexin 32 (Cx32) (Garbay et al., 2000). The expression of these myelin proteins is critical for the formation of stable myelin, as disruptions in their expression or function is often as associated with peripheral neuropathies such as Charcot-Marie-Tooth disease [discussed in section 1.9.1.1].

1.2.1 Compact myelin proteins

P_0 is an integral type 1 membrane glycoprotein which serves as an early marker for the Schwann cell lineage (Bhattacharyya et al., 1991, Lee et al., 1997, Zhang et al., 1995). It is highly expressed by myelinating Schwann cells and accounts for 50-70% of the total myelin proteins (Garbay et al., 2000, Poduslo et al., 1985, Poduslo et al., 1995). P_0 comprises a single transmembrane (TM) region, a positively charged intracellular domain and an extracellular N-terminal domain. P_0 acts as a cell

adhesion molecule and plays a key role in myelin compaction by forming homophilic interactions between lipid bilayers, as well as myelin stability by forming heterophilic interactions that mediate the axon-Schwann cell interaction. Depletion of P_0 in Schwann cells results in poorly compacted myelin, which is unstable and eventually demyelinates, resulting in hypomyelinated peripheral nerves (Giese et al., 1992).

MBP is expressed by Schwann cells and oligodendrocytes. MBP represents roughly 5-15% of the total myelin proteins in the PNS and is believed to participate in stabilising major dense lines (compacted cytoplasmic regions of Schwann cell myelin), stabilising the myelin sheath and also in maintaining the myelin structure, by interacting with myelin lipids and P_0 (Privat et al., 1979, Martini et al., 1995, Quarles et al., 2005). The *shiverer* mouse which contain a 20kb deletion in the MBP gene, that results in MBP not being expressed (Roach et al., 1985), has been shown to exhibit uncontrolled shaking, due to the lack of MBP in the CNS (Privat et al., 1979, Readhead and Hood, 1990). In contract, the absence of MBP in the PNS (specifically within Schwann cells) does not appear to have any dramatic effects (Martini et al., 1995). Studies analysing the sciatic nerves of MBP null mice reported that axon diameter and myelin sheath formation is normal (Martini et al., 1995).

PMP22 is a myelin protein with four hydrophobic transmembrane and two extracellular domains. It is almost exclusively expressed in compact myelin and accounts for 2-5% of the total myelin proteins in the PNS. PMP22 has been shown to form complexes with P_0; an interaction which might be important for its function (D'Urso et al., 1999). Although the functional role of PMP22 in myelination is not clearly understood, PMP22 is important for Schwann cell myelination as both the depletion and overexpression of PMP22 in Schwann cells is associated with peripheral neuropathies such as Charcot-Marie-Tooth type 1A disease. PMP22 null mice demonstrate abnormally thick myelin sheaths which appear to cause axonal compression (Adlkofer et al., 1995). Nonetheless during adulthood the myelin degenerates, resulting in thinly myelin axons and onion bulbs (Adlkofer et al., 1995). Similarly, mice overexpressing PMP22 have been reported to exhibit myelin defects, characterised by severe hypomyelination and slow nerve conduction velocities (Magyar et al., 1996).

1.2.2 Non-compact myelin proteins

MAG is a transmembrane glycoprotein located at the periaxonal membrane of both Schwann cells and oligodendrocytes, and represents 1% of the total proteins in the PNS. MAG is expressed in Schwann cells at the initial stages of myelination and interacts with axonal components; mediating Schwann-axonal contact (Quarles, 2007). MAG is also expressed in the membranes of the Schmitt-Lanterman incisures, lateral loops and inner/outer mesaxons of the myelin sheath. There are currently no reported inherited neurological disorders caused by mutations in the MAG gene in humans (Quarles, 2007). However, studies carried out on MAG knockout mice have revealed that compact myelin formation during development is normal, although abnormalities in the periaxonal region of the myelin sheath were observed (Li et al., 1994, Montag et al., 1994). Furthermore, as these mice aged they appeared show signs of demyelination and eventually axonal degeneration (Quarles, 2007, Weiss et al., 2001, Yin et al., 1998). These studies thus suggest that MAG plays a role in organising the periaxonal space and acts as a ligand in the myelin sheath that binds to the axon receptor to maintain normal myelination and axonal structure. (Quarles, 2007).

Periaxin (Prx) is predominantly expressed at the adaxonal membrane during Schwann cell axonal ensheathment, but then shifts to the abaxonal membrane as Schwann cells myelinate, where it acts to stabilize the formation of Cajal bands (Gillespie et al., 1994, Scherer et al., 1995b, Court et al., 2004). Cajal bands are cytoplasmic channels that form in-between the outermost Schwann cell myelin wrap. Depletion of Prx in mice does not impair myelination, however results in the formation of unstable myelin, which eventually degrades during adulthood resulting in hypomyelination and slow nerve conduction velocities (Gillespie et al., 2000). Prx is therefore suggested to play an important role in establishing stable myelin units.

Cx32 is a gap junction protein predominantly located within the Schmidt-Lanterman incisures and at the paranodes, where it functions as an intracellular channel allowing cytoplasmic continuity and ion diffusion across the myelin sheath (Ressot and Bruzzone, 2000). Cx32 is expressed in parallel with the myelinating phenotype and believed to play a role in myelin maintenance (Scherer et al., 1995a). Depletion or mutations in Cx32 are known to cause Schwann cell demyelination and is related to Charcot-Marie-Tooth type 1X (Scherer et al., 1995a).

1.3 Schwann cell development

Schwann cells of the peripheral nervous system originate from neural crest cells (NCC) via two intermediate cell types; the first, the Schwann cell precursor and the second, the immature Schwann cell. Unlike non-myelinating Schwann cells, in order to form mature myelinating Schwann cells, NCC must undergo transition through three intermediate cell types, the third being the promyelinating Schwann cell (Mirsky et al., 2002). NCC arise from the neural crest at the dorsal neural tube and are specified and maintained by a network of regulatory genes including Snail, Sox8, Myc, Sox9, FoxD3, Slug and Sox10 (Jacob, 2015, O'Donnell et al., 2006, Aybar et al., 2003). While it's important that the expression of these genes is upregulated for NCC specification, it is also important that the expression of genes shown to negatively regulate NCC specification are downregulated, these genes include Sox2 and Kctd15 (Jacob, 2015). Kctd15 interacts with activating enhancer-binding protein 2α (AP-2α) - a transcription factor required for Sox9 activated expression that inhibits its activity and therefore NCC formation (Jacob, 2015, Zarelli and Dawid, 2013).

Upon separating from the dorsal neural tube, NCC migrate through distinct pathways and give rise to a wide range of cell types, including melanocytes in the skin, neurons and glial cells; satellite glia, enteric glia and Schwann cells in the peripheral nervous system (PNS) (Wakamatsu et al., 2000, Monk et al., 2015, Mirsky and Jessen, 1999). The transition of NCC along the Schwann cell lineage into Schwann cell precursors occurs between embryonic day 15 to 16 (E15-16) during rat Schwann cell development (mouse E12-14), and is primarily mediated by the maintained expression of Sox10 (sex determining region Y (SRY) box 10) [discussed further in section 1.5.1]. Sox10 is one of the earliest transcription factors expressed in NCC, and essential for NCC survival, maintenance of pluripotency and peripheral glia specification (Britsch et al., 2001, Finzsch et al., 2010). Sox10 also induces the expression of neuregulin-1 receptor ErbB3, which is activated by the upregulated expression of neuregulin-1, causing NCC to favour peripheral glia specification (Shah et al., 1994, Prasad et al., 2011, Jacob, 2015). Notch signalling also plays an important role in the specification of peripheral glia over neuronal differentiation

(Wakamatsu et al., 2000). More recently, chromatin remodelling enzymes histone deacetylases 1 and 2 (HDAC 1/2) were identified to be essential for the regulation of Schwann cell specification from neural crest cells, through their ability to induce Pax3 expression in NCCs (Jacob et al., 2014). In turn Pax3 acts to maintain high Sox10 levels and to induce the expression of peripheral glial proteins, fatty acid binding protein 7 (FABP7) and Protein zero (P_0) (Jacob et al., 2014).

Schwann cell precursors (SCPs) are specifically marked by the upregulated expression of cadherin 19 and like NCC they are migratory and proliferative (Takahashi and Osumi, 2005, Monk et al., 2015). SCP co-migrate with axons in the developing PNS, and are highly dependent on the axonal derive signal NRG1 which signals via ErbB2/ErbB3 tyrosine kinase receptors on precursor cells for survival. The reliance of Schwann cell precursors on close contact with axons for survival has been proposed to help match precursor numbers to axon numbers, and thus prevent the survival of SCPs that have strayed away from axons (Jessen et al., 1994, Mirsky and Jessen, 1999). In addition to mediating SCP survival, NRG1 further regulates SCP proliferation and migration, as well as SCP maturation, which is co-operatively regulated by fibroblast growth factor (FGF) (Dong et al., 1995, Dong et al., 1999, Jessen and Mirsky, 2005).

Between E16 and E17 in rats (E14 and E15 in mice), SCPs cease migration and begin transition into immature Schwann cells (ISCs), a process driven further by Notch signalling. Enforced Notch signalling *in vivo* accelerates the transition of SCP to ISCs, driving the increased expression of S100β (calcium binding protein) and the lipid surface antigen O4, while also suppressing the expression of AP2α; a negative regulator of the SCP-ISC transition process (Stewart et al., 2001, Woodhoo et al., 2009). Like AP2α, endothelins are upregulated in SCP helping to support survival, nonetheless sustained expression of endothelins acts to delay SCP development by antagonising the maturation effect of β-neuregulin. The expression of endothelins must therefore be downregulated for the timely transition of SCPs-ISCs (Brennan et al., 2000).

Immature Schwann cells, are markedly different from SCPs, they are capable of mediating their own survival and proliferation in the absence of axons, by secreting autocrine growth factors such as neurotrophin-3, insulin-like growth factor (IGF) and

platelet-derived growth factor-BB (PDGF-BB) (Meier et al., 1999). Furthermore immature Schwann cells mediate radial axonal sorting; a process whereby Schwann cells separate large diameter axons (>1 µm) destined to become myelinated, from small diameter axons (<1 µm) that will remain non-myelinated and are organised into Remak bundles [see Figure 1.3].

Radial sorting of axons occurs perinatally and proceeds until about postnatal day 10 (P10) in rodent peripheral nerves (Feltri et al., 2015). Schwann cells initially deposit their basal lamina around groups of mixed calibre axons forming Schwann cell and axon "families", this process is then followed by Schwann cells sending out cytoplasmic processes that resemble lamellipodia into the axon bundles where they selectively separate out large calibre axons, principally A and B fibres such as motor axons and Aδ sensory fibres to the periphery (Feltri et al., 2015, Webster et al., 1973). Upon contact with large calibre axons, immature Schwann cells transition into the promyelin stage, marked by the expression of octamer 6 (Oct6) and establish a 1:1 axon-promyelinating Schwann cell relationship; for Schwann cells to match axon numbers, they undergo progressive proliferation (Jessen and Mirsky, 2005, Webster et al., 1973). Promyelinating Schwann cells then differentiate into myelinating Schwann cells, a process regulated by axonal signalling and the activation of myelin regulatory transcription factors (Feltri et al., 2015). The remaining small calibre axons are ensheathed by immature Schwann cells, which differentiate into non-myelinating Schwann cells forming Remak Bundles.

Abnormalities or impairments in axonal sorting have been shown to result in morphological abnormalities in the peripheral nerve. Firstly, if SCPs fail to migrate along axons, proliferate, survive and generate immature Schwann cells, this causes a complete arrest of radial sorting at the first stage and consequently the majority of axons remain naked. Secondly, if immature Schwann cells fail to deposit basal lamina or to interact properly with axons, this can result in the failure of Schwann cells to appropriately sort axons, resulting in abnormities (Feltri et al., 2015). Three categories for axon abnormalities have been established: (1) Radial sorting arrest/delay; resulting in Schwann cells surrounding large bundles of mixed calibre axons, (2) polyaxonal myelination; caused due to premature differentiation of Schwann cells before completion of radial sorting and results in Schwann cells myelinating multiple axons, (3) Abnormal ensheathment of Remak bundles; non-

myelinating Schwann cells ensheath bundles of small and large calibre axons (Feltri et al., 2015).

The Rho GTPase family members Rac1 and Cdc42 have been shown to play a fundamental role in radial sorting, through regulating the activation of NF2 (Guo et al., 2012, Guo et al., 2013, Benninger et al., 2007). Rac1 has been shown to regulate immature Schwann cell process extensions required for the sorting of axons. In Rac1 null mice immature Schwann cells demonstrate defective cytoplasmic processes that extended in various directions and often failed to envelope axon bundles (Benninger et al., 2007). Cdc42 null mice also demonstrate defective radial sorting, as numerous abnormally large axon bundles containing unsorted small, medium and large axons are observed in the sciatic nerves of these animals (Benninger et al., 2007, Guo et al., 2013). By postnatal day 30 (P30) these mice further showed hind limb dysfunction with abnormal clasping (Guo et al., 2013). Nonetheless, in both Rac1 and Cdc42 null mice, depletion of NF2 (a tumour suppressor gene) rescued the radial sorting and myelination defect, therefore demonstrating that Rac1 and Cdc42 regulation of NF2 activation is essential for normal radial sorting (Guo et al., 2012, Guo et al., 2013).

β1 integrin a Schwann cell laminin receptor, has also be shown to play a fundamental role in radial sorting (Feltri et al., 2002). β1 integrin null Schwann cells develop normally but fail to maintain and extend normal processes around axons, similar to that observed in Rac1 null mice (Benninger et al., 2007, Feltri et al., 2002). Rac1 was later revealed to drive radial sorting through regulating Schwann cell process formation and extension downstream of β1 intergrin (Nodari et al., 2007).

Many additional proteins including laminins (laminin α2, laminin α4 and laminin Ɣ1), surface receptor proteins ErbB2 and ErbB3 and cell signalling molecules Jab1 and β-catenin have been shown to regulate radial sorting, as disruptions in their expression has been shown to cause radial sorting defects during development, impaired Schwann cell myelination and the onset of a peripheral neuropathy (Reviewed by Feltri et al., 2015). Correct radial sorting at all stages is therefore required for Schwann cell myelination and normal function of the peripheral nervous system.

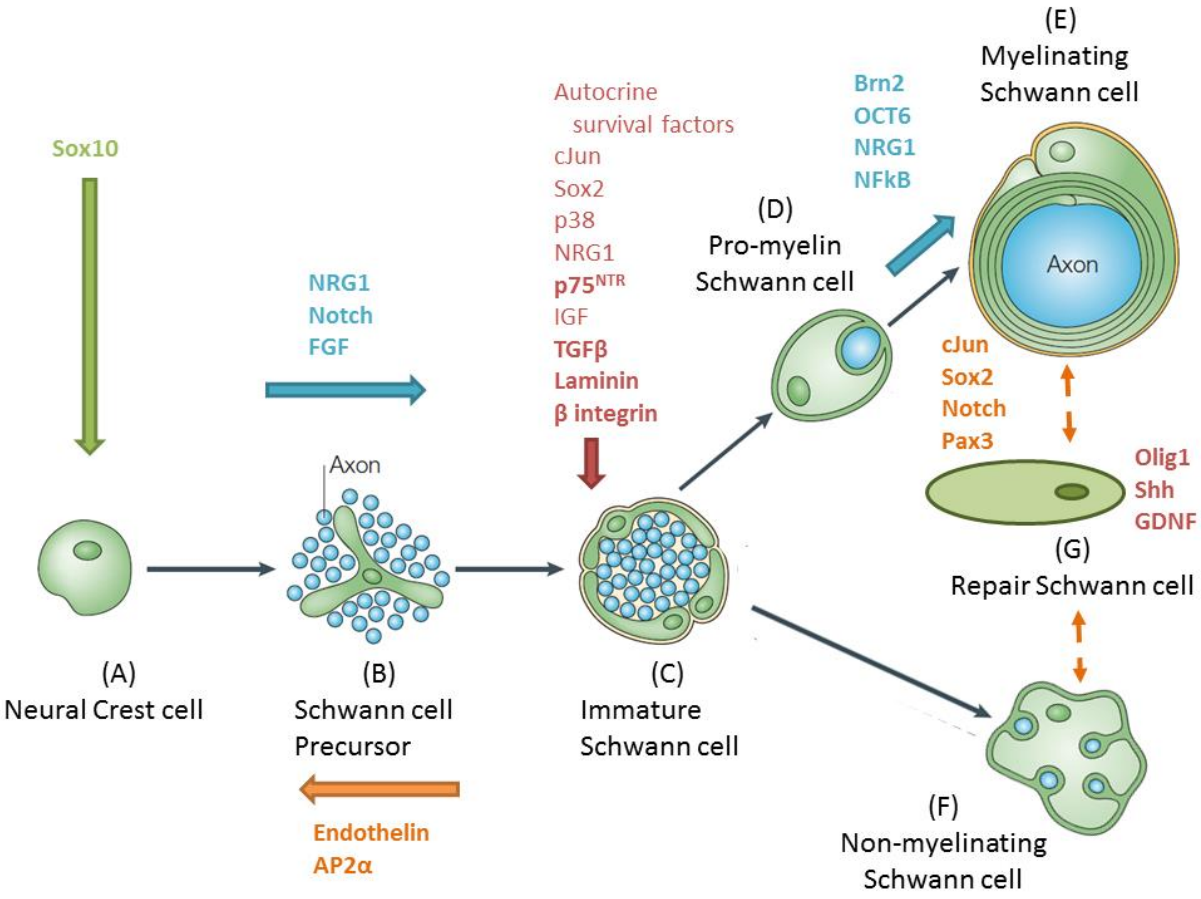

Figure 1. 3: Schwann cell lineage and factors involved in development. Schematic illustration of the main cell types Schwann cells transition through and the molecules expressed during development. (A) Migrating neural crest cells transition to (B) Schwann cell precursors. Schwann cell precursors thereafter transition to (C) immature Schwann cells which then differentiate into two subpopulations of Schwann cells; (D) Promyelinating Schwann cells which associate with large diameter axons in a 1:1 ratio, and further transition into (E) myelinating Schwann cells, or (F) non-myelinating Schwann cells which ensheath groups of small diameter axons, forming Remak bundles. (G) Following nerve injury myelinating and non-myelinating Schwann cells transiently differentiate into Repair Schwann cells to support nerve repair and regeneration. Adapted from (Jessen and Mirsky, 2005).

1.4 Axonal myelination signalling

Schwann cell myelination and myelin maintenance is dependent upon axonal contact, and influenced by axonal diameter, electrical activity and axonal signalling (Taveggia et al., 2010). Importantly axonal cues trigger Schwann cell myelination by signalling through specific Schwann cell receptors. Current literature suggests that Prohibitin 2 expression, Nectin like (Necl) signalling, G-protein coupled receptor 126 (Gpr126) signalling, and Neuregulin-ErbB signalling play fundamental roles in this process (Salzer, 2012, Poitelon et al., 2015).

Axon-Schwann cell contact is vital for the initiation of Schwann cell myelination, in order for Schwann cells to initially contact axons they must respond and polarise towards axonal signals. Schwann cells have been shown to polarise their cytoplasmic processes (which are formed by microtule and filament structures) termed pseudopods, upon Schwann cell-axon contact in response to juxtacrine signals from the axonal membrane. Prohibitin 2, a mitochondrial protein, was recently identified as a novel molecule expressed in Schwann cell pseudopods (in mitochondria and at the cell membrane) and shown to mediate axon-glial contact (Poitelon et al., 2015). Blocking Prohibitin 2 expression in Schwann cells (through shRNA viral infection), was shown to impair their ability to attach to neurons, in Schwann cell-DRG neuronal co-cultures (Poitelon et al., 2015). Moreover, experiments carried out on conditional Prohibitin 2 null mice (P0 Cre^{+}; $Phb2^{fl/fl}$) revealed that these mice demonstrated impaired radial sorting, hypomyelination of axons and severe motor deficit (Ibid). This study by Poitelon et al. (2015) thus highlights how Prohibitin2 expression in Schwann cell pseudopods is essential for Schwann cell-axon contact during development and for normal myelination.

Schwann cells express a number of cell adhesion and recognition molecules on their surface that mediates their association with axons. Nectin-like (Necls) cell adhesion molecules have been shown to play a fundamental role in the interaction of axons and Schwann cells, as well as the initiation of normal myelin formation (Maurel et al., 2007, Spiegel et al., 2007, Golan et al., 2013). Necls are members of the immunoglobulin superfamily of cell adhesions molecules, and consist of five different members Necl1, Necl2, Necl3, Necl4 and Necl5 (Maurel et al., 2007). Necl2 and 4 are expressed in Schwann cell membranes, principally at the internodal region and the Schmidt-Lanterman incisures, while Necl2 and Necl1 are expressed by axons.

Necl4 acts as a glial binding partner for axonal Necl1 at the internode, mediating normal Schwann cell-axon interaction and the distribution of ion channels along axons (Maurel et al., 2007, Spiegel et al., 2007, Golan et al., 2013). Necl4 expression was further shown to be required for the proper establishment of myelinated axons and for the organisation of the underlying axonal membrane. *In vitro* experiments revealed that knockdown of Necl4 by short hairpin RNA, resulted in a striking inhibition of Schwann cell myelination in Schwann cell-DRG co-cultures. Furthermore, the expression of Oct6, a transcription factor expressed by promyelinating Schwann cells and Krüppel box 20 (Krox20), a transcription factor essential for regulating myelination was dramatically inhibited in these co-cultures (Maurel et al., 2007). *In vivo* studies using Schwann cells specific Necl4 null mice experiments further confirmed the importance of Necl4 in Schwann-axon interaction and myelination, however they revealed that the role of Necl4 *in vivo*, differs from that previously identified in earlier *in vitro* studies (Maurel et al., 2007, Spiegel et al., 2007, Golan et al., 2013). Rather than being hypomyelinated, as expected from the earlier studies (Maurel et al., 2007, Spiegel et al., 2007), axons in the nerves of Necl4 null mice were hypermyelinated, and displayed a range of myelin abnormalities including myelin outfolds, myelin degeneration and the displacement of axons. The correct organisation and compartmentalisation of the axonal membrane i.e. the localisation of molecular proteins such as Caspr (a specific marker of the paranode) and ion channels was disrupted [See Figure 1.2], and mice showed a phenotype Charcot Marie Tooth neuropathy [See section 1.9.1.1] (Golan et al., 2013). Necl4 thus plays a fundamental role in establishing axon-Schwann cell interaction, proper myelin formation and the correct organisation of the axonal membrane.

Expression of the adhesion Gpr126 is required autonomously in Schwann cells for Schwann cell myelination (Monk et al., 2009, Mogha et al., 2013) and for the formation of normal Remak fibres (Monk et al., 2011, Mogha et al., 2013). In embryonic zebrafish and mice, the depletion of Gpr126 resulted in the failure of Schwann cells to upregulate the expression of the promyelination transcription factors Oct6 and Krox20 and to myelinate axons. Schwann cells thus appeared to be arrested at the promyelinating stage (Monk et al., 2009, Mogha et al., 2013). Furthermore, Gpr126 mutant mice demonstrated delays in radial sorting, a significant

increase the number of axons per Remak bundle and aberrant abaxonal cytoplasmic protrusions (Monk et al., 2011, Mogha et al., 2013). Treatment with the adenyl cyclase activator forskolin was shown to rescue the myelination defects observed in $Gpr126^{st49}$ mutant zebrafish *in vivo* (Monk et al., 2009), and in Schwann cells cultured from Gpr126 null mice (Mogha et al., 2013). These experiments thus suggest that Gpr126 regulates myelination by activating adenyl cyclase or raising intracellular cAMP. More recent experiments have revealed that Gpr126 is capable of directly elevating cAMP levels in COS-7 cells, by coupling with G_i-proteins and G_s proteins (Mogha et al., 2013). Thus the suggested mechanism by which Gpr126 regulates Schwann cell myelination, is through interactions with G proteins causing elevation of cAMP levels (Mogha et al., 2013). Recent studies carried out *in vitro* have further identified that Gpr126 is activated through binding to collagen IV (Paavola et al., 2014), as well as laminin-211 (Petersen et al., 2015), which are both expressed in the Schwann cell basal lamina (Monk et al., 2015, Petersen et al., 2015). The interaction of Gpr126 with either collagen IV or laminin-211 has been shown to facilitate radial sorting and Schwann cell myelination (Paavola et al., 2014, Petersen et al., 2015)

One of the major axonal signalling molecules that regulates the formation of myelinating and non-myelinating Schwann cells is neuregulin-1, an epidermal growth factor-like ligand. The neuregulin-1 (NRG-1) family comprises more than 15 membrane-associated and secreted protein isoforms, all of which share an epidermal growth (EGF)-like signalling domain required for the activation of their receptors (Nave and Salzer, 2006). The NRG-1 protein isoforms have been subdivided into several subtypes (NRG1 type I-VII), on the basis of their distinct amino-termini. In the nervous system NRG1 type I (NRG1-I) and NRG1-III are the most abundant, and in addition to NRG1-II, play a direct role in mediating Schwann cell myelination (Nave and Salzer, 2006).

NRG1-I (also known as heregulin, neu differentiation factor) and NRG1-II (also known as glial growth factor) have N-terminal immunoglobulin-like domains. In order for these transmembrane forms of NRG1-I and II to signal, they must undergo proteolytic cleavage by the metalloproteinases tumour necrosis factor-α-converting enzyme (TACE), ADAM19 (β-meltrin) or beta amyloid precursor protein–cleaving enzyme1 (BACE1), which causes release of the extracellular signalling domain,

enabling it to act as a soluble signal in a paracrine manner (Horiuchi et al., 2005, Nave and Salzer, 2006). Unlike NRG1-I and NRG1-II, NRG1-III contains a cysteine rich domain (CRD) which acts as a second transmembrane domain, thus following cleavage by BACE1 the protein remains tethered to the cell membrane (Velanac et al., 2012). NRG1-III therefore serves as a juxtacrine axonal signal. While NRG1-I does not appear to play an essential role in Schwann cell myelination during development, Schwann cell derived soluble NRG1-I expression has been shown to be important for Schwann cell redifferentiation and remyelination following nerve injury (Stassart et al., 2013). Following nerve injury, poor Schwann cell remyelination and a decrease in the number of redifferentiated Schwann cells was observed in mice lacking NRG1-I specifically in Schwann cells (Stassart et al., 2013). NRG1-III on the other hand, is the key regulator of peripheral nerve myelination during development; it determines the myelinating phenotype and matches myelin thickness to axon calibre (Monk et al., 2015, Nave and Salzer, 2006, Taveggia et al., 2005). Previous studies have shown that Schwann cells cultured with NRG1-III null neurons failed to myelinate and express myelin proteins, while the overexpression of NRG1-III in Schwann cells enhanced myelin formation (Taveggia et al., 2005). NRG1-III is also important for Schwann cell remyelination after injury; it acts to accelerate the rate of remyelination and functional recovery at early time-points post injury (Fricker et al., 2013). In the absence of axonal NRG1-III Schwann cell remyelination was severely delayed, with axon not reaching full remyelinate until 3 months post injury (Fricker et al., 2013).

Expression levels of NRG1-III on neurons have further been shown to differ, depending on the size and type of neurons; small diameter sensory axons (C-fibre) express minimal levels of NRG1-III, whereas large diameter motor and Aδ fibres express much higher levels (Taveggia et al., 2005). The levels of NRG1-III expressed on the neurons, thus dictates to the Schwann cell its myelin phenotype; high levels of NRG1-III drive Schwann cells to myelination, while low levels cause Schwann cells to undertake a non-myelinating phenotype. Nonetheless, increasing NRG1-III levels in small diameter sensory neurons which are normally unmyelinated, has been shown to result in a myelinated axon fate (Taveggia et al., 2005). While NRG1-III signalling in large diameter axon is essential for driving Schwann cell myelination and normal myelin formation, NRG1-III signalling in small diameter

axons is also important. It has been shown to be critical for proper radial sorting of axons, the complete ensheathment of small diameter axons by non-myelinating Schwann cells, the formation of normal sized Remak bundles and thus normal sensory function (Taveggia et al., 2005, Fricker et al., 2009).

NRGs signal via the epidermal growth factor (EGF) family of receptor tyrosine kinases, comprising ErbB1, ErbB2, ErbB3 and ErbB4. Schwann cells express ErbB3 and ErbB2 receptors which form heterodimers on NRG1 binding to ErbB3. ErbB2 thereafter triggers the activation of a complex sequence of signalling events that mediate myelination (Birchmeier and Nave, 2008). NRG1/ErbB signalling is absolutely essential for Schwann cell development and myelination, as the absence of ErbB2 in Schwann cells results in the formation of abnormally thin myelin sheaths and low expression levels of myelin proteins protein zero (P_0) and peripheral myelin protein 22 (PMP22) (Garratt et al., 2000).

Recent studies have highlighted that the NRG1/ErbB signalling in Schwann cells can activate multiple downstream signalling events, including the activation of calcineurin, Ying Yang 1 (YYI), PI3K (phosphoinositide 3 Kinase) and MAPK (mitogen-activated protein kinase)/ERK signalling pathways [See Figure 1.4] (Krishnan, 2013, He et al., 2010).

Calcineurin-NFATc3/4

Calcineurin is a calcium sensitive serine/threonine protein phosphatase with 2 catalytic subunits; Calcineurin A (CnA), the catalytic domain and Calcineurin B (CnB), the essential catalytic regulatory domain (Rusnak and Mertz, 2000). NRG1 has been suggested to induce phospholipase C-γ (PLC-γ)-dependent Ca^{2+} influx into Schwann cells, which in turn causes activation of cytoplasmic calcineurin. Calcineurin thereafter promotes de-phosphorylation of NFATc3 and NFATc4, enabling their translocate to the nucleus where they binds to DNA, to drive the transcriptional gene expression (Kao et al., 2009). Schwann cells express NFATc3 and NFATc4, which fail to become activated in CnB1 depleted mice; resulting in reduced Krox20 and myelin protein expression, along with Schwann cell hypomyelination (Kao et al., 2009). *In vitro* experiments revealed that NFATc3 and NFATc4 translocate to the nucleus upon activation, where they synergise with Sox10

to drive the transcriptional gene expression of Krox20 and P_0, a process which was also shown to be blocked by Sox2 (Kao et al., 2009).

In vitro experiments by Kipanyula et al. (2013) further revealed that the calcineurin-NFAT signalling pathways are important for potentiating Schwann cell myelination and Krox20 expression in response to cAMP. While activation of the calcineurin-NFAT pathway alone by elevating Ca^{2+} concentrations is insufficient to drive myelination, cAMP treatment alone is sufficient to drive normal Schwann cell myelination. Additionally, Schwann cell myelination is further enhanced and the expression levels of Krox20 and myelin proteins periaxin and P_0 are increased in the presence of cAMP, when the calcineurin-NFAT pathway is activated (Kipanyula et al., 2013).

Activation of the zinc finger transcription factor Ying Yang 1 (YY1), a downstream effector of NRG1 has also been shown to be crucial for Schwann cell myelination (He et al., 2010). Conditional Schwann cell deletion of YYI in mice was shown to result in severe hypomyelination of the sciatic nerves and failure of Schwann cells to express high levels of Krox20 and myelin proteins. Nonetheless this myelin defect was shown to be rescued by the enforced expression of Krox20 in Schwann cells cultured from the sciatic nerves of YY1 null mice, as the percentage of P_0^+ cells was restored to normal. Further experiments by He et al. (2010) revealed that soluble NRG1 stimulates MEK dependent phosphorylation of YY1 on $serine^{118}$, $serine^{184}$ and $serine^{247}$, which in turn promotes the binding of YY1 to the Krox20 promoter and MSE (myelinating Schwann cell enhancer) region, where it drives Krox20 transcriptional activation in cultured Schwann cells (Ogata et al., 2004)

PI3kinase/Akt

The phosphatidylinositol-3-kinase (PI3K) is composed of two subunits, the adaptor subunit p85 and the catalytic subunit p110, and has been shown to be robustly activated in Schwann cells upon NRG1 signalling via the ErbB2/3 receptors (Taveggia et al., 2005, Maurel and Salzer, 2000). The PI3 kinase signalling pathway, phosphorylates and actives the serine-threonine kinases Akt and mTOR, which go onto stimulate downstream molecules that drive myelination (Goebbels et al., 2012). Impairing the PI3K signalling pathways in Schwann cells, by either treating Schwann

cell/DRG co-cultures with a PI3K signalling inhibitor (LY294002) or infecting Schwann cells with an adenovirus carrying a dominant negative mutant of the regulatory subunit p85 (Ax-p85^{DN}), was shown to block the initiation of Schwann cell myelination and reduce the expression of myelin associated glycoprotein (MAG) (Ogata et al., 2004, Maurel and Salzer, 2000). Further experiments also revealed that overexpression of PI3K or activated Akt signalling, significantly enhanced myelin protein expression in Schwann cell/DRG neuronal co-cultures, in addition to enhancing myelin sheath formation during regeneration *in vivo* (Ogata et al., 2004). Recent gain of function studies *in vivo* have extended earlier findings. Mice conditionally depleted of phosphatase and tensin homolog (Pten); a lipid phosphatase, which antagonises PI3K signalling, demonstrate increased activation of the PI3K signalling pathways. This was shown to result in Schwann cell hypermyelination and myelin abnormalities in non-compacted regions; focal myelin thickening in paranodal regions and Schmidt-lantermann incisures (Goebbels et al., 2012). The PI3K-Akt pathway has thus been shown to be a driver of myelination and a direct target of NRG1 signalling.

ERK

Extracellular signal-related kinase (ERK) is a mitogen activated protein kinase (MAPK) signalling pathway capable of regulating both cell differentiation and proliferation. The classical activation of ERK 1/2 signalling is triggered by the sequential phosphorylation and activation of RAS-RAF-MEK 1/2.

In Schwann cells the ERK 1/2 signalling pathway has been shown to exert two opposing functions in a context dependent manner; (1) to drive Schwann cell differentiation and myelination during development and (2) to promote demyelination and inhibit myelin formation following nerve injury [discussed in section 1.6.4].

During Schwann cell development NRG1 dramatically increases the activation of the MAPK ERK 1/2 signalling pathway. While activation of this pathway was originally thought to be redundant during Schwann cell development (Maurel and Salzer, 2000), recent *in vivo* studies using conditional ERK 1/2 double null mice have shown that ERK1/2 signalling is essential for the progression of immature Schwann cells to a myelinating state (Newbern et al., 2011). A significant decrease in the gene and protein expression of Krox20 was observed in the nerves of ERK 1/2 double null

mice, along with a striking reduction in the number of myelinated axons and an increase in the number of unmyelinated axons (Newbern et al., 2011). Furthermore, ERK 1/2 was shown to be a necessary downstream transducer of NRG1/ErbB signals, as loss of ERK 1/2 in glial progenitor cells blocks the survival effects of NRG1 *in vitro* (Newbern et al., 2011).

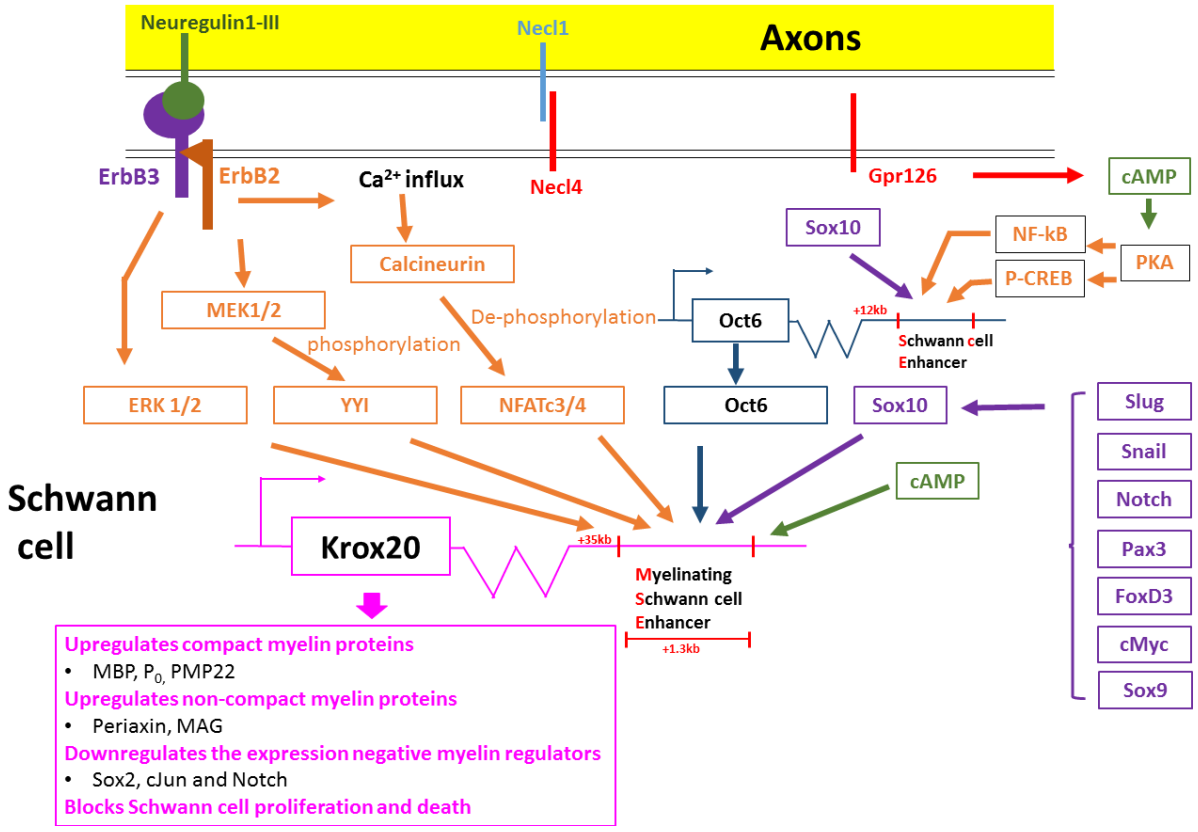

Figure 1. 4: Activated signalling pathways during Schwann cell myelination. Axonal Neuregulin1-type III (NRG1-III) binds to the ErbB3 receptor on Schwann cells. This leads to the activation of the ErbB2/3 receptor complex, which subsequently activates a variety of downstream pathways. These include activation of ERK 1/2 signalling, activation of YY1 through phosphorylation by MEK 1/2, and the activation of NFATc3/4 via calcineurin induced dephosphorylation. G-coupled protein receptor (Gpr) 126, is activated by either collagen IV or laminin 211 (Monk et al., 2015), it thereon functions to elevated levels of cAMP, which activates its main target protein kinase A (PKA), in addition to directly activating Krox20 expression. PKA can phosphorylate and activate both the cAMP response element binding protein (P-CREB) and NF-KB, both of which activate Oct6 (Monk et al., 2009, Svaren and Meijer, 2008). Oct6 is also enhanced by Sox10, which bind to the Oct6 SCE region. During embryonic development, Sox10 has been shown to be activated/upregulated in the neural crest cells by many proteins, including Slug, Snail, Notch, Pax3, FoxD3, cMyc and Sox9 (Jacob, 2015), where it then continues to be expressed throughout Schwann cell development. Together YY1, NFATc3/4, Oct6 and Sox10 have been shown to promote Krox20 transcriptional expression by binding to the Krox20 MSE region. ERK 1/2 has been shown to influence Krox20 expression, however the mechanism is not known (Newbern et al., 2011). Activation of Krox20 is essential as it goes on to induce the expression of proteins and enzymes required for myelination (Nagarajan et al., 2001).

1.5 Positive myelin regulators during Schwann cell development

Schwann cell myelination is tightly controlled by key positive and negative transcriptional regulators. Positive myelin regulators drive Schwann cells along the myelinating lineage, and activate the expression of myelin associated gene, whilst also acting to suppress the expression and activity of negative regulators [Section 1.6]. Sox10, Oct6 and Krox20 have been identified as key positive transcriptional regulators and are discussed below (Jessen and Mirsky, 2008).

1.5.1 Sox10

Sox10 (SRY related box 10) is a high mobility group (HMG) domain transcription factor, and a member of the SoxE subgroup of Sox proteins. Sox proteins of the same group have at least 80% sequence similarly in their DNA-binding HMG domain (Wegner, 2010). The Sox10 protein contains a HMG domain, two activation domains (K2 and Transactivation (TA) domain) as well as a DNA dependent dimerization domain, which enables Sox10 to dimerize either side of a DNA sequence (Barrionuevo and Scherer, 2010). All Sox proteins have been shown to bind to a common 7 base pair (bp) consensus motif '(A/T)(A/T)CAA(A/T)G-3' in DNA. To help ensure that specific Sox proteins bind to different gene sequences and are not competing for the same regions, flanking sequences located in front of and after the consensus motif have been show to aid binding specificity. In particular SoxE proteins bind preferentially to sequences with AG in the 5' flank and G or GG in the 3' flank (Wegner, 2010). On recognition of the DNA sequence, Sox transcription factors bind to the minor grooves of the DNA, causing the grooves to widen and the DNA to bend. It is speculated that this DNA bending enables the Sox proteins to exert their regulatory function (Kamachi and Kondoh, 2013).

Sox10 is a major neural crest regulator and has been shown to be activated in a Sox9 dependent manner (Betancur et al., 2010). Its expression is critical for the specification of neural crest cells into peripheral glia and melanocytes (Britsch et al., 2001, Schreiner et al., 2007). Following peripheral glia specification Sox10 continues to be expression in Schwann cells where it functions to regulated Schwann cell development, myelination and myelin maintenance (Kuhlbrodt et al., 1998, Finzsch et al., 2010). Loss of Sox10 in neural crest cells has been shown to block specification into Schwann cell precursors, resulting in a complete lack of Schwann

cells in the PNS (Britsch et al., 2001). Sox10 has also been shown to be essential for the normal expression of ErbB3 receptor in neural crest cells, as in Sox10 null mice erbB3 expression was reduced. As mentioned earlier in section 1.4, ErbB3 is essential for NRG1 signalling during Schwann cell development (Britisch et al., 2001). Loss of Sox10 in developing embryonic Schwann cells was further shown to block Schwann cells from differentiating beyond the immature Schwann cell stage. Sox10 null mice failed to upregulate Oct6 (a key transcription factor required for driving the transition of immature Schwann cells to the promyelinating stage), Krox20 (a master regulator of myelination) and the gene expression of P_0 and MBP (Finzsch et al., 2010). More recent studies have confirmed that Sox10 plays an essential role in activating the expression of the two key Schwann cell transcription factor Oct6 (Jagalur et al., 2011) and Krox20 (Reiprich et al., 2010), as well as the expression of myelin proteins P_0, periaxin and PMP22 (Schreiner et al., 2007, Srinivasan et al., 2012). Whilst Sox10 is essential for the progression of Schwann cells to the myelinating phenotype and the expression of myelin regulatory genes and proteins, its continued expression in Schwann cells is critical for myelin maintenance (Bremer et al., 2011). Depletion of Sox10 in adult myelinating Schwann cells was shown to result in Schwann cell myelin loss and dedifferentiation (Bremer et al., 2011).

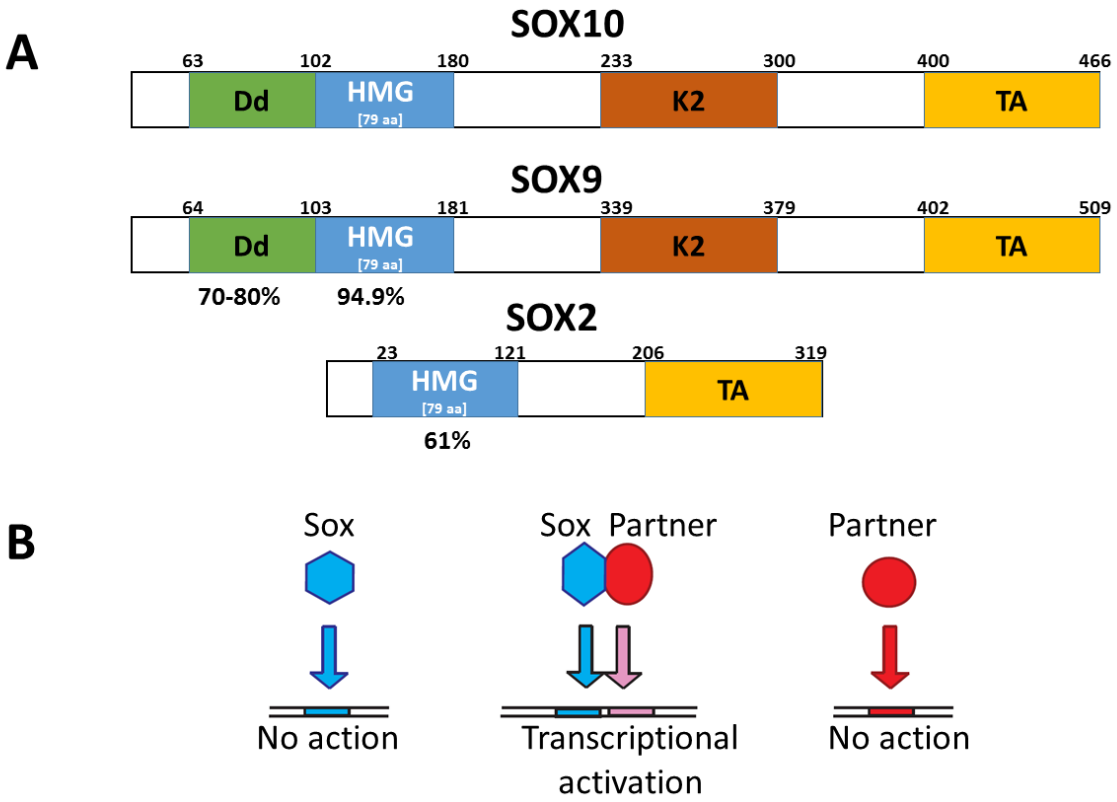

Figure 1. 5: Sox proteins family homology and partner binding. (A) Diagram of the key functional domains of Sox10 (Class E), Sox9 (Class E) and Sox2 (Class B1). The functional domains consist of the dimerization domain (Db, green), the 79 amino acid high mobility group (HMG, blue), the weak activation domain (WA or K2, orange) and the transactivation domain (TA, yellow). The percentage figures demonstrate the similarities of the domains compared to Sox10. Numbers above the domains illustrate amino acid residue counting from the N-terminus. (B) Schematic representative of DNA binding and the requirement of Sox-partner complex; Sox proteins are important for the activation or repression of specific genes, in order for Sox proteins to exert gene regulatory functions, they are generally required to form complexes with partner transcription factors. Binding of Sox proteins to DNA alone does not usually lead to transcriptional activation or repression, thus functional Sox binding sites are commonly accompanied by a second binding site for partner proteins. In Schwann cells Sox10, has been shown to partner with Oct6, Krox20 and NFATc3/4. Whilst Sox2 has been shown to partner with Oct4 in embryonic stem cells and Pax6 during lens development (Kamachi and Kondoh, 2013). Adapted from (Barrionuevo and Scherer, 2010, Kamachi and Kondoh, 2013).

1.5.2 Oct 6

Oct6 (also known as suppressed cAMP inducible protein (SCIP)) is a class III POU domain transcription factor transiently expressed in Schwann cells. The POU domain (named after three transcription factors Pit, Oct, and Unc) is a conserved bipartite DNA binding domain composed of two subunits; the POU-specific domain and the POU-homeodomain, which catalyse high affinity site-specific DNA binding (Verrijzer and Van der Vliet, 1993).

Oct6 is initially expressed in immature Schwann cells, its expression then peaks during the promyelin Schwann cell stage, where it acts to regulate the onset of myelination (Jaegle et al., 2003). Oct6 synergises with Sox10 and together they then bind to the Krox20 myelin specific enhancer (MSE), and drive the transcriptional activated expression of Krox20 (Ghislain and Charnay, 2006, Jagalur et al., 2011). In the absence of Oct6, Schwann cells are transiently arrested at the promyelin stage. Studies carried out in Oct6 null mice, revealed that Schwann cell myelination and myelin protein expression was delayed during development, however by P90 myelination was revealed to be normal (Jaegle et al., 1996). Further experiments revealed that Brain-2 (Brn2), a POU domain transcription factor is able to substitute for Oct6, and partially rescue the delay in Schwann cell development when highly expressed in Oct6 null mice (Jaegle et al., 2003). Double knockout of Oct6 and Brn2 in mice, was shown to worsen the myelinating phenotype; the delay in myelination and time for which Schwann cells were arrested at the promyelination state was shown to be substantially longer then in Oct6 null mice (Jaegle et al., 2003). Although Oct6 acts to initiate Schwann cell myelination, its expression must be reduced following the onset of myelin formation. Continued expression of Oct6 in Schwann cells was shown to cause Schwann cell hypomyelination and prevented the upregulated expression of MBP, P0 and PMP22 *in vivo* (Ryu et al., 2007).

1.5.3 Krox20

Krox20, also known as early growth response 2 (Egr2) is a Cys_2/His_2 type zinc finger transcription factor, recognised as the master regulator of Schwann cell myelination. Krox20 is expressed from E15.5 (in mice), and continues to be expressed in Schwann cells during development and in adulthood, where it functions to regulate

the expression of many myelin components (Topilko et al., 1994, Nagarajan et al., 2001, Decker et al., 2006).

The expression of Krox20 is absolutely necessary for Schwann cell myelination. In Krox20 null mice, Schwann cells completely fail to myelinate axons and express very low levels of myelin proteins P_0 and MBP (Topilko et al., 1994). Electron microscopy analysis confirmed that axons in the nerves of these animals are surrounded by Schwann cells that have made about one and a half turns, this suggested that in the absence of Krox20 Schwann cells are capable of making a 1:1 relationship with axons, however are unable to progress beyond the promyelinating stage (Topilko et al., 1994). Further studies carried out on mice homozygous for the hypomorphic Egr2 allele ($Egr2^{lo/lo}$), confirmed that failure to sufficiently elevate Krox20 expression results in Schwann cells being retained at the immature/ promyelinating stage; this was marked by the sustained expression of Sox2 and Oct6 at P14. Furthermore, $Egr2^{lo/lo}$ mice had severely hypomyelinated axons and exhibited tremors and impaired coordination; phenotypically displaying characteristics of congenital hypomyelination neuropathy (Le et al., 2005a). Continued Krox20 expression in adult Schwann cells has also been shown to be essential for myelin maintenance (Decker et al., 2006). Conditional depletion of Krox20 in adult Schwann cells using a tamoxifen inducible Cre recombination system [see Section 1.6.4] resulted in Schwann cells undergoing demyelination and dedifferentiation (Decker et al., 2006). After nerve injury, Krox20 expression is reduced as Schwann cells demyelinate and dedifferentiate. Nonetheless, indirect evidence suggests that following nerve repair, Krox20 must be re-expressed in Schwann cells, in order to downregulate the expression of negative myelin regulators and increase the expression of myelin-associated genes, thus enabling Schwann cells to remyelinate regenerating axons (Nagarajan et al., 2001, Le et al., 2005a, Parkinson et al., 2008).

Krox20 regulates the expression of many genes critical for the formation of myelin and myelin maintenance. These include myelin associated genes, P_0, MBP, PMP22, MAG, connexin 32 and periaxin, as well as genes encoding enzymes involved in lipid and cholesterol biosynthesis such as 3-hydroxy-3-methyl glutaryl (HMG) CoA reductase and stearoyl CoA desaturase (Nagarajan et al., 2001). Studies have shown that Krox20 regulates the expression of genes associated with myelination by directly binding to regulatory DNA sequences. For example Krox20 induces the

transcriptional gene expression of P_0 by binding to two regulatory sites located in intron 1 (LeBlanc et al., 2006). Krox20 has also been shown to regulate the transcriptional gene expression of MBP, by binding to two conserved sites in the Schwann cell enhancer (termed MbpSCE1) upstream of the MBP gene, and a potential third site in intron 1. The transcriptional gene expression of MAG has also been shown to be induced by Krox20 binding to sites in the second intron of the MAG gene (Jang et al., 2006). Interestingly, Krox20 has been shown to co-localise with Sox10 in regulating many of the myelin genes mentioned above, and that many of these genes contain clustered binding site for Krox20 and Sox10 within their regulatory elements.

For Krox20 to mediate successful myelination, it must interact with the NGF1-A/Egr binding protein (Nab) 1 and 2 transcriptional co-repressors (Mager et al., 2008). This interaction has been shown to be important for the transcriptional repression of specific genes known to oppose myelination such as inhibitors of DNA binding/differentiation 2 (Id2) and Id4 [Section 1.6.7]. Furthermore, double knockout of Nab1 and Nab2 in mice, was shown to phenocopy $Egr2^{lo/lo}$ mice i.e. early lethality and Schwann cells being arrested at the immature/promyelin stage, thus supporting the notion that Krox20/Nab complexes are important for myelination (Le et al., 2005b)

In order for Krox20 to upregulate the expression of myelin associated components during Schwann cell development and following nerve repair, it must first downregulate the expression of gene associated with immature Schwann cells, these include cJun, Sox2 and Notch [discussed in Section 1.6]. *In vitro* experiments have shown that enforced Krox20 by adenoviral infection in Schwann cells suppresses cJun, Sox2 and Notch, while in the absence of Krox20, cJun, Sox2 and Notch levels remain high (Parkinson et al., 2004, Parkinson et al., 2008, Woodhoo et al., 2009). Furthermore, *in vivo* experiments have also confirmed that in the absence of Krox20 or when Krox20 expression is low, Notch and Sox2 remain highly expressed (Le et al., 2005a, Woodhoo et al., 2009)

Some of the functional roles of Krox20 i.e. the upregulation of myelin-associated genes and the suppression of genes associated with immature Schwann cells, have been suggested to be mediated through Dicer, a type-III ribonuclease responsible for

the regulating miRNA maturation. Inactivation of Dicer in Schwann cells was shown to impair the timely upregulated expression of PMP22 and MBP and the downregulated expression of Sox2 and Notch, thus blocking Schwann cells at the promyelinating stage and preventing myelination (Verrier et al., 2010, Pereira et al., 2010).

As Schwann cells transition from the immature/ promyelinating stage into the mature myelinating stage, they must cease proliferation. Krox20 has been show to block Schwann cell proliferation, by reducing their responsiveness to NRG1, and elevating the levels of the cell cycle inhibitor p27. At the immature Schwann cell stage, Schwann cells are also highly susceptible to TGF-β induced cell death. Both NRG1 and TGF-β have been shown to mediate Schwann cell proliferation and cell death via the JNK-cJun signalling pathway (Parkinson et al., 2001, Parkinson et al., 2004). Remarkably Krox20 was revealed to arrest Schwann cell proliferation and inhibit cell death by directly targeting the JNK-cJun signalling pathway and preventing its activation by NRG1 and TGF-β (Parkinson et al., 2004).

1.6 Negative myelin regulators during Schwann cell development and in the injury response.

The cross inhibitory effects exerted between positive and negative myelin regulators enables Schwann cells to transition back and forth between the immature and myelinating phenotype. Schwann cells thus demonstrate a high degree of plasticity, which is essential for nerve repair following injury [discussed in Section 1.7]. Negative myelin regulators are characterised by their ability to oppose promyelin signals, and promote Schwann cell dedifferentiation and myelin loss following nerve injury (Jessen and Mirsky, 2008). Over the last decade a range of myelin regulators such as cJun, Notch, Sox2, Sox4, Pax3, Id2, Egr1 (Krox24) and Egr3 have either been characterised as negative regulator of Schwann cell myelination, or shown to exhibit features of a negative regulator (Bartesaghi et al., 2015, Jessen and Mirsky, 2008).

1.6.1 cJun

The basic leucine zipper transcription factor cJun, is a key component of the AP1 transcription complex, where it forms heterodimers with JunD, JunB/c-Fos and activating transcription factor (ATF) family members (Davis, 2000). cJun is a

downstream effector of the cJun N-terminal kinase (JNK) MAPK signalling pathways. Activation of cJun via phosphorylation of the NH_2-terminal Serine 63 and 73 residues by JNK is important for many biological processes, including cell death and proliferation. Nonetheless, cJun is also able to exert functions independent of being phosphorylated. In Schwann cells the cJun protein has been show to exert many functional effects, which are discussed below (Parkinson et al., 2008).

cJun is highly expressed in immature Schwann cells, however as Schwann cells differentiate and myelinate, its expression is suppressed by the master transcriptional myelin regulator Krox20 (Parkinson et al., 2004, Parkinson et al., 2008). Downregulation of cJun was shown to be necessary for Schwann cell myelination, as enforced expression of both cJun and MAPK kinase 7 (MKK7); an upstream regulator of cJun, was shown to inhibit the induction of myelin proteins P_0 and periaxin in response to cAMP and Krox20 (Parkinson et al., 2008). After nerve injury, cJun was also shown to be re-expressed in Schwann cells, where it plays a central role in driving Schwann cell dedifferentiation and demyelination. Experiments carried out on cJun null mice, revealed that in the absence of cJun the rate of Schwann cell dedifferentiation and myelin loss was strongly delayed (Parkinson et al., 2008).

More recent experiments have revealed that the re-expression of cJun in Schwann cells after injury is also required for axonal survival and the reprogramming of Schwann cells into a repair cell that supports nerve regeneration (Fontana et al., 2012, Arthur-Farraj et al., 2012). Following nerve injury cJun null mice demonstrated a significant reduction in sensory and motor neuron survival after injury (Arthur-Farraj et al., 2012, Fontana et al., 2012). It was revealed that in the absence of cJun, the expression of genes required for axonal survival and growth were markedly reduced, these included GDNF (glial derived neurotrophic factor), Artn (artemin), BDNF (brain derived neurotropic factor) and LIF (leukemia inhibitory factor). *In vitro* experiments further confirmed that cJun was capable of directly regulating GDNF and Artn; the mRNA expression levels of these neurotrophic factors were dramatically increased in Schwann cells infected with an ectopic cJun expressing adenovirus. Moreover, administration of recombinant GDNF and Artn proteins to the injury site of cJun null mice for 28days improved motor neuron survival; supporting the notion that cJun regulates axonal survival following injury (Fontana et al., 2012).

cJun was also revealed to control the downregulation of myelin proteins and the upregulation of proteins associated with regeneration; N-cadherin, $P75^{NTR}$ and NCAM. In addition, cJun was shown to be required for Schwann cell myelin debris and lipid clearance, along with the formation of bands of Büngner and the promotion of axon growth. Consequently, in cJun null mice axon outgrowth was decreased and functional recovery were severely impaired even at 70 days post injury (Arthur-Faraj et al., 2012).

1.6.2 Sox2

Sox2 is a member of the SoxB1 subgroup of high mobility group box domain transcription factors, capable of acting as either a transcriptional activator or repressor depending on the partner protein that it co-operates with, when binding to a DNA domain (Kamachi and Kondoh, 2013). Sox2 is commonly known for its function in maintaining and inducing cellular pluripotency, through interacting with three other factors; Oct3/4, c-Myc and Krüppel-like factor 4 (KLF4) (Takahashi and Yamanaka, 2006).

In Schwann cells, Sox2 has been identified as a marker of the immature Schwann cell stage, it is highly expressed prior to the onset of myelination, but then rapidly declines as Schwann cells begin to myelinate. Following nerve injury Sox2 is again re-expressed (within 5 days), as mature Schwann cells dedifferentiate back to an immature state (Le et al., 2005a, Parkinson et al., 2008). *In vitro* studies have confirmed that Sox2 is suppressed upon the initiation of myelination by the master transcriptional regulator Krox20 (Parkinson et al., 2008). Furthermore, as seen in hypomorphic in $Egr2^{Lo/Lo}$ mice, failure to sufficiently upregulate Krox20 in Schwann cells results in maintenance/ failure to downregulate Sox2 (Le et al., 2005).

Further experiments revealed that Sox2 functions as a negative regulator of Schwann cell myelination *in vitro* (Le et al., 2005a). Adenoviral expression of Sox2 in Schwann cells was shown to prevent the upregulated mRNA expression of myelin associated genes such as Krox20, P_0, periaxin, in response to forskolin treatment. Sox2 lentiviral infection in Schwann cells also revealed that Sox2 blocks myelination, in Schwann cell/DRG neuronal co-cultures (Le et al., 2005a).

1.6.3 Notch

The Notch signalling pathway is highly conserved and plays a central role in regulating cellular communication, development, proliferation and differentiation. Notch is a transmembrane heterodimer receptor, composed of four different members (Notch 1 to 4), and is activated by transmembrane proteins; Delta and Jagged (Bray, 2006). Binding of the Notch ligand to the Notch receptor, triggers proteolytic cleavage events; ADAM 17 metalloprotease catalyses the first cleavage of the extracellular domain, γ-secretase then mediates the second cleavage at the intracellular domain consequently releasing the Notch intracellular domain (NICD) from the Notch transmembrane receptor. The NICD then translocates into the nucleus where it interacts with the DNA binding protein CLS (or RBPJ) and its co-activator Mastermind (MAM), activating the transcription of Notch targets such as Hairy and enhancer of split 1 (Hes 1) and Hes 5 (Bray, 2006).

Notch has been found to act at a number of stages during Schwann cell development where it exerts different functional roles. During Schwann cell development Notch drives the differentiation of Schwann cell precursors into immature Schwann cells, by enhancing the expression of the erbB2 receptor on Schwann cells and thus increasing SCP sensitivity to NRG1; this is required for SCP survival and Schwann cell lineage progression. At the immature Schwann cell stage Notch exerts a mitogenic effect and increases Schwann cell proliferation. Nonetheless, as Schwann cells begin to differentiate into the myelinating stage, Notch signalling is reduced (Woodhoo et al., 2009). This reduction in Notch signalling was shown to be mediated by Krox20, and proven to be important for the timely onset of myelination. Enforced Notch signalling in Schwann cells blocked the upregulated expression of myelin proteins in response to cAMP, in addition to blocking myelination in DRG/Schwann cells co-cultures (Woodhoo et al., 2009). *In vivo*, increased Notch signalling was shown to significantly decrease the number of myelinating Schwann cells at P2 and also decrease myelin thickness at P5 in the nerves of $P0^{Cre+}$;CALSL-NICD mice, in which NICD levels are elevated in Schwann cells. In contrast, inactivation of Notch signalling significantly increased Schwann cell myelin thickness in the nerves of $P0^{Cre+}$;$Notch1^{fl/fl}$ mice at P5 (Ibid).

Notch has also been identified to be upregulated in Schwann cells following nerve injury, where it acts to drives Schwann cell demyelination. After sciatic nerve injury

the rate of Schwann cell demyelination was shown to be dramatically reduced in RBPJ null mice; where Notch signalling is reduced. In contrast increased Notch signalling was shown to accelerate Schwann cell myelin loss, as well as the reduction in MBP expression. Together this data confirmed that Notch acts to negatively regulate myelination during Schwann development and after nerve injury (Woodhoo et al., 2009).

1.6.4 ERK

As discussed in Section 1.4, the ERK 1/ 2 signalling pathways can exert two distinct functional roles in a context dependent manner. Following peripheral nerve injury, ERK 1/2 is rapidly phosphorylated within 15 minutes, in Schwann cells in the distal nerve stump. Its expression thereafter increases, peaking at days 3 and 7 after injury (Napoli et al., 2012, Zrouri et al., 2004, Yamazaki et al., 2009). ERK 1/2 activation in this context, has been shown to play a central role in driving Schwann cell dedifferentiation, regulating the inflammatory response, and preventing Schwann cell remyelination (Harrisingh et al., 2004, Napoli et al., 2012). Studies carried out in Schwann cells *in vitro* and *in vivo* have used a regulatory protein system to analyse the function of ERK. ERK is activated via the Ras/Raf/MEK 1/2 signalling pathways, thus to drive ERK signalling *in vitro* Schwann cells were infected with a retrovirus encoding an inducible Raf fusion protein; which contains the kinase domain of Raf fused to an oestrogen receptor hormone binding domain (ER). In normal baseline condition the Raf-ER construct is inactive, however the addition of tamoxifen (an ER ligand) rapidly activates the Raf/ERK pathway (Harrisingh et al., 2004). Tamoxifen binds to the oestrogen receptor, displacing inhibitory large heat shock proteins and therefore reversing the steric hindrance (Littlewood et al., 1995). A similar method was used to study the functional effects of ERK *in vivo*. Transgenic mice carrying a tamoxifen inducible Raf-kinase/oestrogen receptor fusion protein, expressed under the control of the P_0 promoter (P0-RafTR) were generated. Only when tamoxifen is administrated to the mice, does the RafTR become activated, stimulating the ERK signalling pathway (Napoli et al., 2012).

Activation of Raf in cultured Schwann cells using the Raf-ER system prevented the upregulation of Oct6, Krox20, P0, periaxin and MBP in response to dibutyryl cAMP (db-cAMP), and drove Schwann cell dedifferentiation. Furthermore, the activation of

Raf in established myelinated Schwann cell/DRG co-cultures induced demyelination and the downregulation of P_0, MBP, PMP22 and perixain gene expression. To determine whether the effects mentioned above were mediated through the Raf/ERK pathway, experiments using established myelinated Schwann cell/DRG co-cultured treated with tamoxifen (to induce Raf signalling) in the presence or absence of an ERK signalling inhibitor U0126 were carried out. In the presence of U0126, Raf/ERK signalling failed to drive myelin fragmentation and Schwann cell dedifferentiation. These experiments thus suggest that sustained activation of the Raf/ERK pathway acts to negatively regulate Schwann cell differentiation and myelination.

Recent experiments carried out *in vivo* using P0-RafTR adult mice, have also confirmed that the Raf/ERK signalling pathways causes Schwann cells to downregulate the expression of myelin genes, degrade their myelin sheath and dedifferentiate back to an immature Schwann cell state. Moreover, P0-RafTR adult mice display severe defects in motor function at 10 days after tamoxifen injection. This suggested that sustained Raf/ERK in Schwann cells can cause neuropathological effects. Further *in vivo* experiments identified that the Raf-ERK signalling pathway is also sufficient to drive the inflammatory response in myelinated Schwann cells. P0-RafTR mice treated with tamoxifen showed complete blood nerve barrier breakdown within 5 days, and an influx of inflammatory cells into the nerve.

To determine the functional role of ERK 1/2 in driving Schwann cell demyelination and the inflammatory response after nerve injury, wild type (WT) mice which had undergone nerve crush injury were treated with a MEK 1/ 2 inhibitor PD032501. Animals treated with PD032501 showed delays in Schwann cells downregulating the expression of myelin associated genes and to dedifferentiate. In addition mice displayed an inhibited inflammatory response (Napoli et al., 2012). Together these studies shown that the Raf/ MEK/ ERK 1/2 signalling pathway is sufficient to drive Schwann cell demyelination and initiate an inflammatory response. Activation of this pathway following nerve injury is thus fundamental for Schwann cell plasticity and Wallerian degeneration [discussed in Section 1.7].

1.6.5 p38 MAPK

The p38 MAPK (mitogen-activated protein kinase) signalling pathway plays a central role in regulating cellular proliferation, apoptosis, differentiation and inflammation in response to environmental stimuli such as external stress, inflammatory cytokines or UV radiation. MAPK kinase 3 (MKK3) and MKK 6 pathway specifically activates p38 MAPK by dual phosphorylation at threonine^{180} and tyrosine^{182} residues (Cuenda and Rousseau, 2007). MKK4, an activator of the JNK pathways, has also been identified to specifically activate p38α. Independent of the MAPK kinase pathway, TAB1 (transforming growth factor β activated protein kinase 1 (TAK)-binding protein) can activate p38 MAPK; this method of activation involves TAB1 interacting with p38α, which in turn causes p38α to undergo auto-phosphorylation (Ge et al., 2002, Cuenda and Rousseau, 2007).

There are four isoforms of p38 kinase, p38α, p38β, p38ɣ (ERK6/ SAPK3) and p38δ (SAPK4), although all four isoforms are widely expressed, p38ɣ is most highly expressed in skeletal muscle, while p38δ is most highly expressed in the testis, pancreas, kidneys and small intestine (Yang et al., 2014b). Out of all four isoforms, p38α has been shown to be the most highly expressed and functional isoform in Schwann cells [discussed further in Chapter 5].

p38 MAPK is highly expressed in immature Schwann cells at E17 (in rats), its expression thereafter declines from P1, as immature Schwann cells differentiate into myelinating Schwann cells. This suggests that p38 MAPK is not involved in the regulation of myelin formation (Yang et al., 2012). Following nerve injury, p38 MAPK is rapidly activated within 15 minutes in the distal nerve segment, where it acts to drive Schwann cell demyelination (Zrouri et al., 2004, Yang et al., 2012). Studies by Yang et al. (2012) identified that blocking the re-activation of p38 MAPK following nerve injury, using a specific p38 MAPK inhibitor SB203580 delayed Schwann cell demyelination. At 3 days post injury no significant difference in the MBP positive area was observed in nerves treated with SB203580 compared to uncut nerves. In contrast, nerves not treated with SB203580 were reported to exhibit a significant 54% reduction in the MBP positive area. Further experiments by Yang et al. (2012) also showed that activation of the p38 MAPK signalling pathway in myelinated DRG/Schwann cell co-cultures, caused Schwann cell to demyelinate and reduce the expression of Krox20 and MAG, in the absence of trauma [discussed in more detail

in Chapter 5] (Yang et al., 2012). This study highlights that the p38 MAPK signalling pathway plays an important role in the injury response, and acts as a negative regulator of Schwann cell myelination.

1.6.6 Sox4

Sox4 is a class C Sox family transcription factor, recently identified to be expressed during the early postnatal stages of Schwann cell development (P2-P10). Its expression thereafter declines, but has been shown to be high in three different neuropathic mutant mouse models; Sh3tc2$^{-/-}$ (a model of CMT type-4C) (Arnaud et al., 2009), Pmp22$^{-/-}$ (a mouse model of CMT type-1A) and Lpin1$^{-/-}$ (Lpini encodes for the phosphatidate phosphatase enzyme, which is required for triacylglycerol biosynthesis) (Nadra et al., 2008). To elucidate the functional role of Sox4 in Schwann cells, Bartesaghi et al. (2015) generated mice that overexpressed Sox4 specifically within Schwann cells (Sox4 tg). While the Sox4 mRNA expression was shown to be elevated in the Sox4 tg mice into adulthood, increased Sox4 protein expression was only detected at postnatal day 0. Analysis of Sox4 tg nerves at P2 revealed that Sox4 overexpression reduced MBP, P_0, Krox20 and Oct6 expression and caused Schwann cell hypomyelination. Nonetheless, this effect was only temporary as myelin thickness returned to normal and the expression of MBP, P_0, Krox20 and Oct6 was shown to be upregulated by P5 (Bartesaghi et al., 2015). Schwann cells were reported to tightly regulate the protein expression of Sox4, by targeting it for degradation, thus making it impossible to significantly increase Sox4 protein levels. As Sox4 protein expression is elevated in Sh3tc2$^{-/-}$ mice and not degraded, these mice were crossed with Sox4 tg mice to generate Sh3tc2$^{-/-}$, Sox4 tg mice; this enabled the functional effects of Sox4 to be determined, by seeing whether increasing Sox4 expression would worsen the phenotype of sh3tc2$^{-/-}$ mice. Indeed Sh3tc2$^{-/-}$,Sox4 tg mice demonstrated a worse phenotype and increased g-ratio compared to Sh3tc2$^{-/-}$ mice (Bartesaghi et al., 2015). Together this data suggests that Sox4 is capable of negatively regulating Schwann cell myelination.

1.6.7 Pax3, Id2, Egr1 and Egr3

The transcription factors Pax3, Egr1 (Krox24) and Egr3 and the transcriptional regulator Id2 have also be identified to be expressed at the immature Schwann cell stage and/or to negatively regulate Schwann cell myelination (Jessen and Mirsky,

2008). Pax3 is a paired domain transcription factor expressed in Schwann cell precursors, and maintained in non-myelinating Schwann cells (Kioussi et al., 1995). Schwann cells infected with a Pax3 expressing adenovirus, showed that Pax3 regulates Schwann cell proliferation and survival, and is able to completely block the upregulated expression of myelin components; Oct6, P_0, MBP and periaxin in response to cAMP and Krox20 (Doddrell et al., 2012, Kioussi et al., 1995). Id2 is a member of the Id helix domain transcription factors and is expressed in immature Schwann cells, its expression thereafter declines as Schwann cells myelinate; where it is repressed by Krox20 in conjunction with Nab 1/2 (Mager et al., 2008). Following nerve injury, Id2 has been shown to be re-expressed (Le et al., 2005a). Depletion of Id2 by RNA interference in cultured Schwann cells, was shown to augment P_0 expression in response to cAMP, thus suggesting that Id2 may exert inhibitory effects on myelination (Mager et al., 2008). No further studies have been carried out to elucidate the functional role of Id2 in Schwann cells during development and after injury, this is therefore yet to be determined. Egr1 (Krox24) and Egr3 are zinc finger transcription factors, closely related to Krox20 and of which bind to the same DNA target sequences. In Schwann cells Egr1 and Krox20 are never co-expressed; Krox20 is solely expressed in myelinating Schwann cells, whereas Egr1 is expressed in Schwann cell precursors, immature Schwann cells and non-myelinating Schwann cells, it is also re-expressed in dedifferentiating Schwann cells within 24 hours of nerve injury (Topilko et al., 1997). As Krox20 and Egr1 are expressed at different times during Schwann cell development, it is suggests that they exert opposite functions (Topilko et al., 1997). Further studies have identified that Egr1 and Egr3 regulate the expression of $P75^{NTR}$ in Schwann cells, by binding directly to the $P75^{NTR}$ promoter and inducing transactivation (Gao et al., 2007). $P75^{NTR}$ is a low affinity neurotrophin receptor expressed in immature Schwann cells, and is important for regulating axon growth and survival, as well as axon myelin thickness (Gao et al., 2007, Jessen and Mirsky, 2008). Double knockout of Egr1 and Egr3 in mice was shown to reduce the expression of $P75^{NTR}$ by 82.5%, which consequently resulted in a decrease in myelin thickness (Gao et al., 2007). Surprisingly Krox20 expression was not altered in Egr1/Egr3 double knockout mice, which suggests that Krox20 and Egr1/Egr3 do not antagonise one another. Unfortunately to date no analysis has been carried out in Egr1/Egr3 double knockout mice to determine with the role of

Egr1/Egr3 in Schwann cell myelination during development or dedifferentiation after injury.

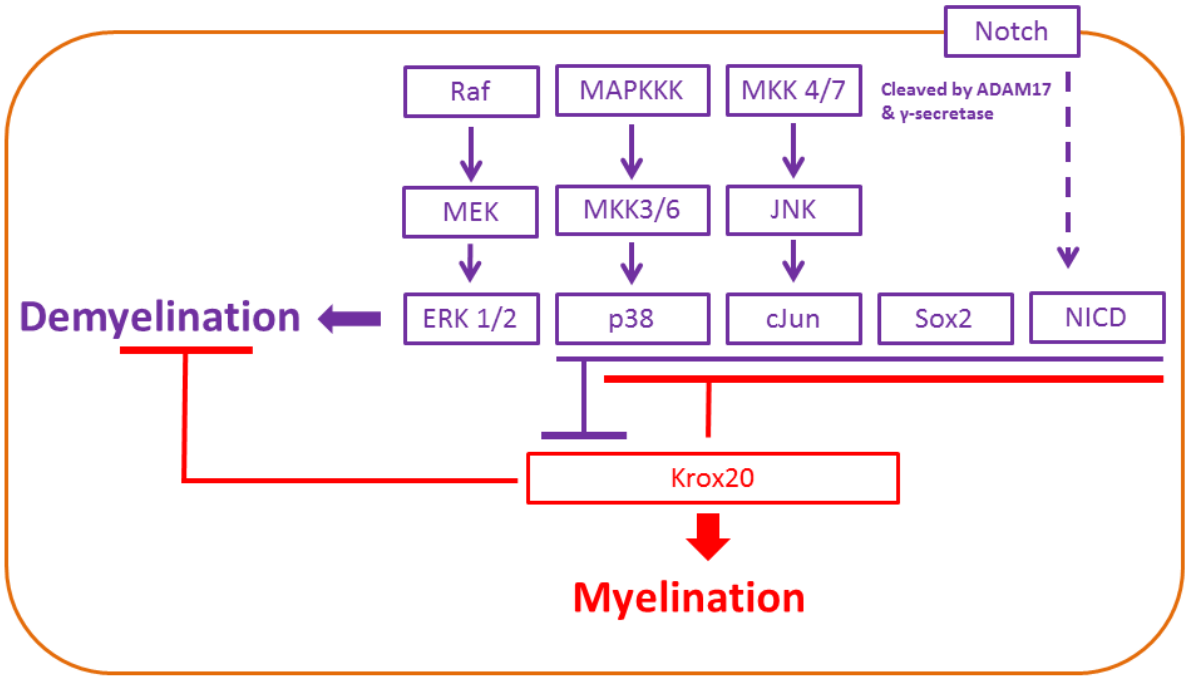

Figure 1. 6: Signals that drive demyelination. The proteins extracellular signal-regulated-kinase (ERK) 1/2, p38, cJun, Sox2 and NICD act to oppose Schwann cell myelination and drive demyelination. ERK 1/2 also functions as a positive regulator of myelination, during early Schwann cell development. ERK is activated by MAPK ERK Kinase (MEK) and Raf. p38 is phosphorylated by MAP kinase kinase 3/6 (MKK3/6) which is phosphorylated by the upstream MAPKK kinase (MAPKKK). cJun is upregulated and phosphorylated by cJun N-terminal kinase (JNK), which is downstream of MKK4/7. The regulator of Sox2 in Schwann cells remains unknown, however Notch1 has been suggested to regulate Sox2 in the PNS (Wakamatsu et al., 2004). The Notch receptor is cleaves by the metalloprotease ADAM17 and γ-secretase, enabling the release of the Notch intracellular domain (NICD). All four of these signalling proteins have been shown to block myelination during Schwann cell development by impairing Krox20 expression. Furthermore, following peripheral nerve injury the re-expression of these proteins have been confirmed to drive Schwann cell demyelination, by suppression Krox20 expression. Adapted from (Napoli et al., 2012, Yang et al., 2012, Le et al., 2005, Woodhoo et al., 2009).

1.7 Schwann cell demyelination, remyelination and repair

Schwann cells demonstrate remarkable plasticity, where they are able to freely transition between the immature Schwann cell (also known as a repair cell after injury) state and the mature myelinating state. This is a key feature in peripheral nerves following injury, making nerve repair in the PNS more effective than in the CNS (Stoll et al., 2002).

Damage to peripheral nerve triggers an injury related response, whereby nerves distal to the site of injury degenerate through a process termed Wallerian degeneration. The nerve proximal to the injury sites regenerate with the aid of Schwann cells, to re-innervate target tissues. Wallerian degeneration is a sequence of events that includes; axonal degeneration, Schwann cell demyelination, dedifferentiation and proliferation, axon/myelin debris clearance, breakdown of the blood nerve barrier and activation of the inflammatory response (Jessen and Mirsky, 2008).

During Wallerian degeneration, Schwann cells degrade their myelin and differentiate into repair/Büngner cells. Repair Schwann cells function to support axonal survival and growth through the production of trophic factors; to support axon guidance by forming bands of Büngner, as well as to promote functional recovery by remyelinating regenerating axons (Fontana et al., 2012, Arthur-Farraj et al., 2012). Repair Schwann cells also assist with myelin debris clearance through a process termed myelinophagy, which is essential to enable axon regrowth through the injury site [discussed in Chapter 4] (Gomez-Sanchez et al., 2015).

Successful nerve regeneration also requires activation of the inflammatory response. Repair Schwann cells secrete inflammatory cytokines such as tumour necrosis factor alpha (TNFα), interleukin 1β (IL1β), IL6, IL10 and leukaemia inhibitory factor (LIF), as well as chemoattractant proteins such as monocyte chemoattractant protein (MCP-1). The expression of these inflammatory cytokines and chemokines at the site of injury encourages the recruitment of immune cells, in particular macrophages, to assist with myelin/axon debris clearance and promote neurite outgrowth (Svennigsen and Dahlin, 2013).

The transition of Schwann cells into a repair competent phenotype is associated with the rapid suppression of key myelin regulators such as Krox20 and myelin proteins

such as P_0 and MBP. In addition, repair Schwann cells also rapidly upregulate the expression of negative myelin regulators; cJun, Sox2, Notch signalling, and activate the ERK 1/2 and p38 MAPK signalling pathways, all of which drive Schwann cell demyelination and dedifferentiation [see Section 1.6]. Repair cells display a similar protein expression profile to immature Schwann cells, as they re-express the cell adhesion (calcium independent) molecules L1 and neuronal cell adhesion molecule (NCAM), in addition to the tyrosine kinase neurotrophin receptor $p75^{NTR}$. Interestingly repair cells also re-express the cell adhesion (calcium dependent) molecule N-cadherin and membrane receptor integrin α1β1, but at much higher levels than that observed in immature Schwann cells (Jessen and Mirsky, 2008, Thornton et al., 2005, Arthur-Farraj et al., 2012). Following N-cadherin re-expression in repair cells, it re-localises to the cell-cell contact junction's where it mediates Schwann cell clustering and the formation of cord like structures, which help to guide axons across the nerve bridge. Once axons are fully regenerated, repair Schwann cells downregulate the expression of negative myelin regulators, redifferentiate back into myelinating Schwann cells and remyelinate axons; this process is essential for complete nerve repair [discussed in Chapter 4 and 5] [see Figure 1.7].

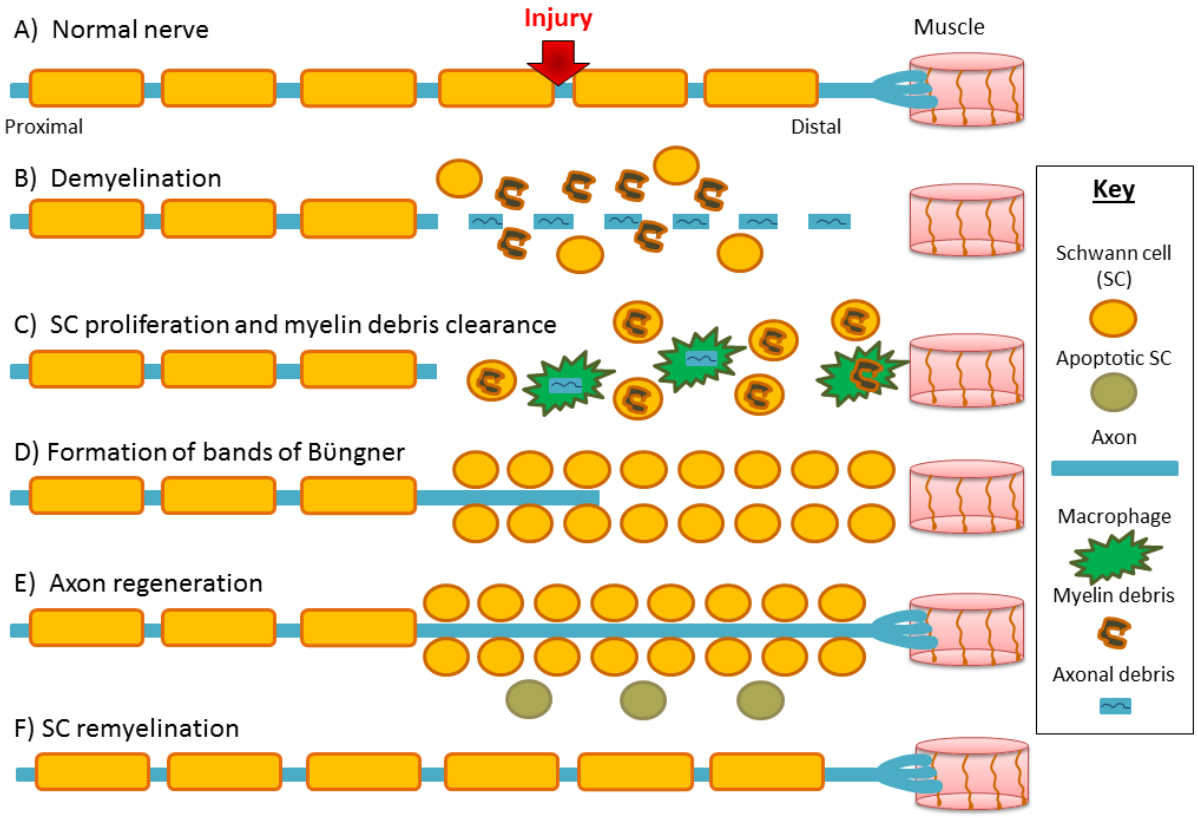

Figure 1. 7: Peripheral nerve regeneration. Following peripheral nerve injury (A) axons (blue) distal to the injury site degenerate and Schwann cells (SC) (yellow) demyelinate, unwrapping axons and dedifferentiate into an immature/repair Schwann cell in a process termed Wallerian degeneration (B). Repair Schwann cells then proliferate and produce chemokines that recruit macrophages to the injury site, where together they clear myelin debris (brown) (C). Repair Schwann cells then clump together forming bands of Büngner, which help to guide axons (D) back to their target tissue for re-innervation (E). Once axons are fully regenerated, repair Schwann cells redifferentiate backing into myelinating Schwann cells and remyelinate axons.

1.8 Differences between the PNS and CNS in nerve repair after injury

Unlike the PNS, the CNS is less effective in nerve repair and regeneration following injury. This is mainly due to the unfavourable environment within the CNS following injury, which consequently impedes regeneration of axons in the CNS.

In the PNS, Schwann cells and macrophages rapidly clear myelin debris, which contains the myelin associated inhibitor (MAI) MAG; known to inhibit axonal outgrowth and regeneration. In contrast, in CNS oligodendrocytes and microglia (macrophage like cells) are less effective at myelin debris clearing (Stoll et al., 2002). What makes matters worse is that myelin debris in the CNS is more enriched in MAI's than in the PNS. Known MAI's in the CNS include MAG, oligodendrocyte myelin glycoprotein (OMGp) and NogoA all of which bind to the same receptor complex, Nogo-66 receptor (Ngr)-$p75^{NTR}$ expressed on neurons; causing nerve growth cone collapse (Filbin, 2003). In the absence of the Ngr receptor, studies have revealed that OMGp fails to inhibit neurite outgrowth (Filbin, 2003).

Astrocytes in the CNS are also renowned for forming glial scars (comprised of astrocytes, microglial and oligodendrocyte precursors) after injury, which acts as a physical barrier blocking axonal regeneration and contains inhibitory molecules such chondroitin sulfate proteoglycans (CSPGs) (Huebner and Strittmatter, 2009). The expression of CSPGs is upregulated by astrocytes, they are the main inhibitory molecule expressed in the glial scar and act to inhibit axon regeneration. CSPGs may be membrane bound or secreted and include neurocan, vesican, brevican, phosphacan, aggrecan and NG2 (Huebner and Strittmatter, 2009).

1.9 Schwann cells in disease

Schwann cells have been shown to cause a range of diseases in human patients. Loss of healthy Schwann cell function commonly results in peripheral neuropathies, whereas Schwann cell transformation has been reported to cause the formation of Schwann cell derived tumours.

1.9.1 Peripheral neuropathies

Peripheral neuropathies are often caused by damage or disease affecting the peripheral nerves; they can be extremely disabling and even fatal. Direct peripheral nerve injuries which cause local damage or systemic illnesses such as diabetes (diabetic neuropathy), cancer and infection (leading to an increased inflammatory response, for e.g. as seen in Guillain-Barre syndrome) are common causes of peripheral neuropathies. Other causes included genetic mutations which directly affect the function of Schwann cells and/ or neurons.

1.9.1.1 Charcot-Marie-Tooth disease

Charcot-Marie-Tooth diseases (CMT), also referred to as hereditary motor and sensory neuropathy (HMSN) is the most common inherited peripheral neuropathy in patients, and has an incidence rate of 1:2500 individuals. CMT is caused by mutations in various genes responsible for the development of the peripheral nerves, currently over 40 gene mutations have been identified in Schwann cells and/or neurons. CMT disease has been classified into four groups, CMT1, CMT2, CMT3 and CMT4; these groups have then been further divided into subgroups due to the numerous different gene mutations [See Table 1 for subgroups of CMT1, CMT2, CMT3 and CMT4].

CMT type 1 (CMT1) is an autosomal dominant demyelinating neuropathy caused by Schwann cell defects. It has an early onset, occurring in the first or second decade of life and results in slow nerve conduction velocities. Nerve biopsies taken from patients with CMT1 often show signals of demyelination, remyelination, onion bulbing, and eventually axon loss (Suter and Scherer, 2003) . Reports estimated that approximately 80% of diagnosed CMT patients are classified as CMT1. Moreover CMT1 type A (CMT1A) is the most common form of CMT1, and is caused due to a 1.4Mb duplication of the PMP22 gene on chromosome 17p11.2 (Patzkó and Shy, 2011).

CMT type 2 is an autosomal dominant axonal neuropathy, patients tends to have normal nerve conduction velocities, but reduced amplitudes of the compound muscle action potential, with an onset occurrence mainly during adulthood. While clinical symptoms of CMT2 tend to overlap extensively with CMT1, CMT2 is often less disabling and causes less sensory loss [symptoms discussed in Chapter 3]. CMT2

type A (CMT2A) is the most common subtype of CMT2, accounting for approximately 20% of CMT2 cases (Patzkó and Shy, 2011). CMT2A is caused due to mutations in the mitofusin 2 genes (MFN2) located on chromosome 1p36 (Suter and Scherer, 2003, Patzkó and Shy, 2011).

CMT type 3, most commonly known as congenital hypomyelinating neuropathy (diagnosed at birth) or Dejerine-Sottas syndrome (diagnosed in infancy), can be either dominant or recessive. CMT3 is a demyelinating neuropathy classified by severe early onset in infants (Suter and Scherer, 2003).

CMT4 is an autosomal recessive severe axonal and demyelinating neuropathy, which is very rare. CMT4 is mostly associated with early onset, where is it often diagnosed at birth or during infancy (Suter and Scherer, 2003).

CMT subtypes	Genetic mutation	Onset
CMT1: Autosomal dominant demyelination neuropathy		
CMT type 1A	PMP22	Onset between 1st and 2nd decade.
CMT type 1B	P_0	Onset between 1st and 2nd decade.
CMT type 1C	SIMPLE	Onset between 1st and 2nd decade.
CMT type 1D/ 4E	Krox20/Egr2	Onset between 1st and 2nd decade
CMT type 1X	Cx32	Occurs at all ages.
CMT2: Autosomal dominant axonal neuropathy		
CMT type 2A	MFN2	Onset by 10 years of age.
CMT type 2B	RAB74	Onset between 2nd and 3rd decade.
CMT type 2C	Unknown	Onset between 2nd and 3rd decade.
CMT type 2D	GARS	Onset between 2nd and 3rd decade.
CMT type 2E	NEFL	Late onset (30 years of age +).
CMT3: Autosomal dominant/recessive severe demyelinating neuropathy		
DSS	AD (PMP22, MBP, Cx32, Krox20, NEFL) ; AR (MTMR2 and PRX)	Delayed motor development before 3 years of age.
CHN	AD (PMP22, MBP, Krox20); AR (Krox20)	Onset occurs at birth
CMT4: Autosomal recessive severe demyelinating neuropathy		
CMT type 4A	GDAP1	Early childhood onset.
CMT type 4B1	MTMR2	Early childhood onset
CMT type 4B2	MTMR13	Childhood onset
CMT type 4C	KIAA1985 (SH3TC2)	
CMT type 4D	NDRG1	Childhood onset
CMT type 4E	Krox20/Egr2	Infantile onset. Progression to wheelchair dependency
CMT type 4F	PRX	Childhood onset. Severe disability by 50 years of age
CMT type 4G	FGD4	
CMT type 4J	FIG4	

Table 1: An overview of Charcot-Marie-Tooth type 1, type 2, type 3 and type 4 subgroups and genes. AD, autosomal dominant; AR, autosomal recessive; DSS, Dejerine-Sottas syndrome; CHN, congenital hypomyelinating neuropathy; PMP22, peripheral myelin protein 22; P_0, myelin protein zero; SIMPLE, small integral membrane protein of late endosome; Egr2, Early growth response 2; Cx32, connexin32; MFN2, mitochondrial protein

mitsofusin 2; RAB7A, small GTPase late endosomal protein gene 7; GARS, glycyl-tRNA synthetase; NEFL, Neurofilament light polypeptide proteins; GDAP1, ganglioside induced differentiation associated protein 1; MTMR, Myotubularin related protein; SH3TC2, SH3 domain and tetratricopeptide repeats 2; NDRG1, N-myc downstream regulated gene 1; FGD4, FYVE, RhoGEF and PH domain containing 4; FIG4, FIG4 homologue. Adapted from (Suter and Scherer, 2003, Reilly and Shy, 2009)

1.9.2 Neurofibromatosis type 1

Neurofibromatosis type 1 (NF1), formally known as von Recklinghausen's disease, is an autosomal dominant disorder affecting roughly 1:3500 individuals worldwide (Jouhilahti et al., 2011). NF1 is a tumour condition caused by mutations (50% of which are sporadic) or loss of the NF1 gene that encodes the tumour suppressor proteins neurofibromin. Common clinical hallmarks of NF1 include numerous benign cutaneous or plexiform neurofibromas, café-au-lait macules (flat brown pigmented marks), learning difficulties and speech disorders (Jouhilahti et al., 2011). Neurofibromas are complex tumours comprising Schwann cells, axons, perineural cells, mast cells and blood vessels and are classified as either cutaneous or plexiform (Zhu et al., 2002, Jouhilahti et al., 2011).

Neurofibromas are thought to originate from Schwann cells, as studies have shown that mice with NF1 null Schwann cells develop neurofibromas (Zhu et al., 2002). Nonetheless, biallelic inactivation of NF1 ($NF1^{-/-}$) in Schwann cells alone is not permissive for plexiform neurofibroma formation; in order for plexiform neurofibromas to develop $NF1^{-/-}$ Schwann cells must also interact with surrounding heterozygous $NF1^{+/-}$ cells in a tumour microenvironment (Zhu et al., 2002). Further studies have also identified that $NF1^{+/-}$ mast cells are an essential component of the tumour microenvironment, permitting neurofibroma growth and maintenance; mice failed to develop plexiform neurofibomas when their $NF1^{+/-}$ bone marrow was replaced with $NF1^{+/+}$ bone marrow (Jouhilahti et al., 2011).

While adult myelinating Schwann cells depleted of $NF1^{-/-}$ do not form neurofibromas in an $NF1^{+/+}$ environment, they are able to form neurofibromas in an $NF1^{+/+}$ environment following nerve injury. It is suggested that nerve injury results in a protumorigenic microenvironment at the wounded site, which is permissive for tumours to form specifically at that region (Ribeiro et al., 2013).

1.9.3 Neurofibromatosis type 2

Neurofibromatosis type 2 (NF2) is an autosomal dominant disorder, that affects approximately 1:25000-30000 births (Hanemann, 2008). NF2 results from mutations in the NF2 gene on chromosome 22q 11.2, which encodes for the tumour suppressor protein Merlin (Moesin/ezrin/radixin like protein); as a result Merlin function is lost (Ferner, 2007). Merlin is thought to interact with multiple intracellular

signalling pathways such as PI3K-Akt, to maintain growth suppression. Thus in the absence of merlin unregulated cellular proliferation occurs (Ferner, 2007).

NF2 results in the formation of many benign tumours; these include schwannomas, meningiomas and ependymomas (detailed below), as well as retinal hamartomas, tumours of the eye and lens opacities (Hanemann, 2008, Ferner, 2007). Schwannomas are pure Schwann cells derived tumours that rarely become malignant and often occur in the vestibular 8th cranial nerve (which is the most frequent, resulting in hearing loss, tinnitus and vertigo), the spinal roots and along the peripheral nerves (Hanemann, 2008). Meningiomas are encapsulated tumours which are most often benign (90% of the time), they occur intracranially or within the spinal canal and arise from arachnoid "cap" (meningothelial) cells that form membranous layers that cover the brain and the spinal cord (Rockhill et al., 2007). Ependymoma account for 2-5% of intracranial tumours and arise from ependymal cells (Hanemann, 2008). These cells line the ventricles of the brain and the central canal of the spinal cord, where they are responsible for the production of cerebral spinal fluid (CSF) (O'Shaughnessy and Bussières, 2006).

1.10 Studying Schwann cell biology *in vivo*

To study Schwann cell biology in vivo, a range of molecular techniques are available which allow for specific genetic modifications. Methods to achieve insertion, deletion or alteration of specific genes include lentiviral vector transfections which allow for the introduction of new genes, lentiviral gene transfer vectors expressing short-hairpin RNA which target specific genes for the deletion (Cotter et al., 2010), the inducible tetracycline-dependent regulatory (tet)-on and tet-off system (Gossen and Bujard, 1992), as well as recombineering which is based on homologous recombination in embryonic stem cells (Sharan et al., 2009). Nonetheless, one of the most commonly used techniques in Schwann cell biology is the Cre/LoxP system, a technique which allows for the quick and precise ablation or modifications of genes in any tissue at any definite time (Sauer, 1998).

1.10.1 Cre-LoxP mediated recombination

The Cre-LoxP system is a DNA recombination tool, widely used to specifically target the expression of genes or carry out DNA deletions or insertions at specific DNA sites. When combined to a specific promoter to drive Cre expression, the Cre-LoxP system can induce conditional gene modification in a particular tissue or cell type, and at specific developmental time-points (Sauer, 1998). It is therefore the most commonly used tool for studying the functional role of particular genes in Schwann cells during development and after nerve injury, in order to understand how alterations in their expression levels may contribute to health or disease *in vivo.*

The Cre recombinase protein is an enzyme found in bacteriophage P1 that mediates site specific recombination, at a 34 base pair site called loxP. The loxP sites consist of two 13bp inverted repeats flanking an 8bp asymmetric core sequence. When two loxP sites are placed either side of an endogenous target DNA sequence, Cre is able to mediate recombination and thus the excision of the targeted DNA sequence; this particular method can be used to conditionally knockout a particular gene [see Figure 1.8] (Sauer, 1998). Alternatively this method can also be used to switch on the expression of a particular gene at a specific time-point. This is beneficial for turning on a gene that may cause morbidity or reduced viability in the transgenic mouse line. In this second case, a STOP cassette floxed by loxP sites could be inserted between the gene of interest and the promoter, thus only upon Cre mediated excision of the STOP signal will the gene be expressed [See Figure 1.9]. (Sauer,1998). A reporter gene such as green fluorescent protein (GFP) can be added either after the second loxP site (when wanting to achieve gene deletion) or after the target gene (when wanting to activate gene expression), this will only be expressed upon Cre-mediated recombination. Cre recombinases can be supplied to a system by either crossing a mouse stain containing the Cre recombinase gene (usually under the control of a specific promoter) *in vivo*, or by infection with a virus containing the gene *in vitro*.

Cre expression can be selectively enforced in Schwann cells when regulated under the control of a Schwan cell specific promotor element. The most common promoter used is the P_0 promoter, which has been shown to successfully drive the expression of Cre. The P_0 Cre transgene (as known as mP_0TOTA Cre) contains the complete mouse P_0 gene (all exons and introns), with 6 kilobases (6 kb) of promoter and the

natural polyadenylation site, which has a mutated ATG start sequence that has been substituted with the Cre recombinase enzyme (Feltri et al., 1999a). As P_0 is expressed in Schwann cells from approximately E13.5-15, Cre driven recombination also occurs at this time. The desert hedgehog (DHH) promoter sequence can also be used to drive Cre (DHH Cre), this gene is expressed in Schwann cell precursors from E12 and therefore causes Cre-recombination at earlier time-points than P_0-Cre (Lindeboom et al., 2003, Jaegle et al., 2003). Alternatively, the 3.9kb periostin promoter sequence (Postn Cre) can be used in order to drive Cre recombination in Schwann cell precursors at an even earlier time-point, E11 (Lindsley et al., 2007). Nonetheless unlike P_0, DHH and periostin are not specific to Schwann cells and are expressed in other cells types. DHH is expressed in the skin of the snout and parts of the vasculature (blood vessel wall endothelial cells) at E12 and in Sertoli cells found in the testis at postnatal day 15 (P15) (Lindeboom et al., 2003). Periostin is found in endocardial cushion cells, and suggested to cause recombination in some PNS neurons.

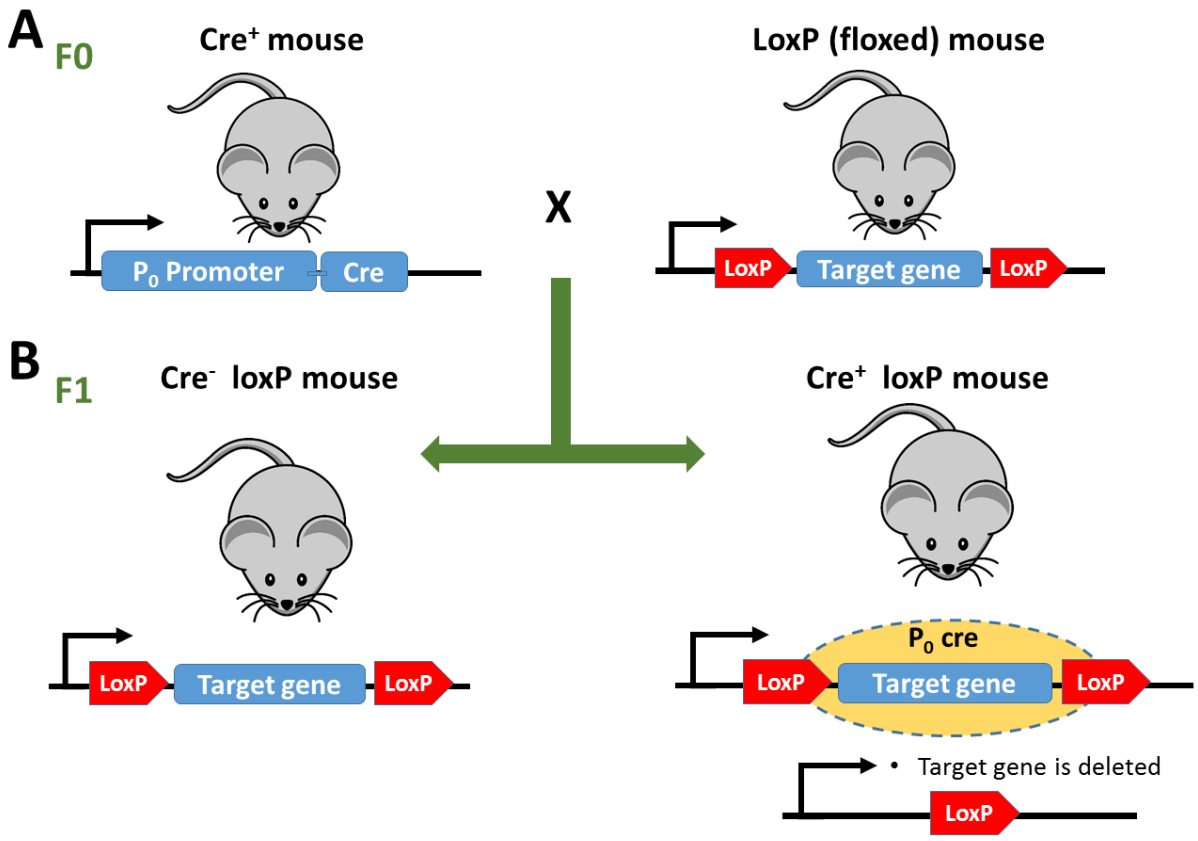

Figure 1. 8: Cre-mediated excisive recombination to achieve target gene deletion in mice. In the F_0 generation mice carrying the Cre transgene (Cre^+) are crossed with mice carrying the target gene, flanked by two loxP sites. In the F_1 generation, Cre-loxP mediated gene excision will occur in mice positive for the Cre transgene and therefore gene function will be altered. In mice negative for the Cre transgene, the loxP flanked target gene will not be excised and therefore the gene function will remain unaltered.

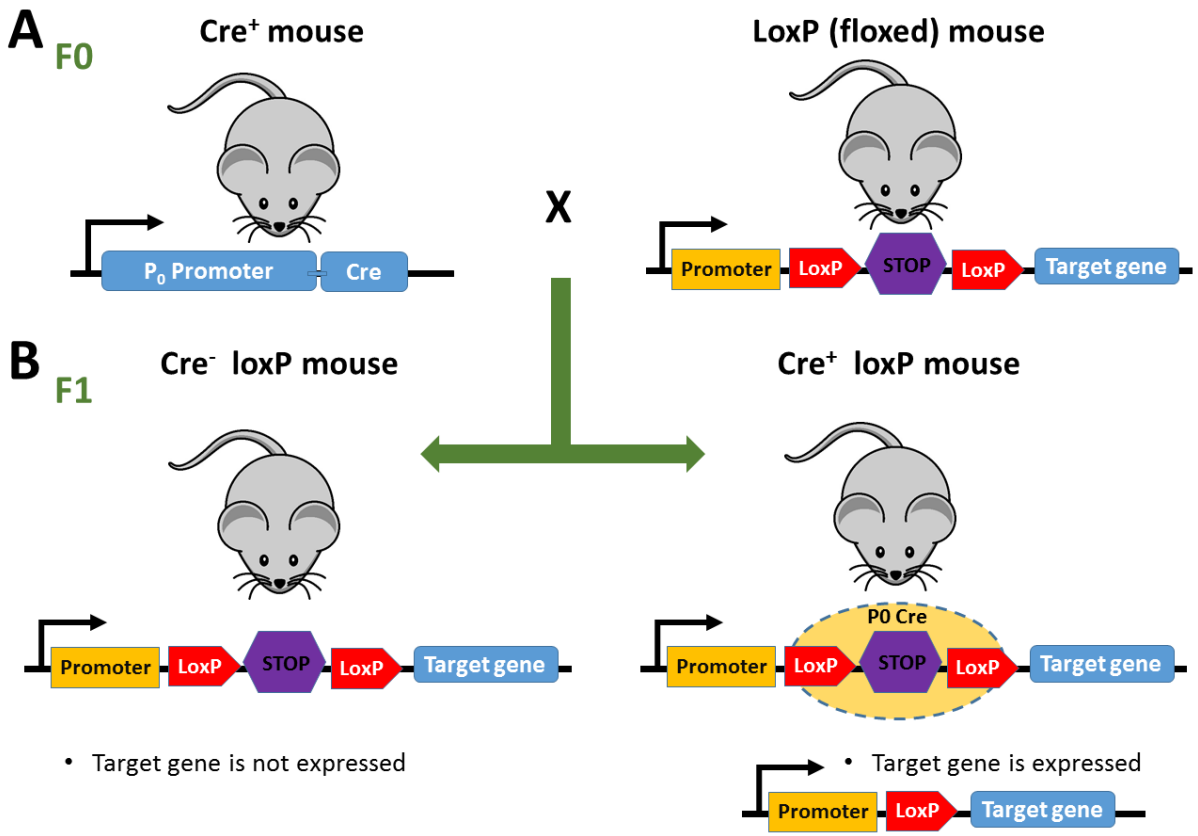

Figure 1. 9: Cre-mediated excisive recombination to achieve target gene expression in mice. In the F_0 generation mice carrying the Cre transgene (Cre^+) are crossed with mice carrying the stop cassette, flanked by two loxP sites. In the F_1 generation, Cre-loxP mediated excision of the STOP cassette will occur in mice positive for the Cre transgene and the target gene will be expressed. In mice negative for the Cre transgene, the loxP flanked STOP cassette will not be excised and therefore the target gene will not be expressed.

1.10.2 The use of P_0 Cre-loxP recombination in the generation of Sox2 overexpressing mice

Gene trapping is an approach used to introduce insertional mutations across the mammalian genome. The method requires mutation to be inserting into an intronic or coding region of genomic DNA, using a specific gene trap vector containing a reporter gene (to identify cell lines where the vector has successfully be inserted). Trap vectors are composed of DNA sequences derived from cDNA or genomic DNA of the trap locus. The Rosa26 gene trap cassette containing a β-galactosidase reporter gene inserted into the Rosa26 locus where it has been shown to be ubiquitously expressed across a wide range of mouse tissue types, including the brain, bone marrow, spleen and muscle from embryonic development (Zambrowicz et al., 1997). The Rosa26 locus (located on mouse chromosome 6) and the Rosa26 gene trap cassette are therefore commonly used for the integration of transgenes. Furthermore, gene insertions into the Rosa26 locus do not cause any adverse effects (for e.g. animal viability or cell phenotype is not affected) and the inserted gene is not subjected to gene silencing (Zambrowicz et al., 1997).

In order to achieve Sox2 overexpression at the Rosa26 locus, a conditional allele of the Rosa26 locus was created by Lu et al. (2010) and referred to as Rosa26R-Sox2-IRES-GFP [See Figure 1.10]. To prevent Sox2 from being expressed under normal conditions by the Rosa26 locus, a neo-STOP sequences flanked by two loxP sites was inserted upstream of the Sox2 gene. Only upon removal of the neo-STOP sequence by Cre-loxP mediated recombination will Sox2 be expressed.

The pRosa26 promoter expresses the gene of interest at low levels, therefore to increase the levels of Sox2 transcription factor after recombination, a synthetic cytomegalovirus early enhancer/ chicken beta actin (CAG) promoter was inserted upstream of the Sox2 gene. The CAG promoter is a hybrid promoter generated by combining the human CMV immediate-early enhancer/promoter (hCMV) and the chicken β-actin promoter, in order to drive gene expression at high levels (Garg et al., 2004).

The human CMV immediate-early enhancer/promoter (hCMV) is able to increase the target gene expression, however in the presence of interferon γ (IFNγ), gene expression levels are reduced. Studies have also shown that the activity of hCMV

promoter varies in different tissues and cell lines, for e.g. it is not transcriptionally active in most cells in the mouse skin (Garg et al., 2004). The chicken β-actin promoter is highly active across a wide range of cell types and modified versions were initially used to efficiently drive the expression of interleukin 5 (IL5) in BMT10 cells (Jun-ichi et al., 1989). When these two individual promoters are coupled together (CAG promoter), they have been shown to be more effective at promoting higher levels of transgene expression, than when used separately. Furthermore, the CAG promoter has been shown to be more effective at driving gene expression across many more cell and tissue types (Alexopoulou et al., 2008, Garg et al., 2004).

In order to easily identify the cells in which Cre-mediated recombination has taken place, an IRES-EGFP (internal ribosomal entry site-enhanced green fluorescent protein) cassette was inserted downstream of the Sox2 gene. Thus in all cells where recombination has taken place and Sox2 is expressed, GFP will also be expressed.

In order to obtain transgenic mice that conditionally overexpress Sox2, mice homozygous for the Rosa26R-Sox2-IRES-EGFP allele were crossed with mice carrying the mTOTA-P_0 Cre transgene [described in section 1.10.1]. P_0 is expressed in Schwann cells at embryonic day 13.5-15 and therefore recombination should occur at this time-point (Feltri et al., 1999a, Lu et al., 2010a). The expected outcome of this cross is that all of the offspring will be heterozygous for the Sox2-IRES-EGFP transgene, with 50% being P_0 Cre positive ($^+$) or P_0 Cre negative ($^-$). In order to generate mice that are also homozygous for the Sox2-IRES-EGFP transgene and Cre^+ / Cre^-, selected heterozygous Sox2-IRES-EGFP Cre^+ mice were then crossed back with homozygous Sox2-IRES-EGFP mice [See Figure 1.11].

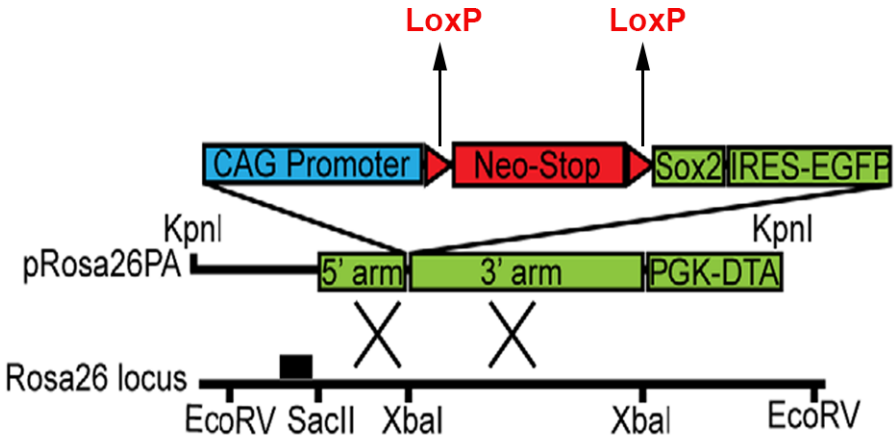

Figure 1. 10 schematic diagram of the Rosa26R-Sox2-IRES-EGFP allele targeting scheme. The Rosa26R-Sox2-IRES-EGFP allele was created by inserting a CAG–loxP-STOP-loxP-Sox2-IRESGFP-polyA cassette into an accepting Rosa-targeting plasmid. GFP is only detected upon Cre mediated recombination and removal of the Neo stop sequence is floxed by the loxP sides. Adapted from (Lu et al., 2010a).

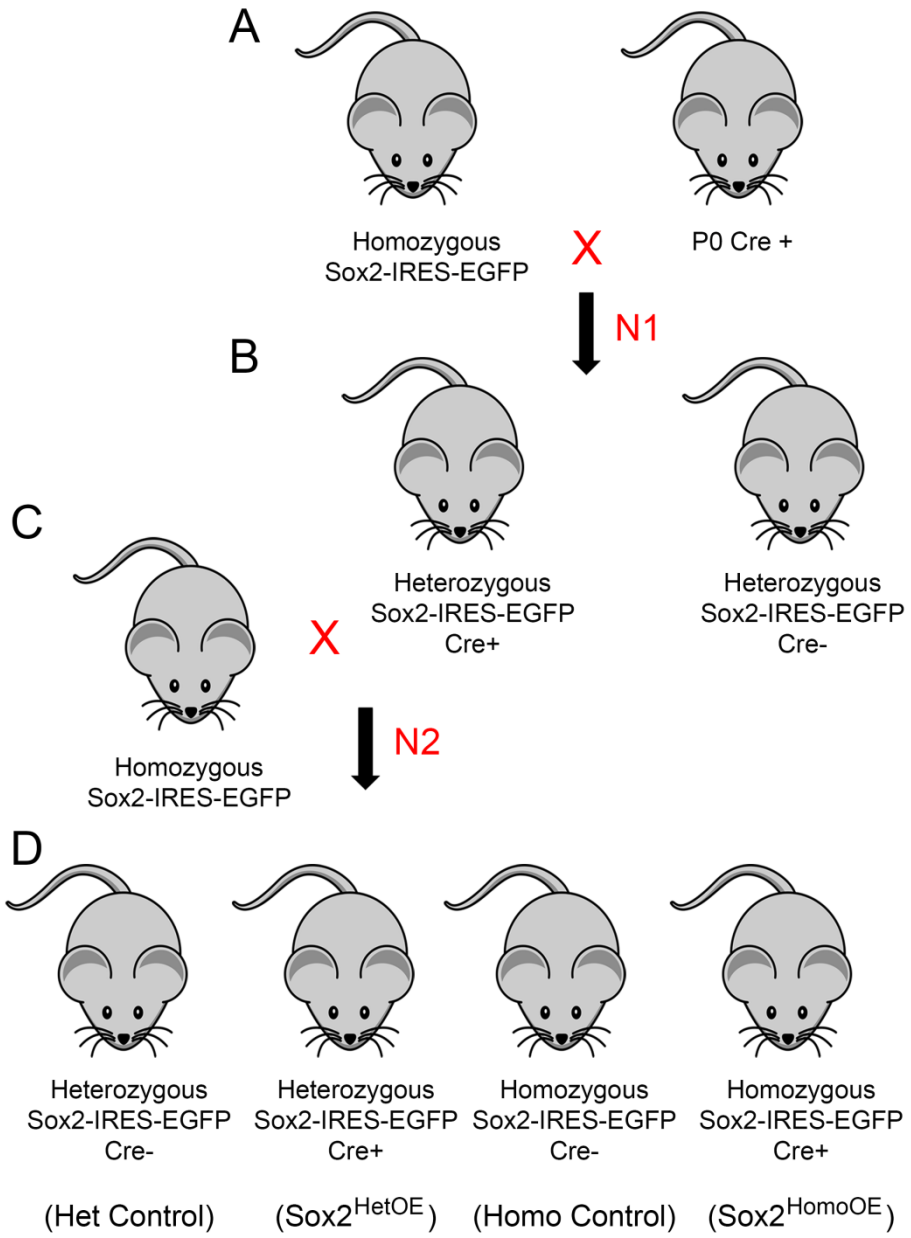

Figure 1. 11 Mouse breeding scheme to generate Sox2 overexpressing mice. Diagram shows the sequences of crosses that were made with transgenic mice during this research. Homozygous Sox2-IRES-EGFP mice were crossed with P_0 Cre^+ mice in order to create generation N1 (A). The resulting offspring were either heterozygous Sox2-IRES-EGFP Cre^- or heterozygous Sox2-IRES-EGFP Cre^+ (B). Heterozygous Sox2-IRES-EGFP Cre^+ mice were then crossed back with homozygous Sox2-IRES-EGFP to generate N2 (C). The resulting offspring were either heterozygous Sox2-IRES-EGFP Cre^- (Het control), heterozygous Sox2-IRES-EGFP Cre^+ ($Sox2^{HetOE}$), homozygous Sox2-IRES-EGFP Cre^- (Homo control) or homozygous Sox2-IRES-EGFP Cre^+ ($Sox2^{HomoOE}$) (D).

1.10.3 The use of P0 Cre-LoxP recombination in the generation of p38α knockout mice.

To obtain Schwann cell specific p38α conditional knockout mice, mice that are homozygous for the p38α transgene, containing loxP sites surrounding exon 2 and 3 [see Figure 1.12], were crossed with mice containing the mTOTA-P_0 Cre transgene [described in section 1.10.1] and are homozygous for the p38α transgene. As discussed in section 1.10.1, recognition of the loxP sites by Cre will result in Cre recombination and thus removal of exons 2 and 3 from the p38α transgene. As reported by Heinrichsdorff et al. (2008), removal of exons 2 and 3 results in p38α becoming inactivated and not being expressed (Heinrichsdorff et al., 2008).

The resulting offspring from the cross mentioned above will be either heterozygous for the p38α transgene and Cre^- or heterozygous for the p38α transgene and Cre^+. In order of obtain mice that are homozygous for the p38α transgene and Cre^+ (conditional p38α knockout), an additional cross is required: mice heterozygous for the p38α transgene and Cre^+ are backcrossed with mice homozygous for the p38α transgene. The resulting offspring from this final cross will be one of 4 genotypes; heterozygous for the p38α transgene and Cre^-, heterozygous for the p38α transgene and Cre^+, homozygous for the p38α transgene and Cre^- (controls) or homozygous for the p38α transgene and Cre^+ (p38α knockout) [See Figure 1.13].

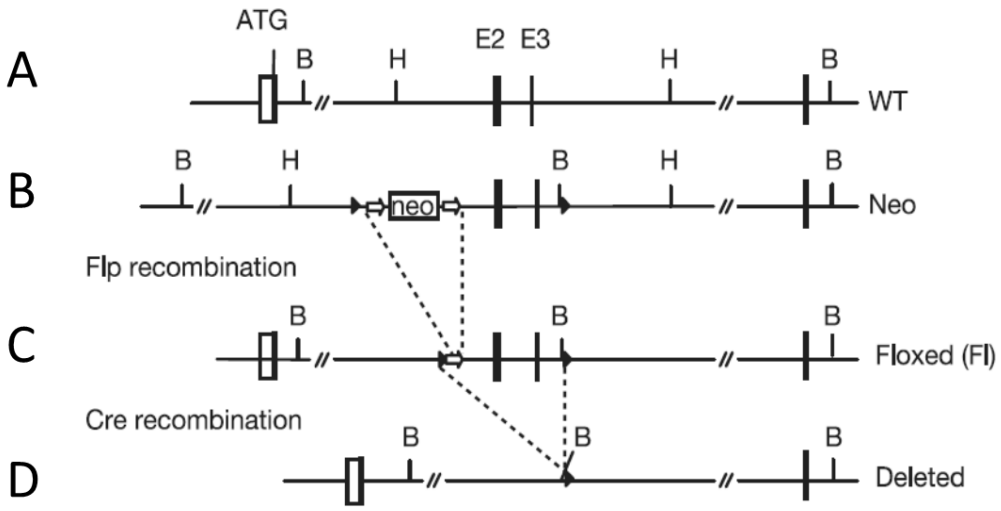

Figure 1. 12: A schematic description of the p38α targeting strategy to generate mice with loxP-flanked p38α alleles. (A) p38α wild type allele containing exons 2 and 3 and the ATP binding site of the kinase domain. (B) p38α transgene containing an inserted neomycin (Neo) resistant cassette, as a selectable marker. The Neo cassette is flanked by two short flippase (FLP) recognition target (Frt) sites: white arrows indicate Frt sites; black arrows indicate loxP sites. (C) Using FLP target recombination the Frt flanked Neo cassette was removed from the p38α transgene. (D) Cre recombination in $p38\alpha^{fl/fl}$:P_0Cre^+ mice [see Figure 1.13] results in deletion of exon 2 and 3 and the generation of a p38α conditional knockout allele. BamHI (B); HindIII (H) restriction endonucleases. Adapted from (Heinrichsdorff et al., 2008).

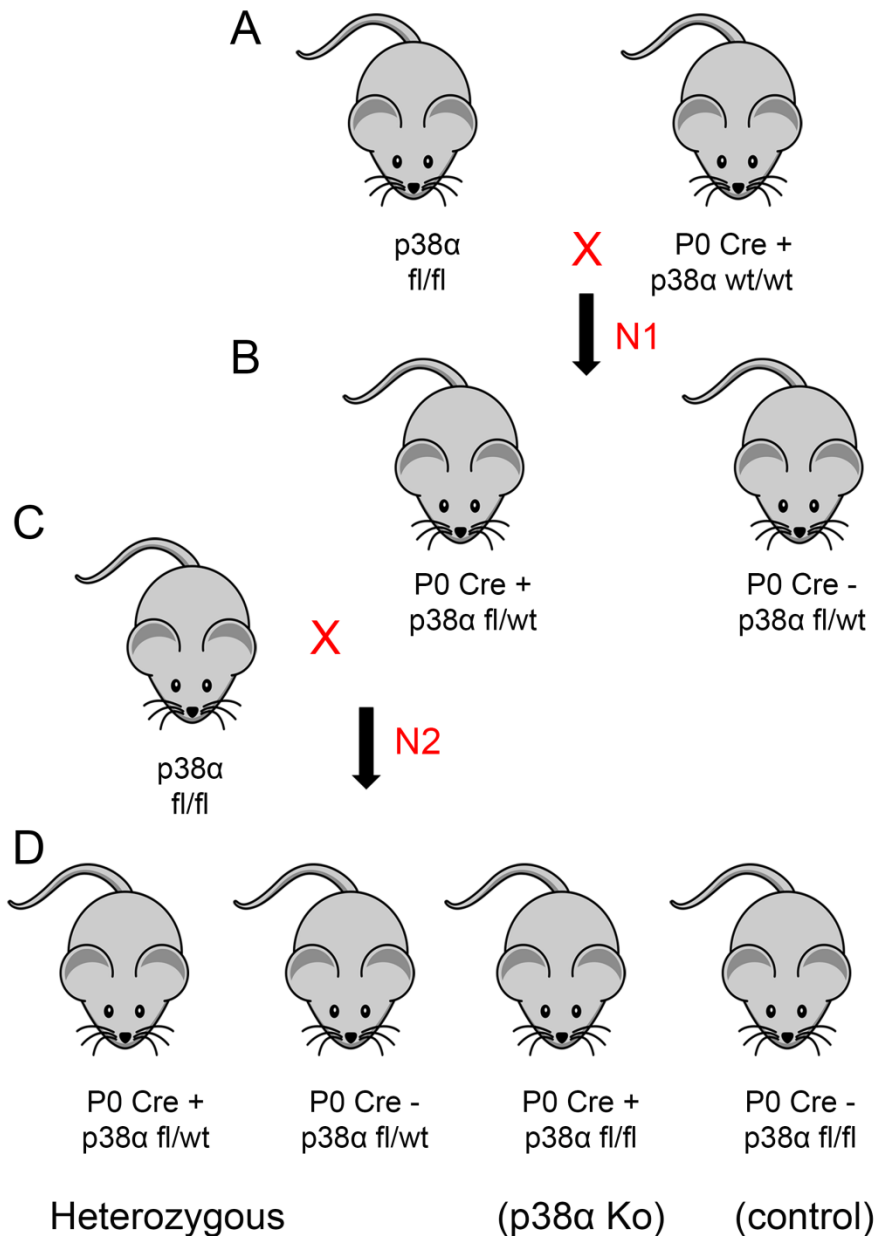

Figure 1. 13: Mouse breeding scheme to generate p38α knockout mice. Diagram shows the sequences of crosses that were made with transgenic mice during this research. (A) p38α flox/flox (fl/fl) mice were crossed with P_0 Cre^+ wild type/wild type mice in order to create generation N1. (B) The resulting offspring were either heterozygous p38α flox/wild type Cre^- or heterozygous p38α flox/wild type Cre^+. (C) In order to generate N2, the selected p38α flox/wild type Cre^+ offspring were then crossed with p38α flox/flox mice. (D) This resulted in p38α flox/flox Cre^+ (p38α conditional knockout mice) offspring which are born at an expected Mendelain ratio of 3:1. p38α flox/flox Cre^- were used as controls in this study.

Chapter 2 Materials and Methods

2.1 Cell culture

2.1.1. Primary Rat Schwann cell preparation

Pure rat Schwann cell cultures were prepared, through serum purification (Brockes et al., 1979). The sciatic nerve and brachial plexus were removed from post-natal day 3 (P3) rodents and placed in L15 medium [Sigma]. Having removed the epineurial sheath, the nerves were placed into a digestion solution containing 50:50 2.5mg/ml trypsin [Invitrogen] and 4mg/ml collagenase [Worthington enzymes, Lakewood, USA] (both dissolved in Earle's balanced salt solution [Sigma]). Nerves were incubated for 45 minutes at 37°C, 5% CO_2 in a Hera cell 240 incubator [Heraeus] and then triturated up to 10 times with a blue pipette tip (maximum volume 1ml) and 20 times with a yellow tip (maximum volume 200µl). The cell suspension was centrifuged at 200xg for 5 minutes in a 5702 centrifuge [Eppendorf, Cambridge, UK], the pellet was resuspended in 2ml of 10% FCS/DMEM containing 10^{-5}M of the anti-mitotic cytosine arabinoside C (Ara C) [Sigma] and the cells plated on to pre-coated 35mm dished [Greiner, Stonehouse, UK] [Table 2.1]. Plates were coated with 100µg/ml poly-L-lysine (PLL) [Sigma, Poole, UK] diluted in 1x phosphate buffered saline (PBS) for 60 minutes at room temperature, washed with 1x PBS and then coated with 4µg/ml laminin [Invitrogen, Paisley, UK] diluted in DMEM for 60 minutes at room temperature (note, the cells were plated without washing the laminin). Cells were incubated for 3 days at 37°C, 5% CO_2 and then changed into growth medium [Table 2.1]. The medium on the cells was changed every 3 days.

Rat Schwann cells	
1g/L	Glucose DMEM
3%	Fetal bovine serum
2µM	forskolin
10ng/ml	Neuregulin
500U/ml	P/S

Table 2. 1: Growth medium used for Schwann cells. Lists the culture medium used to expand primary cells used in this study. The Dulbecco's Modified Eagle Medium (DMEM), serum, growth factors and antibiotics used are all listed. The bottom row indicates the proteins used to coat cell culture plates.

2.1.2. Passaging Cells

Growth medium was removed and cells were washed in PBS, then incubated with trypsin/ethylenediamine tetraacetic acid (EDTA) solution [PAA] (0.5mg/ml trypsin and 0.22mg/ml EDTA dissolved in 1x PBS) for 2 minutes at 37°C. The volume of trypsin/EDTA used for each culture dish is listed in Table 2.2. Approximately 5ml of 10%FCS/DMEM solution was added to suspended cells and centrifuged at 200xg for 5 minutes. The cell pellet was resuspended in growth medium and replated onto fresh PLL/laminin coated plates.

2.2. Cell culture experiments

2.2.1. Plating cells

Cells were cultured for immunocytochemistry and western blotting experiments. For immunocytochemistry, 5000 rat Schwann cells were plated onto coated coverslips in the 15µl droplet onto 100µg/ml poly-D-lysine [Sigma] (diluted in water, 2 hours at room temperature) and 20µg/ml laminin (diluted in defined medium, 30 minutes at 37°C) coated 13mm glass coverslips [Scientific laboratory supplies (SLS), Nottingham, UK] placed in a 24 well plate. After 2 hours each well was topped up with 500µl of defined medium (DM) [For DM composition see Table 2.3].

To harvest cells for protein experiments, 100,000 cells were plated per well of a 6 well plate in growth medium. After cells had grown to confluency, medium was removed and replaced with 3ml/well defined medium. For some experiments 300,000 rat Schwann cells were plated onto 90mm cell culture dishes instead. All culture dishes were coated as required [Table 2.2].

Culture dish	Growth medium volume	Trypsin/EDTA volume
35mm	2ml	0.5ml
90mm	10ml	1.5ml
6 well plate	3ml per well	1ml per well

Table 2. 2: Volume of growth medium and trypsination solution. The volume of solution needed for each size cell culture plate. All plates supplied by Greiner.

Components	Concentration
Hams F12 Medium [Invitrogen]	48%
DMEM Medium [Invitrogen]	48%
Bovine serum albumin (BSA) [Sigma]	350µg/ml
Putrescine [Sigma]	16µg/ml
Transferrin [Sigma]	100µg/ml
Thyroxine (T4) [Sigma]	400ng/ml
Progesterone [Sigma]	60ng/ml
Dexamethasone [Sigma]	38ng/ml
Glutamine [Sigma]	2mM
Penicillin /Streptomycin (P/S) [Invitrogen]	100 U/ ml
Selenium [Sigma]	160ng/ml
Insulin [Sigma]	10^{-6} M

Table 2. 3: Composition of defined medium. Table lists all the components of the defined medium used in this study and their respective final concentration**.**

2.2.2. Defined medium (DM)

The composition of defined medium, which is designed to maintain Schwann cells in a quiescent non-proliferative state, is detailed in Table 2.3 (Jessen et al., 1994, Parkinson et al., 2008). All cells were incubated for 1 hour in defined medium before adenoviral infection. Basal conditions were determined by incubation of cells for 48 hours in DM alone.

2.2.3. Adenoviral infections

Rat Schwann cells were infected with 4µl/ml adenovirus (equivalent to a multiplicity of infection of ~1500) in DM supplemented with 2µM forskolin [For the list of all adenoviruses used in this study see Table 2.4] (Parkinson et al., 2001). After 24 hours, infected media was aspirated and replaced with fresh DM (with no forskolin) for a further 24 hour incubation before fixing or lysing of cells for analysis.

Adenovirus	Expressed protein	Tag	GFP	Backbone	Source [Reference]
Ad GFP	Green fluorescent protein (GFP) alone.	-	Yes	AdEasy-1	Gift from Prof. J Milbrandt [Washington Uni.School of Medicine, St Louis, USA] (Nagarajan et al., 2001)
Ad Sox2	Sox2	Flag	Yes	AdEasy-1	Gift from Prof. J. Milbrandt. (Le et al., 2005a)

Table 2. 4: Adenoviral vectors. Table lists the adenovirus names, expressed protein, antibody tag (Flag or none), co-expression of green fluorescent protein (GFP), adenoviral backbone, vector source and original reference. Ad Easy-1 is based on the adenovirus serotype 5 (Ad5) with deletions in E1 and E3 viral regions to render them replication incompetent (He et al., 1998).

2.3. Transgenic animals

2.3.1. Transgenic animal crossing

Transgenic mouse breeding and experiments were carried out according to Home Office regulations under the UK Animals (Scientific Procedures) Act 1986. Ethical approval for all experiments was granted by Plymouth University Animal Welfare and Ethical Review Board (AWERB).

To identify the effect of Sox2 overexpression in Schwann cells *in vivo,* we crossed homozygous Rosa26R-Sox2-IRES-GFP mice which were a gift from Dr Mark Onaitis (Duke University Medical Centre, Durham, USA) (Lu et al., 2010b) with P0-CRE (mTOTA P0-Cre) mice (Feltri et al., 1999). This allowed us to generated heterozygous Rosa26-Sox2-IRES-EGFP CRE positive $^{(+)}$ and CRE negative $^{(-)}$ offspring. Heterozygous Rosa26-Sox2-IRES-EGFP CRE^{+} offspring were then crossed with homozygous Rosa26-Sox2-IRES-EGFP mice to generate heterozygous and homozygous Rosa26R-Sox2-IRES-GFP CRE^{-} and CRE^{+} mice [For genetic crossing see Figure 1.11]. CRE^{+} animals carrying one copy of the Rosa26-Sox2-IRES-EGFP transgene are referred to as $Sox2^{HetOE}$; CRE^{+} animals carrying two copies of the Rosa26-Sox2-IRES-EGFP transgene are referred to as $Sox2^{HomoOE}$. For analysis of both $Sox2^{HetOE}$ and $Sox2^{HomoOE}$ mice, age and sex-matched heterozygous and homozygous Rosa26-Sox2-IRES-EGFP CRE^{-} animals were used as control animals: Neither heterozygous nor homozygous Rosa26-Sox2-IRES-EGFP CRE^{-} animals express P_0-Cre and therefore do not underdo Cre recombination, which would allow for the overexpression of Sox2. Thus both heterozygous and homozygous Rosa26-Sox2-IRES-EGFP CRE^{-} animals are suitable to be used as controls against both $Sox2^{HetOE}$ and $Sox2^{HomoOE}$ animals.

2.3.2. Transgenic animal genotyping

Genotyping is carried out in order to determine the genetic make-up of a transgenic animal by examining its DNA. The procedure will reveal the alleles that the individual animal has inherited from its parents. In the case of the Sox2 overexpressing mice, we wanted to determine whether the animals had inherited one or two copies of the Rosa26R-Sox2-IRES-GFP allele which contains LoxP sites, to identify if they were heterozygous or homozygous for the Rosa26R-Sox2-IRES-GFP transgene. We also wanted to determine if the animals were P0-CRE^{+}, as heterozygous and

homozygous Sox2-IRES-GFP CRE^- mice were used as controls [See Figure 1.11 for crosses]. In the case of the p38α knockout mice, we were looking for animals that had inherited LoxP sites on both alleles and were P0-CRE^+. Mice which were $p38\alpha^{flox/flox}$ CRE^- were used as controls [see Figure 1.13 for crosses].

Genomic DNA was extracted from ear notch or tail samples using the hot sodium hydroxide and tris (HotSHOT) method (Truett et al., 2000): 75µl of alkaline lysis reagent [Table 2.12] was added to the tissue samples, either ear notches or tail snips. Using a PTC-100 Peltier Thermal Cycler [M.J. Research, Waltham, USA] the samples were heated to 95°C for 1 hour and 30 minutes and then cooled to 4°C. 75µl of neutralisation reagent [Table 2.12] was added to the lysed sample, the sample was then vortexed and stored at -20 ˚C.

In order to check the genotype of the Rosa26R-Sox2-IRES-GFP animals, three 25µl PCR master mix reactions were prepared per lysed tissue sample [For master mix components see Table 2.5]:

(1) In order to determine the P0-CRE status of the animals, 1µl of P0-CRE forward and reverse primers [see Table 2.6] was added to 1 reaction [see Figure 2.1 for an example of the agarose gel];

(2) to identify if whether the Sox2-IRES-GFP mice were carrying one or two copies of the Rosa26R-Sox2IRES-GFP transgene, 1µl of R26 wild type forward and reverse primers [Table 2.6] was added to second reaction [see Figure 2.1 for an example of the agarose gel];

(3) to confirm the presence of the Rosa26R-Sox2-IRES-GFP transgene in the homozygous Sox2-IRES-GFP animals, 1µl of Sox2-IRES-GFP forward and reverse primers [see Table 2.6] was added to a third reaction [see Figure 2.1 for an example of the agarose gel].

In order to determine the check the genotype of the p38α animals, two 25µl PCR master mix reactions were prepared per lysed tissue sample [see Table 2.5]: (1) To determine the P0-CRE status of the animals, 1µl of P0-CRE forward and reverse primers [see Table 2.6] was added to 1 reaction; (2) to determine the p38α LoxP status of the animals, 1µl of p38α LoxP forward and reverse primers [see Table 2.6] was added to another reaction [see Figure 2.2 for an example of the agarose gel].

PCR was carried out using a PTC-100 Peltier thermocycler [for standard PCR programme see Table 2.7 and for variations to the standard programme see table 2.6]. 15µl of each PCR reaction was electrophoresed in 1x tris-acetate-EDTA (TAE) solution, on a 1.5% (w/v) agarose gel [Invitrogen] (diluted in TAE), at 90-100V for 45-60 minutes using a Power Pac 300 [Biorad] and a SubCell® GT tank [Biorad] [For TAE see Table 2.13]. DNA bands were visualised with GelRed Nucleic Acid Gel Stain (10,000x) (1:10,000 in the agarose gel) [Biotium, California, USA] and images captured on a BiodocIt™ Imaging system [UVP, Cambridge, UK] [for variations to standard protocol see Table 2.6

Component	concentrations	Volume
DNA or cDNA		2µl
ddH_20		14.9µl
5 x Green GoTaq® Buffer [Promega]		5 µl
$MgCl_2$ [Promega]	1.5mM	1.5 µl
Forward and reverse primers [MWG, Ebersburgh, Germany]	0.5 picomoles	1 µl
Deoxynucleotide triphosphate (dNTP) [Promega]	200µM	0.5 µl
Taq Polymerase [Promega]	1.25U	0.1 µl

Table 2. 5 : Components of polymerase chain reaction master mix used for both genotyping and semi-quantitative RT-PCR. Table lists all the components used in a PCR mastermix per 25µl reaction.

Gene	Forward primer sequence 5'- 3'	Reverse primer sequence 5'- 3'	Anneal temp (˚C)	No. of Cycles	$MgCl_2$ Conc. (mM)	Size (bp)
P0-CRE (M)	CCACCACCTCT CCATTGCAC	GCTGGCCCAAA TGTTGCTGG	57	35	1.5	492
R26 WT (M)	GGAGCGGAGA AATGGATATG	AAAGTCGCTCT GAGTTGTTAT	50	38	1.5	550
Sox2-IRES-GFP (M)	CTACCTGAGCA CCCAGTCCG	ATAACACCTAC TCAGACAATGC	62	30	1.5	309
p38 (M)	CTACAGAATGC ACCTCGGATG	AGAAGGCTGGA TTTGCACAAG	62	35	1.5	1) 121 2) 188
Neuroserpin (M)	ATCCAATGAGG CTGGTGGTA	CTTCGATCAGC TGTGCTTTG	51.7	35	1.5	140
Krox20 (M)	GCCAAGGCCGT AGACAAA	TTGCCCATGTA AGTGAAGGTC	53	35	1.5	154
Necl 4 (M)	TGCAGTGGTAG AGGCTCAGA	GCCTCATGGGT CAGATAGGA	54	35	1.5	144
Sox2 (M)	CAGCTCGCAGA CCTACATGA	TGGAGTGGGA GGAAGAGGTA	55	35	1.5	152
18S (M)	GAGAAACGGCT ACCACATCC	GGACACTCAGC TAAGAGCATCG	55	39	1.5	339

Table 2. 6: Polymerase chain reaction conditions for each primer pair. Table lists the target gene transcript to be amplified (Gene), the sequence of the forward and reverse primer, the annealing temperature (Anneal. Temp), number of cycles, magnesium chloride concentration and the fragment size in base pairs (bp) for each reaction. In some cases as seen when analysing the p38 gene, two PCR fragments of different sizes (bp) are produced

in mice heterozygous for the transgene; the wild type p38 fragment (121bp) and the p38 floxed “transgene” fragment (188bp) [see Figure 2.2]. (M) denotes a mouse target transcript.

Step Number	Conditions
Step 1	95˚C for 5 minutes
Step 2	95˚C for 45 seconds
Step 3	55˚C for 45 seconds
Step 4	72˚C for 1 minute
Step 5	Back to steps 2-4, 29 times
Step 6	72˚C for 10 minutes
Step 7	4˚C

Table 2. 7: Standard polymerase chain reaction program. For variations to the annealing temperature and number of cycles for individual primers see Table 2.6.

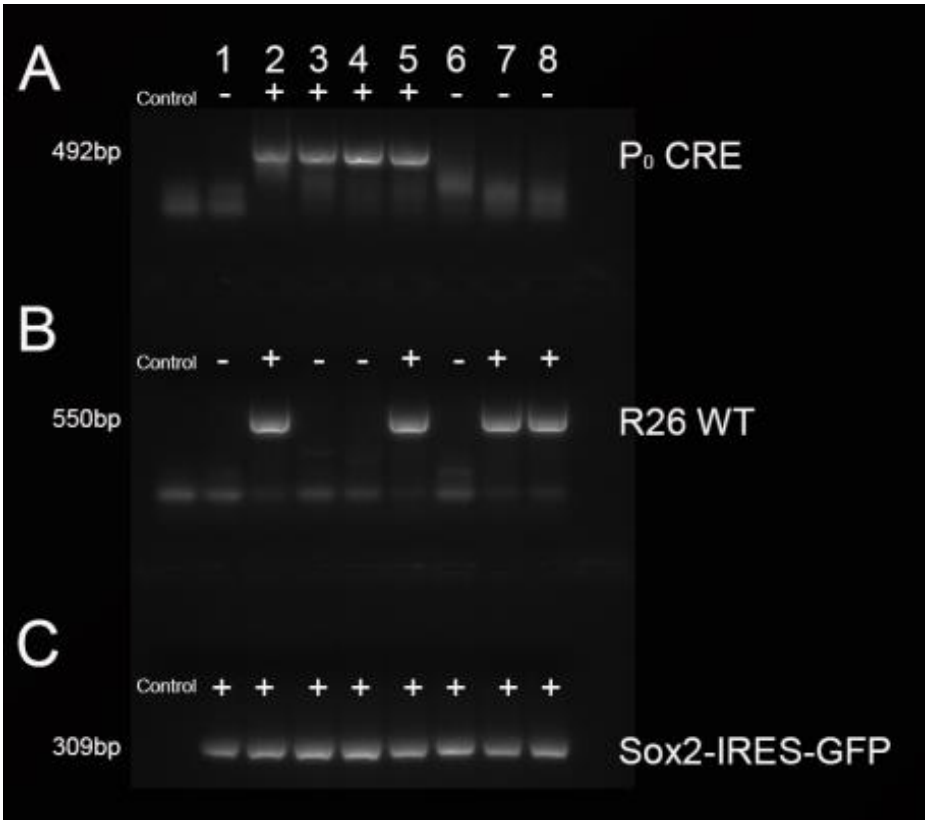

Figure 2. 1: Example of an agarose gel showing P0-CRE, R26 and Rosa26R-Sox2-IRES-GFP genotypes. (A) Samples with a large band at 492bp indicate that these animals inherited the P0-CRE allele e.g. 2, 3, 4, 5. (B) Samples with a large upper band at 550bp indicate that these animals carry the wild type Rosa26 allele e.g. 2, 5, 7, 8. (C) Samples with a band at 309bp indicate that these animals have inherited the Rosa26R-Sox2-IRES-GFP transgene e.g.1, 2, 3, 4, 5, 6, 7, 8. Animals which are heterozygous for the R26 WT allele and the Rosa26R-Sox2-IRES-GFP transgene and are P0-CRE positive will be Sox2 heterozygous over-expressors ($Sox2^{HetOE}$) e.g. 2 and 5. Animals which are homozygous for the Rosa26R-Sox2-IRES-GFP transgene and are P0-CRE positive will be Sox2 homozygous over-expressors ($Sox2^{HomoOE}$) e.g. 3 and 4. Animals which are heterozygous for the R26 WT allele and the Rosa26R-Sox2-IRES-GFP transgene and are P0-CRE negative will be Sox2 heterozygous controls (Het Control) e.g. 7 and 8. Animals which are homozygous for the Rosa26R-Sox2-IRES-GFP transgene and are P0-CRE negative will be Sox2 Homozygous Controls (Homo Control) e.g. 1 and 6.

Figure 2. 2: Example of an agarose gel showing p38α LoxP genotypes. (A) p38 loxP heterozygous samples are represented by double bands, one at 121bp (p38α wild type band) and one at 188bp (p38α floxed band) indicating that these animals have a p38α loxP site on only one allele (wt/fl) e.g. 1, 3, 4, 5, 8. p38α loxP homozygous samples are represented by a single band at 188bp, indicating that these animals have P38α loxP sites on both alleles (fl/fl) e.g. 2, 6, 7, 9.

2.3.3. Nerve dissection for analysis

The sciatic nerve and brachial plexus was removed from mice ranging in age from postnatal day 2 (P2) to adult, and snap frozen immediately in liquid nitrogen, then stored at -80°C for future western blotting analysis. For immunohistochemistry nerves were fixed in 4% w/v paraformaldehyde (PFA) [Sigma] pH 7.4, diluted in 1x PBS [for PBS see Table 2.12], overnight at 4ºC, then washed 3 times for 5 minutes in 1xPBS before being immersed in 30% w/v sucrose [Sigma] diluted in 1x PBS overnight at 4ºC, to allow for cryoprotection. For electron microscopy nerves were fixed in 2.5% (w/v) glutaraldehyde diluted in 0.1M sodium cacodylate buffer [for sodium cacodylate buffer see Section 2.12] overnight at 4°C.

2.3.4. Sciatic nerve injury

Transgenic mice were anaesthetized with isoflurane, the right sciatic nerves were exposed and either crushed or cut approximately 1cm distal to the sciatic notch. For nerve crush, the sciatic nerve was compressed using a pair of round end forceps, as previously described (Dun and Parkinson, 2015). The left contralateral sciatic nerve was left uninjured. Mice were euthanized at the indicated time and both the uninjured and injured distal sciatic nerves were collected for analysis.

2.3.5 Cryosectioning of sciatic nerve

Sciatic nerve samples were placed into a plastic embedding mould [Agar Scientific], filled with Tissue-Tek® optimum cutting temperature (OCT) compound [Sakura Finetek Europe B.V. Netherlands] and frozen slowly in liquid nitrogen. The frozen blocks were then sectioned into 10µm slices using an OTF 5000 Cryostat [Bright Instrument Co. Ltd, UK] and each section was placed on a positively charged SuperFrost® Plus microscope slide [VWR] and allowed to dry before staining.

2.4. Analytical techniques

2.4.1. Reverse transcription polymerase chain reaction (RT-PCR)

RT-PCR is used as a semi-quantitative method to detect the rate of transcription of a target gene by measuring the abundance of the corresponding mRNA. Reverse transcription is used to convert isolated mRNA into cDNA, which can then be amplified by PCR and detected by agarose gel electrophoresis.

Total RNA was harvested from the sciatic nerves of 21 day old mice, using an RNeasy Plus® Mini Kit [Qiagen,Crawley, UK] following the manufacturer's protocol. Briefly sciatic nerves were lysed, DNA removed by passage over a gDNA eliminator column, RNA bound to an RNeasy spin column, washed and RNA eluted in 30µl of RNase free water. RNA concentration (260nm or absorbance at A260) and purity (A260/A280) were measured using a Nanodrop 2000 spectrophotometer [Thermo-Scientific]. For each sample 1µg of RNA was reverse transcribed into cDNA using M-MLV Reverse Transcriptase enzyme [Promega] and random hexamer primers [Promega] following the manufacturer's protocol. Gene expression was then measured by PCR. Each 25µl PCR reaction was made up of 2µl cDNA and 23µl of master mix (For master mix components see Table 2.5). PCR was performed in a PTC-100 or PTC-200 thermocycler [MJ Research,Waltham, USA] [for standard program see Table 2.7 and for variations to the standard protocol see Table 2.6]. 15µl of each PCR reaction was electrophoresed in 1x Tris-acetate-EDTA (TAE) solution, on a 2% (w/v) agarose gel [Invitrogen] (diluted in TAE), at 120V for 45-60 minutes using a Power Pac 300 [Biorad] and a SubCell® GT tank [Biorad] [For TAE see Table 2.12]. DNA bands were visualised with GelRed nucleic acid gel stain (10,000x) (diluted 1:10,000 in the agarose gel) [Biotium, California, USA] and images captured on a BiodocIt™ Imaging system [UVP, Cambridge, UK] [for variations to standard protocol see Table 2.6].

2.4.2. Immunofluorescent staining

Immunofluorescent staining is a technique used to visualise the expression and localisation of a protein within a cell. Primary antibodies are raised against epitopes from proteins of interest and bound by secondary antibodies conjugated with fluorescent chromophores. Chromophores are excited by specific wavelengths of light, and fluoresce; releasing light of a lower frequency/longer wavelength. This can be detected and recorded using a digital camera on a fluorescent microscope.

2.4.2.1. Immunocytochemistry

Culture medium was aspirated and cells were fixed with 500µl/well 4% w/v paraformaldehyde (PFA) [Sigma] pH 7.4, diluted in 1x PBS, for 10 minutes [for PBS see Table 2.12]. 4% PFA was removed and cells washed twice with nonsterile 1x PBS. Coverslips were placed on staining platforms and blocked / permeabilised with antibody diluting solution (ADS) containing 0.2% (v/v) Triton X-100 [Sigma] (ADST) for 30 minutes at room temperature [for ADS see Table 2.12]. Primary (1°) antibody was diluted in ADST and 50µl of primary antibody solution added to each coverslip and incubated overnight at 4°C [for concentrations of specific 1° antibodies see Table 2.8]. The next day coverslips were washed six times in 1x PBS and secondary (2°) antibody diluted in ADS, including Hoechst [Sigma] at a final concentration of 4µg/ml, was applied for 30 minutes at room temperature [for specific 2° antibodies see Table 2.10]. Coverslips were then washed 6 times in 1x PBS, mounted on frosted glass slides [VWR] using 10µl Citifluor antifade glycerol/PBS mounting medium [Agar Scientific, Stansted, UK] and sealed with nail varnish.

2.4.2.2. Immunohistochemistry

Sciatic nerve samples were fixed in 4% w/v paraformaldehyde overnight, washed 3 time for 5 minutes in 1x PBS and then dehydrated in 30% sucrose overnight; all overnight steps were done at 4°C. Sciatic nerve samples were placed into a plastic embedding mould [Agar Scientific], coated with Tissue-Tek® OCT compound [Agar Scientific] and frozen slowly in liquid nitrogen. 8µm thick sciatic nerve sections were cut from the frozen blocks using an OTF 5000 Cryostat [Bright Instrument Co. Ltd, UK], placed onto positively charged SuperFrost® Plus microscope slide [VWR], and allowed to dry before staining.

Slides mounted with tissue samples were washed once for 5 minutes in 1x PBS and a hydrophobic barrier was drawn around the sample using a PAP pen [Fisher Scientific, Loughborough, UK]. If required, samples were fixed with -20˚C methanol (MeOH) for 10 minutes at room temperature. Tissue samples were permeabilised / blocked with either ADST or ADS for 60-90 minutes at room temperature then washed once for 5 minutes in 1x PBS. 1˚ antibodies diluted in either ADS or ADST were added overnight at 4ºC [for concentrations of specific 1° antibodies see Table 2.8]. The next day tissue samples were washed 3 times for 5 minutes in 1x PBS and 2° antibodies (1:250), including Hoechst dye (1/1000) [Sigma] diluted in ADS were applied for 45 minutes at room temperature [for specific 2° antibodies see Table 2.8]. Tissue sections were then washed 3 times in 1x PBS, mounted in Citifluor antifade glycerol/PBS mounting medium and a glass cover slip was sealed over the top of the tissue section with nail varnish.

2.4.2.3. 3-layer protocol

In some instances to increase staining intensity a 3-layer staining protocol was used [Table 2. 8]. Tissue samples were permeabilised / blocked and incubated with 1° antibody following the standard protocol. The 2° antibody was replaced with a biotinylated secondary antibody, raised against the primary antibody species, diluted 1:250 in ADS and incubated for 60 minutes at room temperature. Samples were then washed 3 times for 5 minutes in 1x PBS before incubating with either Alexa Fluor® streptavidin 568 (1:1000) [Invitrogen] or Alexa Fluor® streptavidin 633 (1:1000) [Invitrogen] tertiary layer and Hoechst dye (1/1000) diluted in ADS for 45 minutes at room temperature. Tissue samples were washed 3 time for 5 minutes in 1x PBS, mounted and sealed as standard protocol.

2.4.2.4. Imaging and quantification

Stained slides were visualised under a fluorescence microscope. For counting experiments, all specific antibody staining in cells and across nerve tissue samples were scored as positive and counted. Photos were taken using a Nikon Eclipse 80i Fluorescence microscope [Nikon, Kingston upon Thames, Surrey], an intensilight C-HGF1E lightbox [Nikon] and the NIS Elements software package [Nikon]. Photos were taken using the x10, x20 or x40 objective lenses.

Antibody	Dilution	Fix	Block / 1˚ diluent	2˚antibody	Source
Sox2	1/200	4% PFA	ADST	Anti-rabbit	Millipore [Watford, UK]
Krox20	1/100	4% PFA	ADST	Anti-rabbit	Covance [Princeton, New Jersey, USA]
MBP	1/100	4% PFA	ADS	Biotinylated Anti-goat [Vector Laboratories]	Santa Cruz Biotechnology [Texas, USA]
P0	1/100	First 4% PFA, then MeOH fixation	ADS	Biotinylated anti-mouse [Vector Laboratories, Peterborough, UK]	Gift from Prof. J. Archelos [Uni. of Graz, Graz, Austria]
Ki-67	1/200	4% PFA	ADST	Anti-rabbit	Abcam
cJun	1/200	4% PFA	ADST	Anti-rabbit	Cell Signalling
F4/80	1/250	First 4% PFA, then MeOH fixation	ADS	Anti-rat	Abcam
IBA1	1/300	First 4% PFA, then MeOH fixation	ADS	Biotinylated Anti-rabbit [Vector Laboratories]	Wako Pure Chemical industry
CD3e	1/200	First 4% PFA, then MeOH fixation	ADS	Anti-Hampster	BD Pharmingen
NIMP	1/200	First 4% PFA, then MeOH fixation	ADS	Biotinylated Anti-rat [Vector Laboratories]	Abcam
Survivin	1//100	4% PFA	ADST	Biotinylated anti-Goat [Vector Laboratories]	Santa Cruz Biotechnology [Texas, USA]
Sox10	1/1000	4% PFA	ADST	Biotinylated Anti-rabbit [Vector Laboratories]	Gift from Prof. M. Wegner [Erlangen University, Erlangen,Germany]
N-cadherin	1/400	4% PFA	ADST	Biotinylated Anti-rabbit [Vector Laboratories]	Becton Dickinson
B-catenin	1/200	4% PFA	ADST	Anti-Mouse	Becton Dickinson
Neurofilament	1/500	4% PFA	ADST	Anti-Chicken	Abam

Table 2. 8: Primary antibodies used for immunoflourescent staining. Table lists the primary antibodies alongside the 1° antibody dilution, fix, block / permeabilisation / 1° antibody diluent solution and source. Secondary antibodies used were Alexa Fluor® goat anti-rabbit 568, goat anti-hamster 568 and goat anti-chicken 568, goat anti-rat 568 [Invitrogen]. A biotinylated secondary antibody indicates a 3-layer staining protocol was used.

2.4.3. Western blotting

Western blotting is used to identify the expression levels of different proteins within tissue or cell preparations. Proteins are extracted from tissues or cells using a cell lysis buffer and separated according to their molecular weight through sodium dodecyl sulphate (SDS) polyacrylamide gel electrophoresis (PAGE). Proteins are transferred to membranes and probed with primary and secondary antibodies; the latter conjugated with horseradish peroxidase (HRP). Membranes are then coated with chemiluminescent substrate reagent, which interacts with the HRP enzyme, resulting in an enzymatic reaction which releases light. This can be detected using photographic film and an X-ray film developer.

Cells were lysed in 1x dilution of radio-immunoprecipitation assay (RIPA) buffer containing 1:20 Complete™ Mini EDTA free protease inhibitor cocktail [Roche, Lewes, UK], 1:100 phosphatase inhibitor cocktail II [Sigma] and 1:50 phosphatase inhibitor cocktail C [Santa Cruz] [For RIPA buffer see Table 2.12]. Cell lysate was collected on ice using a cell scraper, heated to 95°C for 5 minutes, cooled on ice, centrifuged at 13 400xg for 15 minutes in a MicroCentaur centrifuge [MSE, London, UK] and the supernatant stored at -80°C.

Sciatic nerve tissue samples were lysed in 1x SDS lysis buffer [for SDS buffer see table 2.12], sonicated for 10 seconds, heated to 95°C for 5 minutes, cooled on ice, centrifuged at 13,400 x g for 5 minutes in a MicroCentaur centrifuge [MSE, London, UK] and the supernatant stored at -80°C.

Protein concentrations were estimated using a BCA™ protein assay [Thermo Scientific, Epsom, UK] following the manufacturer's instructions and absorbance at 562nm measured on a GENIos microplate reader [Tecan, Reading, UK] using the XFluor software add-in [Tecan]. Prior to electrophoresis, 4x reducing sample buffer was added to the lysate, the samples were then boiled at 95°C for 5 minutes [for sample buffer see table 2.12].

Samples were loaded onto either a 10% or 12% w/v polyacrylamide gels (depending on the size of the proteins of interest) alongside 10µl of Precision Plus Protein All Blue Standard [Bio-Rad]. SDS PAGE was performed in 1x running buffer at

constant 150V for 1.5 hour in a Mini Protean® 3 Cell [Bio-Rad]. Protein was transferred to Immuno-Blot™ polyvinylidene fluoride membranes [Bio-Rad] in 1x transfer buffer at constant 250mA for 1.5 hours at room temperature or constant 85mA overnight at 4°C. Membranes were blocked in either 5% (w/v) milk powder [Marvel, Coolock, Republic of Ireland] or 5% (w/v) bovine serum albumin (BSA) [Fisher Scientific] dissolved in 1x Tris buffered saline (TBS) for 2 hours at room temperature [For gels, buffers and solutions see Table 2.12]. Primary antibodies were diluted in the blocking solution and incubated on a roller at 4°C overnight [For specific primary antibody dilutions see Table 2.9]. Following primary antibody incubation, membranes were washed 3 times for 5 minutes in 1x TBS and incubated with HRP conjugated secondary antibodies [Promega], diluted 1:5,000 in 2.5% (w/v) milk powder 1x TBS, for 1 hour at room temperature. Membranes were then washed 3 times for 10 minutes in 1x TBS then incubated with SuperSignalTM West Pico chemiluminescent substrate [Thermo-Scientific] for 5 minutes in the dark. Photographic film, Hyperfilm™ [GE Healthcare, Amersham, UK] was exposed to the membranes for between 5 seconds and 5 minutes, as required, in a Hypercassette™ [GE Healthcare]. Exposed film was developed using a Compact X4 automatic X-Ray film processor [XoGraph Imaging Systems Ltd, Tetbury, UK] following the manufacturer's instructions. Films were scanned using a Fluor-S ^{TM} Multi-imager [BioRad].

Antibody [Source]	Dilution	Block	2˚Antibody	Molecular weight (kDa)
Sox2 [Novus Biological]	1:1000	5% Milk	Anti- Rabbit HRP	37
c-Jun [BD Biological]	1:1000	5% Milk	Anti- Mouse HRP	37-40
MBP [Santa Cruz Biotechnology]	1:2000	5% Milk/	Anti- Goat HRP	17
Protein Zero (P0) Gift from Prof. J. Archelos	1/20000	5% Milk/	Anti- Mouse HRP	25
β-tubulin [Santa Cruz Biotechnology	1/2500	5% Milk	Anti- Mouse HRP	50
Sox10 Gift from Michael Wegner	1/5000	5% Milk/ BSA	Anti-Guinea pig HRP	58
Krox-20 [Covance]	1:1000	5% BSA	Anti- Rabbit HRP	65
Necl 4 (cadm4) [Origene]	1:5000	5% BSA	Anti- Goat HRP	65
p38α [Cell signaling]	1:500	5% BSA	Anti- Mouse HRP	38
p-p38 [Cell signaling]	1:500	5% BSA	Anti- Rabbit HRP	38
P-Erk1/2 [Cell signaling]	1:500	5% BSA	Anti- Rabbit HRP	42-44
Sox10 [Abcam]	1:1000	5% Milk	Anti-Rabbit HRP	55-60

Table 2. 9: Primary antibodies for western blotting. Table lists the primary antibodies used in this study, the source and corresponding dilutions, blocking solutions and secondary antibodies.

2.4.4. Electrophysiology

Electrophysiology is the study of electrical activity of excitable cells. The suction electrode method was used to analyse the extracellular electrophysiology of mouse sciatic nerves. In this technique, glass electrodes are used to record the summation of all the action potentials produced by all the individual axons within a nerve bundle; the compound action potential (CAP). Nerves are placed into saline-filled electrodes, the proximal end connected to an amplifier and the distal end connected to a stimulus recording unit (recordings are usually orthodromically), thus upon stimulation the extracellular compound response can be recorded.

2.4.4.1. Electrophysiological recording of compound action potentials using suction electrodes

Sciatic nerve samples were placed onto an interface perfusion chamber [Harvard Apparatus Inc] for 30-45 minutes and allowed to equilibrate before measurements were initiated. This was done to allow the sciatic nerve to recover from the trauma of the dissection and to regain homeostatic control over its ionic environment. The sciatic nerves were kept at 37ºC at all times, perfused with artificial cerebrospinal fluid (aCSF) [For aCSF buffer see Table 2.12] and oxygenated with 95% O_2, 5% CO_2, which was passed through a water chamber for warming and humidification (Fern et al., 1998, Alix and Fern, 2009).

Upon experimentation, compound action potentials (CAP) were evoked via square-wave constant-voltage current pulses of 150 to 600 µsecs delivered by an isolated stimulus unit (Iso Stim A320; World Precision Instruments, Stevenage, UK) at 30 second intervals. The proximal end of the sciatic nerve was placed into an aCSF filled glass stimulating electrode, containing a chloride silver wire in the lumen and another wrapped around the barrel, near the end of the electrode to provide the current return. The distal end of the sciatic nerve was placed into an aCSF filled recording glass electrode, with a chloride silver wire running through the lumen. A third electrode, the subtraction electrode, was placed next to the recording electrode to suppress the stimulus artefact and electrical noise. All electrodes were connected via a high impedance head stage (Axon Instruments) to an amplifier (Axon Instruments, Cyber Amp 320; Union City, CA), which subtracted the signal from the subtraction electrode, from the signal originating from the recording electrode. The

resulting signal was amplified 10 times, filtered (low-pass1000 Hertz) and digitized (25,000Hz, 1401 mini; Cambridge Electronic Design). The resulting signal was displayed on a computer using Signal software (Cambridge Electronic Design).

2.4.4.2. Electrophysiology data analysis

Nerve conduction velocity (NCV) is the speed at which an electrochemical impulse is propagated down a neural pathway. Conduction velocity speeds largely depend on axon diameter and the level of axon myelination. In this experiment, CAP recordings were used to calculate the NCV of sciatic nerves taken from P20 mice and adult mice which had undergone sciatic nerve crush (21 days post injury). NCV was calculated from two parameters: (1) *Conduction distance* (nerve length), and (2) *latency to peak of compound action potential* (the time difference between the peak of the CAP and the start of the stimulus artefact) (Alix and Fern, 2009) [For mathematical formula see Table 2.10]

Mathematical formulas	
Nerve conduction velocity (NCV) (m/s) =	$\frac{\text{Conduction distance (Nerve Length)}}{\text{Latency of the Peak CAP (Peak of the CAP} - \text{Start of the stimulus artefact)}}$
Static sciatic index (SSI) =	(118.9 x TSF) – (52.2 x PLF) -7.5 TSF = TS experimental – TS normal / TS normal PLF = PL experimental – PL normal / PL normal

Table 2. 10: Mathematical formulas. Table lists the formulas used to calculate NCV and SSI from the given parameters. (TSF) denotes toe spread factor, (TS) denotes toe spread, (PLF) print length factor, and (PL) denotes print length.

2.4.5. Motor-Sensory functional testing

2.4.5.1. Rotarod performance testing

Rotarod performance testing is used to measure motor function, co-ordination and balance. In this experiment rotarod performance testing was used to analyse the motor function of control and $Sox2^{OE}$ mice ages 6 and 8 weeks old. The apparatus was set up in an environment with minimal stimuli (such as noise, movement or light changes). Mice underwent three training trials; they were placed onto a rotating rod which accelerated from 2 to 30 rotations per minute in 250 seconds. The mice were given a 1 hour rest in-between each training trial, it was considered a valid test if the mice ran forward on the rod. The next day mice were re-tested the animals following the above mentioned protocol and the latency to fall off was recorded. The average latency time was used as the outcome value.

2.4.5.2. Static sciatic index

Static sciatic index (SSI) is a method for assessing functional loss and recovery after peripheral nerve injury in mice over a duration of time. Using video analysis of standing animals, parameters (1-5 toes spread and print length) taken from the normal and experimental hindpaw are compared by a mathematic formula [For SSI mathematical formula see Table 2.10] and provide information related to the degree of sensory-motor functional changes (Baptista et al., 2007, Bervar, 2000).

SSI analysis was carried out on mice which had undergone sciatic nerve crush injury. Mice were placed into a clear perspex box and paw print measurements were taken using a video camera, from each mouse before surgery (0 days), 2 hours after surgery (0.1 days) and thereafter at 2-3 day intervals for 21 days following injury. The degree of functional loss and recovery post-surgery was calculated as described above.

2.4.5.3. Toe spread reflex

Toes spread reflex is used to assess the degree of functional recovery following nerve injury. Normally when rodents are lifted by their tail, the legs extend laterally and the toe digits spread, maximising the distance between them. Following nerve injury, the ability to carry out this toe spread reflex is impaired, however in time

improves in relation to the degree of nerve regeneration and functional recovery in animals.

In this experiment, mice which had undergone sciatic nerve crush injury were lifted gently by the tail and toe spread reflex was assessed at 12, 14, 17, 19 and 21 days post injury. A score of 0 was given when there was no leg extension or toe spreading, a score of 1 was given when there was partial leg extension and partial toe spreading and a score of 2 was given when there was full leg extension and full toe spreading (Siconolfi and Seeds, 2001). The total score per genotype (a minimum of 3) at each time-point was given as the toe spread reflex score.

2.4.5.4. Von Frey filament threshold testing

Von Frey filaments are commonly used to measure sensory function. The method involves the application of varying pressures to the mid-plantar surface of the hindpaw in order to determine the mechanical withdrawal threshold.

In the experiment, Von Frey filament threshold testing was carried out on 6 week old mice and mice which had undergone sciatic nerve crush injury at 7, 10, 12, 14, 17, 19 and 21 days post injury. Mice were placed into a plastic cage on a metal mesh floor and Von Frey filaments ranging from 180g to 0.008g were applied to the mid-plantar surface of the right hindpaw (when in contact with the floor) for 5-8 seconds. Filaments were applied in ascending order and the smallest filament to induce a foot withdrawal response was considered the threshold stimulus (Vogelaar et al., 2004).

2.4.5.5. Toe Pinch test

Toe pinch testing is commonly used as a method for measuring sensory function and peripheral nerve regeneration after nerve injury. This technique involves using a pair of fine smooth forceps to lightly pinch the most distal part of the toes in order to generate a response.

In this experiment, pressure and sensitivity tests were carried out on 6 week old mice and mice which had undergone sciatic nerve crush injury at 7, 10, 12, 14, 17, 19 and 21 days post injury. Animals were gently scruffed and the most distal part of toe 3, 4 and 5 on both hindlimbs (normal and experimental) were lightly pinched. A response was considered upon reflex withdrawal or the animal making a sound (Siconolfi and Seeds, 2001).

2.4.6. Electron microscopy

Electron microscopy is a viewing technique used to visualise the ultrastructure of a specimen under high magnification with high resolution. The technique is operated under a vacuum and works by using an electromagnetic lens to focus beams of electron on to a specimen to generate an image. There are two basic types of electron microscopes, the scanning electron microscope (SEM) [For details see section 2.4.6.2] and the transmission electron microscope (TEM) [For details see section 2.4.6.3].

2.4.6.1. Nerve tissue preparation for SEM and TEM

Sciatic nerve samples were dissected and fixed using 2.5% (w/v) glutaraldehyde diluted in 0.1M sodium cacodylate buffer for at least 1 hour. Nerves were rinsed twice in 0.1M sodium cacodylate buffer at room temperature for 1 hour [see Section 2.12], then secondary fixed with osmium tetroxide (1% in sodium cacodylate buffer) for 1 hour. After rinsing twice with sodium cacodylate buffer, the tissue was then dehydrated through an alcohol series, starting with 30% ethanol, then 50%, 70%, 90% and finally 100% ethanol. The rinse with 100% ethanol was repeated twice, and each rinse was left for 15 minutes to ensure adequate exchange of liquids. Once the alcohol dehydration was complete, the 100% ethanol was replaced with Agar low viscosity resin. Tissues were placed into increasing concentrations of resin, 30% (30% resin: 70% ethanol), 50% (50% resin: 50% ethanol), 70% (70% resin: 30% ethanol) and finally 100% resin. The 100% resin change was repeated twice, and each change was left for at least 12 hours to allow the resin to completely infiltrate into the tissue. Tissue samples were then placed into a mould embedding Beem capsules and transferred into a Taab embedding oven [Agar Scientific, UK], where the resin was polymerised at 60^{o}C overnight (12 hours) to form a solid matrix that thoroughly permeates the tissue.

2.4.6.2 Scanning electron microscopy

Scanning electron microscopy (SEM) can be used to take high resolution and magnification images of cell surface morphology. Within the scanning electron microscope, a focused beam of electrons are scanned along the surface of the sample under low vacuum. The electrons interacting with the sample, then produce various signals that can be detected and provide information about the sample

surface topography. In this experiment, the polished surface of a nerve was exposed to a beam of electrons. Backscattered electrons (electrons which come into contact with the specimen and are reflected back) were then detected with a backscatter electron detector and used to form an image. The image formed related to the chemical composition of the specimen, through atomic number contrast; bright intensities correlate with parts of the sample with a high atomic number, and dark areas correlates with parts of the sample with low atomic number. SEM was conducted in the Plymouth Electron Microscopy Centre [PEMC, Plymouth, UK].

Following nerve tissue preparation and resin embedding [see section 2.4.6.1], the resulting hard blocks were removed from the Beem capsule and trimmed with a Leica Ultracut E ultramicrotome using a glass knife, to expose the surface of the tissue specimen. Samples were imaged on a JEOL 6610 LV scanning electron microscope [JEOL, Welwyn Garden City, UK] at 15kV, with a 12mm working distance and at x700 and x1500 magnifications.

2.4.6.3. Transmission electron microscopy

Transmission electron microscopy (TEM) can be used to take high resolution and magnification images of the cellular structures of a specimen. Within the transmission electron microscope, a beam of electrons is transmitted through an ultrathin stained section under a high vacuum. The beam of electrons is then either transmitted through the specimen, absorbed or scattered by internal structures of the specimen. An image is formed from the transmitted electrons below the specimen and is detected by a charge-coupled device (CCD) camera [GATAN Orius]. The image detected by the camera is then displayed on a computer. TEM was conducted in the Plymouth Electron Microscopy Centre [PEMC, Plymouth, UK].

Following nerve tissue preparation and resin embedding [see section 2.4.6.1], the resulting hard blocks were removed from the Beem capsule and sectioned with a Leica Ultracut E ultra-microtome using a diatome diamond knife [Agar Scientific]. The resulting sections (80nm thick) were then places onto supporting 200 mesh thin bar copper grids [Agar Scientific]. The copper grids with the sections were then stained using a saturated solution of uranyl acetate for 15 minutes, washed in double distilled water for 30 seconds, then stained with a solution of Reynold's lead citrate

for 15 minutes [for staining solutions see Table 2.11]. Samples were imaged on a JEOL 1400 transmission electron microscope [Jeol, Welwyn Garden City, UK] at 120kV, using a variety of magnifications.

Solutions	Components [sources]
Uranyl acetate	1g uranyl acetate powder [Agar Scientific] dissolved in 1.5ml of 70% ethanol
Reynolds lead citrate	1pellet (0.1-0.2g) of sodium hydroxide [Agar Scientific] 0.25g lead citrate powder [Agar scientific] dissolved in 50ml double distilled water

Table 2. 11: TEM staining solution. Details of the components used to make up the staining solutions for TEM.

2.5 Statistical testing

All numerical data are presented as mean ± 1 standard error of the mean. Unless otherwise stated, n=3 was used for all experiments. Statistical significance was assessed using Student's t-Test, one way ANOVA with Bonferroni *post-hoc* or Kruskal-Wallis with Dunn's *post-hoc* test and a significance threshold of p value (p) <0.05. Statistical significance on graphs was shown as follows P<0.05 as *, P<0.01 as **, P<0.001 as *** and non-significant (NS).

2.6 General laboratory solutions

Composition of all general laboratory solutions shown in Table 2.12.

Solutions	Components [source]
10x phosphate buffered saline (PBS)	80.0g sodium chloride [Sigma] 2.0g potassium chloride [Sigma] 2.0g mono-potassium phosphate [Sigma] 11.5g sodium phosphate [Sigma] dissolved in 1L water
1x antibody diluting solution (ADS)	20.0ml donor calf serum [Sigma] 3.6g lysine monohydrochloride [Sigma] 400µl 10% sodium azide dissolved in 180ml 1x PBS
Alkaline lysis reagent	25 mM NaOH [Sigma] 0.2 mM disodium EDTA (pH12- dissolve in H_2O without adjusting pH)
Neutralising reagent	40 mM Tris-HCl [Sigma] (pH5- dissolve in H_2O without adjusting pH)
10x tris buffered saline (TBS)	160.0g sodium chloride [Sigma] 48.8g Trizma® base [Sigma] dissolved in 2L water
10% polyacrylamide running gel	4.8ml water 2.5ml Trizma®-HCl 1.5M (pH 8.8) [Sigma] 2.5ml 40% acrylamide/bis [Bio-Rad] 100µl 10% SDS [Sigma] 75µl ammonium persulphate (APS) 10µl Temed [Sigma]
12% polyacrylamide running gel	4.5ml water 2.3ml Trizma®-HCl 1.5M (pH 8.8) [Sigma] 3ml 40% acrylamide/bis [Bio-Rad] 100µl 10% SDS [Sigma] 75µl ammonium persulphate (APS) [Sigma] 10µl Temed [Sigma]
10 x Western running buffer	45.5g Trizma® base [Sigma] 216g Glycine [Sigma] 15g SDS Dissolved in 1.5 litres of water
10 x Western transfer buffer	45.5g Trizma® base 216.0g glycine dissolved in 1.5L water
1 x Western transfer buffer	100.0ml 10x western transfer buffer 200.0ml methanol [Rathburn Chemicals, Walkerburn, UK] 700.0ml water 3.8ml 10% SDS

Solutions	Components [source]
1x western stripping buffer	1.5g glycine [Sigma] 0.1g SDS [Sigma] 1.0ml Tween20 [Sigma] dissolve in 100ml ultrapure water adjust to pH2.2
2x SDS lysis buffer	4% (w/v) SDS 20% (v/v) glycerol [Sigma] 60mM Trizma®-HCl (pH 6.8) 0.001% (w/v) Bromophenol Blue [Sigma] 4% (w/v) β-mercaptoethanol [Sigma]
4x reducing loading buffer	8% (w/v) SDS 40% (v/v) glycerol 250mM Tris-HCL(pH 6.8) 200mM dithiothreitol (DTT) [Sigma] 0.4% (w/v) Bromophenol Blue
RIPA buffer	50mM Tris (pH 7.5) 150mM Sodium chloride (NaCl) 1mM Ethylene glycol-bis (2 aminoethylether) tetraacetic acid (EGTA) [Sigma) 1mM Ethylenediaminetetraacetic acid (EDTA) [Sigma] 1% (v/v) Triton x-100 [Sigma] 0.5% (w/v) Deoxycholic acid [Sigma] 0.1% (w/v) SDS [Sigma] 1mM Sodium orthovanadate [Sigma] 10µg/ml Leupeptin [Sigma] Dissolved in 100ml water
50x tris-acetate-EDTA (TAE) solution	242.0g Trizma® 57.1ml glacial acetic acid 100.0ml 0.5M EDTA (pH 8.0) dissolve in 1L water
0.1M sodium cacodylate buffer	2.15g sodium cacodylate dissolve in 100ml water
Artificial cerebral spinal fluid (aCSF)	126 mM NaCl [Sigma] 3 mM KCl [Sigma] 2 mM NaH_2PO_4 [Sigma] 2 mM $MgCl_2$ [Sigma] 26 mM $NaHCO_3$ [Sigma] 10 mM Glucose [Sigma] 2 mM $CaCl_2$ [Sigma] pH 7.45 and bubbled with 95% O_2, 5% CO_2

Table 2. 12: Composition of general laboratory solutions. Details of the components and a brief protocol for preparation of general laboratory solutions used in this study.

Chapter 3 Schwann cell myelination and sensory-motor function is impaired by Sox2 overexpression during development *in vivo*

3.1 Introduction

Schwann cells in the peripheral nervous system are renowned for their remarkable plasticity, which is regulated by the transcriptional activation of both positive and negative myelin regulators. Many positive regulators such as Krox20 (Egr2), Oct6 (SCIP or Tst1), Sox10, NFkB and NFATc4 have been identified by both *in vitro* and *in vivo* analysis, but there is relatively little data on potential negative regulators of myelination that may be as important in both regulating the correctly timed onset of myelination and potentially in the pathology of demyelinating neuropathies of the PNS (Parkinson et al., 2004, Finzsch et al., 2010, Bremer et al., 2011, Kao et al., 2009, Salzer, 2008).

While the transcription factors Pax3, cJun, Id2 and Sox2, activation of the Notch pathway, as well as signalling through the ERK1/2 and p38 mitogen activated protein (MAP) kinases, have been shown to inhibit myelination of Schwann cells *in vitro*, there is only direct genetic evidence that increased activation of the Notch or ERK1/2 signalling pathway in Schwann cells inhibits or is sufficient to drive the de-myelination of Schwann cells *in vivo* (Doddrell et al., 2012, Harrisingh et al., 2004, Le et al., 2005a, Parkinson et al., 2008, Woodhoo et al., 2009, Yang et al., 2012, Jessen and Mirsky, 2008, Mager et al., 2008). The high mobility group (HMG) domain transcription factor Sox2 has been shown using an *in vitro* assay, Schwann cell/dorsal root ganglion co-cultures and adenoviral overexpression of Sox2 in Schwann cells, to inhibit the induction of Krox20 and myelination of axons but an *in vivo* demonstration of the potential inhibitory role of Sox2 *in vivo* within the intact nerve has not been shown.

3.2 Results

3.2.1 Sox2 overexpressing mice exhibit a phenotype of a peripheral neuropathy

Patients suffering with Charcot Marie Tooth (CMT) disease such as congenital hypomyelinating neuropathy (CHN) and CMT-type 1 (CMT-1) disease, clinically present symptoms such as muscle weakness, muscular atrophy of the hands, sensory loss, characteristic foot abnormalities, tremors, ataxia and areflexia (Jani-Acsadi et al., 2008). Mouse models of CMT disease have also been shown to mimic some of the phenomena that occur in human CMT (Kinter et al., 2013, Saporta et al., 2012, Wrabetz et al., 2006). CMT mouse models can therefore provide us with a good reference to the disease and the ability to gain a deeper understanding of the mechanisms that cause and/or enhance disease progression (Sereda et al., 1996, Sereda and Nave, 2006, Tanaka and Hirokawa, 2002).

Sox2 has been previously shown to be upregulated in mouse models of CHN and to impair Schwann cell myelination *in vitro* (Le et al., 2005a). In order to determine whether Sox2 was capable of blocking myelination and inducing a phenotype similar to that of CMT *in vivo*, we generated mice which conditionally overexpressed Sox2 in Schwann cells. To achieve this we crossed P_0 Cre+ mice with mice homozygous for the Sox2-IRES-EGFP transgene. This allowed us to generate heterozygous Rosa26 Sox2IRES-EGFP CRE positive (+) and CRE negative (-) offspring. Heterozygous Rosa26 Sox2IRES-EGFP CRE^+ animals were then backcrossed with homozygous Rosa26 Sox2IRES-EGFP mice to generate heterozygous and homozygous Rosa26R-Sox2IRES-GFP CRE^- (hereafter referred to either Sox2 Het or Homo control mice) and CRE^+ mice. CRE^+ animals carrying one copy of the Rosa26 Sox2IRES-EGFP transgene are referred to as $Sox2^{HetOE}$; CRE+ animals carrying two copies of the Rosa26 Sox2IRES-EGFP transgene are referred to as $Sox2^{HomoOE}$ mice [See Figure 1.11] (Feltri et al., 1999a, Lu et al., 2010a). In these experiments both heterozygous and homozygous Rosa26 Sox2IRES-EGFP CRE^- animals are suitably used as controls against $Sox2^{HetOE}$ and $Sox2^{HomoOE}$ animals [see section 2.3.1 for details].

During development from postnatal day 21 (P21), we observed that $Sox2^{HomoOE}$ mice appeared to be slightly smaller compared to age matched control litter mates, this

became even more obvious as $Sox2^{HomoOE}$ mice reached adulthood. By P60, we observed that $Sox2^{HomoOE}$ mice displayed typical characteristic of a peripheral neuropathy such as hindlimb clasping when lifted by the tail, foot abnormalities, ataxia and muscle weakness [Figure 3.1]. These observations suggested that overexpression of Sox2 within Schwann cells resulted in the onset of a peripheral neuropathy within these mice (Sereda et al., 1996, Sereda and Nave, 2006).

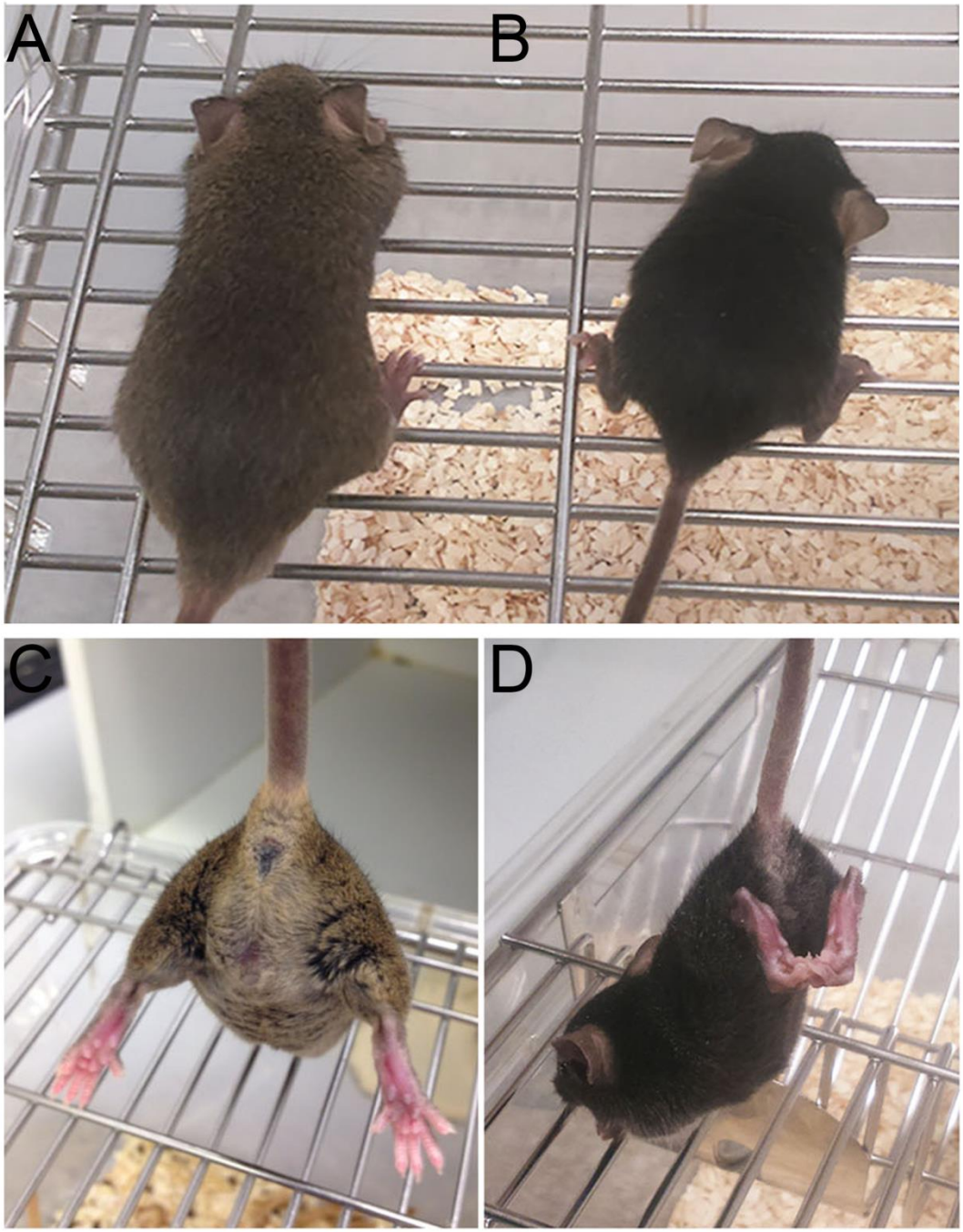

Figure 3. 1: Sox2^{HomoOE} mice display characteristics of CMT disease. P60 Sox2^{HomoOE} mice were smaller and showed signs of hindlimb clasping(B and D), whilst Sox2 control (Homo and Het) littermates were normal in size and displayed normal hindlimb spreading when lifted by the tail (A and C).

3.2.2 Sox2 overexpression impairs Schwann cell myelination

In the PNS mature Schwann cells myelinate motor axons in a 1:1 ratio by extending their plasma membrane and spirally ensheathing the axonal segment. Multiple spirals formed around an individual axon condense into a multilamellar compact sheath, enabling axonal protection and saltatory conduction. Nonetheless, in many peripheral neuropathies such as CHN and CMT-1 disease, Schwann cells fail to sufficiently myelinate axons resulting in severe axonal hypomyelination (Decker et al., 2006, Le et al., 2005a, Jessen and Mirsky, 2005).

As mentioned previously, Sox2 has been shown to be upregulated in mouse models of CHN and to impair Schwann cell myelination *in vitro* (Le et al., 2005a). To determine whether Sox2 was capable of blocking myelination *in vivo*, sciatic nerves were removed from Sox2 control (Het and Homo), $Sox2^{HetOE}$ and $Sox2^{HomoOE}$ mice and the morphology of the nerves was examined at postnatal day 7, 21 and 60 by electron microscopy.

In the sciatic nerves of $Sox2^{HetOE}$ mice at P7, axons were significantly shifted towards having thinner myelin, compared to axons in the sciatic nerves of Sox2 Het control mice [Figure 3.2]. In Sox2 Het control mice the average myelin thickness was at 0.33 ± 0.005 µm (mean ± 1 standard error of the mean), whereas in $Sox2^{HetOE}$ mice the average myelin thickness was significantly lower at 0.28 ± 0.004 µm ($P<0.001$, n=3). Similarly, in the sciatic nerves of $Sox2^{HomoOE}$ mice at P7, axons shifted towards having thinner myelin, compared to Sox2 Homo control mice; the average myelin thickness of Sox2 Homo control nerves 0.38 ± 0.008 µm, whereas the average myelin thickness of $Sox2^{HomoOE}$ nerves was significantly lower at 0.27 ± 0.01 µm ($P<0.001$, n=3) [data not shown]. Counts made on the total percentage of unmyelinated axons in a 1:1 relationship with Schwann cells showed that there was a significant increase in the percentage of unmyelinated axons in the sciatic nerves of $Sox2^{HetOE}$ mice (27.6 ± 3.4 %) ($P<0.05$) and $Sox2^{HomoOE}$ mice (28 ± 2.09 %) ($P<0.001$) compared to Sox2 (Het and Homo) control mice (7.5 ± 0.56 %) at P7 [Figure 3.2] (n=3 $Sox2^{HetOE}$, n=3 $Sox2^{HomoOE}$, n=6 Sox2 control). Further analysis at P21 revealed that overexpression of Sox2 resulted in a significant shift in the population of axons towards having a higher g-ratio. The average g-ratio observed

in $Sox2^{HetOE}$ mice was 0.71 ± 0.003, whereas the average g-ratio observed in Sox2 Het control mice was 0.68 ± 0.002 ($P<0.001$, n=3) [Figure 3.3]. The percentage of unmyelinated axons in a 1:1 relationship with Schwann cells was also significantly increased in the sciatic nerves of $Sox2^{HetOE}$ mice (15.3 ± 1.34 %) at P21 compared to Sox2 Het control mice (1.13 ± 0.17%) ($P = 0.001$, n=3) [Figure 3.3]. Myelin thickness was not analysed in the nerves of $Sox2^{HomoOE}$ and Sox2 Homo control animals at P21.

We next wanted to determine whether overexpression of Sox2 resulted in Schwann cell hypomyelination in adult mice. We therefore analyse the sciatic nerves of Sox2 Het control, $Sox2^{HetOE}$ and $Sox2^{HomoOE}$ mice at P60. Surprisingly, at P60 there was no longer a significant difference in myelin thickness between Sox2 Het control and $Sox2^{HetOE}$ mice ($P>0.05$, n=3); the average g-ratio for Sox2 Het control mice was 0.66 ± 0.02 and the average g-ratio for $Sox2^{HetOE}$ mice was 0.65 ± 0.02. Further analysis also revealed that no significant difference in the total population of unmyelinated axons was observed between Sox2 Het control mice (0.17 ± 0.17%) and $Sox2^{HetOE}$ mice (0%) at P60 ($P>0.05$, n=3) [Figure 3.4]. We therefore analysed the expression of the Sox2-IRES-EGFP transgene in the $Sox2^{HetOE}$ animals and found that expression of both Sox2 and GFP declined from P21 onwards and was undetectable at later time-points, either by western blot of by immunocytochemistry [data not shown & unpublished data by Dr Xin-Peng Dun in our group]. We were unable to conclude at this time why expression levels of Sox2 and GFP decline in these $Sox2^{HetOE}$ mice, but it does show that loss of Sox2 expression in a hypomyelinated nerve will allow myelination to proceed and complete by P60 in the mouse peripheral nervous system.

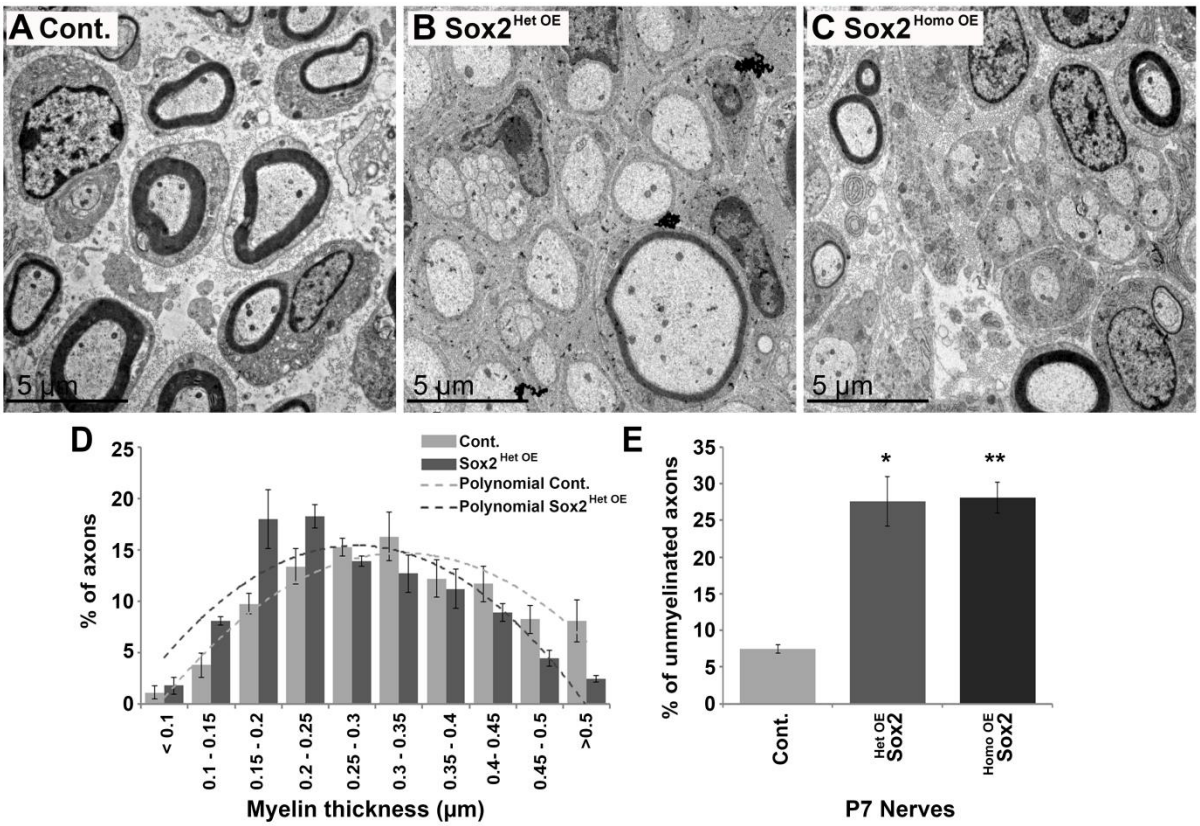

Figure 3. 2: Inhibition of myelination by Sox2 overexpression at P7. Transmission electron micrographs of sciatic nerve sections taken from Sox2 Het control (A), Sox2^{HetOE} (B) and Sox2^{HomoOE} mice (C) at P7. Graph (D) showing the percentage distribution of axons in relation to their myelin thickness; note a shift in the population of axons towards having thinner myelin in the sciatic nerves of Sox2^{HetOE} mice. (E) Graph showing a significant increase in the population of unmyelinated axons in the sciatic nerves of Sox2^{HetOE} (P=0.026) and Sox2^{HomoOE} mice (P=0.007), compared to control P7 mice (n=3 Sox2^{HetOE}, n=3 Sox2^{HomoOE}, n=6 Sox2 (het and homo) control).

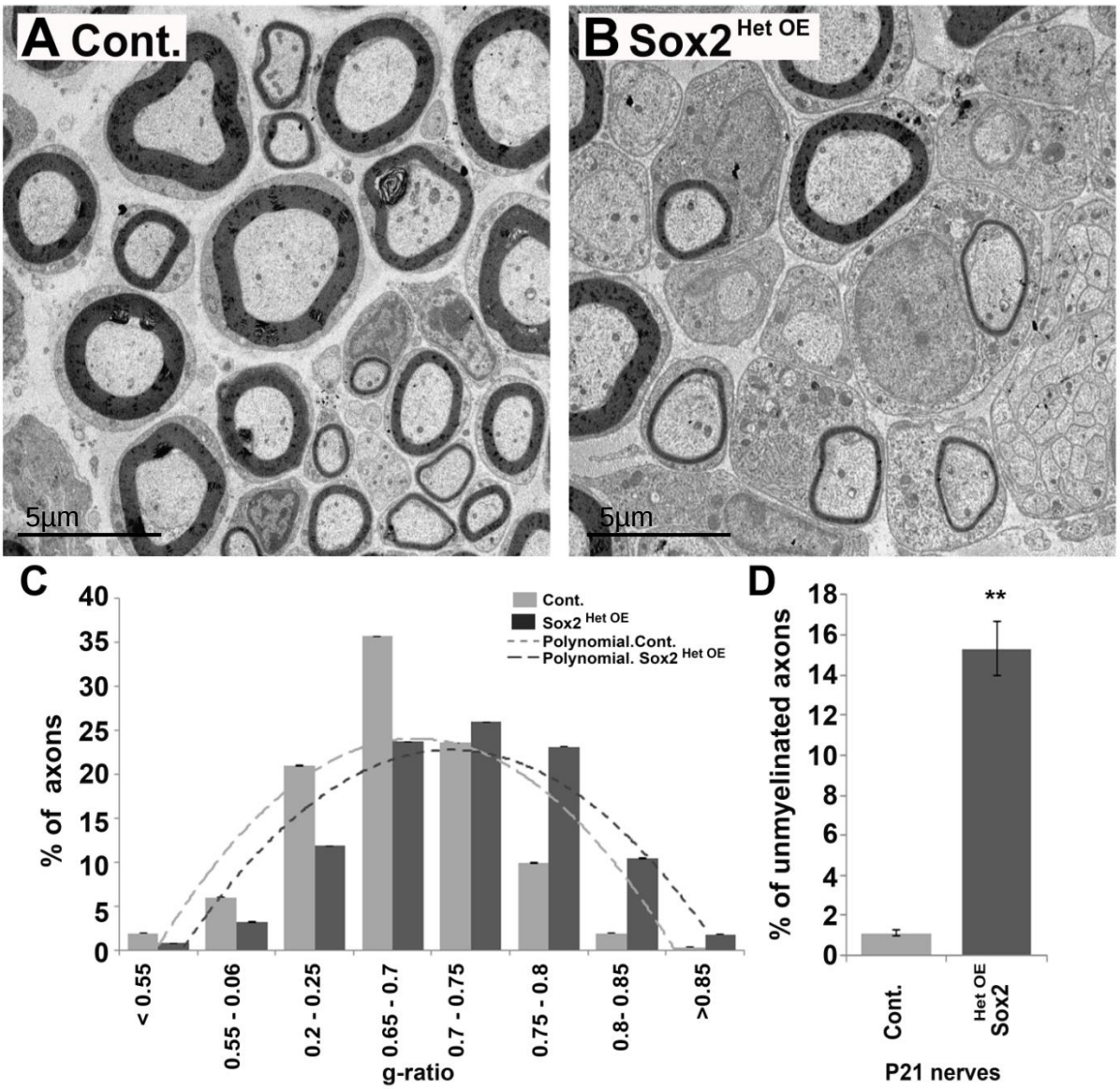

Figure 3. 3: Inhibition of myelination by Sox2 overexpression at P21. (A & B) Transmission electron micrographs of sciatic nerve sections taken from Sox2 Het control (A) and Sox2^{HetOE} mice (B) at P21. Graph (C) showing the percentage distribution of axons in relation to their g-ratio; note a shift in the population of axons towards having an increased g-ratio (i.e. thinner myelin), in the sciatic nerves of Sox2^{HetOE} mice. (D) Graph showing a significant increase in the population of unmyelinated axons in the sciatic nerves of Sox2^{HetOE} mice compared to Sox2 Het control mice P21 ($P = 0.001$, n=3 per genotype).

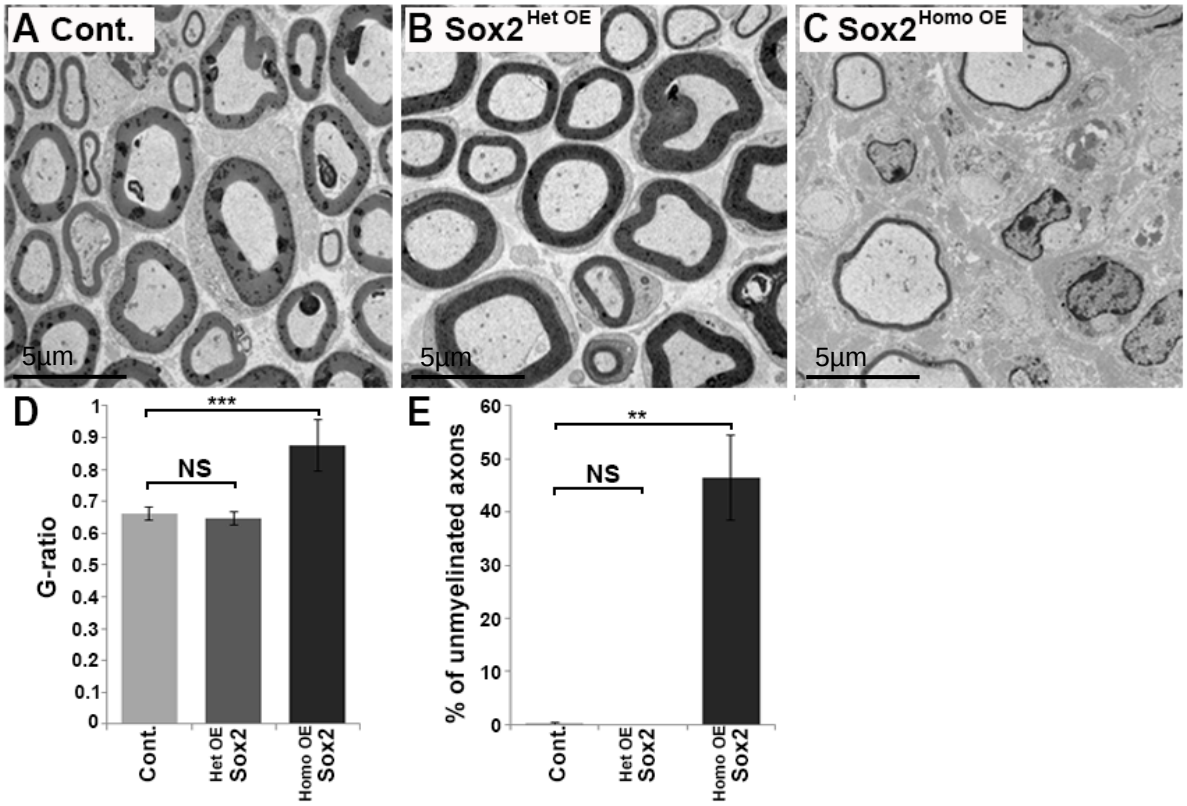

Figure 3. 4: Inhibition of myelination seen in Sox2^{HomoOE} at P60. (A, B, C) Transmission electron micrographs of sciatic nerve sections taken from Sox2 Het control (A), Sox2^{HetOE} (B) and Sox2^{HomoOE} mice (C) at P60. (D) Graph showing the average g-ratio of axons; note there is significant increase in the g-ratio of Sox2^{HomoOE} mice, compared to control mice ($P < 0.001$, n=3 per genotype). (E) Graph showing the population of unmyelinated axons in the sciatic nerves of Sox2 Het control, Sox2^{HetOE} and Sox2^{HomoOE} mice; note there is a significant increase in the number of unmyelinated axons in Sox2^{HomoOE} mice compared to control mice ($P<0.01$, n=3 per genotype).

We next compared myelin thickness in the nerves of Sox2 Het control and $Sox2^{HomoOE}$ nerve mice at P60. We revealed that myelin thickness was significantly reduced in the nerves of $Sox2^{HomoOE}$ mice, compared to Sox2 Het control mice at P60 ($P<0.001$, n=3); in Sox2 Het control mice the average g-ratio was 0.66 ± 0.2, whereas in $Sox2^{HomoOE}$ mice the average g-ratio was significantly higher at 0.87 ± 0.08 [Figure 3.4]. A significant increase in the total population of unmyelinated axons was also observed in the sciatic nerves of $Sox2^{HomoOE}$ mice (46.5 ± 8.04%) at P60 compared to sciatic nerves of Sox2 Het control mice (0.17 ± 0.17%) ($P<0.01$, n=3) [Figure 3.4]. As nerves taken from $Sox2^{HomoOE}$ mice remained severely hypomyelinated we carried out further analysis to determine the expression of the Sox2-IRES-EGFP transgene in the animals. In contrast to what was observed in $Sox2^{HetOE}$ mice, Sox2 and GFP were both highly expressed within the nerves of $Sox2^{HomoOE}$ mice at P60 [Figure 3.7 A-F] and P90 [Figure 3.8 A-F]. Thus having two copies of the Sox2-IRES-EGFP transgene appears to retains the expression of Sox2 and GFP past P21, although we cannot confirm why this is.

In summary, overexpression of Sox2 is able to alter peripheral myelination during development. This was determined by an overall reduction in myelin thickness observed at P7 in both $Sox2^{HetOE}$ and $Sox2^{HomoOE}$ mice, at P21 in $Sox2^{HetOE}$ mice and at P60 in $Sox2^{HomoOE}$ mice. In addition, overexpression of Sox2 also increased the total number of unmyelinatinated axons in a 1:1 relationship with Schwann cells during development, and in adult $Sox2^{HomoOE}$ mice.

To confirm whether the increased number of unmyelinated axons was due to a block in Schwann cell development and radial sorting at the immature phase (prior to Schwann cells forming a 1:1 ratio with axons), further analysis looking at unmyelinated axons was carried out on nerves taken from P7 and P21 $Sox2^{HetOE}$ sciatic nerves and P7 and P60 $Sox2^{HomoOE}$ sciatic nerves. EM analysis revealed that all axons in the sciatic nerves of $Sox2^{HetOE}$ mice at P7 and P21 were ensheathed by either an individual Schwann cell forming a 1:1 ratio with axons $\geq$1µm, or a non-myelinating Schwann cell which groups axons <1µm into structures known as Remak bundles; no naked axons (unassociated) were observed [data not shown]. Similarly at P7 and P60 all axons in the sciatic nerves of $Sox2^{HomoOE}$ mice were ensheathed by either individual Schwann cells forming a 1:1 ratio or non-myelinating Schwann cells [Figure 3.5].

These observations show that Sox2 overexpression does not affect the early stages of axon radial sorting by immature Schwann cells, as clear Schwann cell basal laminae can be observed surrounding individual Schwann cells. However, as seen in Figure 3.5, panel A (asterisks) there does appear to be some delay in the sorting of some large diameter axons in the sciatic nerves of P7 $Sox2^{HomoOE}$ nerves. Nonetheless, this appears to be corrected by P60, as all large diameter axons appear to be sorted into a 1:1 ratio. Thus, Sox2 expression does not result in any long term defects in the segregation of axons; by P60 all large calibre axons (axons >1µm) are sorted into a 1:1 relationship with promyelinating Schwann cell and smaller calibre axons (axons <1µm) are sorted into Remak bundles. We therefore conclude that Schwann cells which overexpress Sox2 are capable of radial sorting and normal development up until the promyelinating stage, which is when Sox2 appears to affect Schwann cell myelination.

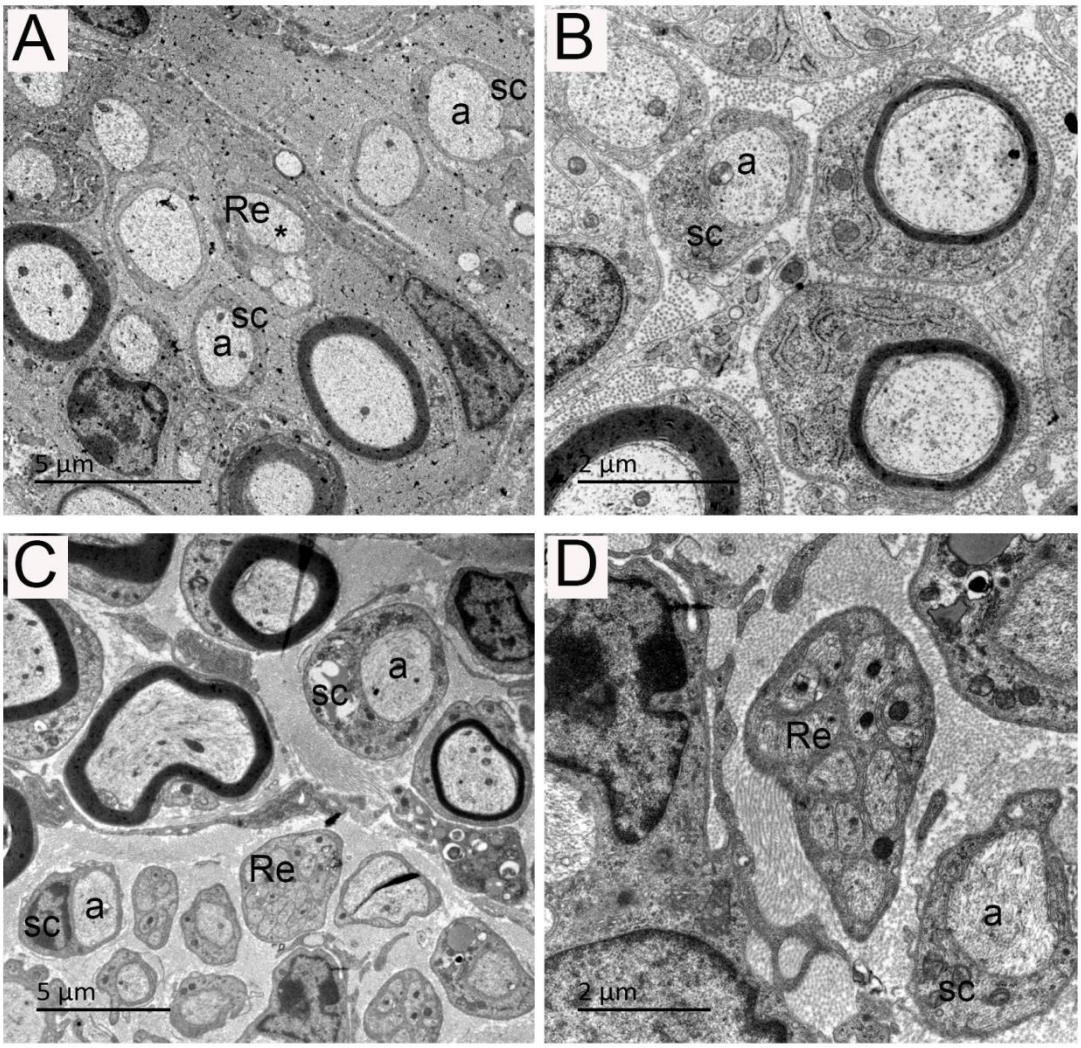

Figure 3. 5: Sox2 overexpression does not affect axonal sorting. Transmission electron micrographs of sciatic nerve sections taken from P7 (A-B) and P60 (C-D) $Sox2^{HomoOE}$ mice. Morphological analysis of unmyelinated axons reveal that all axons are sorted into a 1:1 ratio with Schwann cells at both P7 (A & B), and P60 (C & D). a, Axon; SC, Schwann cell; Re, Remak bundle, *, asterisks identifying a large diameter axon (axon >1µm) in a Remak bundle, panel A.

3.2.3 Sox2 overexpression impairs myelin protein expression

Sox2 is initially expressed during Schwann cell development, and is a marker of immature Schwann cells. More recently Sox2 has been shown to be re-expressed upon nerve injury and following demyelination both *in vitro* and *in vivo* (Woodhoo et al., 2009, Lee et al. 2005, Decker et al., 2006). Furthermore, Sox2 has been shown to negatively regulate the expression of myelin associated genes, including Krox20, Protein Zero (P_0), Gap junction beta-1 protein (GJB1) and N-myc downstream regulated gene 1 (NDRG1) *in vitro*, consequently blocking the ability of Schwann cells to myelinate axons (Le et al., 2005a)

The zinc finger transcription factor Krox20 (also known as Egr2), is a known master regulator of myelination and plays an essential role in activating the expression of myelin associated genes; myelin basic protein (MBP), P_0, peripheral myelin protein 22 (PMP22), as well as the induction of lipid and cholesterol synthesizing enzymes (Topilko et al., 1994, Nagarajan et al., 2001, Parkinson et al., 2004). The expression of Krox20 is critical for Schwann cell myelination and myelin maintenance, as Krox20 null and mutant mice with a hypomorphic Krox20 allele demonstrate severe hypomyelination of the peripheral nerves and impaired expression of myelin associated genes (Topilko et al., 1994, Nagarajan et al., 2001, Le et al., 2005a, Decker et al., 2006). P_0 has also been shown to play a critical role in Schwann cell myelination, as it is involved in the adhesion and compaction of the multi-layered myelin sheath. Reduced expression, mutations and complete loss of P_0 function does not affect Schwann cells forming a 1:1 relationship with large diameter axons ($\geq$1µm in diameter). However, the absence of P_0, reduced P_0 expression and heterozygous P_0 mutations in mice, have all been shown to result in the formation of abnormal and unstable myelination, which begins to degenerate at approximately P21, resulting in reduced motor function and the development CMT-1B (Giese et al., 1992, Hayasaka et al., 1993, Saporta et al., 2012). P_0 is therefore essential for stable compact myelin formation and myelin maintenance. As both Krox20 and P_0 play critical roles in myelination, it was thus essential to determine whether Sox2 was capable of negatively regulating their protein expression, in addition to the expression of other myelin proteins such as MBP, as a mechanism for Sox2 induced hypomyelination [observed in Section 3.2.1].

Sciatic nerves taken from Sox2 Homo control and $Sox2^{HomoOE}$ mice at P7, P21, P60 and P90 were analysed for changes in the expression of myelin proteins by immunohistochemical analysis and western blotting.

At P7, immunohistochemical analysis revealed that Sox2 and green fluorescent protein (GFP) (which is coexpressed with Sox2) [see Section 1.9.2] were highly expressed within the sciatic nerves of $Sox2^{HomoOE}$ mice, whereas no Sox2 or GFP expression was detected in the sciatic nerves of Sox2 Homo control mice (n=3) [Figure 3.6]. Immunolabelling of sciatic nerve sections with antibodies for MBP further revealed that Sox2 reduced the expression of MBP and the number of MBP positive myelin rings in the sciatic nerves of $Sox2^{HomoOE}$ mice, compared to Sox2 Homo control mice (n=3) [Figure 3.6]. These experiments were repeated by western blot, which further revealed that high levels of Sox2 reduced the expression of MBP, as well as Krox20 and P_0 in the sciatic nerves of $Sox2^{HomoOE}$ mice, compared to Sox2 Homo control mice (n=3) [Figure 3.6]. Again at P21, western blot analysis revealed a similar effect; high levels of Sox2 dramatically reduced the expression of Krox20 and MBP within the sciatic nerves of $Sox2^{HomoOE}$ mice, compared to Sox2 Homo control mice (n=3) [data not shown]. An Affymetrix gene array experiment carried out by Dr R.Doddrell, using RNA harvested from rat Schwann cells infected with Sox2/GFP or GFP expressing adenovirus, revealed that β-tubulin 2A expression remains unaltered in the presence of Sox2 overexpression (unpublished data in our group from Dr R.Doddrell and Dr Xin-Peng Dun). β-tubulin 2A was therefore used as a loading control for all experiments.

At P60, immunohistochemical analysis revealed high levels of Sox2 and GFP expression within the sciatic nerves of $Sox2^{HomoOE}$ mice, whereas no Sox2 or GFP expression was detected in the sciatic nerves of Sox2 Homo control mice (n=8 $Sox2^{HomoOE}$, n=6 Sox2 Homo control). Immunolabelling of sciatic nerves with antibodies for Krox20, revealed that Krox20 was clearly reduced in $Sox2^{HomoOE}$ mice, compared to Sox2 Homo control mice (n=4). Accordingly, a reduction in the expression of MBP and the number of MBP positive myelin rings was observed in the sciatic nerves of $Sox2^{HomoOE}$ mice, as well as a reduction in the expression of P_0 and the number of P_0 positive myelin rings, compared to Sox2 Homo control mice (n=4) [Figure 3.7]. These experiments were repeated by western blot which showed

that Sox2 decreased the expression of Krox20 and myelin proteins P_0 and MBP (n=4) [Figure 3.7].

At P90, immunohistochemical analysis revealed that Sox2 and GFP was still highly expressed within the sciatic nerves of $Sox2^{HomoOE}$ mice, whereas no Sox2 or GFP expression was detected in the sciatic nerves of Sox2 Homo control mice (n=3). Similarly, the expression of MBP and the number of MBP positive myelin rings were both reduced within the sciatic nerves of $Sox2^{HomoOE}$ mice, compared to Sox2 Homo control nerves (n=3) [Figure 3.8]. Western blot analysis at P90 further revealed that Sox2 expression remained high the sciatic nerves of $Sox2^{HomoOE}$ mice and was able to reduce both Krox20 and MBP protein expression (n=3) [Figure 3.8].

We therefore confirm that Sox2 is able to inhibit the expression of myelin associated proteins, in both early developing (P7 and P21) and adult (P60 and P90) Schwann cells. This adds to the increasing evidence that Sox2 is a true negative regulator of Schwann cell myelination *in vivo*.

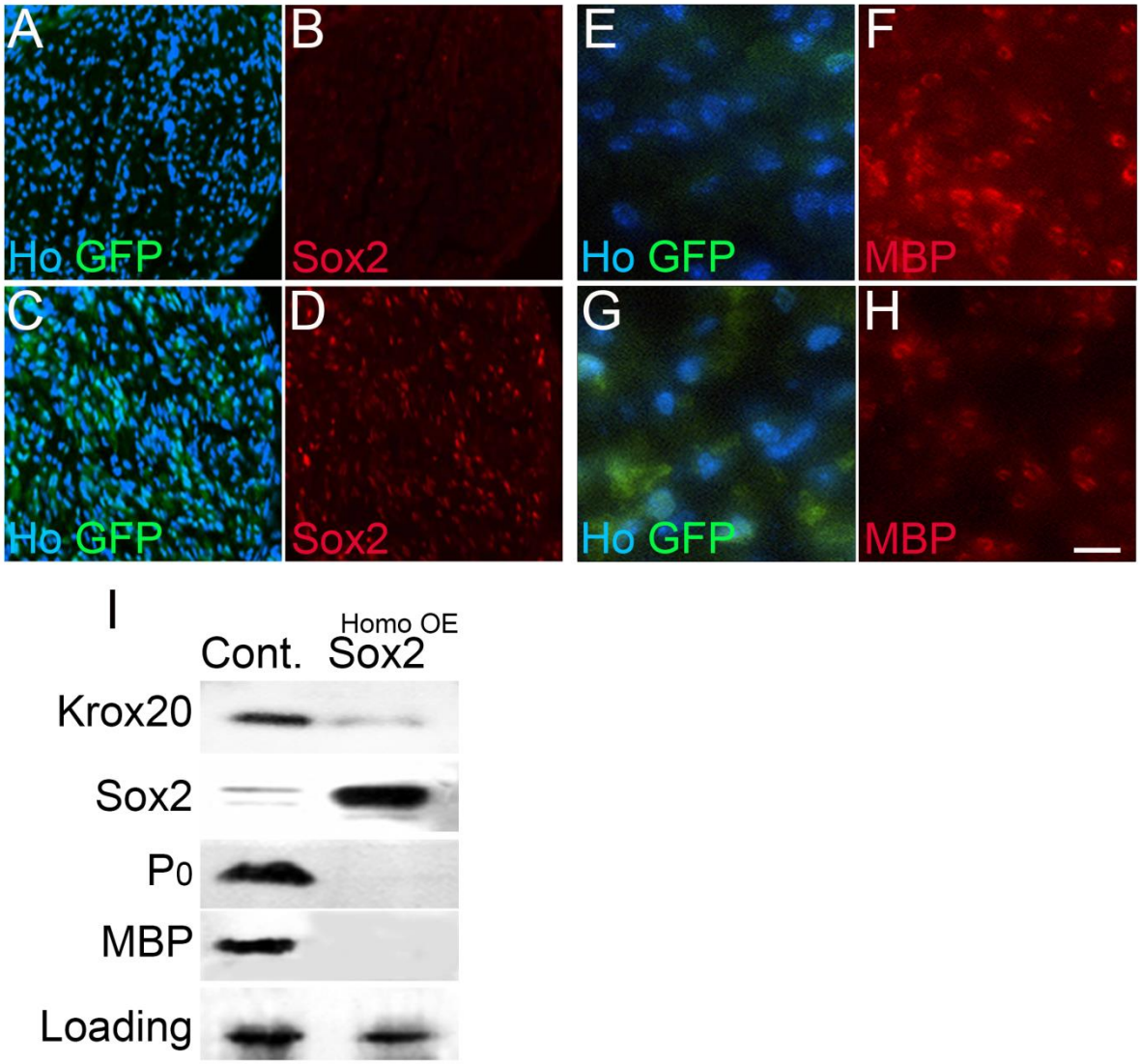

Figure 3. 6: Sox2 impairs myelin protein expression during development. Immunofluorescent staining for Sox2 (A-D) shows that control nerves do not express Sox2 (B), whilst $Sox2^{HomoOE}$ nerves show high expression of Sox2 (D) at P7. Note, control nerves do not express GFP (A), whereas GFP is expressed in the nerves of $Sox2^{HomoOE}$ mice (C). Immunofluorescent staining for MBP (E-H) shows that control nerves express high levels of MBP and more frequent myelin ring structures (F), compared to $Sox2^{HomoOE}$ nerves, which express reduced levels of MBP and have fewer myelin rings structures (H) at P7. Western blot (I) showing reduced expression of Krox20, P_0 and MBP in $Sox2^{HomoOE}$ nerves compared to control nerves at P7 (n=3). Images taken using 40x objective, scale bar is 20µm.

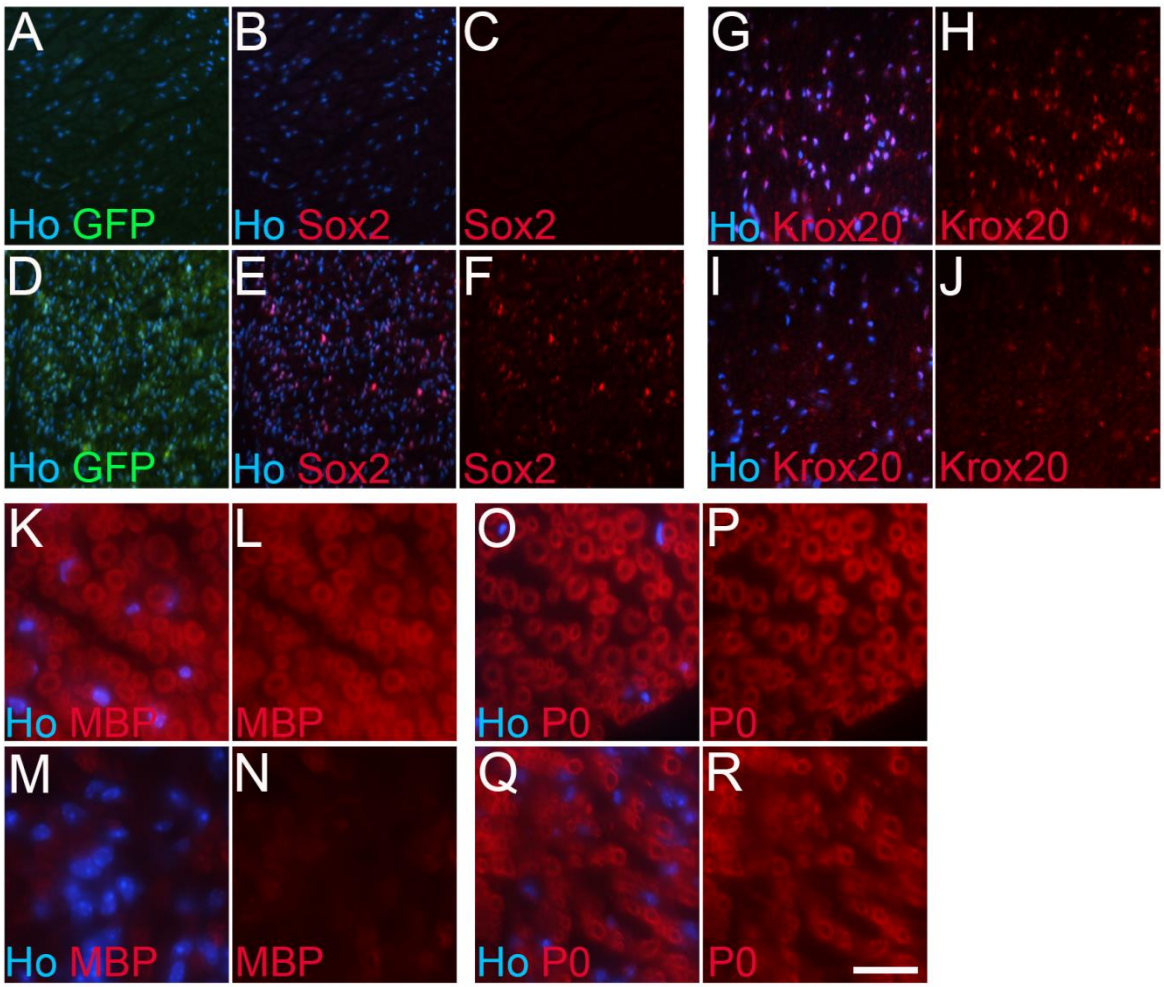
A
Ho GFP
B
Ho Sox2
C
Sox2
G
Ho Krox20
H
Krox20
D
Ho GFP
E
Ho Sox2
F
Sox2
I
Ho Krox20
J
Krox20
K
Ho MBP
L
MBP
O
Ho P0
P
P0
M
Ho MBP
N
MBP
Q
Ho P0
R
P0

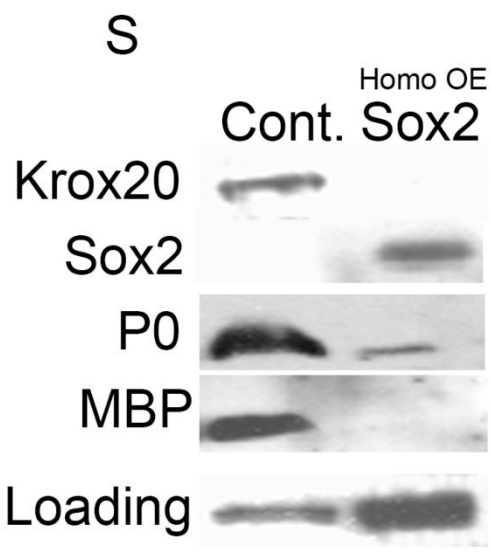
S
Homo OE
Cont. Sox2
Krox20
Sox2
P0
MBP
Loading

Figure 3. 7: Sox2 impairs Schwann cell myelin protein expression at P60. Immunofluorescent staining using antibodies against Sox2 (A-F) shows that Sox2 Homo control nerves do not express Sox2 (B & C), whereas $Sox2^{HomoOE}$ nerves show high expression of Sox2 (E & F) at P60 . Note, control nerves do not express GFP (A), whereas $Sox2^{HomoOE}$ nerves highly express GFP (D). Immunofluorescent staining using antibodies against Krox20 (G-J) shows that Sox2 Homo control nerves have a high abundance of Krox20 positive nuclei (G & H), whereas $Sox2^{HomoOE}$ nerves have few Krox20 positive nuclei (I-J). Immunofluorescent staining using antibodies against MBP (K-N) shows that Sox2 Homo control nerves express high levels of MBP and numerous MBP positive myelin ring structures (K & L), whereas $Sox2^{HomoOE}$ nerves express reduced levels of MBP and have fewer myelin rings structures (M & N) at P60. Immunoflurescent staining using antibodies against P_0 (O-R) shows that Sox2 Homo control nerves have thicker and more numerous P_0 positive myelin ring structures (O & P) compared to $Sox2^{HomoOE}$ nerves (Q & R). Western blot (S) showing reduced expression of Krox20, P_0 and MBP and high expression of Sox2 in the sciatic nerves of $Sox2^{HomoOE}$ mice, compared to Sox2 Homo controls at P60 (n=4). Images taken using 40x objective, scale bar is 20µm.

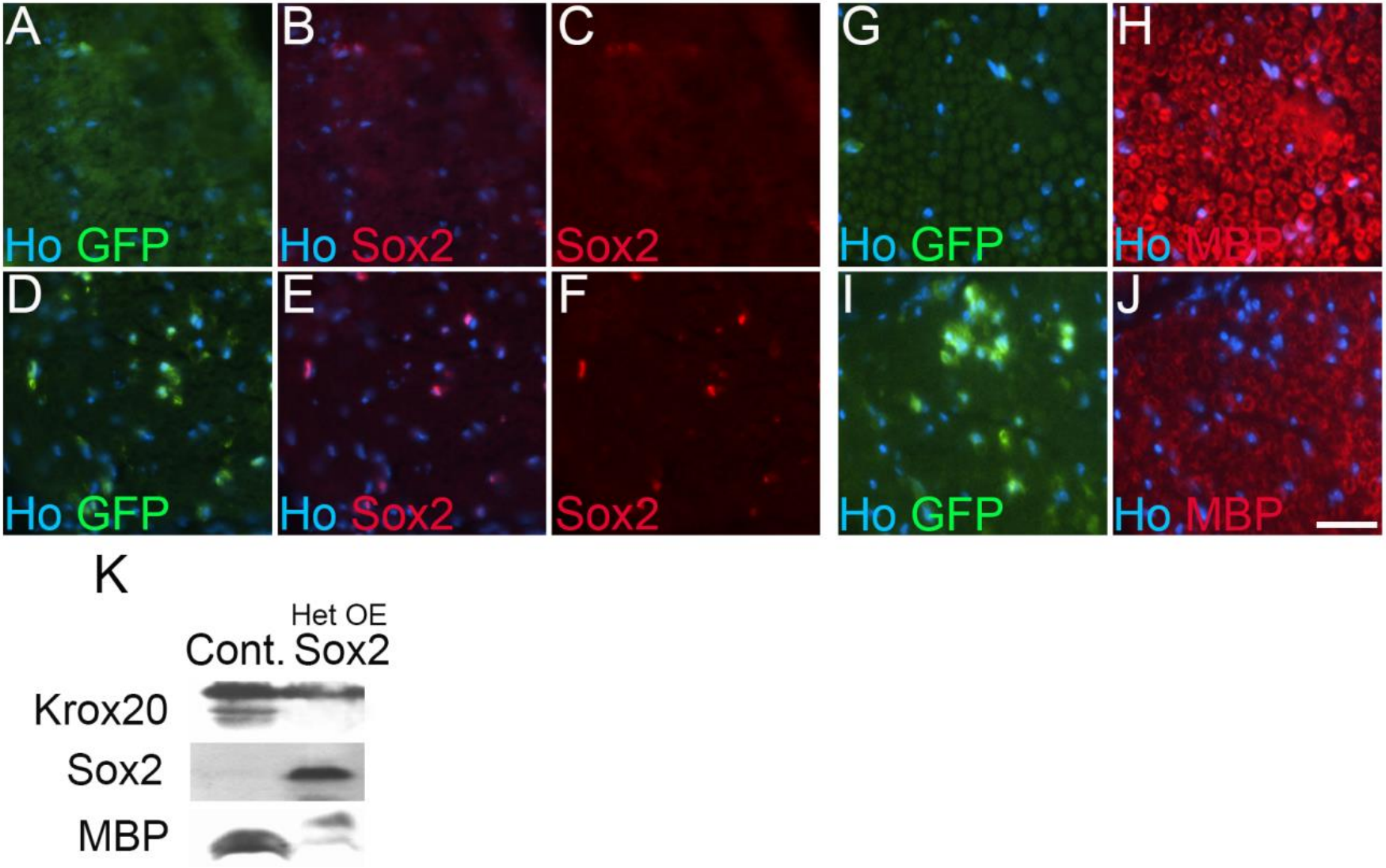
A
Ho GFP
B
Ho Sox2
C
Sox2
G
Ho GFP
H
Ho MBP
D
Ho GFP
E
Ho Sox2
F
Sox2
I
Ho GFP
J
Ho MBP
K
Het OE
Cont. Sox2
Krox20
Sox2
MBP

Figure 3. 8: Sox2 impairs myelin protein expression at P90. Immunofluorescent staining for Sox2 (A-F) shows that control nerves do not express Sox2 (B & C), whereas $Sox2^{HomoOE}$ nerves show high expression of Sox2 (E & F) at P90. Immunofluorescent staining for MBP (G-J) shows that control nerves express high levels of MBP and numerous MBP positive myelin ring structures (H), whereas $Sox2^{HomoOE}$ nerves express reduced levels of MBP and have fewer myelin rings structures (J) at P90. Western blot (K) showing overexpression of Sox2 leads to reduced Krox20 and MBP expression in the sciatic nerves of $Sox2^{HomoOE}$ mice, compared to controls at P90 (n=3). Images taken using 40x objective, scale bar is 20µm.

3.2.4 cJun expression is maintained in the sciatic nerves of Sox2 overexpressing mice

Like Sox2, cJun has been identified as a marker of immature Schwann cells and a negative regulator of myelination (Parkinson et al., 2008, Parkinson et al., 2004). Furthermore, Parkinson et al. (2008) identified that cJun and Sox2 are co-expressed in Schwann cells after sciatic nerve injury, however it is unclear whether these two transcription factors co-regulate one another. We therefore wanted to identify whether cJun levels were also elevated within the sciatic nerves of Sox2 overexpressing mice.

Sciatic nerve sections taken from P7 and P60 Sox2 Homo control and $Sox2^{HomoOE}$ mice were immunolabelled with antibodies against cJun. At P7 a minimal difference in cJun expression was observed between Sox2 Homo control and $Sox2^{HomoOE}$ nerves (n=3). However at P60 a more striking difference in the number of cJun positive nuclei was observed; whilst minimal cJun expression was detected in the sciatic nerves of Sox2 Homo control mice, clearly elevated nuclear cJun expression was detected in the sciatic nerves of $Sox2^{HomoOE}$ mice (n=3) [Figure 3.9].

These results further support our previous findings that Sox2 maintains Schwann cells at the immature Schwann cells state, marked by the expression of an additional immature Schwann cell marker, cJun. Furthermore, our results support previous studies show that Sox2 and cJun are co-expressed in immature Schwann cells.

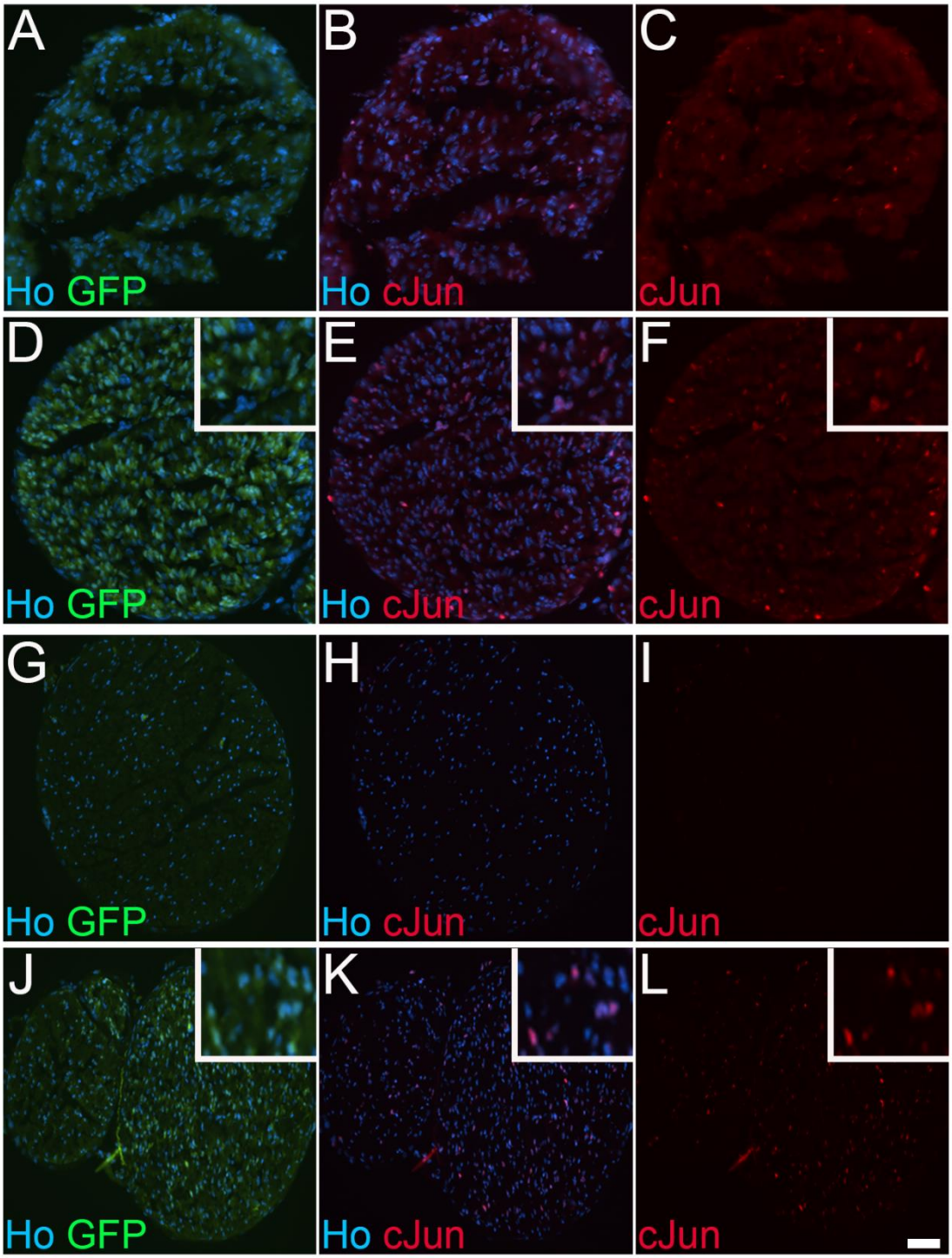

Figure 3. 9: cJun expression is elevated in Sox2 overexpressing nerves. Sciatic nerve sections taken from P7 and P60 Sox2 Homo control and $Sox2^{HomoOE}$ mice were immunolabelled with antibodies against cJun. Immunofluorescent staining for cJun at P7 (A-F) shows that $Sox2^{HomoOE}$ nerves express slightly higher levels of cJun (D-F) compared to Sox2 Homo controls (A-C). At P60 $Sox2^{HomoOE}$ nerves showed strong nuclear expression of cJun (J-L), whereas only minor levels of cJun was detected in Sox2 Homo control nerves (G-I) (n=3). Images taken using 20x objective, (D,E,F, J, K, L inset 200x), scale bar is 20µm.

3.2.5 Sox2 maintains N-cadherin expression *in vivo*

Enforced expression of Sox2 in Schwann cells, has been shown to directly drive the re-localisation of N-cadherin, a transmembrane protein which mediates cell-cell adhesion in a calcium dependent manner, and thus cause the clumping of Schwann cells into clusters (Parrinello et al., 2010, unpublished observation by Dun et al., submitted: under review). Like Sox2, N-cadherin is highly expressed in Schwann cell precursors and immature Schwann cells, but its expression begins to reduce as Schwann cells differentiate into myelinating cells (Wanner et al., 2006, Crawford et al., 2008). Furthermore, N-cadherin is re-expressed in dedifferentiated Schwann cells following nerve injury and is re-localized to the cell contact junctions under the regulation of Sox2, allowing for Schwann cell sorting (Parrinello et al., 2010). As these studies have all confirmed that Sox2 is able to influence N-cadherin localisation, and that N-cadherin is a marker of undifferentiated Schwann cells *in vitro*, we wanted to examine whether the localisation and expression of N-cadherin is altered in the sciatic nerves of Sox2 Homo control and $Sox2^{HomoOE}$ mice at P60 by immunofluorescent staining.

Sox2 Homo control nerve sections stained with antibodies for N-cadherin showed weak N-cadherin expression. In contrast, N-cadherin was up regulated in the sciatic nerves of $Sox2^{HomoOE}$ mice and formed a clear honeycomb like structure (n=3) [Figure 3.10]. These results suggest that Sox2 is able to directly increase the expression of N-cadherin in Schwann cells *in vivo*; making this the first study to confirm that Sox2 is able to regulate N-cadherin expression in an intact nerve. As N-cadherin is a marker of immature Schwann cells, these results provide additional evidence that Sox2 maintains Schwann cells in an undifferentiated state.

β-catenin is a known binding partner of N-cadherin and has been shown to co-localise with N-cadherin at the Schwann cell-Schwann cell interface, as well as the Schwann cell-axon interface during Schwann cell development (Lewallen et al., 2011). Further studies also confirmed that both N-cadherin and β-catenin are necessary for axonal induced Schwann cell proliferation and may also play a role in establishing Schwann cell polarity and the initiation of myelination (Gess et al., 2008, Lewallen et al., 2011). We therefore wanted to test whether Sox2 overexpression *in vivo* would also cause relocalisation of β-catenin.

Experiments carried out *in vitro* revealed that β-catenin expression was increased in Sox2 adenoviral infected Schwann cells, in contrast only faint β-catenin expression was detected in GFP adenoviral infected Schwann cells (unpublished observation by Dun et al., submitted: under review). Furthermore, immunofluorescent staining for β-catenin *in vivo* revealed weak cell membrane staining in the sciatic nerves of Sox2 Homo control mice, however strong cell membrane staining was detected in the sciatic nerves of $Sox2^{HomoOE}$ mice at P60 (n=3) [Figure 3.11].

These findings further supports the evidence that continued Sox2 expression maintains Schwann cells in an immature state and is able to either maintain or up regulate the protein expression of both N-cadherin and β-catenin *in vivo*.

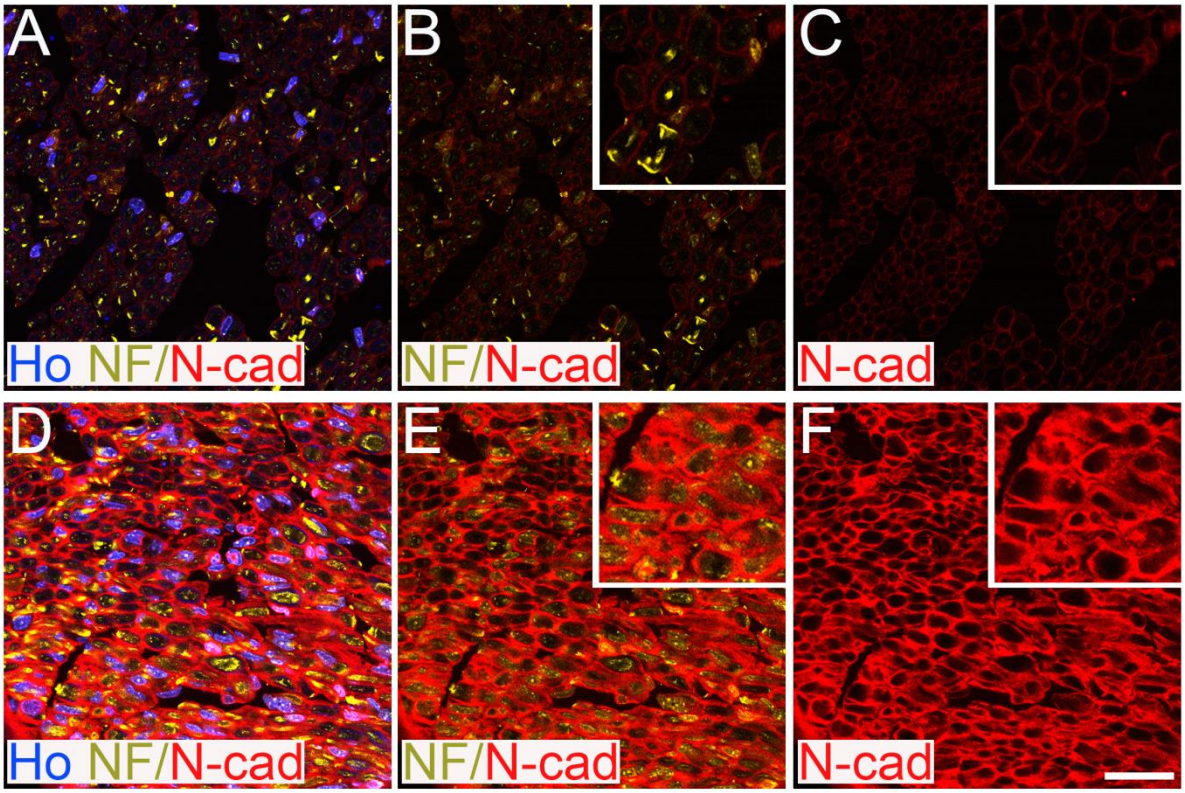

Figure 3. 10: N-cadherin expression is elevated in Sox2 overexpressing nerves. Immunofluorescent staining for neurofilament and N-cadherin (A-F) revealed weak expression of N-cadherin in the sciatic nerves of Sox2 Homo control mice (A-C), whereas strong expression of N-cadherin was observed in the sciatic nerves of $Sox2^{HomoOE}$ mice at P60 (D-F) (n=3). Images taken using 40x objective, (B, C, E, F, inset 80x), scale bar is 20µm.

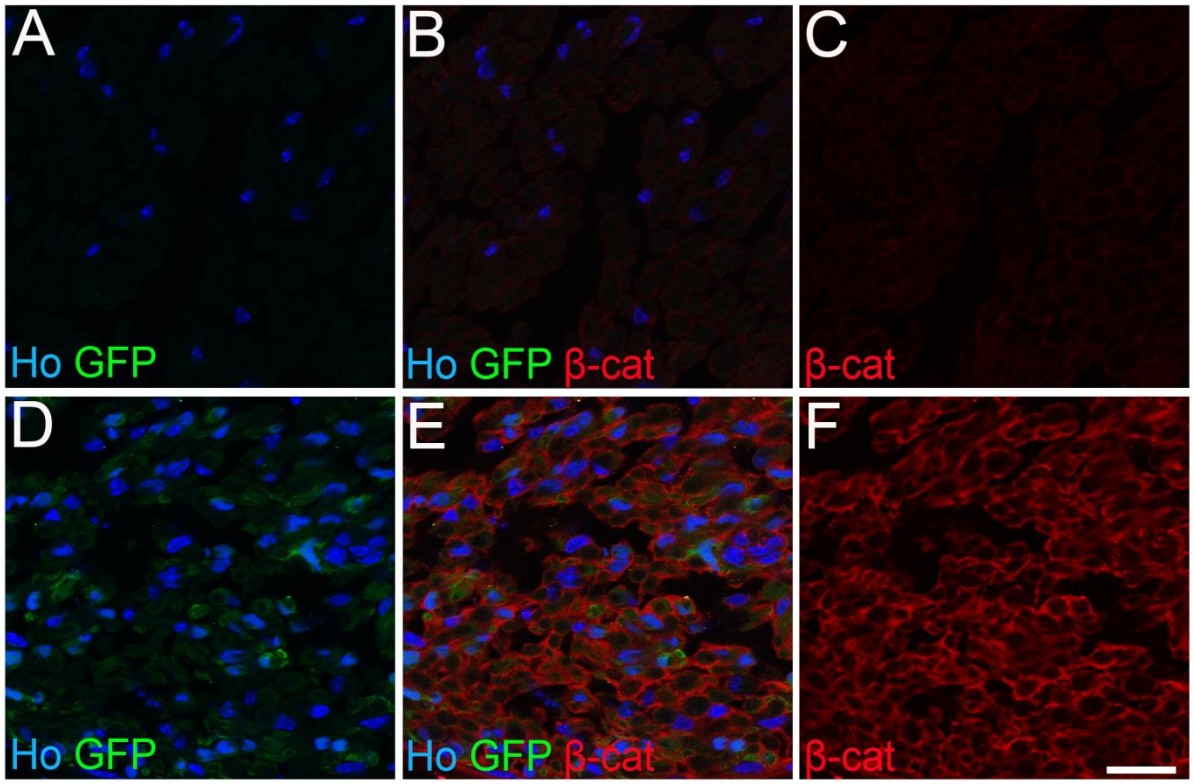

Figure 3. 11: β-catenin expression is elevated in Sox2 overexpressing nerves. Immunofluorescent staining for β-catenin (A-F) revealed weak expression of β-catenin in the sciatic nerves of Sox2 Homo control mice (B-C), whereas strong expression of β-catenin was observed in the sciatic nerves of $Sox2^{HomoOE}$ mice at P60 (E-F) (n=3). Images taken using 40x objective, scale bar is 20µm.

3.2.6 Sox2 reduces the expression of Sox10 *in vitro* and *in vivo*

Sox2 has previously been shown to block the induction of Krox20 *in vitro* by cAMP (Le et al., 2005a). More recently, it was further identified that Sox2 is able to block the ability of Sox10 and NFATc4 to synergistically bind and activate the Krox20 Myelin Specific Enhancer (MSE) region, as well as the P_0 promoter, thus preventing the transcriptional activation of Krox20 and P_0 (Kao et al., 2009). However, the effect of Sox2 on the induction of transcription factors upstream of Krox20 and P_0, such as Sox10 is still unknown. We therefore sough to identify whether Sox2 overexpression would impair Sox10 expression *in vitro* and *in vivo*.

To test this *in vitro*, Schwann cells were infected with either control GFP or Sox2/GFP expressing adenovirus for 24 hours in defined medium supplemented with 2μM forskolin, which was then removed and replace with defined medium without forskolin for a further 24hours. The expression of Sox2 and Sox10 was then examined by immunofluorescent staining.

Schwann cells infected with control GFP-expressing adenovirus showed pronounced expression of GFP and low levels of Sox2 expression, whereas Schwann cells infected with Sox2/GFP-expressing adenovirus showed clear expression of GFP and marked expression of Sox2 (n=3) [Figure 3.12 A-D]. Analysis of Sox10 expression revealed that Schwann cells infected with control GFP-expressing adenovirus showed pronounced expression of Sox10 within their nucleus, whereas Schwann cells infected with Sox2/GFP-expressing adenovirus showed very faint Sox10 expression (n=3) [Figure 3.12 E-H].

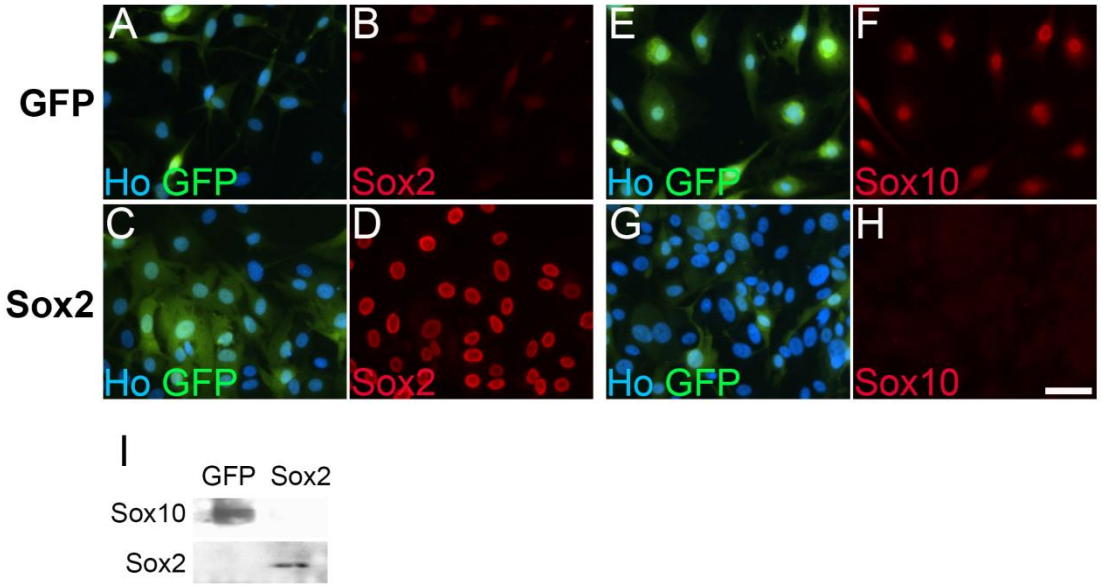

Figure 3. 12 :Sox2 blocks Sox10 expression *in vitro*. Rat Schwann cells were infected with control GFP (A, B, E, F) or Sox2/GFP (C, D, G, H) expressing adenovirus. Immunofluorescent staining for Sox2 (A-D) shows high express of Sox2 in the cells infected with Sox2/GFP (D), whereas only faint Sox2 expression could be detected in control cells (B). Immunofluorescent staining for Sox10 (E-H) shows high expression of Sox10 in control cells (F), whereas Sox10 expression was undetectable in Sox2 infected cells (H) (n=3). Western blot (I) shows reduced expression of Sox10 in the presence of high Sox2 expression (n=1). Images taken using 40x objective, scale bar is 20µm.

Further analysis by western blot, showed that the expression of Sox10 was blocked in Schwann cells infected with Sox2/GFP-expressing adenovirus compared to Schwann cells infected with control GFP-expressing adenovirus (n=1) [Figure 3.12 I]. These results identify that Sox2 is able to block the expression of Sox10 by Schwann cells *in vitro* which could explain the mechanisms by which Sox2 impairs the expression of Krox20 and myelin proteins P_0 and MBP.

As enforced Sox2 expression was sufficient to block Sox10 expression *in vitro*, the next most important question was whether Sox2 was able to block Sox10 expression *in vivo*. To test this we followed up these experiments by analysing the expression of Sox10 in the sciatic nerves of Sox2 Homo control and $Sox2^{HomoOE}$ mice by immunohistochemistry and western blotting. At P7 and P14, western blot analysis revealed that Sox10 expression was quite similar in the sciatic nerves of $Sox2^{HomoOE}$ mice and Sox2 Homo control mice (n=3 at P7, n=2 at P14). Nonetheless, immunohistochemical analysis revealed that Sox10 expression was slightly reduced within the sciatic nerves of P7 $Sox2^{HomoOE}$ mice compared to Sox2 Homo control mice at P7 (n=3) [Figure 3.13]. Lastly we analysed the expression of Sox10 in P60 $Sox2^{HomoOE}$ mice, where the phenotype of the mice appears to be much more severe. We observed a more dramatic reduction in the expression of Sox10 at this time-point, as well as an shift in the expression of Sox10 towards being more cytoplasmic, rather than nuclear in the nerves of $Sox2^{HomoOE}$ mice, compared to Sox2 Homo control mice at P60 (n=3) [Figure 3.13].

Our preliminary data suggests that maintained overexpression of Sox2 leads to reduced Sox10 expression and affects Sox10 nuclear localisation. As Sox10 is an essential transcription factor required for Schwann cell myelination and myelin maintenance, antagonising Sox10 expression could be a mechanism by which Sox2 reduces myelination during development, and progressively enhances hypomyelination in adult $Sox2^{HomoOE}$ Schwann cells (Bremer et al., 2011).

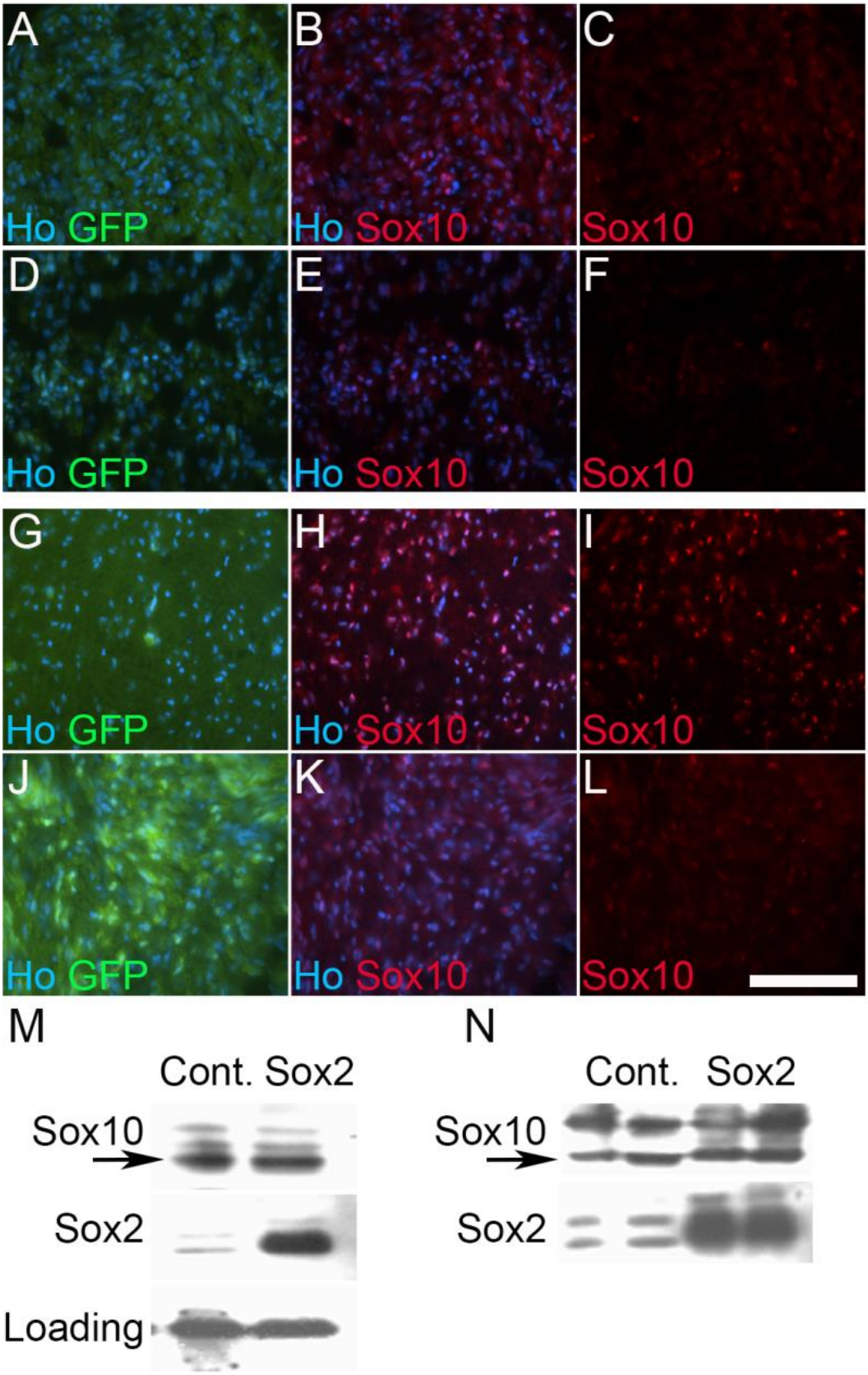
A
Ho GFP
B
Ho Sox10
C
Sox10
D
Ho GFP
E
Ho Sox10
F
Sox10
G
Ho GFP
H
Ho Sox10
I
Sox10
J
Ho GFP
K
Ho Sox10
L
Sox10
M
Cont. Sox2
Sox10
Sox2
Loading
N
Cont. Sox2
Sox10
Sox2

Figure 3. 13: Sox10 expression is slightly altered *in vivo* by Sox2 overexpression. Sciatic nerves taken from P7 (A-F) and P60 (G-L) Sox2 Homo control and $Sox2^{HomoOE}$ mice were immunolabelled with antibodies against Sox10. Immunofluorescent staining showed weaker Sox10 expression within the sciatic nerves of $Sox2^{HomoOE}$ mice (D-F), compared to Sox2 Homo control (A-C) at P7 (n=3). Immunofluorescent staining at P60 again showed weaker and less nuclear localised Sox10 expression within the sciatic nerves of $Sox2^{HomoOE}$ mice (J-L) compared to Sox2 Homo control mice (G-I) (n=3). Western blots (M-N) showing similar levels of Sox10 expression in response to elevated Sox2 levels at P7 (M) (n=3) and P14 (N) (n=2). Images taken using 40x objective, scale bar is 20µm.

3.2.7 Sox2 reduces the expression of myelin associated genes, in addition to upregulating the expression of serine protease inhibitor neuroserpin

Sox2 overexpression has been shown to suppress the expression of myelin related genes, including Krox20, MBP and periaxin, as well as the expression of Nectin like 4 (Necl4), an adhesion molecule essential for normal Schwann cell myelination (Le et al., 2005a, Maurel et al., 2007, Spiegel et al., 2007) (unpublished data in our group by Dr R.Doddrell). We therefore wanted to confirm whether Sox2 was also capable of suppressing the gene expression of Krox20 and Necl4 *in vivo*.

RNA was extracted from the sciatic nerves of Sox2 Het control and $Sox2^{HetOE}$ nerves at P20, reverse transcribed and analysed using semi quantitative RT-PCR. We were able to identify that both Krox20 and Necl4 gene expression was reduced in the sciatic nerves of $Sox2^{HomoOE}$ mice compared to Sox2 Homo control mice at P20 [Figure 3.14] (n=1 per genotype).

An Affymetrix gene array experiment carried out by Dr R.Doddrell, using RNA harvested from rat Schwann cells infected with Sox2/GFP or GFP expressing adenovirus, identified that overexpression of Sox2 massively up regulates the mRNA expression of Neuroserpin (55 fold increase). Neuroserpin is a secreted serine protease inhibitor which has previously been identified to regulate the expression and localization of N-cadherin in PC12 cells (Lee et al., 2008). As we have observed that Sox2 appears to increase the expression of N-cadherin in the nerves of $Sox2^{HomoOE}$ nerves, we wanted to follow this up and determine whether Sox2 also influenced the gene expression of Neuroserpin *in vivo.* Using semi-quantitative PCR we were able to reveal that overexpression of Sox2 resulted in a 1.7 fold increase in the expression of Neuroserpin in the sciatic nerves of $Sox2^{HetOE}$ mice at P20; however this data is preliminary and more repeats need to be carried out [Figure 3.14] (n=1 per genotype).

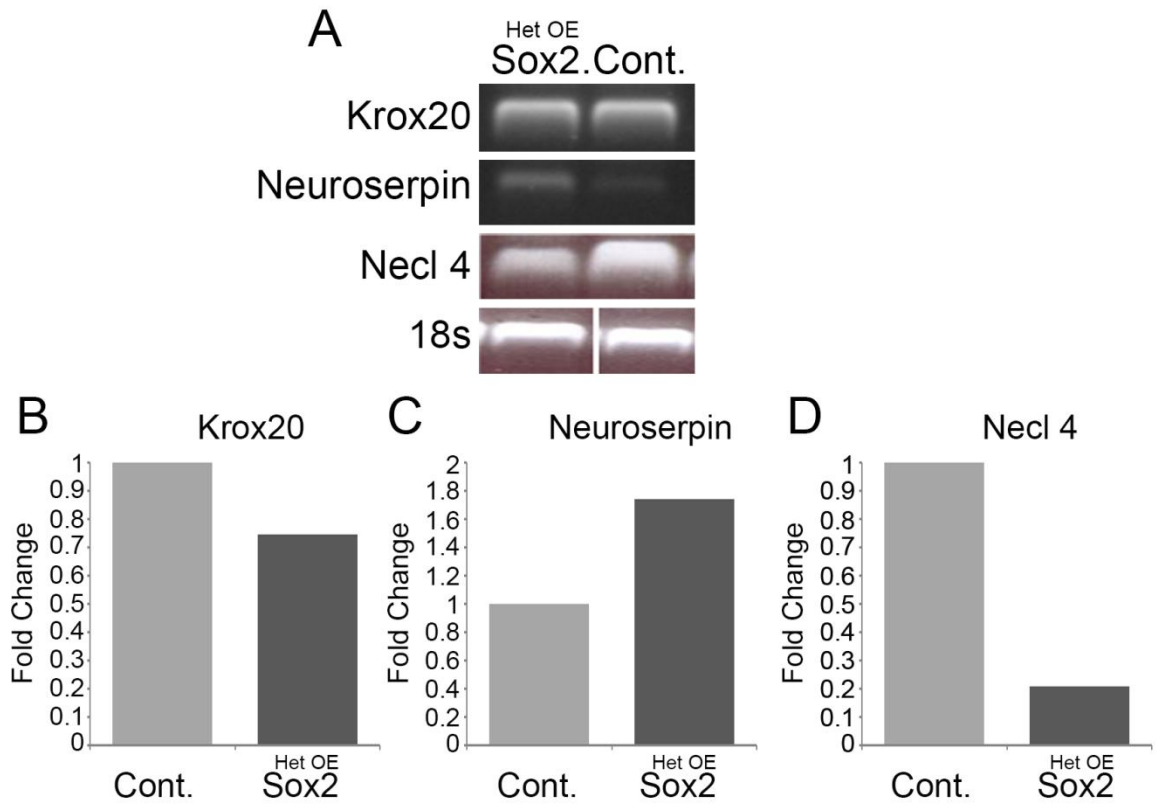

Figure 3. 14: Sox2 alters the gene expression of Krox20, Necl4 and Neuroserpin. Agarose gel electrophoresis of reverse transcription PCR reactions (A), using RNA prepared from the sciatic nerves of Sox2 Het control and $Sox2^{HetOE}$ mice to analyse the expression of Krox20, Neuroserpin and Necl4. Graph (B) showing Sox2 overexpression represses the gene expression of Krox20 (n=1). Graph (C) showing Sox2 overexpression up-regulates the gene expression of Neuroserpin (n=1). Graph (D) showing Sox2 overexpression represses the gene expression of Necl4 (n=1).

3.2.8 Sox2 enhances Schwann cell proliferation

When previously analysing the sciatic nerves of Sox2 Homo control and Sox2^{HomoOE} mice for changes in myelin proteins by immunohistochemical analysis, we observed an increased number of nuclei in the sciatic nerves of Sox2^{HomoOE} mice. To determine whether Sox2 overexpression did in fact alter the number of nuclei within these nerves compared to Sox2 Homo control nerves, sciatic nerve sections were stained with Hoechst dye and nuclei counts were made at P3, P7 and P60.

At P3, Sox2^{HomoOE} nerves showed a 7 ± 5% increased number of nuclei per nerve section (610.5 ± 31 nuclei per nerve section) compared to Sox2 Homo control nerves (565 ± 39.8 nuclei per nerve section), although this was not significant (P=0.4, n=4) [Figure 3.15]. At P7, the number of nuclei present in the sciatic nerves of Sox2^{HomoOE} (693 ± 67 nuclei per nerve section) was increased by 35 ± 12%, compared to Sox2 Homo control nerves (512.2 ± 70 nuclei per nerve section), although again this was not yet significant (P=0.068, n=5) [Figure 3.16]. Nonetheless, at P60 the number of nuclei present in the sciatic nerves of Sox2^{HomoOE} mice (870.3 ± 66 nuclei per nerve section), was significantly increase by 70 ±13% compared to Sox2 Homo control nerves (511.3±62 nuclei per nerve section) (P<0.01, n=3) [Figure 3.17]. Overall these results confirm that Sox2 increases the number of nuclei within the sciatic nerves of Sox2^{HomoOE} mice, however at this stage it was not clear if this is due to an increase in Schwann cell proliferation, a reduction in Schwann cell apoptosis or an increased infiltration of other cells.

To confirm whether Sox2 enhances the number of nuclei in the nerves of Sox2^{HomoOE} mice, by increasing Schwann cell proliferation, sciatic nerve sections taken from Sox2 Homo control and Sox2^{HomoOE} mice at P3, P7 and P60 were stained with antibodies for Ki67, a cellular marker of proliferation. It has previously been published that Sox2 enhances proliferation in stem cells and different cancer cell types, but more specifically that Sox2 is capable of enhancing the proliferative capacity of Schwann cells in response to the mitogen β-neuregulin (Chen et al., 2008, Le et al., 2005a, Lu et al., 2010a).

At P3, no significant change in Schwann cell proliferation was observed in the sciatic nerves of Sox2^{HomoOE} mice (106.25 ± 21 Ki67 positive nuclei per nerve section) compared to Sox2 Homo control nerves (108 ± 57 Ki67 positive nuclei per nerve

section) (P>0.05, n=4) [data not shown]. However, at P7 a significant increase in Schwann cell proliferation (1.9 fold increase) was observed in the sciatic nerves of $Sox2^{HomoOE}$ mice compared to Sox2 Homo controls; in the sciatic nerves of $Sox2^{HomoOE}$ mice there was an average total of 43.6 ± 6.62 Ki67 positive nuclei per nerve section, whereas in the sciatic nerves of Sox2 Homo control mice there was an average total of 22.83 ± 5.7 Ki67 positive nuclei per nerve section (P<0.05, n=5 $Sox2^{HomoOE}$, n=6 Sox2 Homo control) [Figure 3.18]. Similarly, at P60 a significant increase in Schwann cell proliferation (3.3 fold increase) was observed in the sciatic nerves of $Sox2^{HomoOE}$ mice compared to Sox2 Homo controls; in the sciatic nerves of $Sox2^{HomoOE}$ mice there was an average total of 10.75 ± 1.65 Ki67 positive nuclei per nerve section, whereas in the sciatic nerves of Sox2 Homo control mice there was an average total 3.25 ± 1.1 Ki67 positive nuclei per nerve section (P<0.01, n=4) [Figure 3.19]. These results show clearly for the first time that Sox2 is able to directly enhance Schwann cell proliferation *in vivo*.

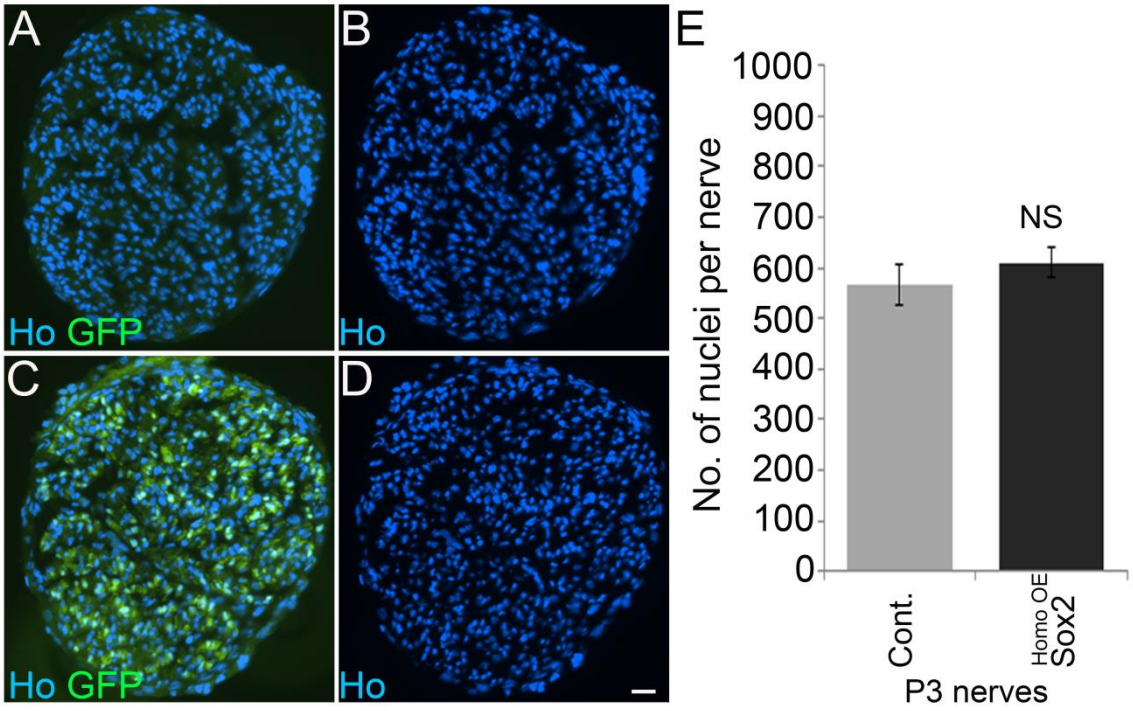

Figure 3. 15: Number of nuclei in the nerves of P3 control and Sox2 overexpressing mice. P3 Sox2 Homo control (A and B) and Sox2^{HomoOE} nerve sections (C and D) stained with Hoechst nuclear dye. Graph (E) showing a slight increase in the average number of nuclei per transverse nerve section taken from Sox2^{HomoOE} mice, compared to Sox2 Homo controls at P3: note this change was not significant ($P>0.05$, $n=4$ per genotype). Images taken using 20x objective, scale bar is 20µm.

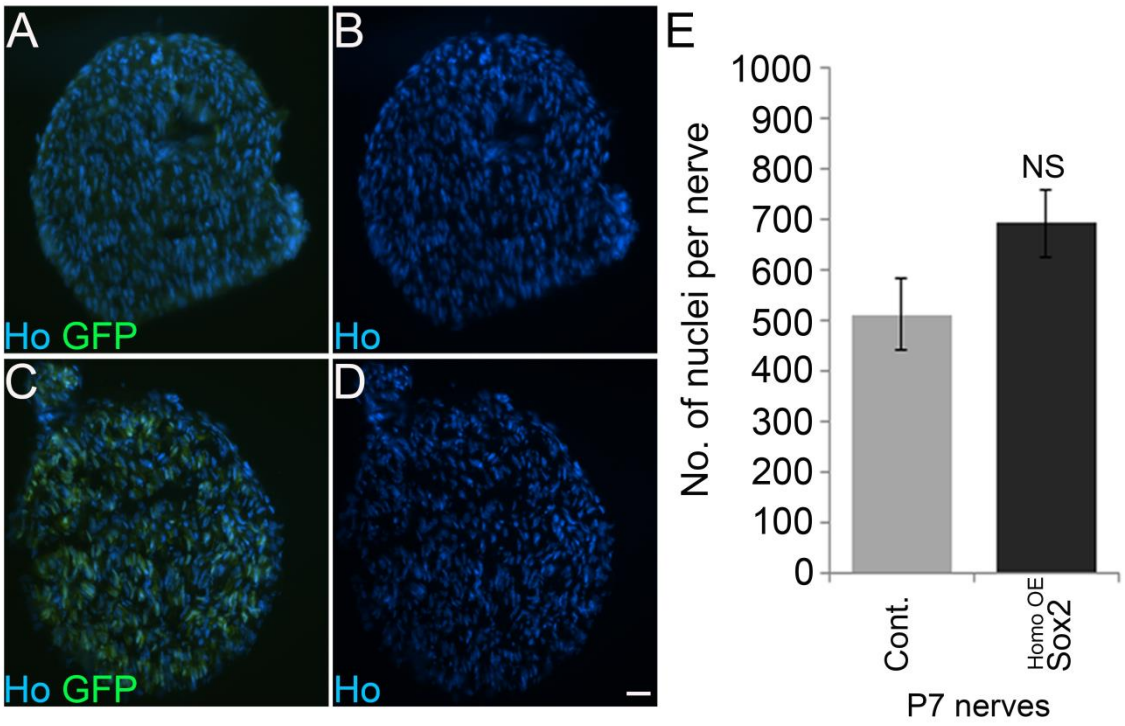

Figure 3. 16: Number of nuclei in the nerves of P7 control and Sox2 overexpressing mice. P7 Sox2 Homo control (A and B) and $Sox2^{HomoOE}$ nerve sections (C and D) stained with Hoechst nuclear dye. Graph (E) showing the number of nuclei per Sox2 Homo control and $Sox2^{HomoOE}$ transverse nerve section at P7: note an increased number of nuclei in the nerves of $Sox2^{HomoOE}$ mice, compared to Sox2 Homo controls, although this was not significant ($P>0.05$, n=5 per genotype). Images taken using 20x objective, scale bar is 20µm.

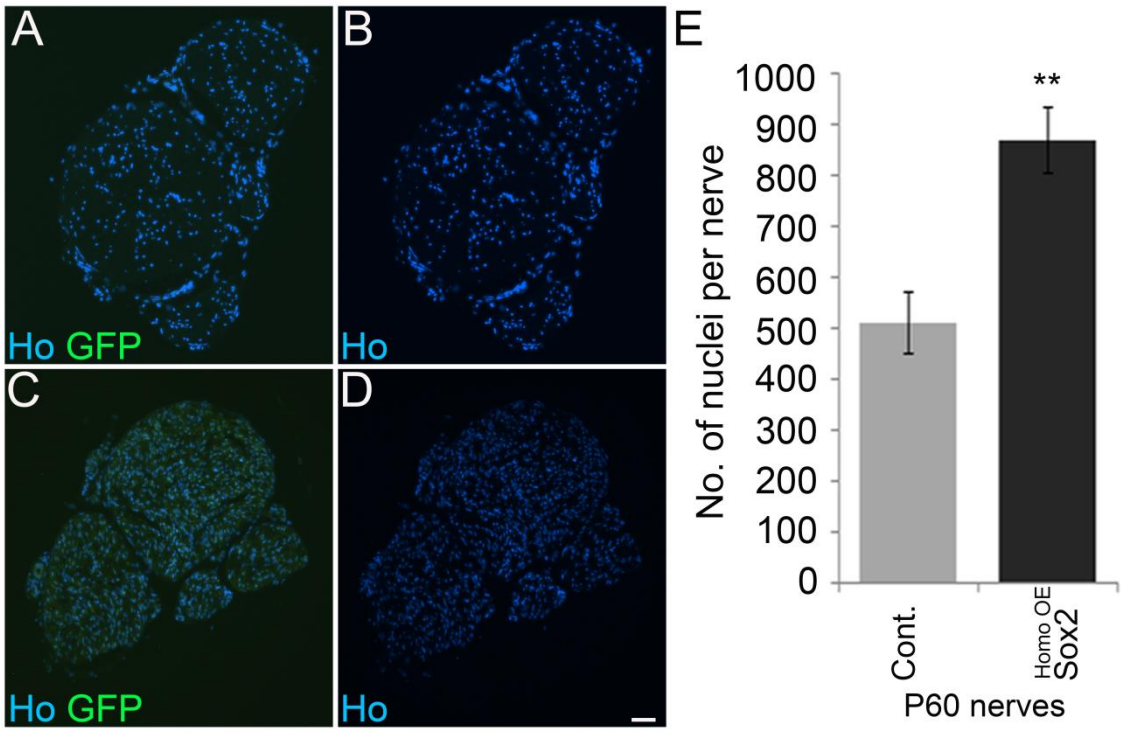

Figure 3. 17: Increased number of nuclei in the nerves of P60 Sox2 overexpressing mice. P60 Sox2 Homo control (A and B) and Sox2^{HomoOE} nerves sections (C and D) stained with Hoechst nuclear dye. Graph (E) showing a significant increase in the number of nuclei per transverse nerve in Sox2^{HomoOE} mice, compared to Sox2 Homo controls at P60 ($P<0.01$, n=3 per genotype). Images taken using 20x objective, scale bar is 20µm.

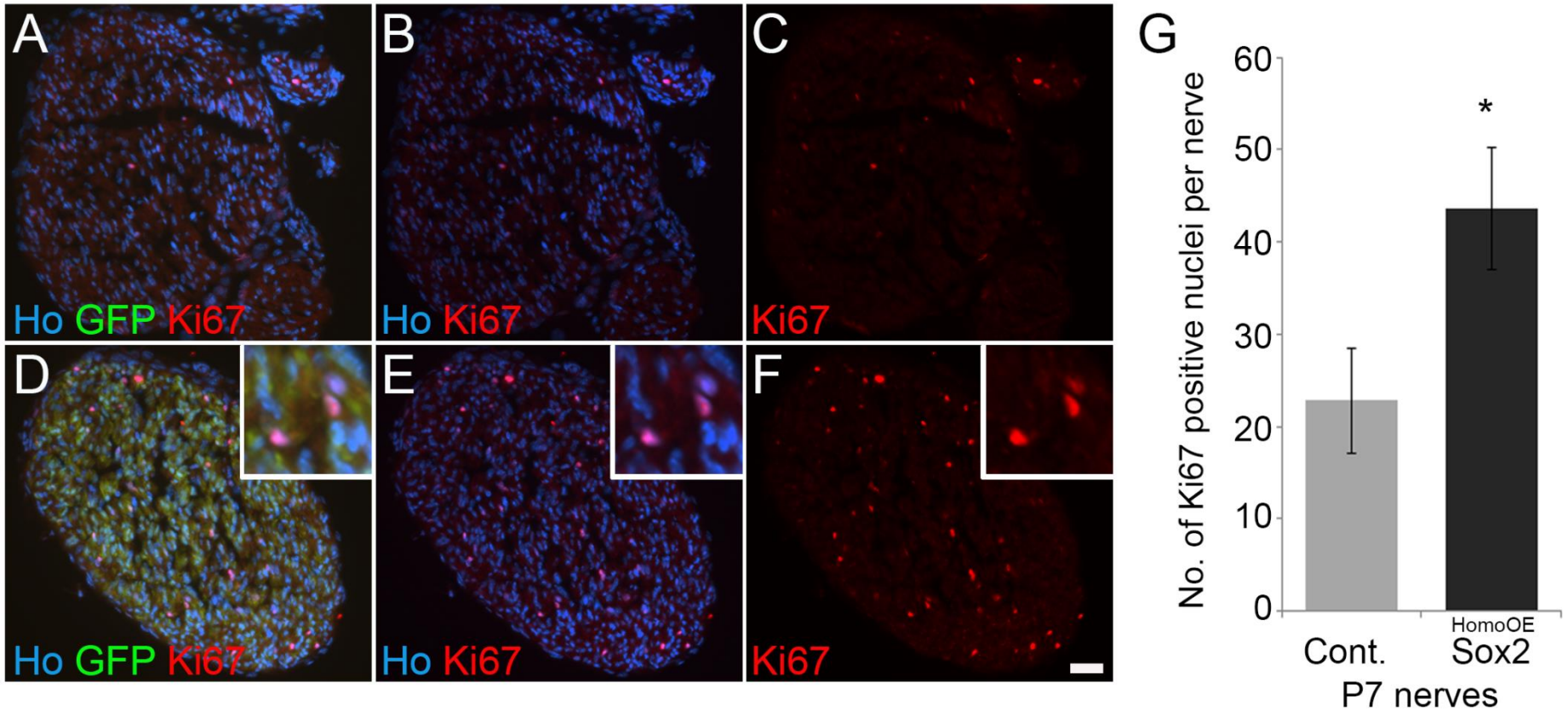

Figure 3. 18: Sox2 increases Schwann cell proliferation at P7. Sciatic nerves taken from P7 (A-F) Sox2 Homo control and $Sox2^{HomoOE}$ mice were immunolabelled with antibodies against Ki67. Immunofluorescent staining shows fewer Ki67 positive nuclei in the sciatic nerves of Sox2 Homo control mice (A-C) compared to $Sox2^{HomoOE}$ mice (D-F) at P7. Graph (G) showing the total number of Ki67 positive nuclei in the sciatic nerve section of Sox2 Homo control and $Sox2^{HomoOE}$ mice at P7 ($P<0.05$, n=5 $Sox2^{HomoOE}$, n=6 Sox2 Homo control). Images taken using 20x objective, (D,E,F, inset 100x), scale bar is 20µm.

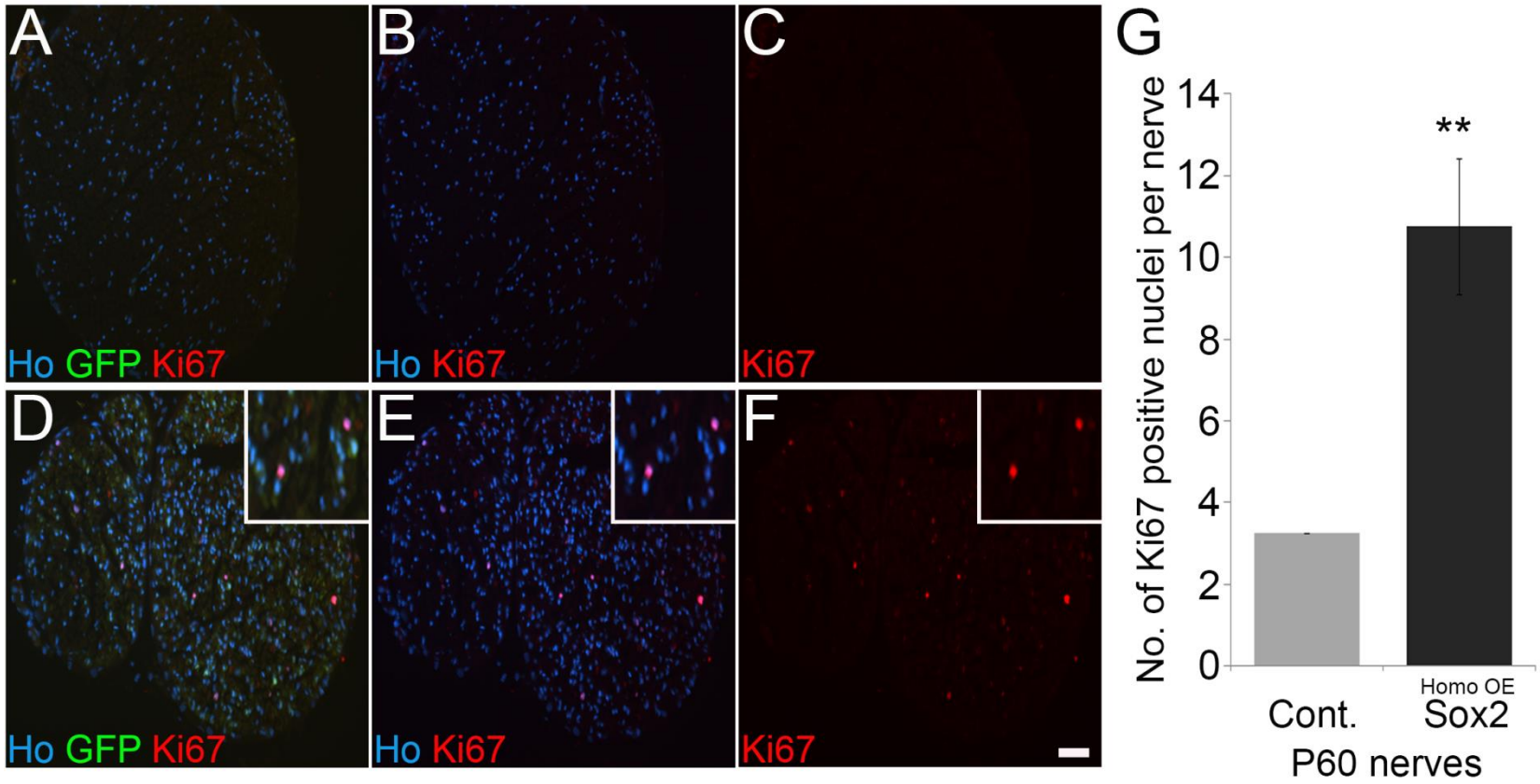

Figure 3. 19: Sox2 increases Schwann cell proliferation at P60. Sciatic nerves taken from P60 Sox2 Homo control and $Sox2^{HomoOE}$ mice were immunolabelled with antibodies against Ki67 (A-F). Immunofluorescent staining shows fewer Ki67 positive nuclei in the sciatic nerves of Sox2 Homo control mice (A-C) compared to $Sox2^{HomoOE}$ mice (D-F) at P60. Graph (G) showing the total number of Ki67 positive nuclei in the sciatic nerve section of Sox2 Homo control and $Sox2^{HomoOE}$ mice at P60 ($P<0.01$, n=4 per genotype). Images taken using 20x objective, (D,E,F, inset 100x), scale bar is 20µm

3.2.9 Sox2^{HomoOE} nerves show an increased influx of immune cells

Across many slow progressive demyelinating neuropathies such as CMT1-A, B and X an elevated number of immune cells such as T-lymphocytes and F4/80 positive macrophages appears to be a striking feature, with numbers of immune cells increasing with age and disease progression (Mäurer et al., 2002, Kohl et al., 2010a, Groh et al., 2010, Groh et al., 2015). Schwann cells in CMT mouse models have been shown to mediate macrophage recruitment and activation through the elevated expression of chemokines such as MCP1/CCL2 (Kohl et al., 2010a, Groh et al., 2010). These activated macrophages then go on to secrete cytokines which lead to the recruitment of T-lymphocytes, which thereon attract more macrophages and T-lymphocytes, resulting in a progressive inflammatory/pathogenic environment, with axonal damage and Schwann cell demyelination (Mäurer et al., 2002, Kiefer et al., 2001, Kobsar et al., 2003).

To assess whether Sox2^{HomoOE} mice also exhibit an increased number of immune cells, we immunolabelled sciatic nerve sections taken from Sox2 Homo control and Sox2^{HomoOE} mice with antibodies for both macrophages (F4/80 and Iba1) and T-cells (CD3).

Double immunolabelling of sciatic nerve sections with antibodies for both F4/80 and Iba1 revealed that at P7, there was an increased number of macrophages present in the sciatic nerves of Sox2^{HomoOE} mice (29.6 ± 14.4), compared to Sox2 Homo control nerves (15.5 ± 13.2), however this was not significant (P=0.17, n=5 Sox2^{HomoOE}, n=4 Sox2 Homo control) [Figure 3.20]. Nonetheless, there appeared to be a significant increase in the number of macrophages present in the sciatic nerves of P60 Sox2^{HomoOE} mice (48.5 ± 9.9) compared to control mice (6.3 ± 2.2) ($P<0.05$, n=4 Sox2^{HomoOE}, n=3 Sox2 Homo control) [Figure 3.20]. Immunolabelling of sciatic nerve sections with antibodies for CD3 (a T cell receptor complex marker) revealed that at P7, no T-lymphocytes were present in the sciatic nerves of either Sox2 Homo control or Sox2^{HomoOE} mice (n=4) [data not shown]. However at P60, a slight increase in the number of CD3 positive T-lymphocytes was observed in the sciatic nerves of Sox2^{HomoOE} mice (3.75 ± 1.8), compared to Sox2 homo control mice (0.7 ± 0.3), although this was not significant (P=0.13, n=4 Sox2^{HomoOE}, n=3 Sox2 Homo control) [Figure 3.21]. These results suggest that like many other demyelinating neuropathy

mouse models, Sox2 overexpressing mice also exhibit an increased number of immune cells, which progressively increases with age.

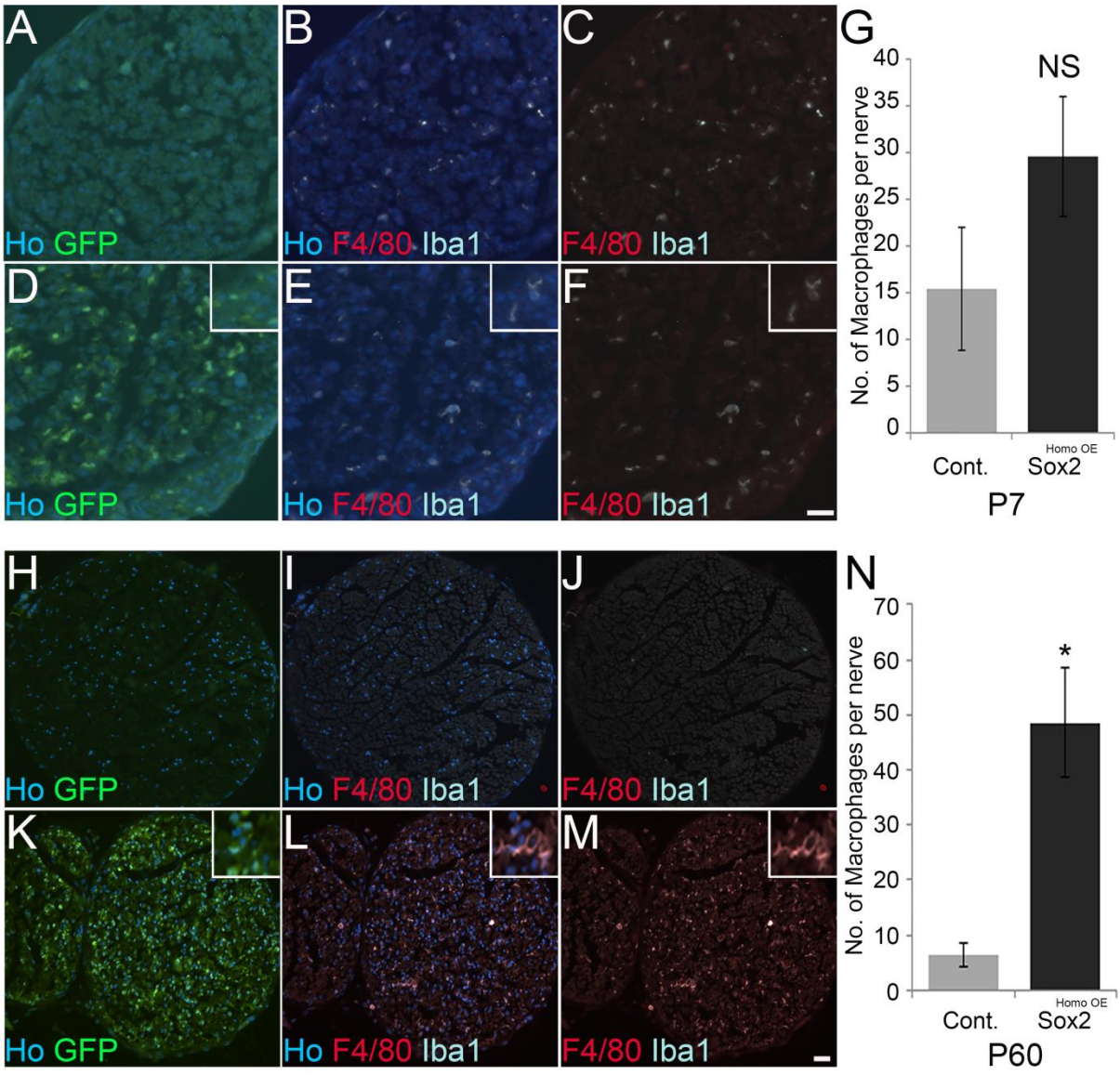

Figure 3. 20: Sox2 overexpressing nerves have an increased number of macrophages. Immunofluorescent staining for F4/80 and Iba1 shows that P7 Sox2 Homo control nerves have fewer F4/80 and Iba1 positive cells (B-C) compared to $Sox2^{HomoOE}$ nerves (E-F). Graph (G) displaying the total number of macrophages present in the sciatic nerves of Sox2 Homo control and $Sox2^{HomoOE}$ mice at P7 (n=4 control, n=5 $Sox2^{HomoOE}$). (H-M). Immunofluorescent staining for F4/80 and Iba1 at P60 show fewer F4/80 and Iba1 positive cells in the sciatic nerves of Sox2 Homo control mice (I-J), compared to $Sox2^{HomoOE}$ mice (L-M). Graph (N) displaying the total number of macrophages present in the sciatic nerves of Sox2 Homo control and $Sox2^{HomoOE}$ mice at P60 (n=3 control, n=4 $Sox2^{HomoOE}$). Images taken using 20x objective, (D,E,F, K, L, M inset 50x), scale bars are 20µm

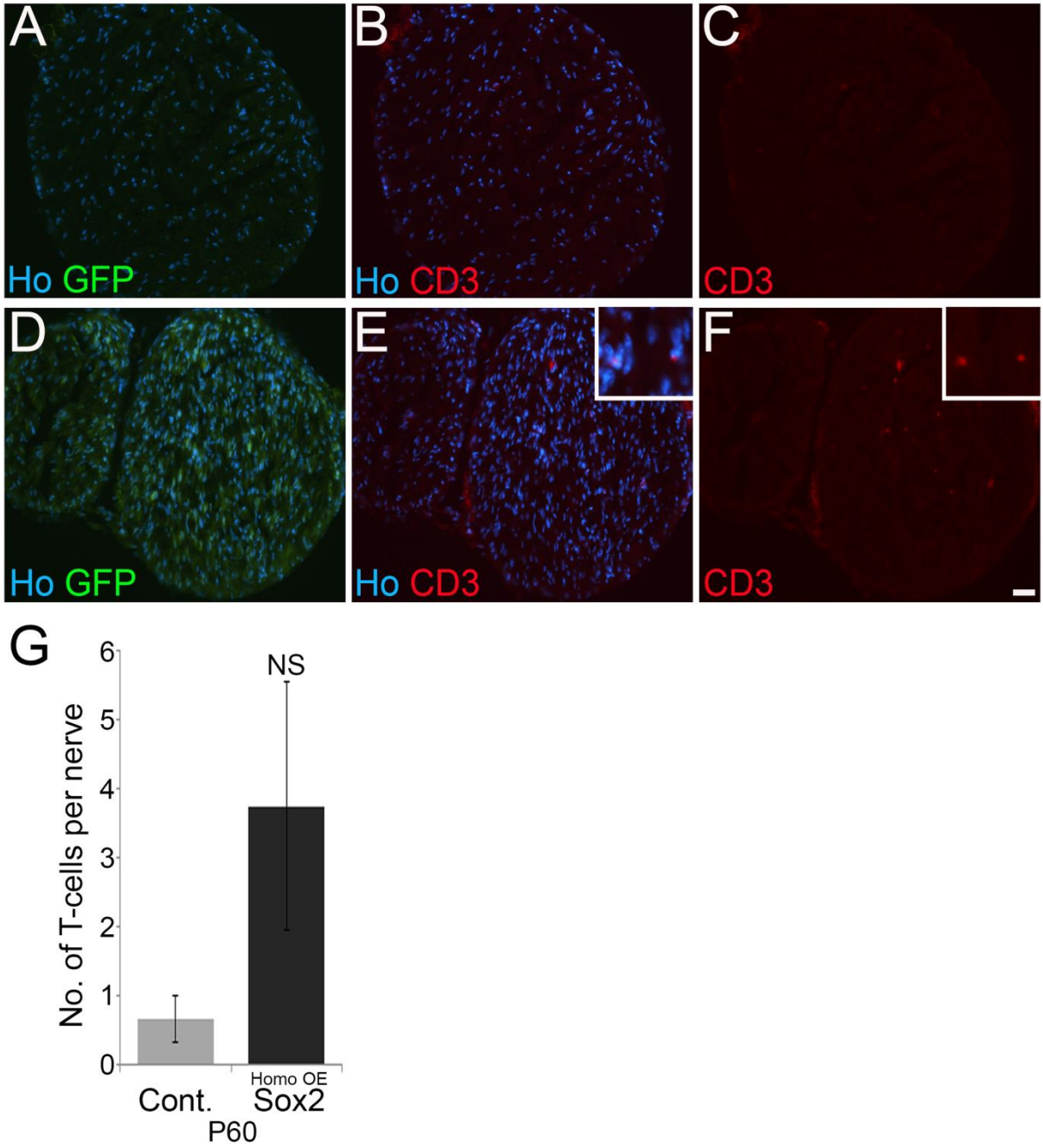

Figure 3. 21: Sox2 overexpressing nerves have an increased number of T-cells. Immunofluorescent staining for CD3 shows that P60 Sox2^{HomoOE} mice have more numerous CD3 positive T-cells within the sciatic nerve (D-E), compared to Sox2 Homo control nerves (A-C). Graph (G) illustrating the total number of T-cells in the sciatic nerves of Sox2 Homo control and Sox2^{HomoOE} mice at P60 (n= 3 Sox2 Homo control, n= 4 Sox2^{HomoOE}). Images taken using 20x objective, (E,F inset 50x), scale bar is 20µm.

3.2.10 Sox2 overexpression leads to reduced motor and sensory function

To further characterise the phenotype of the Sox2 overexpressing mice, electrophysiological, functional and sensory testing was carried out.

Nerve conduction studies are commonly used in neurological diagnosis and are the primary tests used to classify CMT disease, as they provide clues as to whether the neuropathy is demyelinating or axonal. In most cases demyelinating neuropathies are distinguishable by uniformly slower nerve conduction velocities (Jani-Acsadi et al., 2008, Sereda and Nave, 2006). To determine if Sox2 overexpression in Schwann cells altered the conduction efficiently of peripheral nerves, extracellular compound action potentials were recorded from the sciatic nerves of Sox2 Het control and $Sox2^{HetOE}$ mice. These extracellular compound action potential recordings were then analysed and used to calculate nerve conduction velocities.

We observed that at P20, nerve conduction velocities were significantly reduced in the sciatic nerves of $Sox2^{HetOE}$ mice (13.41 ± 0.72 m/s) compared to Sox2 Het control mice (15.37 ± 0.44 m/s) ($P<0.05$, n=13 $Sox2^{HetOE}$, n=11 Sox2 Homo control) [Figure 3.22]. Similarly at P24, a reduction in nerve conduction velocity (NCV) was also observed in $Sox2^{HetOE}$ mice (30.43± 2.86 m/s) compared to Sox2 Het control mice (37.8 ± 5.31 m/s) (n=2 per genotype) [data not shown]. To determine if NCV was also altered in adult mice, further analysis was carried out on P60 mice. Likewise, $Sox2^{HomoOE}$ mice exhibited slower nerve conduction velocities (16m/s) compared to Sox2 Homo control mice (49m/s) (n=1 per genotype) [data not shown]. These experiments demonstrate that overexpression of Sox2 in Schwann cells results in a decreased efficiency of peripheral nerves to conduct electrical signals. These results however are not surprising as we have previously seen that overexpression of Sox2 significantly impairs Schwann cell myelination [see Section 3.2.2] and therefore would expect that this would impact of the speed and ability of impulses to propagate along the nerves of $Sox2^{OE}$ mice.

Patients with CMT disease typically show signs of ataxia and reduced sensory function. Similarly in mouse models of CMT type-1 disease, mice have also been show to exhibit signs of unsteady gait and abnormalities in motor performance (Wrabetz et al., 2006, Saporta et al., 2012). We therefore wanted to further

characterise the phenotype of the $Sox2^{OE}$ mice, by carrying out motor/sensory functional testing. Control and $Sox2^{OE}$ mice at 6 and 8 weeks of age were therefore placed onto a rota-rod and the latency to fall was recorded. At 6 weeks of age, no significant difference in latency to fall was observed between Sox2 Het control and $Sox2^{HetOE}$ mice ($P>0.05$, n=4 $Sox2^{HetOE}$, n=7 Sox2 Homo control) [Figure 3.22]. However, a significant reduction in latency to fall was observed in $Sox2^{HomoOE}$ mice at 6 weeks of age, compared to Sox2 Het control mice ($P<0.001$, n=6 $Sox2^{HomoOE}$, n=7 Sox2 Homo control) [Figure 3.22]. Again, at 8 weeks of age no significant difference in latency to fall was observed between Sox2 Het control and $Sox2^{HetOE}$ mice ($P>0.05$, n=4 $Sox2^{HetOE}$, n=4 Sox2 Homo control), whilst a significant difference in latency to fall was observed between $Sox2^{HomoOE}$ mice and Sox2 Het control mice ($P<0.05$, n=6 $Sox2^{HomoOE}$, n=4 Sox2 Homo control) [Figure 3.22].

We next went onto analyse the sensory function of Sox2 control and $Sox2^{OE}$ mice at 6 weeks of age. Toe pinch testing revealed that whilst 100% of both Sox2 (Het and Homo) control and $Sox2^{HetOE}$ mice responded to light pressure, only 40% of $Sox2^{HomoOE}$ mice were able to respond (n=7 Sox2 control, n=3 $Sox2^{HetOE}$, n=5 $Sox2^{HomoOE}$) [Figure 3.23]. Furthermore, Von Frey hair testing revealed that $Sox2^{HomoOE}$ mice had a significant impaired ability to respond to light touch stimulus compared to Sox2 (Het and Homo) control mice ($P<0.01$), however no significant difference in responsiveness was observed between $Sox2^{HetOE}$ and Sox2 control (Het and Homo) mice at 6 weeks of age ($P>0.05$) (n=11 Sox2 control, n=5 $Sox2^{HetOE}$, n=5 $Sox2^{HomoOE}$) [Figure 3.23].

Together these results are consistent with our previous findings that overexpression of Sox2 in Schwann cells impairs nerve function and further suggest that Sox2 overexpression induces a phenotype similar to that of a peripheral neuropathy.

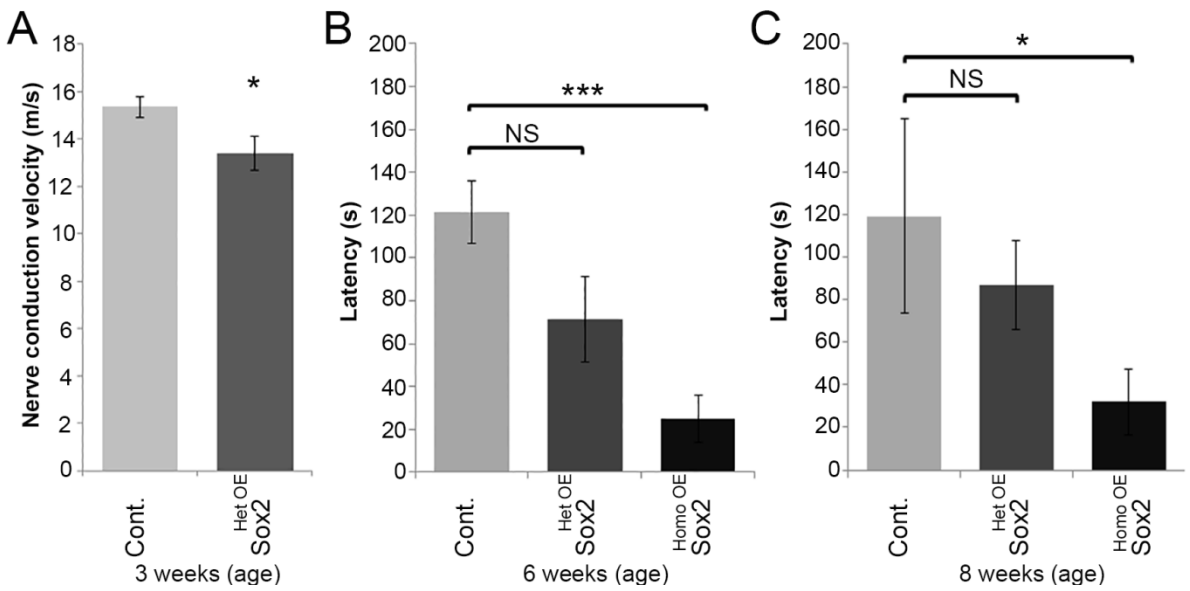

Figure 3. 22 Nerve conduction velocity and motor function is reduced in Sox2 overexpressing mice. Graph (A) comparing the nerve conduction velocity of sciatic nerves taken from control and $Sox2^{HetOE}$ mice at P20 (n=11 control, n=13 $Sox2^{HetOE}$). Graphs (B & C) showing the latency to fall using rotarod testing of control, $Sox2^{HetOE}$ and $Sox2^{HomoOE}$ mice at 6 weeks (B) and 8 weeks (C) of ages. (6 weeks: n=7 control, n=4 $Sox2^{HetOE}$, n=6 $Sox2^{HomoOE}$. 8 weeks: n=4 control, n=4 $Sox2^{HetOE}$, n=6 $Sox2^{HomoOE}$).

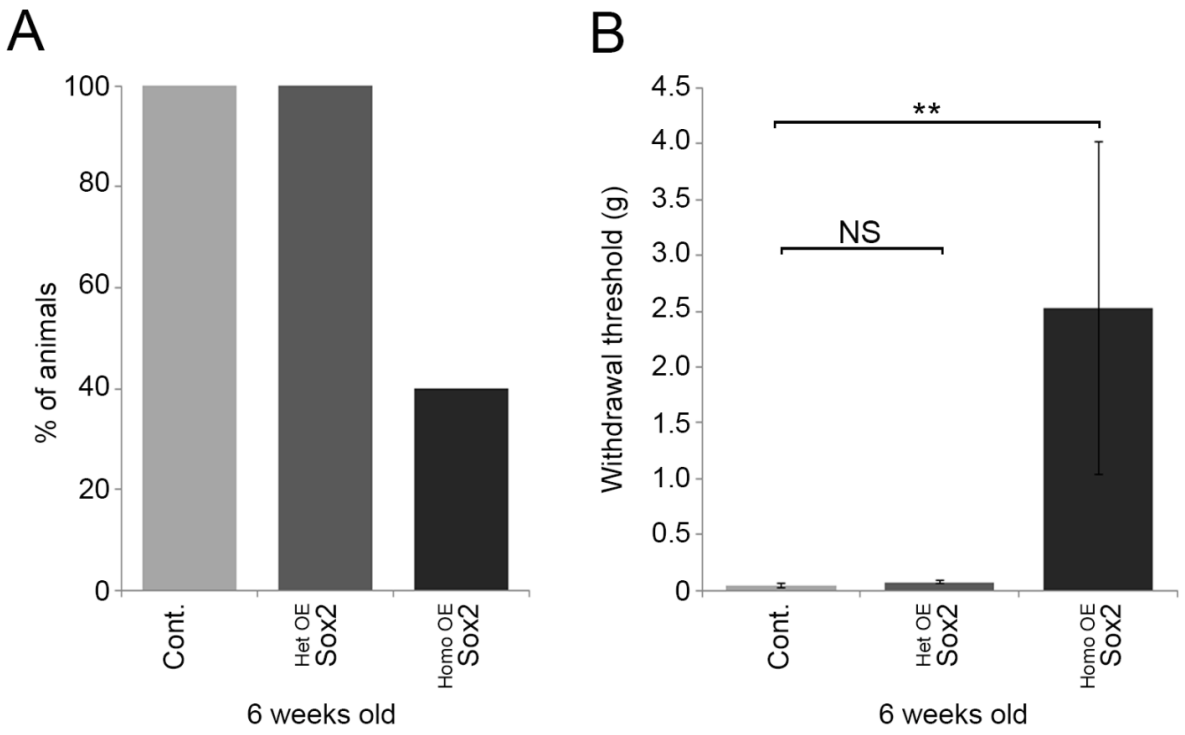

Figure 3. 23: Sensory function is reduced in Sox2^{HomoOE} mice. Graph (A) showing the percentage of control, Sox2^{HetOE} and Sox2^{HomoOE} mice which responded to toe pinch testing at 6 weeks of age (n=7 control, n=3 Sox2^{HetOE}, n=5 Sox2^{HomoOE}). Graph (B) showing the withdrawal threshold (g) for control, Sox2^{HetOE} and Sox2^{HomoOE} mice at 6 weeks of age to various Von Frey filaments (n=11 control, n=5 Sox2^{HetOE}, n=5 Sox2^{HomoOE}).

3.3 Discussion

The results in this chapter clearly show that Sox2 functions as a negative regulator of Schwann cell myelination and sustained expression of Sox2 during development and in adulthood leads to the onset of a phenotype similar to that of a peripheral neuropathy, such as congenital hypomyelinating neuropathy and Charcot-Marie-Tooth type-1 disease.

3.3.1 Sox2 impairs Schwann cell myelination

Schwann cells that come into contact with large diameter axons (>1µm) are destined to differentiate into a myelinating Schwann cell and ensheath axons in a 1:1 ratio. In contrast, Schwann cells that make contact with small diameter axons (<1µm), differentiate into non-myelinating Schwann cells, and ensheath multiple axons with a thin layer of cytoplasm (Bhatheja and Field, 2006). Axons have been shown to be responsible for determining the phenotype of Schwann cells, through their expression levels of Neuregulin-1 (Nrg1) type-III which acts as an instructive signal for myelination. Expression levels of Nrg1 type-III in axons has been shown to correlate with their level of myelination; small diameter axons express low levels of Nrg1 type-III and thus do not drive Schwann cells to myelinate, whereas large diameter axons express high levels of Nrg1 type-III and induce Schwann cells to myelinate (Nave and Salzer, 2006). Nonetheless, overexpression of Nrg1 in Nrg1 type III transgenic mice, has been shown to drive the hypermyelination of small diameter axons (Michailov et al., 2004). High expression levels of Nrg1-III (notably on large diameter axons) signal via the ErbB2/ErbB3 heterodimer receptors expressed on Schwann cells. This activates a range of signalling cascades; including the phosphatidylinositol 3-Kinase (PI3K)/Akt signalling, phospholipase C-gamma (PLC-γ) dependent NFATc4 activation, Oct6 activated expression and cAMP elevation within promyelinating Schwann cells, all of which aim to activate Krox20; a zinc finger transcription factor required to drive myelination (Kao, 2009). Krox20 is essential for the suppression of negative myelin regulators such as cJun, Notch and Sox2, and the increased expression of myelin proteins such as P_0 and MBP (Parkinson et al., 2008, Parkinson et al., 2004, Le et al., 2005a, Woodhoo et al., 2009).

Studies have shown that Schwann cells overexpressing Sox2 fail to myelinate co-cultured dorsal root ganglia (DRG) axons and upregulate the expression of myelin

related genes *in vitro,* indicating that suppression of Sox2 is essential for Schwann cell myelination (Le et al., 2005a). *In vitro* evidence thus suggests that Sox2 is a negative regulator of Schwann cell myelination, however the functional role of Sox2 on myelination *in vivo* remains open for investigation, as previous studies have demonstrated that the functional role of a protein *in vitro*, may not parallel *in vivo* (Lewallen et al., 2011, Golan et al., 2013). Although the role of Sox2 on Schwann cell myelination has not been fully studied, increasing evidence *in vivo* confirms Sox2 to be a marker of immature Schwann cells (Decker et al., 2006, Bremer et al., 2011, Le et al., 2005a). We thus set out to investigate the effect Sox2 overexpression would have on Schwann cell function, by generating Schwann cell specific Sox2 overexpressing mice.

Phenotypically $Sox2^{HomoOE}$ mice displayed characteristics similar to mouse models of congenital hypomyelinating neuropathy (CHN) and Charcot-Marie-Tooth type 1 (CMT-1) disease; they were smaller in size, had poor movement and displayed hindlimb clasping when lifted by the tail (Le et al., 2005). Histologically, $Sox2^{HomoOE}$ sciatic nerves were very similar to those of patients with CHN; at P7, P21 and P60 the nerves were very hypomyelinated, with a high percentage of axons being unmyelinated, the nerves did not display axonopathy or onion bulbing, hallmarks that differentiate CHN from other neuropathies. Whilst CHN can be either non-progressive or slowly progressive, we observed a slowly progressive phenotype in our $Sox2^{HomoOE}$ mice; we saw that myelin thickness decreased and the number of unmyelinated axons increased with age.

In order to determine the mechanism by which Sox2 impairs Schwann cell myelination, we analysed the expression of myelin proteins. Overexpression of Sox2 was shown to reduce the gene and protein expression of Krox20, as well as the protein expression of P_0 and MBP throughout Schwann cell development and in adult nerves. Krox20 expression is essential during development for the activation of Schwann cell differentiation, as disrupted Krox20 expression has been shown to block Schwann cells at the early promyelinating stage (Topilko, 1994). In addition, Krox20 is essential for the initiation of myelination and for myelin maintenance, as it coordinates the expression of numerous myelin associated genes including; P_0, MBP, peripheral myelin protein 22, periaxin and myelin associated glycoprotein

(MAG), as well as genes encoding enzymes required for cholesterol and myelin lipid biosynthesis, such as HMG-CoA reductase, choline kinase and stearyl coA desaturase (Le et al., 2005a, Nagarajan et al., 2001, Decker et al., 2006, LeBlanc et al., 2005, Topilko et al., 1994). It thus comes to no surprise that mutations in Krox20, or disruptions to its expression are associated with the development of various peripheral myelopathies; CHN, CMT and Dejerine–Sottas syndrome (Le et al., 2005a, Nagarajan et al., 2001, Timmerman et al., 1999, Warner et al., 1998)

The major peripheral myelin protein, P_0 also plays an essential role in Schwann cell myelination, enabling myelin compaction and adhesion between myelin layers. Mutations or disruptions in its expression have therefore been associated with impaired/irregular myelination and the onset of peripheral neuropathies such as CMT-1B (Giese et al., 1992, Saporta et al., 2012). MBP on the other hand is less essential for myelin formation, but plays an important role in the compaction and stabilisation of intracellular peripheral myelin (Notterpek et al., 1999, Shine and Sidman, 1984, Martini et al., 1995). Whilst mice lacking MBP (MBP^{--}) myelinate normally, mice with compound heterozygous mutations in both MBP and P_0 (P_0^{+-} /MBP^{+-}) show a worse peripheral myelinopathy than single mutant P_0 (P_0^{+-}) mice (Martini et al., 1995).

From previous studies mentioned above, it's clear that Krox20, P_0 and MBP are important for Schwann cell myelination and that the ability of Sox2 to directly repress their expression will result in detrimental consequences. As Sox2 overexpressing mice show a simultaneous reduction in the expression of all three components (Krox20 and P_0, and MBP), we believe this explains the mechanism by which Schwann cell myelination is impaired in these mice, and why $Sox2^{HomoOE}$ mice demonstrate characteristics of peripheral neuropathies associated with disrupted Krox20, P_0 and MBP expression.

In addition to targeting Schwann cell myelin proteins, overexpression of Sox2 dramatically reduced the protein and gene expression of a well characterised cell adhesion molecule Necl4 *in vitro* (unpublished data from Dr R.Doddrell), as well as in the nerves of $Sox2^{HetOE}$ mice (unpublished data from Dr Xin-Peng Dun; this study). Necl4 is a transmembrane protein which mediates glial-axon interaction by binding to

axonal Necl1 and Necl2 (Maurel et al., 2007, Spiegel et al., 2007). Whilst Necl1, Necl2 and Necl3 are dispensable for myelination, Necl4 plays an essential role in facilitating normal myelin formation (Maurel et al., 2007, Spiegel et al., 2007, Golan et al., 2013). Knockdown of Necl4 by shRNA (Maurel et al., 2007) and the expression of dominant mutant forms of Necl4 (Spiegel et al., 2007) have been shown to result in a marked reduction in Schwann cell myelination *in vitro*. A more recent study analysing Necl4 null and Necl4 mutant transgenic (*mbp-Cadm4dCT*) mice further confirmed that Necl4 is essential for the proper establishment of myelinated nerve fibres (Golan et al., 2013). However, in contrast to the *in vitro* studies, Golan et al., (2013) showed that disrupted Necl4 expression *in vivo* causes an initial delay in myelin formation, followed by hypermyelination and myelin abnormalities. Although the Necl4 null and Necl4 mutant mice are not histologically similar to Sox2 overexpressing mice, which we might have expected from earlier *in vitro* studies, they do similarly show reduced motor function and hindlimb clasping (Maurel et al., 2007, Spiegel et al., 2007, Golan et al., 2013). We might predict that the ability of Sox2 to suppress Necl4 may be a contributing factor to the impaired normal myelination. Although we do not observe hypermyelination within the nerves of Sox2 overexpressing mice, this could be due the dual ability of Sox2 to also suppress the expression of Krox20, a key regulator of myelin lipid synthesis and myelin protein expression (Nagarajan et al., 2001). Necl4 is also reported to be essential for the establishment of correct axon-glial contact points; Necl4$^{-/-}$ mice showed abnormal distribution of Caspr (a paranodal protein marker), and an accumulation of Caspr and Kv1 channels (marker of the internodal region) away from the Na^{+} channel-containing nodes of Ranvier. This was suggested to reflect unwinding of the paranodal loops in the absence of Necl4 [See Figure 1.2] (Golan et al., 2013).

3.3.2 Sox2 downregulates the expression of Sox10

Sox10 is highly expressed throughout Schwann cell development and is essential for the specification and differentiation of peripheral glial from neural crest cells (Britsch et al., 2001). Sox10 thereafter plays a fundamental role in regulating Schwann cell development and differentiation by activating the gene expression of Oct6, a key POU domain transcription factor required for the transition of immature Schwann cells into promyelinating Schwann cells (Finzsch et al., 2010, Jagalur et al., 2011). In

order to drive promyelinating Schwann cells into the myelinating stage, Sox10 then synergises with both Oct6 and NFATc4 independently, to activate the transcription of Krox20, by binding to the Myelin Specific Enhancer (MSE) region (1.3kb cis-regulatory element of the Krox20 promoter). In addition to activating Krox20, Sox10 activates the transcription of P_0, by co-operating with NFATc4 and binding to the P_0 promoter, as well as synergising with Krox20 to further enhance P_0 expression, by binding to the P_0 gene within intron 1 (Kao et al., 2009, Jagalur et al., 2011, LeBlanc et al., 2006).

As Sox10 plays such a fundament role in Schwann cell development, we were surprised to observe that overexpression of Sox2 reduced the expression of Sox10 *in vitro* and at later time-points in adult $Sox2^{HomoOE}$ mice (P60), nonetheless this function is consistent with its role as a negative regulator of myelination. We expect that the ability of Sox2 to alter the expression of Sox10 is likely to be a major part of the mechanism by which Sox2 impairs myelination and thus myelin protein expression, as selective deletion of Sox10 has been shown to stall Schwann cells at the immature Schwann cell phase, and prevents the upregulated expression of Oct6, Krox20, MBP and P_0 (Finzsch et al., 2010). Sox2 was also shown to reduce the expression of Oct6 expression *in vitro* (unpublished data by Dr R.Doddrell in our group), which further supports our hypothesis that Sox2 is able to regulate Sox10, thus reducing its ability to regulate its downstream targets.

In addition to being crucial for Schwann cell differentiation and myelination, studies have also confirmed that Sox10 expression is essential for myelin maintenance, but not for the survival of adult Schwann cells (Finzsch, 2010; Bremer, 2011). As we observed an apparent progressive decline in the expression of Sox10 between P7 and P60 in our $Sox2^{HomoOE}$ mice, as shown by fluorescent imaging [Figure 3.13], this further explains why myelin thickness decreased with increased age.

Although we observed *in vivo* that Sox2 is capable of reducing Sox10 expression at later stages of Schwann cell development, Sox2 did not completely eliminate Sox10 expression from Schwann cells. For this reason we believe this is why the phenotype observed in the $Sox2^{HomoOE}$ mice is less severe than that previously observed in studies carried out on Sox10ΔeST mice (Schwann cell specific Sox10 deleted mice) which show symptoms of shiverer type tremors, an abnormal, straddled position of

the hindlimb, poor motor coordination and which eventually die by 7 weeks of age (Finzsch et al., 2010). Furthermore, studies on homozygous $Sox10^{LacZ/lacZ}$ mutant mice (in which the complete open reading frame of Sox10 has been replaced with a LacZ sequence) reported that these mice die during embryonic development and do not develop any peripheral glia; Schwann cells or satellite cells (Britsch et al., 2001).

While Sox genes are regulated by a range of different mechanisms including auto-regulation, regulation by other Sox proteins and post transcriptional modification, it is not known how Sox2 and Sox10 genes are regulated in Schwann cells, or how they may regulate one another (Kamachi and Kondoh, 2013). It would be of great interest to determine whether Sox2 reduces the gene expression of Sox10, as well as downstream targets of Sox10 which are not co-regulated by Oct6 or Krox20, such as S100B and ErbB3 receptor expression (Fujiwara et al., 2014, Prasad et al., 2011, Britsch et al., 2001). Many genes have been reported to be regulated by Sox10 in Schwann cells, including desert hedgehog (Küspert et al., 2012), myelin proteins P_0 and PMP22 (Jones et al., 2011, Peirano et al., 2000, Finzsch et al., 2010), LGI4, ciliary neurotrophic factor (CNTF) (Ito et al., 2006, Srinivasan et al., 2012), and more recently Id2, Id4, Sox5, Notch1, HMGA2, Mycn and Hes1 (Personal communications with members of John Svaren group, University of Wisconsin-Madison), however most are co-regulated by Krox20. In order for Sox proteins to exert their gene regulatory function, they are often required to form complexes with partner transcription factors (Kamachi and Kondoh, 2013). As Sox10 often forms complexes with Krox20, it's difficult to identify sole targets of Sox10 alone.

It would be equally interesting to examine the mechanism by which Sox2 reduces Sox10 expression, for example whether Sox2 interacts directly with Sox10 thus reducing its activation. In addition to investigating whether Sox2 prevents Sox10 from binding to the promoter region of its downstream targets. This could be achieved through chromatin immunoprecipitation (ChIP) experiments, using antibodies against Sox10 in wild-type and in Sox2 overexpressing nerves in adult P60 nerves. Furthermore, it would be interesting to determine whether the addition of exogenous Sox10 to cultured Sox2 adenoviral infected Schwann cells, restored myelination in Schwann cell/DRG co-cultures.

3.3.3 Sox2 maintains Schwann cells in an immature state

Immature Schwann cells are marked by the expression of Sox2, cJun, and Notch, all of which aid to enhance Schwann cell proliferation (Le et al., 2005a, Parkinson et al., 2004, Woodhoo et al., 2009)(David Parkinson, unpublished data). As immature Schwann cells differentiate and myelinate, the expression of these immature Schwann cell markers declines, coinciding with their expression being restricted to the immature state during development (Parkinson et al., 2004; Le et al., 2005, Woodhoo et al., 2009). Overexpression of Sox2 in Schwann cells reduced myelin thickness and significantly increased the percentage of unmyelinated axons, which were in a 1:1 ratio with Schwann cells. As Sox2 is highly expressed within immature Schwann cells and is capable of impairing myelination, we expected that Sox2 would restrict Schwann cells to the immature / promyelinating stage (Le et al., 2005; this study). In support of this, we observed high expression levels of cJun within the nerves of $Sox2^{HomoOE}$ mice compared to controls. cJun has previously been shown to only be expressed within immature and repair (dedifferentiated) Schwann cells, as cJun protein levels and the JNK-cJun signalling pathway are suppressed by Krox20; which is upregulated in Schwann cells as they transition from immature/repair cells into myelinating Schwann cell (Parkinson et al., 2004).

To further determine whether Schwann cells were retained at the immature or promyelinating Schwann cell stage, it would be of interest to carry out further experiments analysing the expression levels of promyelinating Schwann cell markers, such as Oct6 and Brn-2 within the sciatic nerves of control and $Sox2^{HomoOE}$ mice. We might expect that if Sox2 maintains Schwann cells at the immature/ promyelinating phase, levels of Oct6 would be increased within the nerves of $Sox2^{HomoOE}$ mice, compared to controls.

Although Oct6 expression induced by cAMP was previously shown to be completely impaired in Sox2 adenoviral infected Schwann cells *in vitro* (unpublished data by Dr R.Doddrell in our group), we might expect Oct6 to still be weakly expressed within the nerves of $Sox2^{HomoOE}$ mice, similarly to its upstream regulator Sox10 which was shown to also be weakly expressed within $Sox2^{HomoOE}$ mice, in contrast to the vitro analysis, where Sox10 was completely impaired. This further highlights the difference between *in vitro* and *in vivo* experiments. Oct6 and Brn2 are highly expressed within Schwann cells from P1 to P8, however their expression begins to

decline from then onwards, until they can no longer be detected at P30/P32. Thus in order to make a comparative analysis of differences in the expression of Oct6 and Brn-2 in the nerves of control and $Sox2^{HomoOE}$ mice, analysis should be carried out from P30 onward (Jaegle et al., 2003, Arroyo et al., 1998).

Overall it is clear that Sox2 acts to antagonise the Schwann cell promyelination pathway, by maintaining Schwann cells at the immature/promyelinating Schwann cell phase. This was supported by the high expression of two immature Schwann cell makers, cJun and the cell adhesion molecule N-cadherin (which will be discussed further in section 3.3.4) within the nerves of $Sox2^{HomoOE}$ mice. The ability to proliferate is also a hallmark of immature Schwann cells, as mature myelinating Schwann cells lose their ability to proliferate (Parkinson et al., 2004). As we observed an increased level of proliferation in the nerves of $Sox2^{HomoOE}$ mice (this will be discussed in more detail in section 3.3.6), this provides additional support to the evidence that Schwann cells are retained in an immature state.

3.3.4 Sox2 regulates cell adhesion proteins

Due to their exceptional plasticity, Schwann cells play a remarkable role in the ability of the peripheral nervous system to regenerate following nerve injury. One of the critical functions of Schwann cells during nerve repair is to dedifferentiate and assist with the guidance of regrowing axons across the wounded site and back to their targets (Parrinello et al., 2010). This process firstly requires Schwann cells to cluster together and form cord like structures, which is regulated by Sox2 (Parrinello et al., 2010). Following nerve injury, fibroblasts migrate into the nerve bridge (the site of injury) and express ephrin B ligand, which binds to EphB2 receptors expressed on Schwann cells, causing Schwann cell upregulation of Sox2 expression. Sox2 was shown to play an important role in Schwann cell clustering by inducing the re-localisation of N-cadherin to cell-cell contact junctions, thus promoting cell sorting: the separation of Schwann cells and fibroblasts into two separate groups (Parrinello et al., 2010). Upon N-cadherin relocalisation, protein levels of N-cadherin appeared elevated, however no increase in N-cadherin messenger RNA (mRNA) was observed (Parrinello et al., 2010). This suggested that the Sox2 caused post transcriptional changes that lead to increased stabilization of the N-cadherin protein.

N-cadherin is also strongly expressed in immature Schwann cells during development, however as Schwann cells differentiate and begin to myelinate, the expression of N-cadherin is downregulated and E-cadherin expression is upregulated (Crawford et al., 2008). In early Schwann cell development N-cadherin localises to the Schwann cell-axon interface, mediating both Schwann cell-axon and Schwann cell-Schwann cell interaction, as well as neurite outgrowth (Wanner et al., 2006, Wanner and Wood, 2002). As neural outgrowth comes to an end and the requirement for Schwann cell-cell interaction is reduced in order to allow for structural transformation within the nerve (such as myelination), the expression of N-cadherin expression is reduced, coinciding with the decrease in Sox2 expression during Schwann cell differentiation and maturation (Wanner et al., 2006). As expected, N-cadherin was weakly expressed within the nerves of adult Sox2 control mice, however strong expression of N-cadherin was detected within the nerves of adult $Sox2^{HomoOE}$ mice (Wanner and Wood, 2010). The data revealed that Sox2 was able to regulate and maintain N-cadherin expression in Schwann cells during development, however the mechanism by which Sox2 is able to achieve this remains unclear. Further experiments would need to be carried out to determine whether Sox2 is able to increase the expression of N-cadherin by analysing both N-cadherin protein and gene expression at different time-points during development, in both control and $Sox2^{HomoOE}$ nerves. Nonetheless, as previously reported by Parrinello et al. (2010), we might expect that Sox2 post-transcriptionally modified or stabilized N-cadherin protein, rather than increasing its gene expression levels. Analysis of the Affymetrix gene array carried out by Dr R.Doddrell in our group, did not reveal N-cadherin to be significantly increased in Sox2 adenoviral infected Schwann cells, compared to GFP adenoviral infected Schwann cells (controls) (1.9 fold increase, P=0.12).

As N-cadherin has only been reported to be expressed in Schwann cells prior to myelination and after nerve injury, this data further supports our theory that Schwann cells are maintained in an immature state by the overexpression of Sox2.

N-cadherin is classically though to transduce intracellular signals by interacting with β-catenin, which in turn associates with the actin cytoskeleton though binding α-catenin; forming a cadherin-β-catenin-α-catenin signalling complex (Meng and Takeichi, 2009, Ivanov et al., 2001). In Schwann cells, β-catenin co-localises with N-

cadherin at the Schwann cell-axon interface and co-immunoprecipitates with N-cadherin on the initiation of myelination (Lewallen et al., 2011). β-catenin was also shown to compensate for N-cadherin in its absence, reducing the severity of the delay in Schwann cell myelination (Lewallen et al., 2011). In the nerves of $Sox2^{HomoOE}$ mice, β-catenin was highly expressed, whereas only weak expression of β-catenin was detected in control nerves. We expect that as a downstream effector of N-cadherin, N-cadherin and β-catenin would co-localised within the nerves of $Sox2^{HomoOE}$ mice as demonstrated by Lewallen et al. (2010), however as both antibodies for these proteins were raised in the same species (mouse) we were unable to double labelled nerve sections for both proteins. Nonetheless, we were able to demonstrate for the first time that Sox2 is capable of either increasing or maintaining high protein expression levels of both N-cadherin and β-catenin in Schwann cells *in vivo*.

In order to determine whether Sox2 increased the expression of N-cadherin and β-catenin, or rather whether it stabilized the protein expression further analysis would need to be carried out. Western blot experiments using sciatic nerve lysates taken from control and $Sox2^{HomoOE}$ mice at different time-points throughout Schwann cell development for e.g. at P0, P7, P14, P21 and P60 could be carried out to determine whether Sox2 increases the expression of both N-cadherin and β-catenin. In laryngeal cancer Hep-2 cells, Sox2 has also been shown to enhance N-cadherin and Wnt/β-catenin protein expression, thus promoting migration, invasion and epithelial-mesenchymal transition (Yang et al., 2014a). It is possible that this functional role of Sox2 to regulate N-cadherin and β-catenin expression is conserved across different cell types. Furthermore, although the study by Yang et al., (2014) did not analyse N-cadherin and β-catenin protein localisation, it is possible that the ability of Sox2 to drive N-cadherin and β-catenin relocalisation is also a conserved function.

3.3.5 Sox2 increases the mRNA expression of Neuroserpin

Neuroserpin, also known as Serpini 1, is a member of the serpin superfamily, and has been shown to play an important role regulating a range of biological processes by inhibiting the function of members of the trypsin-like serine protease family. Serpins are able to selectively target and inhibit the function of proteases, through their exposed mobile reactive centre loop (RCL). The RCL covalently attaches to the

target protease via an ester bond, and induces the serpin to undergo the stressed to relaxed transition, consequently causing the protease to be moved from the top to the bottom of the serpin, where it is distorted into a conformation that allows for the acyl enzyme intermediate to be hydrolysed, leading to its inactivation (Rashid et al., 2014, Huntington et al., 2000).

Neuroserpin has been shown to be primarily synthesised and secreted by axons in the central and peripheral nervous system, where it regulates proteolytic events, such as inhibiting the activation of tissue plasminogen activator (tPA) and to a smaller degree urokinase plasminogen activator (UPA). A balance in the expression of plasminogen activators in the brain is important as deficiencies or overexpression can have adverse effects leading to impaired learning; mice lacking tPA show interference with long-lasting long term potentiation and reduced performance in two-way active avoidance learning (Huang et al., 1996), whilst mice overexpressing UPA perform poorly in tasks of spatial, olfactory, and taste-aversion learning (Meiri et al., 1994). Given its function in modulating proteolytic events, neuroserpin has been suggested to participate in modulating synaptic reconstruction during neuronal development and synaptic plasticity in the adult nervous system (Osterwalder et al., 1996, Krueger et al., 1997).

Mutations in serpins results in a delay in protein folding and a delay in their ability to be cleared from the endoplasmic reticulum, leading to the onset of a class of conditions referred to a serpinopathies (Roussel et al., 2011). Neuroserpin, has been associated with many neurological diseases, including dementia, cerebrovascular disease, epilepsy, multiple sclerosis and schizophrenia (Yepes and Lawrence, 2004). In particular, mutations in the neuroserpin gene leads to aberrant polymeration of neuroserpin in the endoplasmic reticulum, causing a form of dementia known as Familial Encephalopathy with Neuroserpin Inclusion Bodies (FENIB). The disease is characterised by eosinophilic neuronal inclusion of neuroserpin in the cerebral cortex and the substantia nigra (Roussel et al., 2011). Mutations in neuroserpin have also been associated uncontrolled tPA activity, and therefore increased seizure occurrence and neurotoxicity (Yepes and Lawrence, 2004, Kaur et al., 2004).

Previously published data has shown that neuroserpin also plays a role in regulating cell-cell contact, by increasing the expression of N-cadherin at the plasma

membrane contact regions of cells. This was shown in PC12 cells overexpressing neuroserpin, as increased levels of neuroserpin correlated within increased cell–cell adhesion, cell cluster size as well as N-cadherin expression (Lee et al., 2008). Furthermore, PC12 cells infected with a mutant form of neuroserpin (NS_{R362A}) incapable of recognising tissue plasminogen activators (tPA), still demonstrated increased cell-cell adhesion similar to PC12 cells overexpressing wild type neuroserpin. This demonstrated that the functional ability of neuroserpin to regulate cell adhesion was independent of its enzymatic inhibitory function (Lee et al., 2008). Nonetheless, the mechanism by which neuroserpin regulates N-cadherin expression remains unknown.

Schwann cells infected with a Sox2 overexpression adenovirus demonstrated cell clustering, similar to that observed in PC12 cells overexpressing neuroserpin (Lee et al., 2008, Dun et al., paper submitted: under review). Neuroserpin mRNA was show to be massively upregulated by Sox2, identified by an Affymetrix array screen (55 fold increase) and semi-quantitative RT-PCR analysis carried out on Schwann cells infected with a GFP expressing adenovirus (controls) and Schwann cells infected with a Sox2 expressing adenovirus (unpublished data by Dr R.Doddrell; Dun et al (paper submitted: under review)). Neuroserpin mRNA was also upregulated in the sciatic nerves of $Sox2^{HomoOE}$ mice, further confirming neuroserpin to be a direct target of Sox2 both *in vitro* and *in vivo*.

Dr R.Doddrell (unpublished data) identified a four consensus Sox core-binding elements (SCBE) consisting of A/T, A/T, CAA, A/T in a 500bp DNA region 9kb upstream of the neuroserpin promotor (Mertin et al., 1999). As Sox2 is commonly known to act as a transcriptional enhancer or repressor, it therefore possible that Sox2 may regulate the expression of neuroserpin through binding one of these identified SCBEs upstream of the neuroserpin promoter, thus enhancing its transcriptional activation.

We proposed that Sox2 was able to regulate N-cadherin expression by enhancing the expression of neuroserpin. Sox2 was show to dramatically increase the expression of neuroserpin both in cells and secreted into the cell culture medium, as well as the expression of N-cadherin. Nonetheless, enforced expression of neuroserpin within Schwann cells failed to induce Schwann cell clustering as well as

to upregulate the expression of N-cadherin and induce re-localisation to the cell membrane (Dun et al. paper submitted: under review). Furthermore, silencing of neuroserpin expression through siRNA in Schwann cells, did not affect the ability of Schwann cells to cluster when stimulated by fibroblasts [unpublished data Dr S.Parrinello, UCL, London, UK].

These results demonstrated that contradictory to the data published by Lee et al. (2008), in PC12 cells neuroserpin does not appear to directly mediate cell clustering, nor does it mediate N-cadherin expression and relocalisation in Schwann cells (Dun et al. paper submitted: under review).

Little is known about the transcriptional regulation of neuroserpin *in vivo,* and therefore the strong regulation of neuroserpin we have shown by Sox2 in Sox2^{HomoOE} nerves if of great potential interest. Sox2 is highly expressed in the CNS during early development and is known to preserve neural progenitor cells identify, it would thus be of interest to determine whether Sox2 partly regulates neuroserpin expression during CNS development.

Neuroserpin is highly upregulated following ischemic nerve injury and shown to be neuroprotective by preventing ischemia induced neuronal apoptosis, microglia activation, and promoting the preservation of the blood brain barrier (Yepes and Lawrence, 2004, Gu et al., 2015, Cinelli et al., 2001). As Sox2 is highly upregulated in Schwann cells following peripheral nerve injury (Parrinello et al., 2010, Parkinson et al., 2008), it would also be interesting to see if Sox2 is upregulated in CNS following ischemic injury, and whether it is responsible for upregulating neuroserpin allowing for neuroprotection.

3.3.6 Sox2 increases proliferation in Schwann cells

Overexpression of Sox2 has widely been reported in several tumours, including lung cancer, breast cancer, ovarian cancer and glioma (Weina and Utikal, 2014, Lu et al., 2010a, Chen et al., 2008). It was further reported to enhance proliferation in these cancers and to also be oncogenic (Lu et al., 2010a, Chen et al., 2008, Yang et al., 2014a, Weina and Utikal, 2014). In particular Sox2 was shown to be highly expressed within the squamous cell tumours and adenocarcinomas isolated from patients with lung cancer, as well as in breast cancer, with levels of Sox2 expression correlating with tumour grade and cyclin D1 expression (a marker of proliferation). In

the nervous system, overexpression of Sox2 was shown to inhibit neuronal differentiation, and to also play a functional role in enhancing proliferation in crest cells (Wakamatsu et al., 2004). More specifically in Schwann cells, overexpression of Sox2 enhanced the proliferative response of these cells to β-neuregulin. While, Sox2 has been shown to enhanced proliferation in many cells types, the effect of Sox2 on Schwann cell proliferation in the presence of a range of mitogenic stimulus (such as Nrg1 and BDNGF) driving proliferation *in vivo* has not been examined.

In agreement with its previously published role in enhancing proliferation, we showed for the first time that Sox2 was capable of promoting proliferation in Schwann cell in the nerves of $Sox2^{HomoOE}$ mice during development (postnatal day 7) and during adulthood (postnatal day 60). This data further supports to the ability of Sox2 to maintain Schwann cells in an immature state, as mature Schwann cells are non-proliferative.

In breast cancer cells, Chen et al. (2008) identified that Sox2 promoted proliferation by synergising with β-catenin and binding to a Sox core binding element region (C(T/A)TTG(T/A)(T/A)) located between 86 to 234bps proximal to the CCND1 gene promoter. Together Sox2 and β-catenin promoted the gene expression of CCND1, and thus its protein product cyclin D1; a critical regulator of G1/S cell cycle transition in breast cancer cells (Chen et al., 2008). It would be interesting to see if Sox2 activated the transcription expression of cyclin D1 in Schwann cells, thus promoting Schwann cell proliferation.

$p27^{kip1}$ plays a role in regulating the cell cycle by binding and inhibiting multiple cyclin-dependent kinases and was recently shown to have a regulatory effect on Sox2. Overexpression of p27 in both mouse embryonic fibroblasts and transduced embryonic stem cells reduced Sox2 expression, while silencing p27 expression in fibroblasts, lungs, retina and the brain resulted in a defective repression of Sox2, as well as delayed silencing of Sox2 during the differentiation of pluripotent cells (Li et al., 2012). p27 was shown to regulate the transcriptional expression of Sox2 by forming a complex with p130, E2F4 and SIN3A at a critical regulatory element responsible for Sox2 expression, termed the Sox2-SRR2 enhancer (Li et al., 2012, Sikorska et al., 2008). A further study by Herreros-Villanueva et al. (2013) revealed that Sox2 is also able to regulate the gene expression of $p27^{kip1}$ in pancreatic cancer

cells (LC3.6 cells) by directly binding to the promoter/enhancer regions, and promoting cell cycle progression (Herreros-Villanueva et al., 2013). From these studies it appears that $p27^{kip1}$ is able to directly suppress Sox2 expression, however when the expression of Sox2 is rapidly upregulated as seen in many cancers, Sox2 feeds back and blocks the expression of $p27^{kip1}$, causing increased cell cycle progression.

More specifically in relation to Schwann cells, Krox20 has been shown to mediate the induction of p27, thus inducing Schwann cell exit from the cell cycle during development (Parkinson et al., 2004). As Sox2 reduced Krox20 expression and overexpression of Sox2 in pancreatic cancer cells has been shown to block $p27^{kip1}$ function, it would be interesting to see whether the expression of $p27^{kip1}$ is altered, along with its downstream cyclin-dependent kinase targets, in the nerves of $Sox2^{HomoOE}$ mice compared to Sox2 controls mice.

Sox2 has been shown to be expressed in 40-50% of schwannomas; a benign Schwann cell tumour which forms in the nerves sheath, resulting from uncontrolled proliferation (Shivane et al., 2013). More recently, Sox2 was shown to disrupt the Hippo signalling pathway (a key regulator of proliferation and apoptosis) in osteosarcoma cells and glioblastoma tumours, by transcriptionally repressing the tumour suppressor scaffolding protein NF2 (neurofibromin 2, merlin) and upregulating YAP (Yes associated protein) expression, which functions as an oncogene in many cancers (Basu-Roy et al., 2015). The Hippo-pathway is conserved across multiple cells types including Schwann cells, and mutations in the NF2 gene or disruptions to its expression is associated with schwannoma formation (Rouleau et al., 1993, Hanemann, 2008). As Sox2 has been shown to increase proliferation (in this study) and alter the Hippo-pathway (Basu-Roy et al., 2015), it would be of interest to see whether sustained overexpression of Sox2 alters the NF2 expression in $Sox2^{HomoOE}$ Schwann cells and leads to schwannoma development in nerves taken from $Sox2^{HomoOE}$ mice at later time-points, such as 6 months or 12 months of age. In order to check for the presence of schwannomas, nerve sections taken from control and $Sox2^{HomoOE}$ mice could be stained with Haematoxylin and Eosin (H&E) and then analysed for characteristics of schwannoma tumours. Schwannomas often show Antoni patterning; highly cellular areas composed of bundles of Schwann cells that have a spindle like morphology (Antoni type A

pattern), or loosely textured or microcytic areas composed of Schwann cells which may merge with one another (Antoni type B pattern). Furthermore, schwannomas often have areas of nuclear alignment or palisading, forming parallel nuclear arrays or Verocay bodies (cellular areas, surrounded by nuclear palisades) (Hilton and Hanemann, 2014).

3.3.7 Overexpression of Sox2 causes an inflammatory nerve environment

Models of inherited peripheral demyelinating neuropathies such as Charcot Marie Tooth (CMT) type 1A, B and X disease demonstrate substantially enhanced nerve inflammation, which leads to the amplification of disease progression (Martini and Willison, 2015). Both the innate and adaptive immune response have been implicated in models for inherited peripheral neuropathies (Martini and Willison, 2015). Macrophages have been shown to be recruited to the peripheral nerves in models of CMT-1 disease, where they sense and move towards defective Schwann cells and play a pivotal role in mediating myelin and axonal damage (Carenini et al., 2001, Groh et al., 2015, Kobsar et al., 2005). Blocking the activation of macrophages by colony stimulating factor-1 (CSF-1), a secreted cytokine produced by endoneurial fibroblasts, resulted in a robust reduction in the number of macrophages in the nerves of CMT-1B and -1X mouse models and severely ameliorated the neuropathy; improved axonal structures and improved nerve function (Klein et al., 2015, Groh et al., 2012). Furthermore, reducing but not eliminating the expression of monocyte chemoattractant protein 1 (MCP-1/ CCL2), a chemokine produced by Schwann cells and involved in macrophage attraction and activation, reduced the recruitment of macrophages and alleviated the demyelinating phenotype in CMT-1B and CMT-1A mouse models (Fischer et al., 2008a, Kohl et al., 2010a).

T-and B-lymphocytes are also recruited and increase demyelination in the nerves of CMT-1B (P_0het) and CMT-1X (connexin 32 mutant) mouse models (Carenini et al., 2001, Kobsar et al., 2003); CMT-1B and CMT-1X mouse models crossbred with Rag1 (recombinase activating gene 1) deficient mice lacking mature T-and B-lymphocytes, showed marked amelioration of demyelination, fewer axonopathic changes and a reduction in macrophage number (Kobsar et al., 2003). Surprisingly however, removing T-and B-lymphocytes from CMT-1A (PMP22 overexpressing

transgenic mice) mouse models did not alleviate disease progression (Kohl et al., 2010b). These studies demonstrate the critical role macrophages and immune cells play in enhancing demyelination and neuropathology.

Having discovered that Sox2 overexpression results in a phenotype similar to models of CMT-1 disease [See section 3.2.1-3.2.3] in $Sox2^{HomoOE}$ mice, we set out to investigate whether our mouse model also demonstrated a strong influx of inflammatory immune cells. $Sox2^{HomoOE}$ mice showed an increased number of both macrophages and T-lymphocytes into their poorly myelinated nerves. A slight increase (although not significant) in immune cells was observed from early developmental time-points (P7) in $Sox2^{HomoOE}$ mice, and increased with age (up until P60); which further correlated with the worsening phenotype and disease progression observed in these mice. A similar observation was previously observed in CMT-1A, CMT-1X and CMT-1B mouse models, whereby the number $F4/80^{+}$ macrophages and $CD8^{+}$ T-lymphocytes were significantly elevated with increasing age and disease progression (Carenini et al., 2001, Kobsar et al., 2005, Kobsar et al., 2003). A shown in this study and previous studies, macrophages in demyelinating nerves outnumber that of T-lymphocytes, suggesting that they are the major culprit in disease progression (Kobsar et al., 2003, Kobsar et al., 2005, Carenini et al., 2001). It would be interesting to see whether administration of the CSF-1 receptor inhibitor, which was previously identified by Klein et al., (2015) to reduce macrophage influx and act as a treatment for CMT-1 neuropathies, would ameliorate the worsening phenotype observed in $Sox2^{HomoOE}$ mice, as a potential anti-inflammatory therapy.

The MEK 1/2-ERK 1/2 signalling pathways were revealed to be upregulated in the CMT-1A mouse model and to regulate the expression of MCP-1 (Kohl et al., 2010a). Furthermore, blocking the MEK 1/2-ERK 1/2 signalling cascade using a pharmacological inhibitor (PD184352), reduced the expression of MCP-1 (Kohl et al., 2010a). Activation of the MEK 1/2-ERK 1/2 pathways via a tamoxifen induced Raf kinase transgene in healthy Schwann cells was shown to induce Schwann cell demyelination, motor defects, the recruitment of inflammatory cells into the peripheral nerve and activate the expression of MCP-1 (Napoli et al., 2012). As the MEK 1/2- ERK 1/2 cascade has been proven to play a pivotal role in linking Schwann cell pathology with the inflammatory response, it would be of interest to

see whether the MEK 1/2- ERK 1/2 signalling cascade is elevating in the nerves of $Sox2^{HomoOE}$ mice, along with its downstream target MCP-1, in order to attempt to understand the mechanism by which overexpression of Sox2 leads to an increased recruitment of macrophages.

A recent study by Xia et al. (2015) identified Sox2 to be highly expressed in neutrophils, where it acts as a cytoplasmic pattern recognition receptor. Upon the recognition of microbial DNA, Sox2 was shown to trigger the expression of genes encoding for pro-inflammatory molecules, in a TAB2-TAK1 dependent manner, which leads the activation of NF-kB and AP-1; thus causing an immune response. Although highly upregulated in neutrophils, Sox2 was not expressed in any other immune cells including macrophages, eosinophils or basophils (Xia et al., 2015). This study highlights a new and novel role for Sox2 in regulating the immune response and suggests new possibilities for Sox2 being involved in triggering an inflammatory response in a range of cells. A previous study by Napoli et al. (2012), identified that activation of the Raf-ERK signalling pathway in Schwann cells caused blood nerve barrier (BNB) breakdown, and an influx of immune cells into the nerve. As we observe such as dramatic increase in immune cells in the nerves of adult $Sox2^{HomoOE}$ mice, it would be interesting to see whether overexpression of Sox2 causing blood nerve barrier (BNB) breakdown, as a mechanism that allows for the infiltration of immune cells into the nerve. BNB breakdown could be analysed in by injecting mice with Evans blue, an azo dye with a high affinity for serum albumin. Following BNB breakdown, Evans blue can be traced from the blood vessels into the endoneurium and perineurium (Napoli et al., 2012).

Although we have observed a striking increase in the number of macrophages recruited to the nerves of $Sox2^{HomoOE}$ mice, we are unsure whether the environment in the nerves of these mice is pro-inflammatory and thus destructive. TNF-α and IL-1β have been linked to macrophage activation and tissue destruction, whilst cytokines such as IL-10 and IL-4 have been shown to mediate an anti-inflammatory environment (Ellis and Bennett, 2013). To clarify whether the overexpression of Sox2 in Schwann cells orchestrates a pro-inflammatory environment, future experiments using an antibody array should be carried out comparing the cytokine profile of nerves taken from control and $Sox2^{HomoOE}$ mice. Analysis of the Affymetrix gene array carried out by Dr R.Doddrell in our group (mentioned earlier in Section 3.2.7),

identified that Sox2 did not significantly alter the transcript of IL-10 (-1.5x, P=0.4), IL-1α (-2.0x, P=0.5) or IL-1β (-1.2x , P=0.8), but did significantly alter the transcript of MCP-1 (-3.1x, P=0.02), CSF-1 (-4.7x, P=0.03), granulocytes-macrophage colony-stimulating factor (-1.4x, P=0.6), and vascular endothelial growth factor -B (1.6x P=0.004).

3.3.8 Overexpression of Sox2 in Schwann cells causes functional impairment

Overexpression of Sox2 in Schwann cells causes severe hypomyelination of axons, as well as a significant increase in the number of unmyelinated axons in the nerves of $Sox2^{HetOE}$ (during development) and $Sox2^{HomoOE}$ mice. As a result these mice demonstrated a phenotype similar to that of mouse models of CMT-1 and patients diagnosed with CMT-1; they exhibit poor movement, slower nerve conduction velocities and reduced motor function (Klein et al., 2015, Saporta et al., 2012, Jani-Acsadi et al., 2008, Wrabetz et al., 2006). CMT disease is also classically associated with reduced sensitivity to heat and touch in the feet and lower legs of diagnosed patients, we therefore analysed whether the overexpression of Sox2 impaired sensory function within the nerves of $Sox2^{HomoOE}$ mice and revealed that sensitivity to toe pinching and Von Frey filament testing was severely reduced (Reilly, 2001). In some cases of CMT-1 and CMT-2 diagnosed patients experience neuropathic and nociceptive pain, however as we did not test for this we cannot state whether this was experienced by $Sox2^{HomoOE}$ mice (Gemignani et al., 2004, Carter et al., 1998). The results obtained from carrying out functional testing coincided with our hypothesis that as a negative regulator of Schwann cell myelination, Sox2 overexpression induced a phenotype similar to CMT-1 demyelinating neuropathy.

The mechanisms by which Sox2 reduces sensory function is unclear. We believe that it could be due to a direct effect of Sox2 impairing myelination of fast conducting Aδ sensory fibres, which are involved in relaying information regarding acute pain and pressure, or as an indirect effect caused by potential damage to sensory nerve fibres due to an influx of inflammatory cells [this is discussed in more detail in section 4.3.4].

3.3.9 Deleting Sox2 as a therapy for peripheral demyelination

Our results show that Sox2 acts as a negative regulator of Schwann cell myelination by impairing the expression of myelin proteins and hindering Schwann cell myelination, resulting in a phenotype similar to that of a peripheral neuropathy such as CMT-1 disease in our $Sox2^{HomoOE}$ mice. Unpublished data from Dr Maurizio D'Antonio's group (at San Raffaele University) has further identified that the transcription factors Sox2, cJun and Id2 are upregulated in the nerves of P0S63del transgenic mice (CMT-1B mouse model). Serine 63 mutations in P_0 protein (P0S63del) results in the protein being retained in the endoplasmic reticulum (ER), causing ER stress, activation of the unfolded protein response (UPR) and Schwann cell demyelination (Wrabetz et al., 2006). P0S63del mutations also affects the ability of wild type P_0 to exit the ER and assist in myelin formation (Fratta et al., 2011). As Sox2 is upregulated in P0S63del mice, it could be assumed that it contributes to the disease pathology. Sox2 null mice generated by cross breeding Sox2 conditional floxed mice with P_0Cre mice showed increased myelin thickness at P3, although myelin thickness appears to be undistinguishable from control nerves by P7 (unpublished data by Dr Xin-Peng Dun in our group; unpublished data by Dr Francesca Florio at San Raffaele University). As Sox2 is a negative regulator of Schwann cell myelination and ablation of Sox2 has been shown to increases Schwann cell myelin thickness, we might expect that removal of Sox2 from P0S63del transgenic mice (CMT-1B) would alleviate the disease progression and improve myelination. This was however not proven to be the case, ablation of Sox2 from P0S63del nerves worsens the phenotype; mice demonstrated an enhanced reduction in myelin basic protein expression and an increase in the percentage of unmyelinated axons compared to P0S63del nerves (unpublished data by Dr Francesca Florio at San Raffaele University). In P0S63del nerves Sox2 may therefore provide a protective effect by reducing the expression of P0S63del and thus reducing ER stress and activation of the unfolded protein response (UPR) (unpublished data by Dr Francesca Florio at San Raffaele University). As we can see from this unpublished study, Sox2 does not always exert a pathological effect and may in some cases be protective. Sox2 has also been shown to be upregulated in the mouse model of CMT-1A (*Tg(Pmp22)Kan* Mice) which overexpress PMP22 (Fledrich et al., 2014). It would be interesting to see whether the upregulated

expression of Sox2 in CMT-1A disease is also protective; reducing the protein expression of PMP22 via its negative myelin regulatory function might be beneficial.

The transcription factor cJun, a negative regulator of Schwann cell myelination (Parkinson et al., 2008), has been shown to be highly upregulated in pathological nerves but not healthy nerves (Hutton et al., 2011). Patients diagnosed with axonal neuropathies, CMT-1A and acquired demyelination neuropathies showed high cJun immunoreactivity in the nuclei of Schwann cells and in the cytoplasm, whereas no cJun expression was detected in normal nerves (Hutton et al., 2011). Experiments carried out on C3 mice (mouse model of CMT-1A), further revealed that cJun was highly expressed within the nerves of these animals, compared to controls (Hantke et al., 2014). Selective deletion of cJun in C3 mice (C3/Schwann cell-cJun$^{-/-}$) was shown to worsen the phenotype, resulting in an increased sensory-motor deficit and an increase in sensory axon loss, caused by PMP22 overexpression (Hantke et al., 2014). This study highlighted that in CMT-1A disease, Schwann cells upregulate their expression of cJun as an adaptive response to disease, allowing for axonal protection and the support of sensory-motor performance.

During development, inhibition of cJun by Krox20 promotes Schwann cell myelination and normal Schwann cell development (Parkinson et al., 2004). Studies therefore analysed whether ablation of cJun in Schwann cells would promote Schwann cell remyelination and regeneration following nerve injury as a potential therapy. Experiments carried out on cJun null mice following nerve injury revealed that cJun plays a protective role in promoting motor neuron survival, in addition to promoting the Schwann cell repair program and axon regeneration (Fontana et al., 2012, Arthur-Farraj et al., 2012). The JNK-cJun pathways has also recently been identified to be a key regulator of myelinophagy during Wallerian degeneration, which is essential for effective Schwann cell myelin degeneration, myelin clearance and thus nerve repair and regeneration following injury (Gomez-Sanchez et al., 2015). Blocking the JNK-cJun pathways by either treating wild type mice with JNK inhibitor (SP600125) or conditional depleting cJun from Schwann cells in mice (cJun null mice), revealed that myelin protein breakdown and autophagic flux was significantly reduced at 5 days after injury (Gomez-Sanchez et al., 2015). These

studies demonstrate that both cJun and Sox2 can exert protective and beneficial effects in response to disease and injury when regulated correctly.

3.3.10 Sox2 in the PNS vs CNS

Previous work has shown that Sox2 plays an essential role in the development of the peripheral nervous system, as misexpression or mutations of Sox2 result in failure to form the neural crest and impaired differentiation of neural crest cells into peripheral neurons and glia (Wakamatsu et al., 2004). Schwann cells express Sox2 during the immature Schwann cell stage, however for immature Schwann cells to myelinate, Sox2 levels must be reduced (Le et al., 2005a). We further confirm that maintained expression of Sox2 in Schwann cells during development impairs myelination and leads to the development of a peripheral neuropathy. Despite what we observe in Schwann cells, the function of Sox2 appears to be different in oligodendrocytes.

Reactivation of Sox2 mediated by tumour suppressor protein Brca1 and the chromatin remodelling protein Brahma in cultured oligodendrocyte precursors (OPCs) was previously shown to cause cell fate reversal of OPCs and conversation into multipotent neural stem-like cells (NSLCs) (Kondo and Raff, 2004). However, a more recent study by Hoffmann et al. (2014) identified Sox2 to be involved in promoting the terminal differentiation of oligodendrocytes. Despite being highly expressed throughout oligodendroglia development, Sox2 was shown not to exert any functional effect in these cells; removal of Sox2 did not alter proliferation or survival, nor did it affect emigration of OPCs from the ventricular zone to their final destination in the mantle and marginal zone (Hoffmann et al., 2014). Instead, Sox2 was shown to be involved in regulating the timely translation of two critical transcription factors required for early oligodendrocyte differentiation, maturation and myelination; Sox2 repressed the expression of miR145, thus enabling the translation of myelin gene regulatory factor (myrf) and mediator complex subunit 12 (Med12) (Hoffmann et al., 2014, Emery et al., 2009, Vogl et al., 2013). Sox2 was also shown to directly bind to the promoter of MBP, driving its expression in differentiating oligodendrocytes (Hoffmann et al., 2014).

In contrast to the study by Hoffmann et al. (2014), Zhao et al. (2015) stated that they were unable to confirm the involvement of Sox2 in oligodendrocyte terminal differentiation. Zhao et al. (2015) identified that Sox2 does in fact play a functional in

in regulating OPC proliferation and survival, as cultured OPCs taken from Sox2 null mice showed lower expression of the proliferation marker Ki67 and also an increased number of cells with pyknotic nuclei (indicative of cell death), compared to cultured OPCs taken from control mice. Even though this study stated that Sox2 is not involved in OPC differentiation, an impairment in OPC differentiation was observed in Sox2-deficient cells compared to controls, this was indicated by a reduction in $Olig2^{+}/MBP^{+}$ cells. Nonetheless, Zhao et al. (2015) attributed this impairment to a reduction in the number of Sox2-depleted OPCs in culture rather than their inability to differentiate and myelinate; it was however noted that Sox2 may be required to prime OPCs for full differentiation, which coincides partly with the study by Hoffmann and colleagues (ibid).

The study by Zhao et al. (2015) further stated that overexpression of Sox2 in OPCs impaired differentiation and therefore downregulation of its expression is required for normal myelination. While Hoffmann at al. (2014) showed that Sox2 was involved in OPC terminal differentiation, they did not stated that Sox2 was required at later time-points, as Sox2 was shown to be very weakly expressed in the spinal cord at P30. Thus, it is possible that Sox2 may only be involved in the timely onset of differentiation and that maintained expression may have negative effects.

Following toxin induced CNS demyelination, Sox2 was also identified to be re-expressed in OPCs, where it regulated proliferation, OPC recruitment and survival (Zhao et al., 2015). Zhao et al. (2015) reported that remyelination was impaired in OPC specific Sox2 null mice following demyelination, however suggested this to be a consequence of reduced OPC recruitment, rather than the role of Sox2 in OPC differentiation. This suggestion was further supported by experiments which showed that depletion of Sox2 in OPC during the differentiation stage (11-14 days post lesion) did not affect OPC differentiation, whilst depletion of Sox2 in OPCs during the recruitment stage, significantly reduced differentiation (Zhao et al., 2015).

The study by Zhao et al. (2015) eluded to a similar role of Sox2 in OPCs, to that which we observe in immature Schwann cells; the ability to regulate proliferation and impair differentiation when overexpressed. The study further identified a new role of Sox2 in regulating the OPC recruitment and expansion following demyelination. On the other hand Hoffmann et al. (2014) identified a new and novel role for Sox2 in

driving oligodendrocyte terminal differentiation, and its ability to compensate for Sox3 in this process, when Sox3 is depleted from oligodendrocytes. These studies both highlight exciting new functions for Sox2 in oligodendroglial cells, however due to their conflicting conclusions regarding the involvement of Sox2 in oligodendrocyte differentiation, its role in this process remains uncertain.

3.3.11 Conclusion

Sox2 is able to retain Schwann cells in an immature highly proliferative state, by reducing the expression of Krox20; an essential transcriptional regulator of Schwann cell myelination, as well as its downstream myelin protein targets P_0 and Krox20. We have also shown that Sox2 alters the expression and nuclear localisation of Sox10 in Schwann cells at later developmental time-points, however further experiments need to be carried out clarify this. As Sox2 impairs Schwann cell myelination, this leads to hypomyelination of axons, reduced nerve conduction velocity, and impaired motor and sensory function. Surprisingly, overexpression of Sox2 was further shown to enhance the recruitment of immune cells to hypomyelinated nerves, which is also observed in mouse models and patients with CMT-1. We confirm that Sox2 is a negative regulator of Schwann cells myelination and maintained expression of Sox2 induces a phenotype similar that seen in mouse models of CMT-1 disease.

Chapter 4 Sox2 overexpression impairs nerve repair and functional recovery following injury.

4.1 Introduction

Following peripheral nerve injury, axons distal to the site of injury degrade and Schwann cells dedifferentiate into a repair Schwann cell state, helping to facilitate nerve repair and regeneration. Recent studies have identified that in order for Schwann cells to dedifferentiate and orchestrate an effective injury response that allows for nerve regeneration, they must downregulate the expression of myelin related genes, and re-express markers of immature Schwann cells, such as cJun and Notch, and re-activate the p38 and extracellular-regulated kinase 1/2 (ERK1/2) mitogen-activated protein kinase (MAPK) signalling pathways (Arthur-Farraj et al., 2012, Jessen and Mirsky, 2008, Napoli et al., 2012, Yang et al., 2012, Woodhoo et al., 2009). This change in Schwann cell signalling and gene expression thereon facilitates neuronal survival, blood nerve barrier breakdown, the recruitment of macrophages and the clearance of axonal and myelin debris, thus providing an environment suitable for axonal regrowth and regeneration. Once axons have regenerated and re-innervated their target tissues, Schwann cells must downregulate the expression of immature markers, redifferentiate and remyelinate regenerating axons in order to complete the repair process (Navarro et al., 2007).

Recent studies have identified that Sox2 is also re-expressed in Schwann cells following nerve injury, and helps to facilitate the re-localisation of N-cadherin to cell-cell contact junctions on Schwann cell membranes, enabling Schwann cell sorting and the guidance of axons across the nerve bridge (Parkinson et al., 2008, Arthur-Farraj et al., 2012, Parrinello et al., 2010). Although re-expression of Sox2 is important during the early stages of nerve injury, it is not clear how continued expression of Sox2 will affect nerve regeneration and functional recovery of motor and sensory neurons. We therefore aimed to investigate the effect of continued Sox2 expression on Schwann cell function, nerve repair and functional recovery for up to 21 days post crush injury (21DPI).

4.2 Results

4.2.1 Sox2 overexpression impairs Schwann cell remyelination after injury

We have previously shown (Chapter 3) that overexpression of Sox2 leads to severe hypomyelination in adult $Sox2^{HomoOE}$ mice and the progressive onset of a hypomyelination peripheral neuropathy. In contrast, $Sox2^{HetOE}$ mice show declined expression of Sox2 and GFP from P21 onwards, with myelination returning to normal by adulthood in these animal (P60); no significant difference was observed between the g-ratio of $Sox2^{HetOE}$ (0.65 ± 0.02) and control mice (0.66±0.03) ($P>0.05$) [Figure 3.4]. As we wanted to investigate the effect of continued Sox2 expression following sciatic nerve injury in adult mice with normal myelinated axons, we decided to carry out these experiments using $Sox2^{HetOE}$ and Sox2 Het control animals between the ages of 6 and 8 weeks. We hypothesized that following PNS injury the accompanying dedifferentiation of Schwann cells would cause re-activation of Sox2 and GFP expression in the $Sox2^{HetOE}$ animals. Immunohistochemical analysis showed re-expression of GFP expression in the sciatic nerves of $Sox2^{HetOE}$ animals at 7 day post cut injury (7 DPC) and 14 and 18 days post crush injury (14 and 18 DPI), compared to Sox2 Het controls at similar time-points [data not shown]. Furthermore, increased levels of Sox2 were maintained at 21 DPI in $Sox2^{HetOE}$ animals, compared to Sox2 Het controls; in which Sox2 and GFP were undetectable (n=4) [Figure 4.4].

Using both transmission and scanning electron microscopy, we evaluated Schwann cell remyelination in the sciatic nerves of Sox2 Het control and $Sox2^{HetOE}$ mice taken distal to the site of injury (distal nerve stump) at 21DPI.

To verify that myelination was normal in the sciatic nerves of Sox2 Het control and $Sox2^{HetOE}$ mice, were analysed scanning electron micrographs of uninjured nerve taken from both these animals. We observed that myelination was normal in the sciatic nerves of Sox2 Het control and $Sox2^{HetOE}$ mice prior to injury, as numerous thick and compact myelin sheaths were detected (n=2 Sox2 Het control, n=4 $Sox2^{HetOE}$) [Figure 4.1]. We next analysed sciatic nerve sections taken distal to the site of injury, from the same Sox2 Het control and $Sox2^{HetOE}$ animals at 21 DPI. In the nerves of Sox2 Het control mice, myelination was normal at 21 DPI; numerous

thick compact myelin sheaths were observed, suggesting that remyelination had occurred normally. In contrast, remyelination appeared to be impaired in the distal nerves of $Sox2^{HetOE}$ mice 21DPI; myelin sheaths were much thinner and there appeared to be a reduction in the overall number of myelin sheaths (n=2 Sox2 Het control, n=4 $Sox2^{HetOE}$) [Figure 4.1].

We next analysed the same uninjured and injured nerves via transmission electron microscopy (TEM), in order to obtain higher resolution images at higher magnification. This allowed for accurate measurements of myelin thickness and counts of unmyelinated axons to be made.

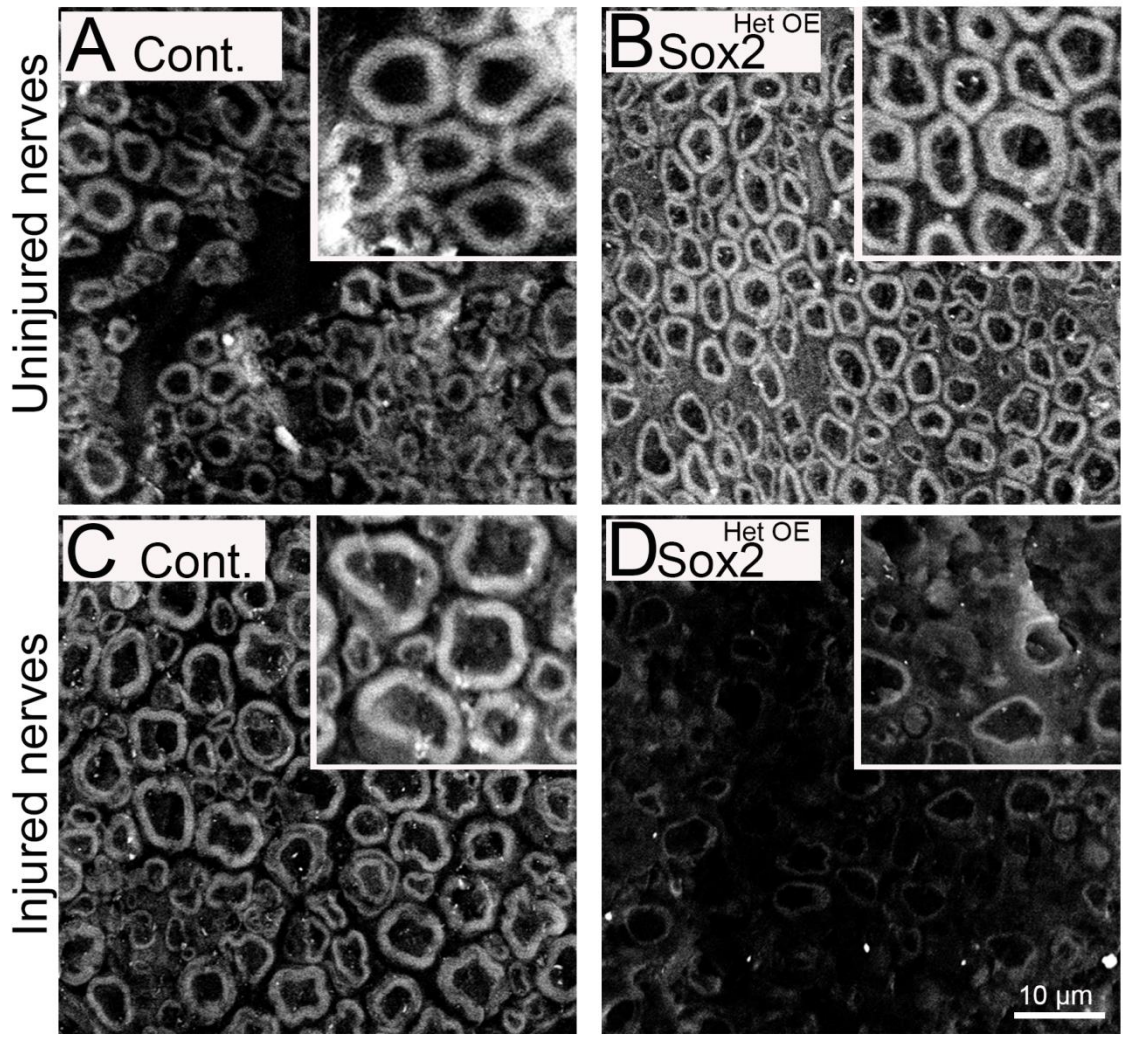

Figure 4. 1: Scanning electron micrographs of uninjured and injured sciatic nerves. Uninjured sciatic nerves (A & B) taken from sox2 Het control (A) and $Sox2^{HetOE}$ adult mice (B) show numerous thick myelin rings. Injured (crushed) distal sciatic nerves (C & D) taken from Sox2 Het control (C) and $Sox2^{HetOE}$ (D) mice 21DPI; note $Sox2^{HetOE}$ nerves are hypomyelinated with fewer myelin rings, compared to Sox2 Het control nerves (n=2 Sox2 Het control, n=4 $Sox2^{HetOE}$). A,B,C and D, inset 2x magnification.

Transmission electron micrographs showed that while axons in the Sox2 Het control nerves were remyelinated normally, many axons within the sciatic nerves of $Sox2^{HetOE}$ mice were hypomyelinated 21 DPI. The average g-ratio for Sox2 Het control mice was 0.69 ± 0.027, whereas the average g-ratio for $Sox2^{HetOE}$ mice was significantly increased to 0.86 ± 0.028 ($P<0.01$, n=4). Furthermore, the total percentage of unmyelinated axons at 21DPI was significantly increased from 1.1 ± 0.3 % in the sciatic nerves of Sox2 Het control mice, to 27.8 ± 10.2% in the sciatic nerves of $Sox2^{HetOE}$ mice ($P< 0.05$, n=4) [Figure 4.2]. Analysis of axonal diameter size revealed that there was also a significant shift in the percentage of axons towards having a larger diameter in the sciatic nerves of $Sox2^{HetOE}$ mice, compared to Sox2 Het controls; the average axonal diameter in Sox2 Het control nerves was 1.38 ± 0.02 µm, whereas the average axonal diameter in $Sox2^{HetOE}$ nerves was significantly larger at 1.62 ± 0.02 µm ($P <0.001$, n=4) [Figure 4.2].

Further analysis by TEM was carried out on the distal sciatic nerve stump sections taken from Sox2 Het control and $Sox2^{HetOE}$ mice, to determine whether axonal sorting was normal 21 days post injury (21 DPI). In the sciatic nerves of both Sox2 Het control mice and $Sox2^{HetOE}$ mice, all small diameter axons (<1µm) had effectively been sorted into groups and ensheathed by non-myelinating Schwann cell forming Remak bundles. Additionally, all larger calibre axons (>1µm) appeared to have been effectively sorted, and were in a 1:1 relationship with a Schwann cell (n=4) [Figure 4.2 and 4.3].

We further investigated the ultrastructure of the regenerating nerves using TEM and observed an abundant number of macrophages, still present within the sciatic nerves of $Sox2^{HetOE}$ mice, compared to Sox2 Het controls 21 DPI. More strikingly, the macrophages present within the nerves appeared to be associated with demyelinating axons and to also be degenerating myelin, suggesting that remyelination and demyelination was occurring. In the sciatic nerves of Sox2 Het control mice a couple of macrophages remained and myelin ovoid structure could still be observed 21 DPI, however this was to a much lesser extent, compared to $Sox2^{HetOE}$ mice (n=4) [Figure 4.3].

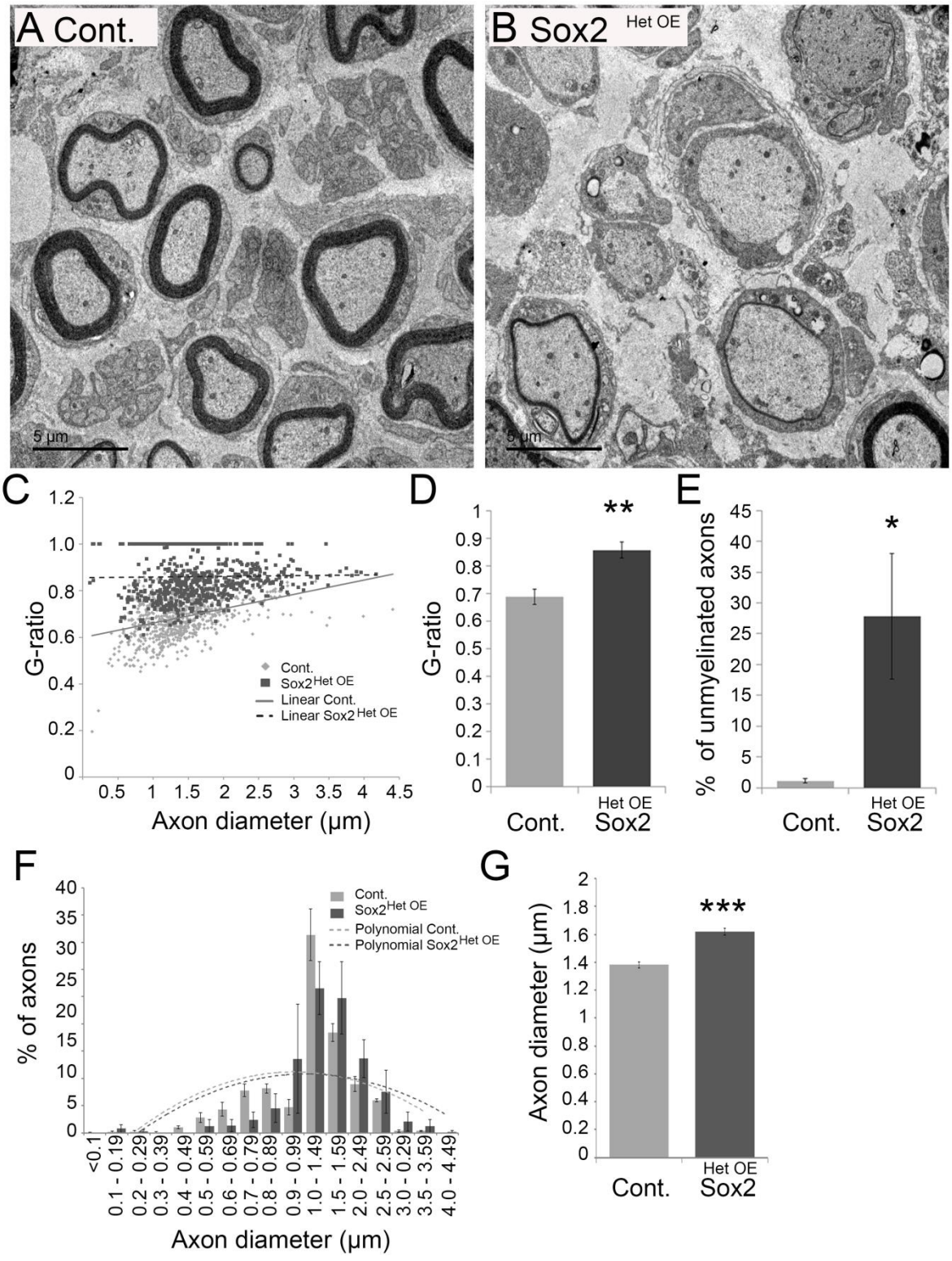

Figure 4. 2: Overexpression of Sox2 hinders remyelination. Transmission electron micrographs of sciatic nerves sections taken from control (A) and Sox2^{HetOE} nerves (B) at 21 DPI (n=4). (C) Scatter plot displaying the g-ratios of individual axons in relation to their axon size (n=4). (D) Graph showing the average g-ratio of control and Sox2^{HetOE} nerves 21 DPI;

note the g-ratio is significantly increased in $Sox2^{HetOE}$ mice compared to controls (P=0.005, n=4). (E) Graph showing the total percentage of unmyelinated axons in the sciatic nerves of control and $Sox2^{HetOE}$ mice (n=4). (F) Graph showing the percentage distribution of axons in relation to their size; note, a shift in the population of axons towards having a larger diameter in the sciatic nerves of $Sox2^{HetOE}$ mice at 21 DPI (n=4). (G) Graph showing the average axon diameter of control and $Sox2^{HetOE}$ nerves at 21 DPI; note the axon diameter is significantly larger in the sciatic nerves of $Sox2^{HetOE}$ mice at 21 DPI (P<0.001, n=4).

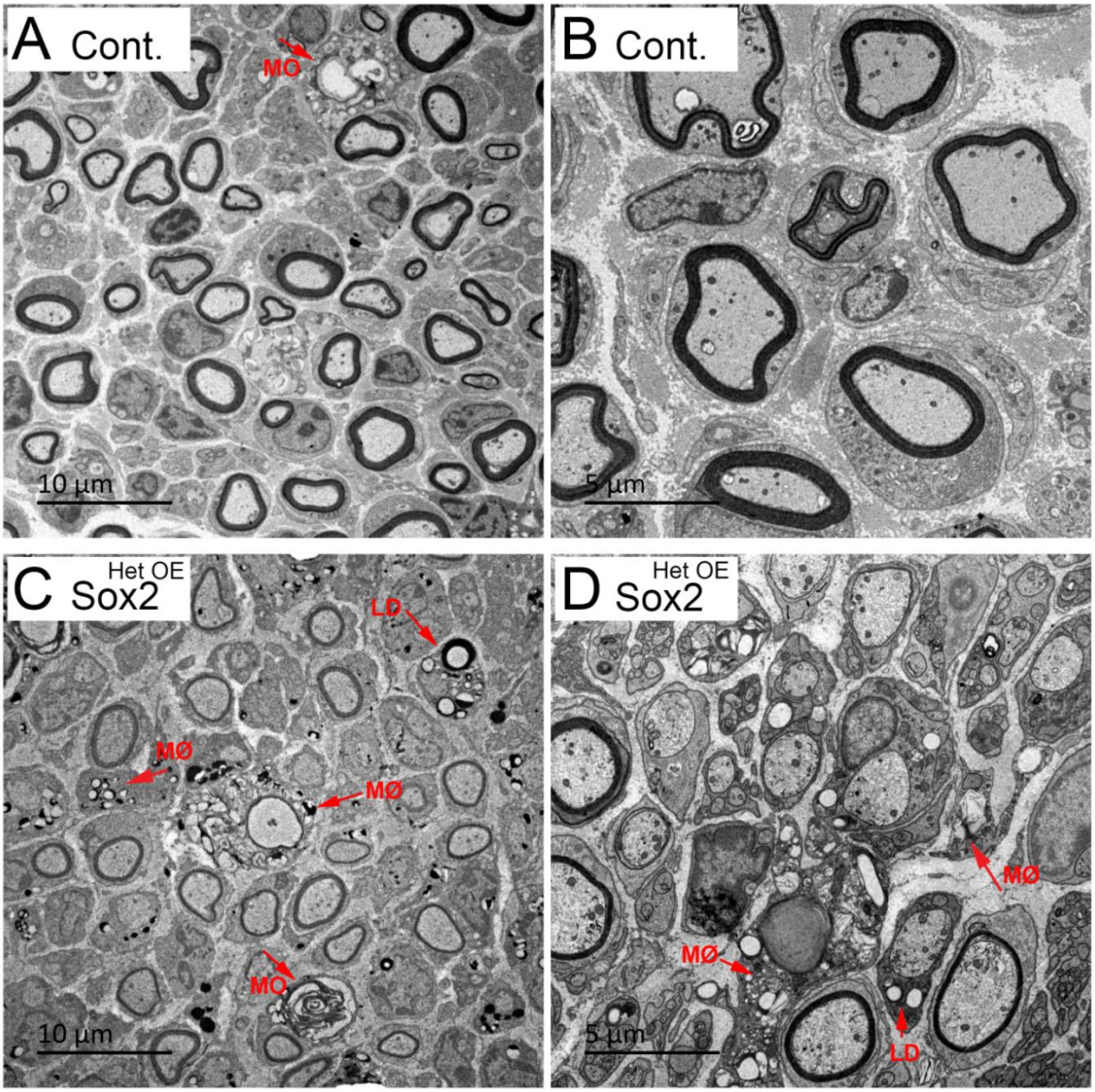

Figure 4. 3: Increased number of macrophages and myelin debris in the nerves of Sox2 overexpressing mice at 21 DPI . Transmission electron micrographs of Sox2 Het control (A & B) and $Sox2^{HetOE}$ (C & D) nerves at 21 DPI. In the nerves of $Sox2^{HetOE}$ mice, numerous macrophages and lipid droplets can be observed at both low (C) and high (D) magnifications. In comparison, very few macrophages and lipid vacuoles can be detected within the nerves of Sox2 Het control mice (A & B). MØ, Macrophage; MO, Myelin Oviod; LD, Lipid droplet.

4.2.2 Sox2 overexpression impairs the re-expression of myelin proteins after injury

As we have observed that continued Sox2 expression impairs Schwann cell remyelination, we next wanted to investigate whether continued Sox2 expression hindered the re-expression of myelin proteins following sciatic nerve injury. To test this we carried out immunohistochemical and western blot analysis on the distal sciatic nerve stump taken from Sox2 Het control and $Sox2^{HetOE}$ mice at 21 DPI.

The expression of Sox2 and GFP remained high, with Sox2 localising to the nucleus in the sciatic nerves of $Sox2^{HetOE}$ mice at 21 DPI. In comparison, the expression of Sox2 was clearly reduced, and no GFP was observed in the sciatic nerves of Sox2 Het control mice at 21 DPI (n=3) [Figure 4.4].

Further analysis of myelin associated proteins revealed that MBP re-expression was severely impaired within the distal sciatic nerve stump of $Sox2^{HetOE}$ mice at 21 DPI; expression levels of MBP were extremely low and very few MBP positive myelin rings could be observed (n=3) [Figure 4.4]. Similarly, expression levels of Krox20 appeared to be very low, with very few Krox20 positive nuclei being detected within the distal sciatic nerve stump of $Sox2^{HetOE}$ mice (n=3) [data not shown]. In contrast, MBP was highly expressed within the distal sciatic nerve stump of Sox2 Het control mice, with numerous MBP positive myelin rings being observed (n=3) [Figure 4.4]. In addition increased levels of Krox20, and numerous Krox20 positive nuclei were observed in the distal sciatic nerve stump of Sox2 Het control mice at 21 DPI (n=2) [data not shown].These experiments were repeated by western blot and showed that continued expression of Sox2 at 21 DPI impaired the re-expression of both MBP [data not shown] and P_0 [Figure 4.4] (n=3 control, n=4 $Sox2^{HetOE}$).

From these results we can conclude that continued expression of Sox2 following sciatic nerve injury impairs the ability of Schwann cells to re-express myelin associated proteins and effectively remyelinate regenerating axons, even though axon/Schwann cell association is normal at 21 DPI [See Figure 4.2 and Figure 4.3].

As we previously identified in Chapter 3 that Sox2 overexpression maintains Schwann cells in an immature state, which was further confirmed by the maintained expression of other immature Schwann cell markers such as cJun and N-cadherin. We therefore wanted to identify whether overexpression of Sox2 after nerve injury

would further retain Schwann cells in an immature/repair Schwann cell state, and thus the upregulated expression of other immature Schwann cell markers. To confirm this, we immunolabelled distal nerve stump sections taken from Sox2 Het control and $Sox2^{HetOE}$ mice with antibodies for cJun at 21 DPI.

Surprisingly, cJun expression was still detectable and clearly localised at the nucleus within the nerves of Sox2 Het control mice at 21 DPI; this was unexpected as analysis by electron microscopy had shown that all Schwann cells appeared to have redifferentiated and remyelinated normally. Further analysis of $Sox2^{HetOE}$ nerves 21 DPI revealed that cJun expression was highly detectable and to a much more elevated extent, than in the Sox2 Het controls. Furthermore the expression of cJun appeared to be much more evenly distributed throughout nerves of $Sox2^{HetOE}$ mice (n=2) [Figure 4.5].

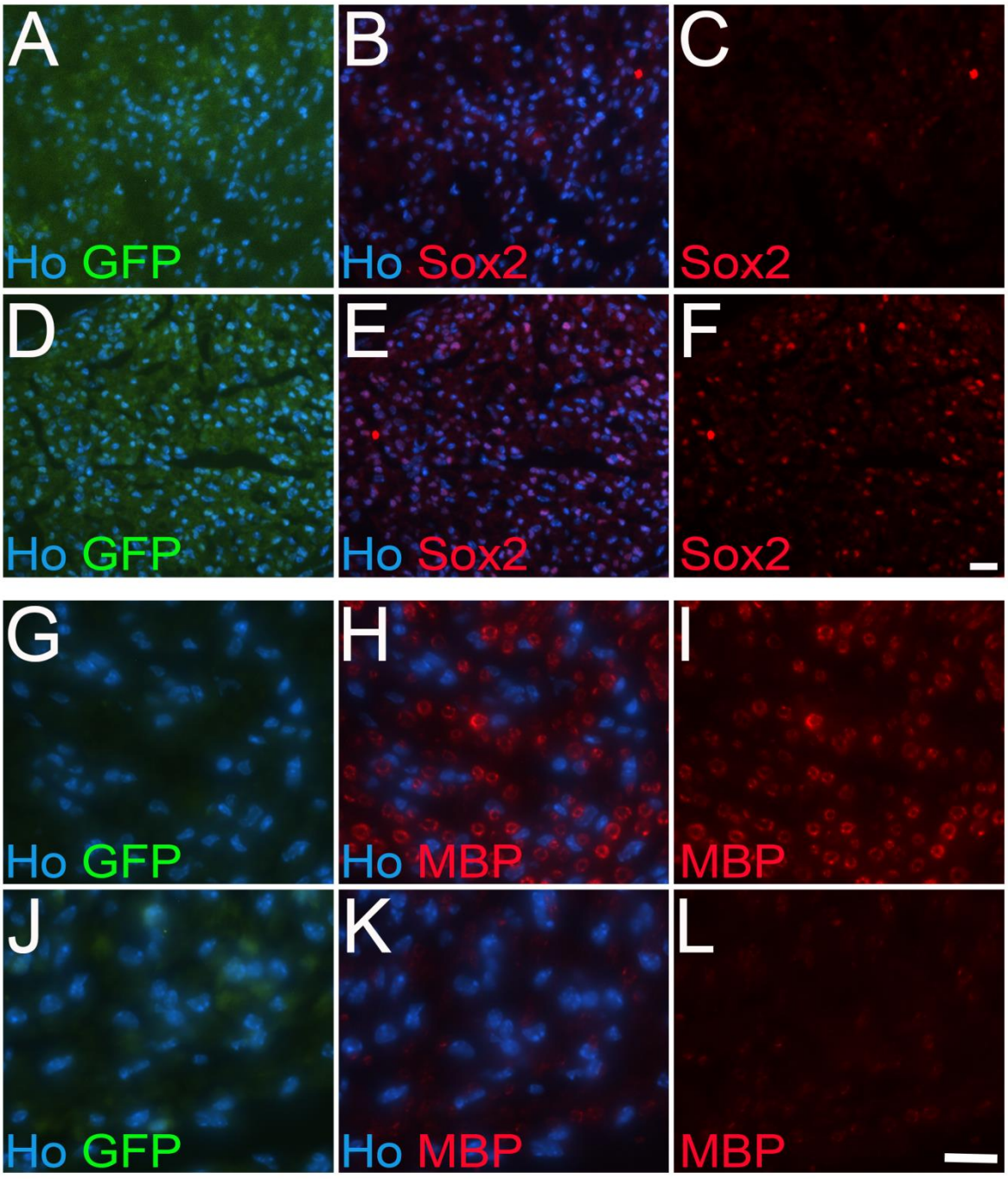
A
Ho GFP
B
Ho Sox2
C
Sox2
D
Ho GFP
E
Ho Sox2
F
Sox2
G
Ho GFP
H
Ho MBP
I
MBP
J
Ho GFP
K
Ho MBP
L
MBP

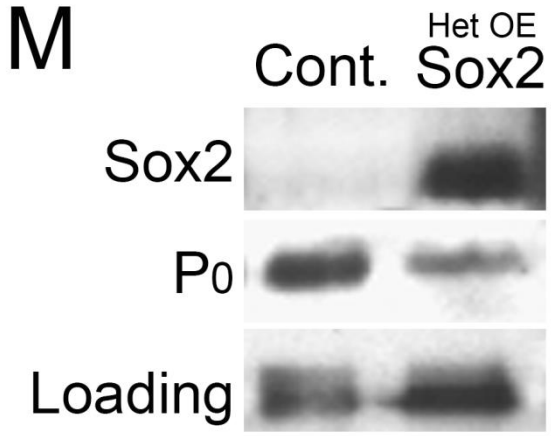
M
Cont.
Het OE
Sox2
Sox2
P0
Loading

Figure 4. 4: Overexpression of Sox2 impairs the re-expression of myelin proteins following injury. Immunolabelling with antibodies against Sox2 revealed that control nerves no longer express Sox2 at 21 DPI (A-C), whereas Sox2 is still highly expressed within $Sox2^{HetOE}$ nerves (D-F) at 21 DPI (n=3). Immunolabelling of distal sciatic nerve sections with antibodies for MBP (G-L) revealed that control nerves strongly express MBP and have numerous MBP positive rings (H & I) at 21 DPI, whereas $Sox2^{HetOE}$ nerves show weak expression of MBP and have very few MBP positive rings (K & L) at 21 DPI (n=3). Western blot (M) showing high expression of Sox2, and reduced expression of P0 and MBP in the distal nerve stump of $Sox2^{HetOE}$ mice at 21 DPI (n=3 control, n=4 $Sox2^{HetOE}$). Images (A-F) taken using 20x objective, images (G-L) taken using 40x objective, scale bars are 20µm.

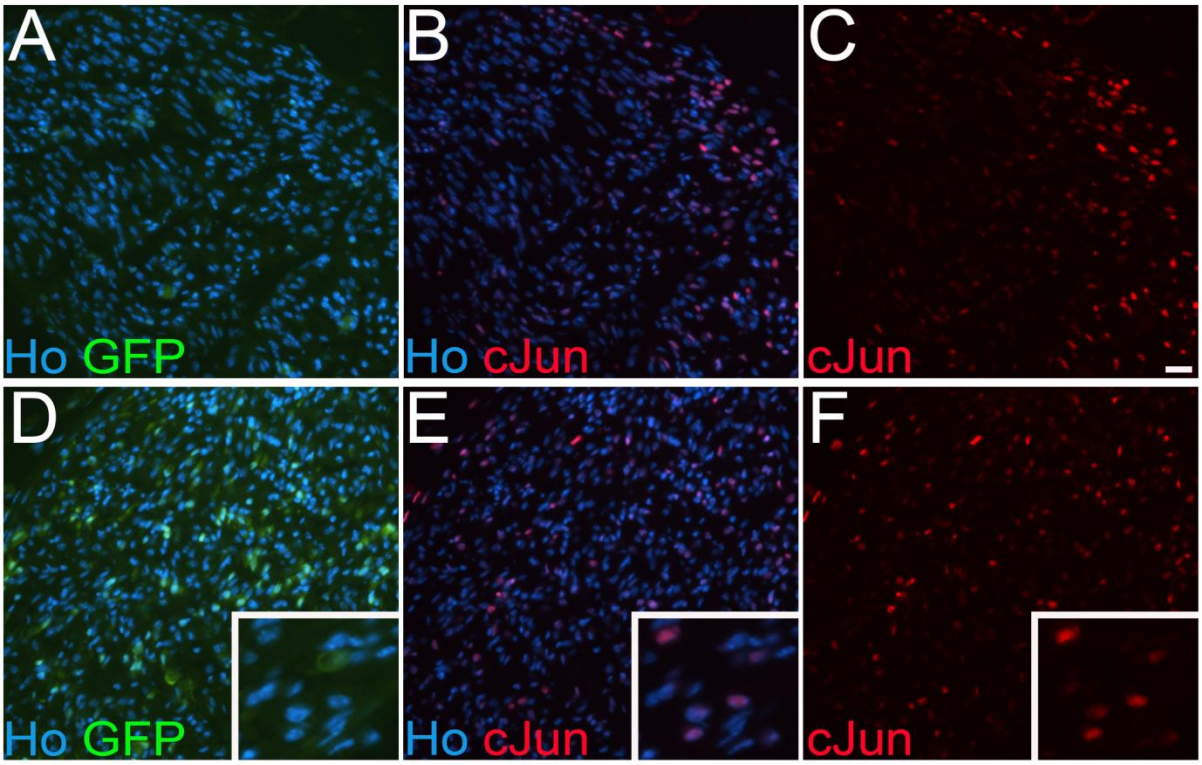

Figure 4. 5: cJun is elevated in the nerves of Sox2 overexpressing mice at 21 DPI. Distal sciatic nerve sections taken from Sox2 Het control and $Sox2^{HetOE}$ mice at 21 DPI were Immunolabelling with antibodies against cJun (A-F). Immunofluorescent staining shows higher levels of cJun expression and more numerous cJun positive nuclei in the nerves of $Sox2^{HetOE}$ mice (D-F), compared to Sox2 Het control mice (A-C) (n=2). Images (A-F) taken using 20x objective (D,E,F, inset 50x), scale bar is 20µm.

4.2.3 Overexpression of Sox2 maintains Schwann cells in a highly proliferative state 21DPI

To test whether Sox2 overexpression altered Schwann cell proliferation after injury, distal sciatic nerve stump sections taken from Sox2 Het control and $Sox2^{HetOE}$ mice at 3, 14, 18 and 21 DPI were stained with antibodies for Ki67.

At 3 DPI, there did not appear to be a rapid increase in the levels of proliferation, as very few Ki67 positive nuclei were detected in the sciatic nerves of both Sox2 Het control and $Sox2^{HetOE}$ mice. Furthermore, counts made on the total number of Ki67 positive nuclei per nerve revealed that at 3 DPI, Sox2 overexpression did not significantly increase the number of Ki67 positive nuclei within the nerves of $Sox2^{HetOE}$ mice compared to Sox2 Het controls (n=2 per genotype) [data not shown].

Analysis of Sox2 Het control and $Sox2^{HetOE}$ sciatic nerves at 7 DPC revealed that proliferation was increased within $Sox2^{HetOE}$ sciatic nerves, distal to the site of injury (89.7 ± 13.3 Ki67 positive nuclei per nerve section), compared to Sox2 Het control sciatic nerves, distal to the site of injury (67.2 ± 16.6 Ki67 positive nuclei per nerve section). Nonetheless, statistical analysis identified that the increased number of in Ki67 positive nuclei in nerves of $Sox2^{HetOE}$ mice was not significant ($P>0.05$, n=3) [Figure 4.6].

At 14 DPI, staining for Ki67 revealed that there was an increase in the number of proliferating cells within the distal sciatic nerve stump sections taken from both Sox2 Het control and $Sox2^{HetOE}$ mice; a total number of 289 Ki67 positive nuclei was detected in the distal nerves of Sox2 Het control mice and a total number of 296 Ki67 positive nuclei was detected within the distal nerves of $Sox2^{HetOE}$ mice (n=1 per genotype). Surprisingly, although Schwann cell proliferation appears to have peaked at this time-point, Sox2 overexpression did not appear to dramatically increase Schwann cell proliferation above the control threshold. Nonetheless, analysis at 18 DPI revealed that the total number of Ki67 positive nuclei was dramatically increased in the nerves of $Sox2^{HetOE}$ mice (42 ± 24 Ki67 positive nuclei per nerve section), compared to Sox2 Homo control mice (4 Ki67 positive nuclei per nerve section) (n=1 control, n=2 $Sox2^{HetOE}$) [Figure 4.7]. Similarly, at 21 DPI, a significant increase in Schwann cell proliferation was observed at this time-point in the distal sciatic nerve stump of $Sox2^{HetOE}$ mice (20.75 ± 3.7 Ki67 positive nuclei), compared to the distal

sciatic nerve stump of Sox2 Het control mice (6.5 ± 2.9 Ki67 positive nuclei) ($P < 0.05$, n=4 per genotype) [Figure 4.8].

These results suggest that overexpression of Sox2 directly after sciatic nerve injury does not significantly enhance proliferation above the normal threshold. However, continued Sox2 expression following axon regeneration maintains Schwann cells in a highly proliferative state. Data collected by Dr Xin-Peng Dun in our group [unpublished data], further confirmed that Sox2 expression following nerve injury is essential for Schwann cell proliferation, as a significant reduction in Schwann cell proliferation was observed in the distal nerve stump of Schwann cells specific Sox2 null mice, compared to control mice at 7 DPC. Overall these results support previous findings, that Sox2 plays a role in enhancing Schwann cell proliferation (Le et al., 2005a).

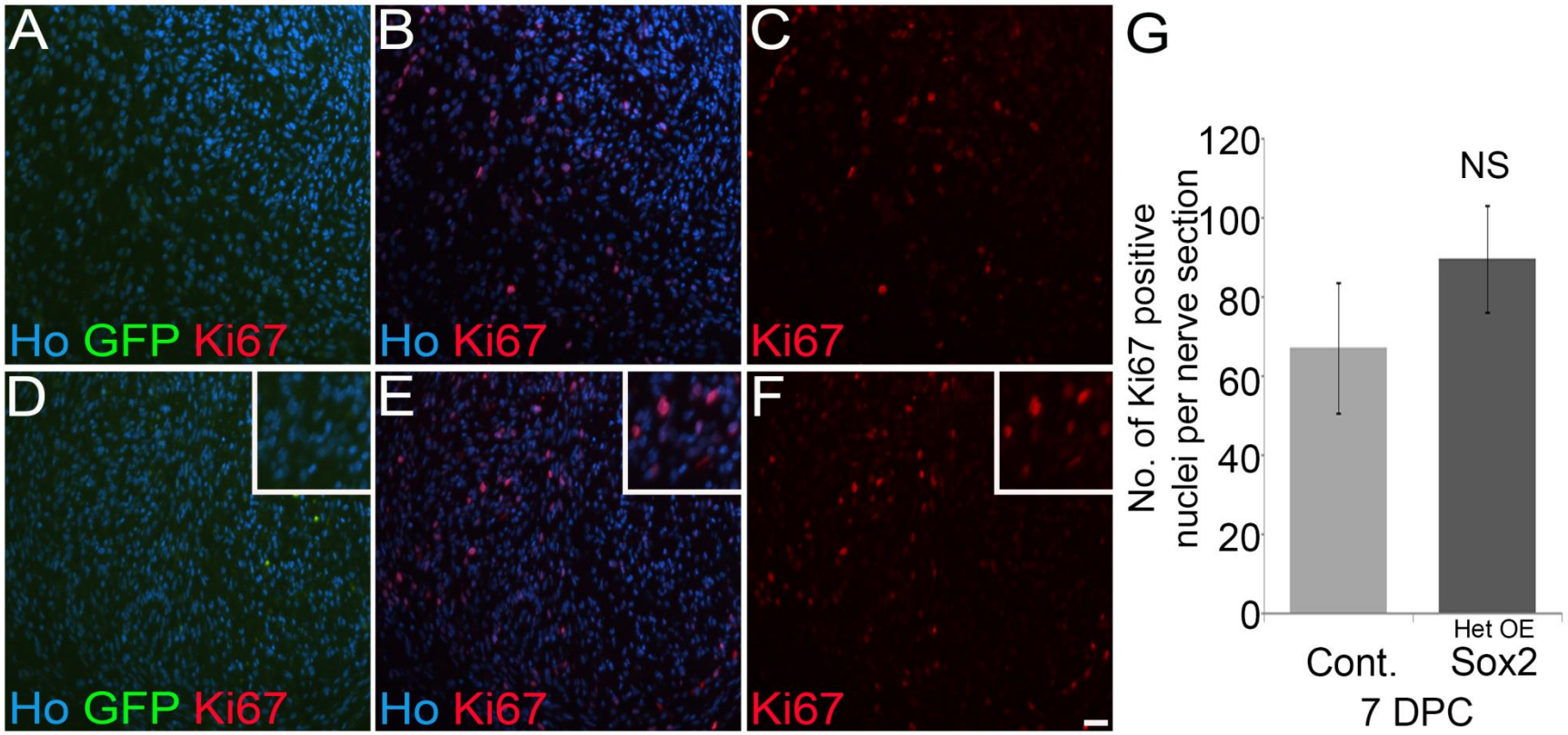

Figure 4. 6: Overexpression of Sox2 increases Schwann cell proliferation at 7 DPC. Distal sciatic nerve stump sections taken from Sox2 Het control and $Sox2^{HetOE}$ mice at 7 DPC were immunolabelled with antibodies against Ki67 (A-F). Immunofluorescent staining shows slightly more numerous Ki67 positive nuclei in the nerves of $Sox2^{HetOE}$ mice (E & F), compared to Sox2 Het control mice (B & C) at 7DPC. Graph (G) showing the total number of Ki67 positive nuclei in the sections of distal sciatic nerves taken from Sox2 Het control and $Sox2^{HetOE}$ mice 7 DPC; note no significant change ($P>0.05$, $n=3$). Images taken using 20x objective (D,E,F, inset 40x), scale bar is 20µm.

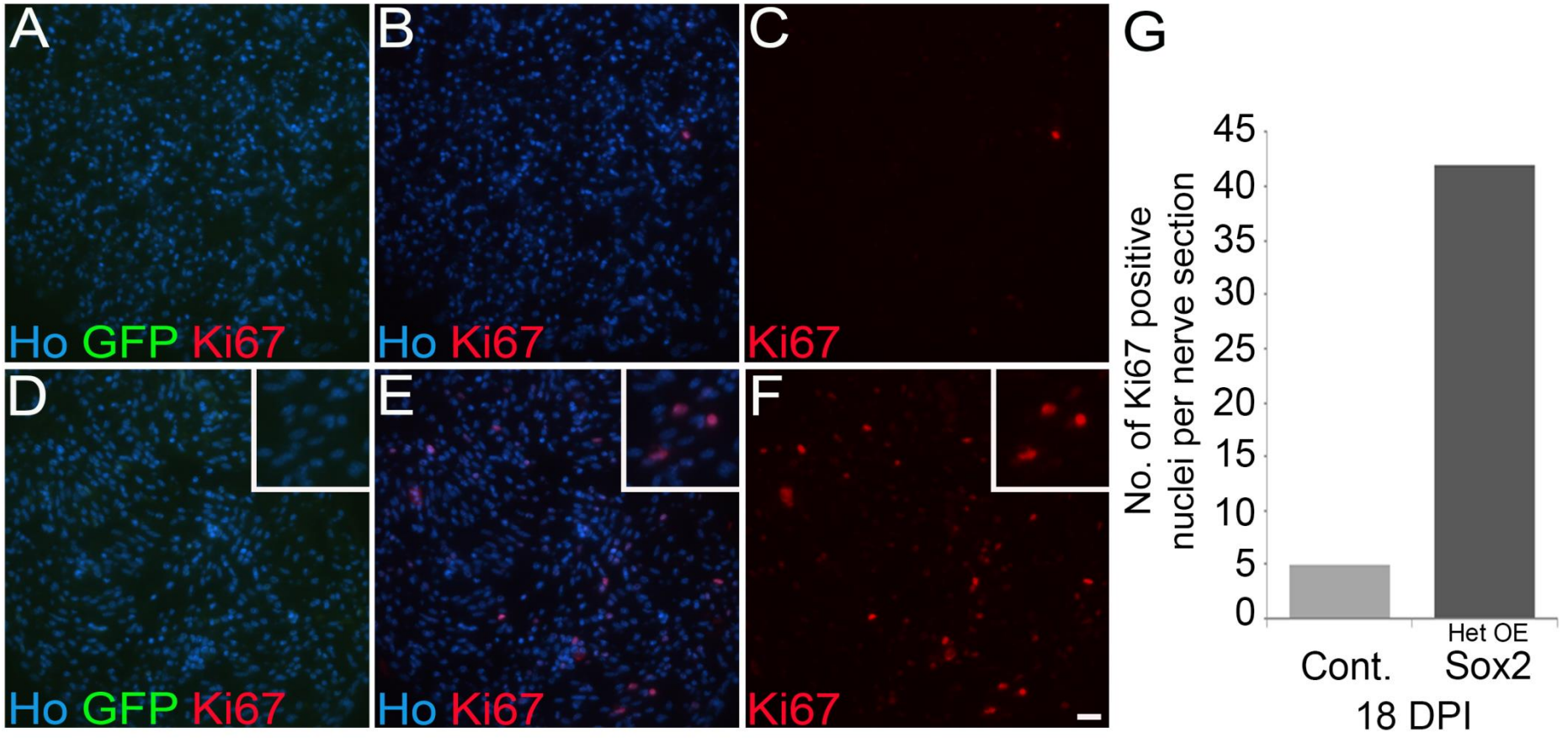

Figure 4. 7: Overexpression of Sox2 increases Schwann cell proliferation at 18 DPI. Distal sciatic nerve stump sections taken from Sox2 Het control and Sox2^{HetOE} mice at 18 DPI were immunolabelled with antibodies against Ki67 (A-F). Immunofluorescent staining shows more numerous Ki67 positive nuclei in the nerves of Sox2^{HetOE} mice (E & F), compared to Sox2 Het control mice (B & C) at 18 DPI. Graph (G) showing the total number of Ki67 positive nuclei in sections of distal sciatic nerves taken from Sox2 Het control and Sox2^{HetOE} mice at 18 DPI (n=1 control, n=2 Sox2^{HetOE}). Images taken using 20x objective (D,E,F, inset 40x), scale bar is 20µm.

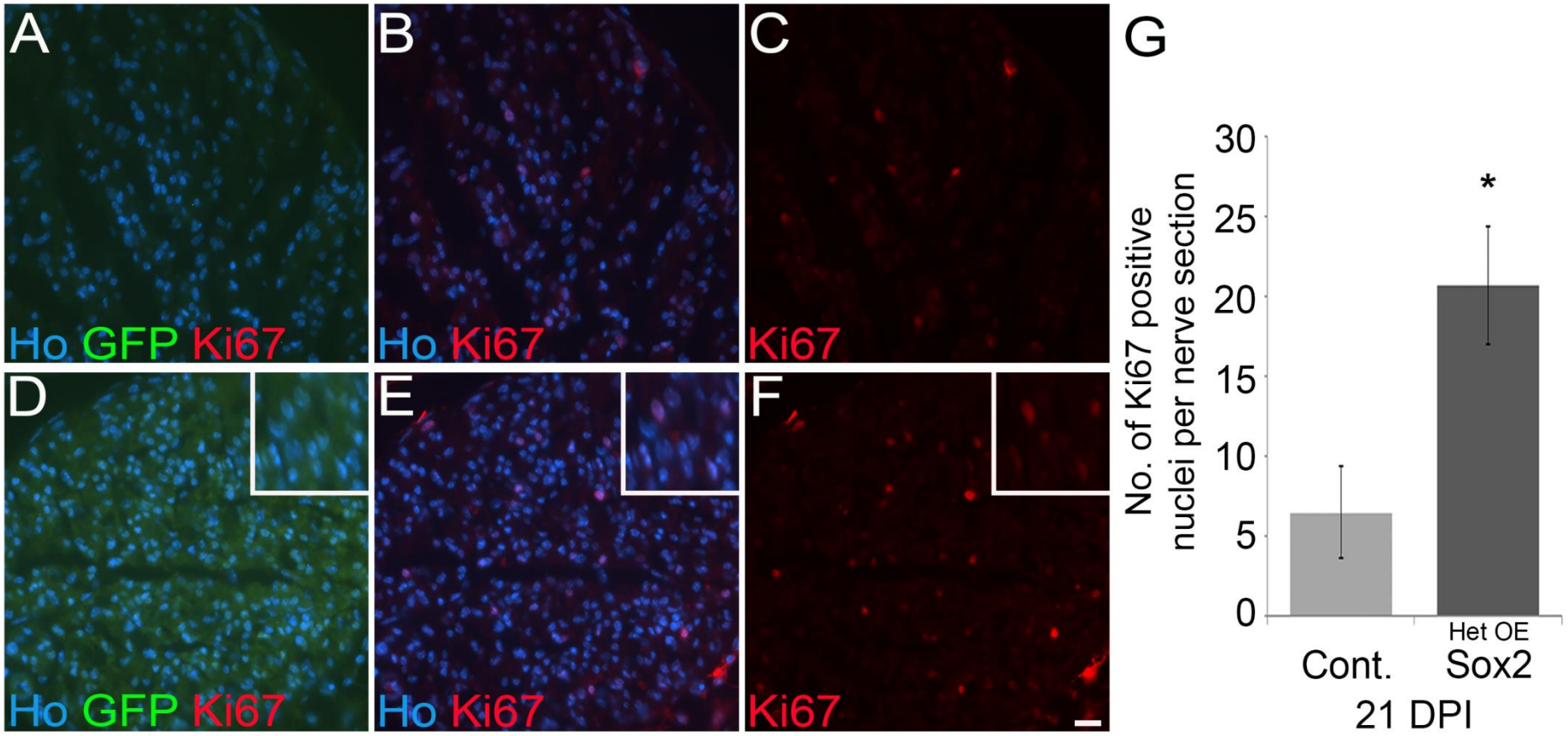

Figure 4. 8: Overexpression of Sox2 increases Schwann cell proliferation at 21 DPI. Distal sciatic nerve stump sections taken from Sox2 Het control and $Sox2^{HetOE}$ mice at 21 DPI were Immunolabelled with antibodies against Ki67 (A-F). Immunofluorescent staining shows numerous Ki67 positive nuclei in the nerves of $Sox2^{HetOE}$ mice (E & F), compared to Sox2 Het control mice (B & C) at 21 DPI. Graph (G) showing a significant increase in the total number of Ki67 positive nuclei in sections of distal sciatic nerves taken $Sox2^{HetOE}$ mice, compared to Sox2 Het control mice at 21 DPI ($P<0.05$, $n=4$). Images taken using 20x objective (D,E,F, inset 50x), scale bar is 20µm.

4.2.4 Sox2 overexpression leads to an increased number of macrophages within the distal nerve stump at 21DPI

Following peripheral nerve injury, axons distal to the site of injury trigger a process known as Wallarian degeneration, resulting in a cascade of degenerative and regenerative cellular and molecular changes within both the nerve and the Schwann cell. During this event, the blood nerve barrier is breached and Schwann cells upregulate the expression of various cytokines and chemokines including TNFα, IL-α, Monocyte Chemotactic Protein -1 (MCP-1) and Macrophage Inflammatory Protein-1α (MIP-1α), which promote the activation and recruitment of macrophage to the site of injury (Rotshenker, 2011, Hall, 2005, Napoli et al., 2012, Tofaris et al., 2002).

In section 4.2.1 we identified the presence of numerous macrophages still within the distal sciatic nerve stump of $Sox2^{HetOE}$ mice at 21 DPI by TEM. To follow this up, we wanted to quantify and determine whether overexpression of Sox2 resulted in a significant increase in the total number of macrophages within the nerves of $Sox2^{HetOE}$ mice, compared to Sox2 Het control mice following crush injury. To test this, we double immunolabelled distal sciatic nerve stump sections taken from both Sox2 Het control and $Sox2^{HetOE}$ mice at 21DPI, with antibodies for F4/80 and Iba1 (macrophage markers). $Sox2^{HetOE}$ nerves showed prominent F4/80 and Iba1 staining, with numerous F4/80+ and Iba1+ cells localised next to a nucleus. In contrast, although Sox2 Het control nerves showed F4/80 and Iba1 double positive cells, fewer were identified. We quantified the number of F4/80 and Iba1 positive macrophages and revealed that there was a significant increase in the number of macrophages present within the nerves of $Sox2^{HetOE}$ mice (124 ± 20.5 F4/80+ / Iba1+ cells), compared to Sox2 Het control mice (60 ±11.3 F4/80+ / Iba1+ cell) at 21DPI ($P<0.05$) (n = 6 Sox2 Het control, n= 5 $Sox2^{HetOE}$) [Figure 4.9].

In order to confirm that the increase in macrophage numbers in the nerves of $Sox2^{HetOE}$ mice was in fact due to the overexpression of Sox2 following nerve crush injury, we also stained uninjured sciatic nerves taken from the same Sox2 Het control and $Sox2^{HetOE}$ mice, with antibodies for F4/80 and Iba1. We were able to reveal that there was no significant difference in the number of macrophages present within the nerves of uninjured Sox2 Het control and $Sox2^{HetOE}$ mice ($P>0.5$); in Sox2 Het control mice the average number of macrophages was 14.3 ± 7.5 per nerve

section, and in Sox2^{HetOE} mice the average number of macrophages was 10.5 ± 3.7 per nerve section (n=3 per genotype) [Figure 4.9].

In addition to macrophages, neutrophils and T-lymphocytes are also recruited into nerves following injury, helping to mediate the inflammatory response and promote functional recovery. Neutrophils are the first immune cell to appear to the site of injury, infiltrating around 3 DPI, whilst T-lymphocytes and macrophages appear slightly later at around 5 DPI (Napoli et al., 2012, Hall, 2005). As we observed an increased number of macrophages within the nerves of Sox2^{HetOE} mice, compared to Sox2 Het control mice at 21 DPI, we next wanted to determine whether there was also an increase in other inflammatory cells within the nerves of Sox2^{HetOE} mice. To test this, we stained distal nerve stump sections take from Sox2 Het control and Sox2^{HetOE} mice at 21 DPI with antibodies specific for neutrophil marker NIMP, and T-lymphocyte marker CD3.

We were able to reveal that there was an increase in the number of NIMP+ cells within the distal nerve stump of Sox2^{HetOE} mice (24. 33 ± 9.61 NIMP+ cells), compared to Sox2 Het control nerves (7 ± 2.27 NIMP+ cells) at 21 DPI, however this was not significant (P=0.21, n=4) [Figure 4.9]. The total number of CD3+ cells was also increased within the distal nerve stump of Sox2^{HetOE} mice (20.75 ± 3.7 CD3+ cells), compared to Sox2 Het control nerves (11± 2.9 CD3+ cells), however again this increase was not significant (P=0.085, n=4) [Figure 4.9].

These results confirmed that continued overexpression of Sox2 following nerve injury increases the number of inflammatory cells within the regenerating nerves at 21 DPI. The presence of macrophages and other inflammatory cells in the nerve following regeneration is likely to impact on the ability of Schwann cells to remyelinate, consequently hindering functional recovery and having implications in neuropathic pain (Ellis and Bennett, 2013, Liu et al., 2000, Ristoiu, 2013).

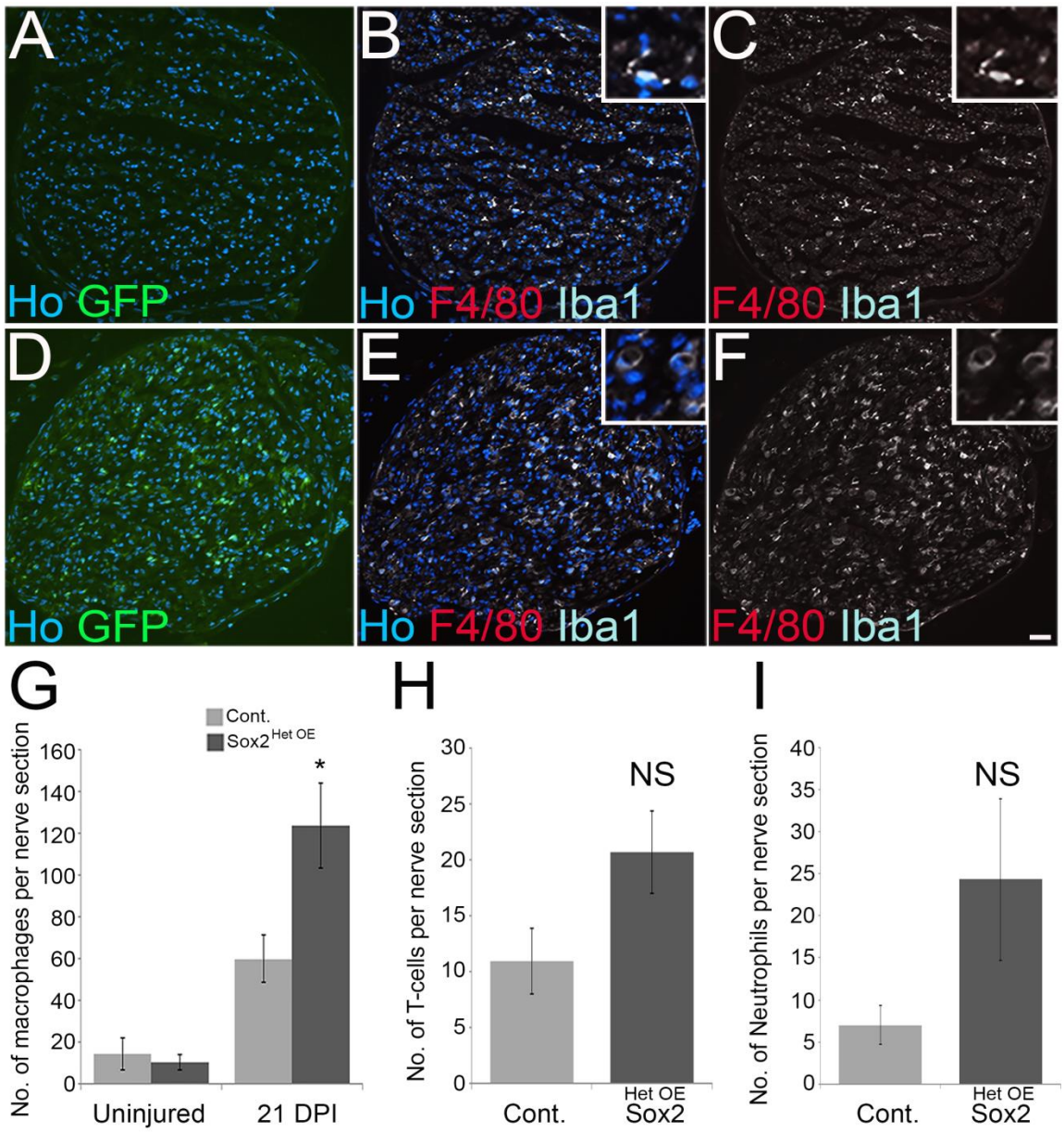

Figure 4. 9: Overexpression of Sox2 leads to an increased number of immune cells present in the distal nerve stump at 21 DPI. Immunofluorescent staining with antibodies specific for macrophage markers F4/80 and Iba1 (A-F) shows that Sox2^{HetOE} mice have numerous F4/80+ and Iba1+ cells within their nerves at 21 DPI (E & F). In contrast Sox2 Het control mice have very few F4/80+ and Iba1+ cells present in their nerves at 21 DPI (B & C). (G) Graph showing the total number of macrophages present in the uninjured and injured nerves of Sox2 Het control and Sox2^{HetOE} mice at 21 DPI (n=3 per genotype for uninjured nerves; n=6 control, n=5 Sox2^{HetOE} for injured nerves). (H) Graph showing the total number of CD3^{+} T-cells in the injured nerves of Sox2 Het control and Sox2^{HetOE} mice at 21 DPI (n=4 per genotype). (I) Graph showing the total number of NIMP^{+} neutrophils in the injured nerves of Sox2 Het control and Sox2^{HetOE} mice at 21 DPI (n=4 per genotype). Images taken using 20x objective (B,C,E,F, inset 50x), scale bar is 20µm.

4.2.5 Sox2 overexpression hinders functional recovery following nerve injury

Peripheral nerve injury, leads to loss of motor and sensory function, however following Wallerian degeneration and proper guidance of regenerating axons, nerves are able to repair and re-innervate their target tissue, leading to full functional recovery being seen in rodents between 3-4 weeks after crush injury (Yang et al., 2008). Nonetheless, having observed that Sox2 overexpression directly leads to a marked reduction in remyelination at 21 DPI, we wanted to identify whether continued Sox2 expression this would affect functional recovery of regenerating nerves. To test this, we compared nerve conduction velocities of uninjured and injured sciatic nerves taken from both Sox2 Het control and $Sox2^{HetOE}$ mice at 21 DPI. In addition, functional recovery of motor axons was assessed by measuring and analysing static sciatic index (SSI) of Sox2 Het control and $Sox2^{HetOE}$ animals before sciatic nerve crush injury, directly after nerve injury and thereon every 2-3 days up until 21days post injury.

Compound action potentials were recorded from uninjured and injured sciatic nerves taken from both Sox2 Het control and $Sox2^{HetOE}$ mice 21DPI, and used to calculate nerve conduction velocities. We were able to confirm that no significant difference in nerve conduction velocity was observed between Sox2 Het control (61.9 ± 4.1 m/s) and $Sox2^{HetOE}$ (61.2 ± 7.3 m/s) uninjured sciatic nerves ($P>0.05$, n=6 per genotype). Nonetheless, following sciatic nerve injury a decrease in nerve conduction velocity was observed in the sciatic nerves of $Sox2^{HetOE}$ mice (36.2 ± 3.9 m/s), compared to Sox2 Het control mice (43.4 ± 7.9 m/s) at 21 DPI; although this did not appear to be significant ($P>0.05$, n=6 per genotype) [Figure 4.10].

We next went on to analyse functional recovery using SSI. Prior to sciatic nerve injury, no significant difference in motor function was observed between Sox2 Het control and $Sox2^{HetOE}$ animals ($P>0.5$, n=11 Sox2 Het control, n=9 $Sox2^{HetOE}$). Directly following sciatic nerve injury, motor function was dramatically impaired in both Sox2 Het control and $Sox2^{HetOE}$ animals; this was identified by the inability of these animals to spread their paw (toes spread test) and a dramatic reduction in SSI. At 7 DPI slight functional recovery could be observed in both Sox2 Het control and $Sox2^{HetOE}$ animals, with no significant difference in recovery being observed between

these mice (P=0.16, n=13 per genotype). However at 10 DPI it was clear that functional recovery in $Sox2^{HetOE}$ mice was significantly slower than in Sox2 Het control mice (P<0.05, n=11 Sox2 Het control, n=12 $Sox2^{HetOE}$) [Figure 4.10]. Functional recovery of motor neurons thereon continued to be significantly slower in $Sox2^{HetOE}$ mice compared to Sox2 Het control mice, up until 21DPI (P<0.01). By 21DPI, motor function was back to normal in the Sox2 Het control mice, with no significant difference being observed between SSI measurements before injury and SSI measurements at 21 DPI (P>0.05, n=11 prior to injury, n=5 at 21DPI). However, as a significant difference was observed between SSI measurements taken before injury and SSI measurements taken at 21 DPI in $Sox2^{HetOE}$ animals (P<0.001, n=9 prior to injury, n=7 at 21DPI); thus revealing that motor function had not returned back to normal in these animals by 21 DPI. Further analysis of Sox2 Het control and $Sox2^{HetOE}$ SSI measurements at 21 DPI, confirmed that functional recovery was significantly reduced in $Sox2^{HetOE}$ animals, compared to Sox2 Het controls at 21 DPI (P<0.001, n=5 Sox2 Het control, n=7 $Sox2^{HetOE}$) [Figure 4.10].

In order to further characterise whether Sox2 overexpression impaired recovery of motor function, we assessed toe spread reflex in Sox2 Het control and $Sox2^{HetOE}$ animals at 12, 14, 17, 19 and 21 DPI (n=6 per genotype). A scored of either 0, 1 or 2, was given in regards to the animals toe spread reflex ability [See Section 2.4.5.3]. By 14 DPI, 100% of Sox2 Het control animals had regained some motor function, this was demonstrated through their ability to extend their leg with slight toe spreading (score of 1), in contrast only 33% of $Sox2^{HetOE}$ animals showed regain of slight motor function (score of 1), the remaining 67% of $Sox2^{HetOE}$ animals showed no sign of regained motor function (score of 0). At 17 DPI, again 100% of Sox2 Het control animals showed some motor function with a toe spread reflex score of 1, whilst only 33% of $Sox2^{HetOE}$ animals scored a toe spread reflex value of 1 and the remaining 67% of $Sox2^{HetOE}$ animals scoring a toe spread reflex value of 0. These results further identified that there had been no additional improvement in motor function among both Sox2 Het control and $Sox2^{HetOE}$ animals between 14 and 17 DPI. At 19 DPI and 21 DPI, an improvement in motor function was observed in both Sox2 Het control and $Sox2^{HetOE}$ animals, although recovery of motor function appeared to be much slower in $Sox2^{HetOE}$ animals. 50% of Sox2 Het control animals had regained full motor function, this was demonstrated through their ability to fully extend their leg

and spread their toes (Score of 2), whilst the remaining 50% of Sox2 Het control animals scored a toe spread value of 1. In contrast, only 33% $Sox2^{HetOE}$ animals scored a toe spread reflex value of 2, another 33% scored a toe spread value of 1, and the remaining 33% scored a toe spread value of 0, at both 19 DPI [data not shown] and 21DPI [Figure 4.10]

Our SSI and preliminary toe spread data further support our hypothesis that continued Sox2 expression following nerve injury, reduces nerve repair and regeneration and further impairs functional recovery of motor axons.

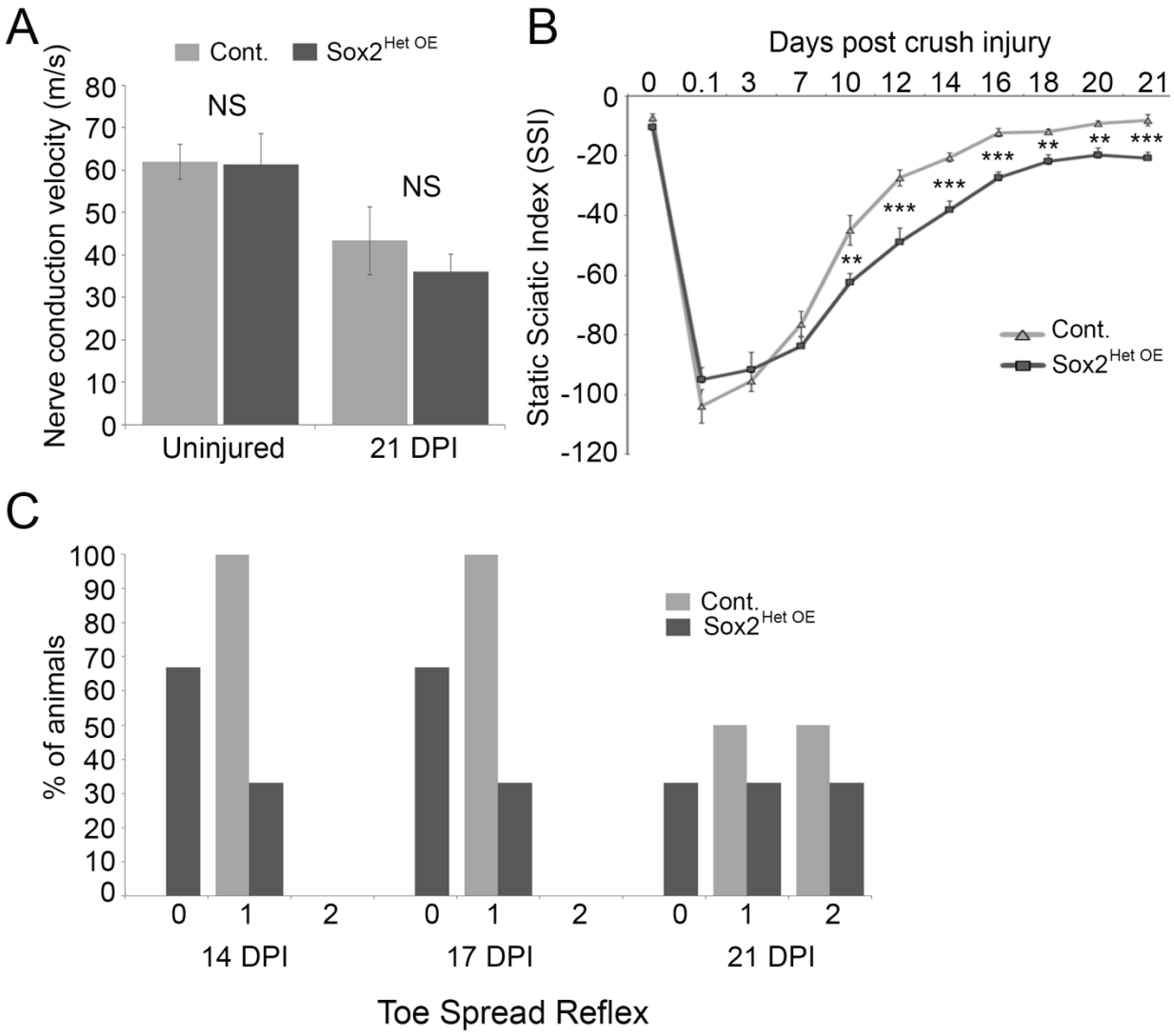

Figure 4. 10: Overexpression of Sox2 reduces functional recovery in Sox2^{HetOE} mice. (A) Graph displaying the nerve conduction velocities of uninjured and injured nerves taken from Sox2 Het control and Sox2^{HetOE} mice at 21 DPI (n=6). (B) Graph showing the functional recovery of control and Sox2^{HetOE} mice following nerve injury; a significant difference in function recovery was observed between Sox2 Het control and Sox2^{HetOE} mice from 10 DPI to 21 DPI. (C) Graph showing the toe spread reflex (score 0: no leg extension or toe spread; Score 1: partial leg extension and partial toe spreading; score 2: full leg extension and full toe spreading) of Sox2 Het control and Sox2^{HetOE} mice after crush injury (n=6).

4.2.6 Sox2 overexpression hinders recovery of sensory function following nerve injury

For successful recovery of sensory function following nerve injury, sensory axons distal to the site of injury must undergo Wallerian degeneration, proximal axons must then successfully regrow within a permissive environment and re-innervate their target tissue. As we have previously seen that continued Sox2 expression following nerve injury reduces nerve conduction velocity and functional recovery at 21 DPI, we next wanted to determine whether continued Sox2 expression would affect recover of sensory function. To test this we analysed the responsiveness of Sox2 Het control and $Sox2^{HetOE}$ mice to toe pinching and light pressure testing at 7, 10, 12, 14, 17, 19 and 21 DPI.

In Sox2 Het control and $Sox2^{HetOE}$ mice, sciatic nerve crush injury abolished the response to toe pinching in toes 3, 4 and 5 from 1DPI. Sox2 Het control animals started to regain responsiveness to toe pinch testing in toe 3 from 10 DPI (16% of animals) [data not shown], whilst $Sox2^{HetOE}$ animals did not begin to regain responsiveness until 17DPI (16% of animals). By 21 DPI 100% of Sox2 Het control animals were able to respond to toe pinch testing in toe 3, whilst only 33% of $Sox2^{HetOE}$ animals were able to respond (n=6 per genotype) [Figure 4.11]. In toe 4, Sox2 Het control animals regained responsiveness to toe pinch testing from 17DPI (16% of animals), with 33% of Sox2 Het control animals being able to respond by 21DPI. In contrast $Sox2^{HetOE}$ animals did not regain responsiveness in toe 4 until 21DPI and only 16% of animals were able to respond at this time-point (n=6) [Figure 4.11]. In toe 5, Sox2 Het control animals regained responsiveness to toe pinch testing from 17DPI (16% of animals) and by 21DPI, 50% of Sox2 Het control animals were able to respond. In contrast $Sox2^{HetOE}$ animals did not regain the ability to respond to in toe 5 by 21DPI (n=6) [Figure 4.11].

We next went on analyse responsiveness to light touch using Von Frey filaments. In Sox2 Het control and $Sox2^{HetOE}$ mice, sciatic nerve crush injury abolished the response to light touch. By 10 DPI, both Sox2 Het control and $Sox2^{HetOE}$ mice had regained the ability to respond to light touch, furthermore Sox2 Het control mice showed an increased responsiveness to light touch (70 ± 25g) compared to $Sox2^{HetOE}$ mice (92 ± 23g), however this was not significant ($P>0.05$, n=6 per

genotype). At 12, 14, 17, 19 and 21 DPI Sox2 Het control mice continued to show improved responsiveness to light touch at a faster rate than $Sox2^{HetOE}$ mice, however this improved difference was again not significant ($P<0.05$, n=6) [Figure 4.11]. By 21 DPI, $Sox2^{HetOE}$ mice were able to respond to Von Frey filaments as light as 0.06 ± 0.02g, whilst Sox2 Het control mice were able to respond Von Frey filaments much lighter at 0.01 ± 0.002g, although this change was not significant ($P=0.07$, n=6).

Although continued Sox2 expression does not significantly impair recovery of sensory function, we can conclude that it does reduce the rate of recovery following nerve injury. We can assume that functional recovery in some sensory axons such as C fibres is not significantly impaired as they are do not require myelination. However, mechanoreceptors such as A delta (Aδ) sensory fibres which are responsible for responsiveness to touch and pressure, do in fact require thin layers of myelin in order to respond to stimulus in a timely manner. As Sox2 overexpression leads to hypomyelination, this might explain why sensory recovery is slightly slower in $Sox2^{HetOE}$ mice.

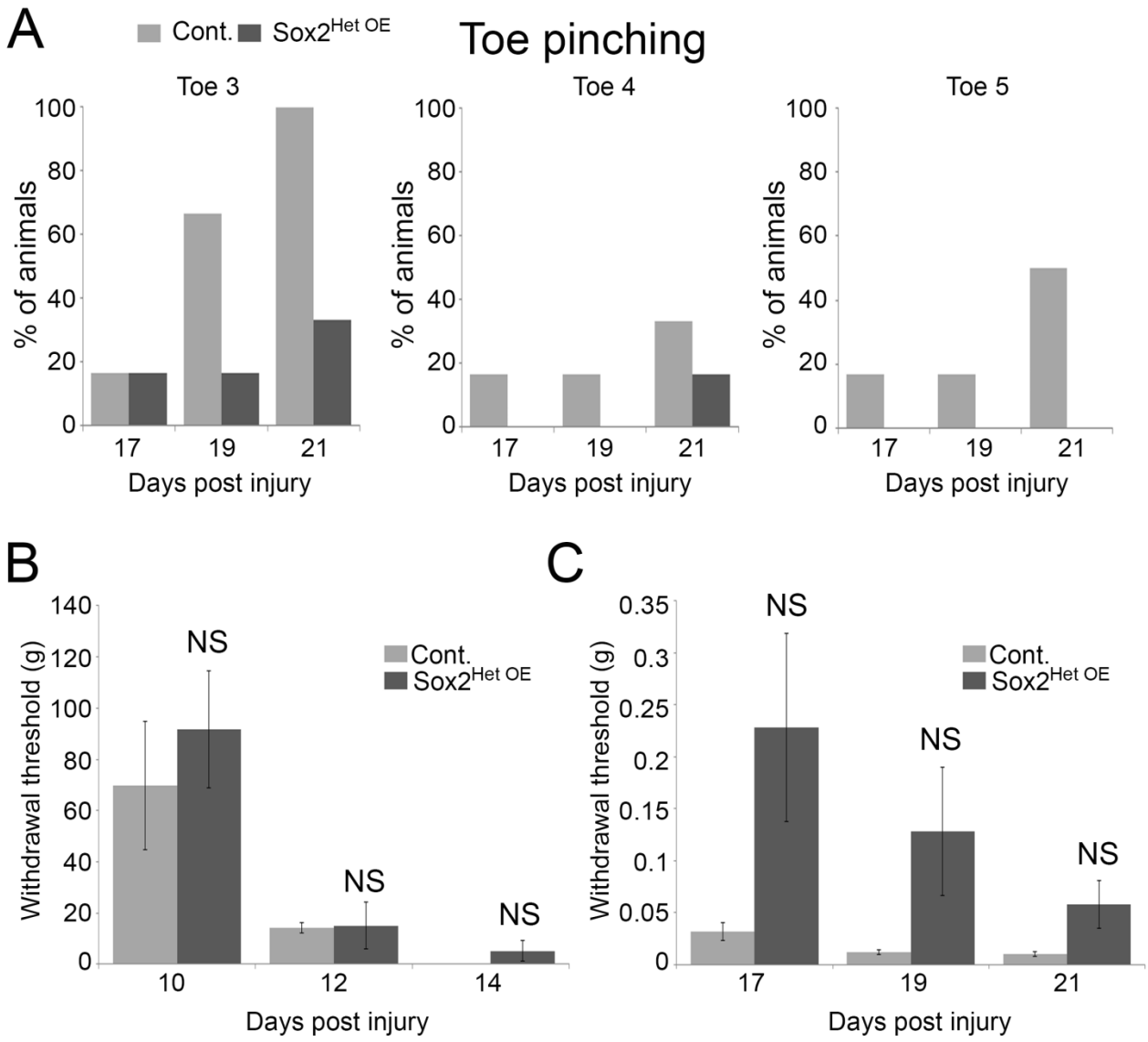

Figure 4. 11: Overexpression of Sox2 reduces sensory function recovery following injury. (A) Graph showing the percentage of Sox2 Het control and $Sox2^{HetOE}$ mice responding to pinching of distal parts of toes 3, 4 and 5 at 17, 19 and 21 DPI (n=6). (B) Graph showing the responsiveness of Sox2 Het control and $Sox2^{HetOE}$ mice to light pressure at 10, 12 and 14 DPI. (C) Graph showing the responsiveness of Sox2 Het control and $Sox2^{HetOE}$ mice to light pressure at 17, 19 and 21 DPI (n=6).

4.3 Discussion

Expression of Sox2 following nerve injury is beneficial in the process of Wallerian degeneration as it regulates two processes essential for nerve repair and regeneration: Schwann cell demyelination and the guidance of regenerating axons back to their target tissues. Nonetheless, our data confirms that Sox2 expression must eventually be repressed to allow for the timely transition of repair cells into a myelinating Schwann cell state, allowing remyelination of regenerating nerve fibres, and thus successful nerve repair and functional recovery.

4.3.1 Maintained Sox2 expression impairs remyelination following nerve injury

Following nerve injury, Schwann cells undergo a process of adaptive cellular reprogramming. It is essential that cJun is activated in these cells, along with other negative myelin regulators Sox2, Notch and the ERK 1/2 and p38 mitogen activated protein kinase (MAPK) signalling pathway. Reactivation of these factors causes Schwann cells to degrade their myelin sheath and differentiate into a transient repair cell termed a Büngner cell; which is similar to an immature Schwann cell (Jessen et al., 2015, Arthur-Farraj et al., 2012, Le et al., 2005a, Yang et al., 2012, Napoli et al., 2012, Harrisingh et al., 2004). These repair cells express high levels of trophic factors including glial derived nerve growth factor (GDNF), Artemin (Artn), leukemia inhibitory factor (LIF) and brain derived nerve growth factor (BDNF) which help to support the survival of regenerating axons and promote axon growth (Fontana et al., 2012, Arthur-Farraj et al., 2012). Furthermore, the repair cells form regenerative tracts, termed bands of Büngner which help to guide regenerating axons back to their target (Parrinello et al., 2010). As axons regrow and re-innervate their target site, the repair cell then downregulates the expression of cJun, Sox2, Notch and the activated ERK 1/ 2 and p38 MAPK signalling pathway. Repair cells then upregulate the expression of myelin associated genes, such as Krox20, P_0 and MBP enabling them to differentiate back into a myelinating Schwann cell. Finally, Schwann cells remyelinate regenerating axons, allowing for complete nerve repair and functional recovery.

Previous studies have confirmed that the early expression of these negative myelin regulators following nerve injury is essential for Schwann cells to effectively transition

into repair cells and promote nerve regeneration. In Schwann cell specific cJun depleted (cJun null) mice following nerve injury, Schwann cells fail to dedifferentiate and upregulate genes associated with trophic support, and to downregulate genes associated with myelination (Parkinson et al., 2008, Arthur-Farraj et al., 2012). Furthermore, in cJun null mice proteins associated with cell adhesion and the formation of bands of Büngner (N-cadherin, p75NTR, and NCAM) are dysregulated, resulting in the formation of abnormal regenerative tracts (Arthur-Farraj et al., 2012). cJun null mice also exhibit impaired myelin breakdown by autophagy, a striking increase in the death of both small and large dorsal root ganglion (DRG) neurons, as well as a decrease in axon growth. Functional recovery (sensory & motor) is thus severely impaired in cJun null mice, while control mice demonstrate almost full recovery by 3-4 weeks. Consequently, cJun was proven to govern all major aspects of the injury response including neuronal survival, Schwann cell reprograming, myelin degradation and clearance and the formation of regenerative tracts (Arthur-Farraj et al., 2012, Gomez-Sanchez et al., 2015).

Studies analysing the role of ERK 1/2 signalling in Schwann cells following nerve injury, reveal that inhibition of the ERK 1/2 MAPK signalling pathways using the pharmaceutical inhibitor PD0325901, results in a delay of Schwann cell downregulation of the expression of myelin-related genes and dedifferentiation (Napoli et al., 2012). In contrast, prolonged activation of the ERK 1/2 signalling pathways following nerve injury retains Schwann cells in a dedifferentiated state, resulting in delayed motor functional recovery (Ibid). Similarly, studies analysing the functional role of p38 MAPK in Schwann cells have identified that blocking its activation (using a pharmaceutical inhibitor SB203580) results in the impairment of Schwann cells to demyelinate, following nerve injury (Yang et al., 2012).

Experiments by Woodhoo et al. (2009), further confirmed the functional role of Notch in regulating Schwann cell demyelination following injury. Absence of RBPJ (the key transcriptional regulator of the Notch canonical signalling pathway) resulted in a dramatic reduction in Schwann cell demyelination following injury, whilst increased Notch signalling accelerates demyelination as demonstrated by elevated expression of the intracellular proportion of the Notch receptor; NICD using P_0-Cre$^+$CALSL-NICD mice (Woodhoo et al., 2009). From these studies it is clear that the expression of these negative myelin regulators is essential for the initiation of Schwann cell

dedifferentiation and demyelination to aid with nerve repair. The study by Napoli et al. (2012) where ERK1/2 signalling is prolonged, further confirms that that the downregulation of these negative regulators is essential for the transition of Schwann cells back to the myelinating state, and for the complete functional recovery of motor-sensory neurons.

Sox2 has been shown to play an essential role in the re-localisation of N-cadherin to Schwann cell contact junctions, enabling Schwann cells to form bands of Bungner that aid with axon guidance and regeneration (Parrinello et al., 2010). Data collected by Dr Xin-Peng Dun in our group [unpublished data] further confirmed using Schwann cell specific Sox2 knockout (Sox2 null) mice, that axon regeneration is severely disorganised in these animals following nerve cut injury, compared to controls. Although Sox2 has been identified as being important for axon guidance and regeneration, the role of Sox2 on Schwann cell differentiation and myelination following nerve injury *in vivo* had not been studied. Using $Sox2^{HetOE}$ mice we thus set out to investigate the effect of maintained Sox2 expression on nerve repair and regeneration.

During development $Sox2^{HetOE}$ mice expressed high levels of Sox2, which caused reduced Schwann cell myelination and myelin protein expression, compared to controls up until postnatal day 21 (P21). However, from P21 the Sox2-IRES-EGFP transgene appeared to switch off; neither Sox2 nor GFP was detected in the sciatic nerves of P60 $Sox2^{HetOE}$ mice. Furthermore myelination had returned to normal in these animals at P60, and no significant difference in motor or sensory function was observed between $Sox2^{HetOE}$ and control mice from 6 weeks of age onwards (see Chapter 3 Figure 3.4, Figure 3.22 & Figure 3.23]. We hypothesized that following PNS injury the accompanying dedifferentiation of Schwann cells would cause reactivation of Sox2 and GFP expression in the $Sox2^{HetOE}$ animals. Western blot and immunolabelling showed higher levels of Sox2 and GFP induction in $Sox2^{HetOE}$ animals compared to controls and that Sox2 expression was maintained at 21 days post crush injury (21 DPI) in these animals compared to controls; in which Sox2 is undetectable at this later time-point following repair and remyelination of the nerve.

Continued Sox2 expression following sciatic nerve crush injury was revealed to significantly impair Schwann cell remyelination and increase the percentage of

unmyelinated axons in a 1:1 relationship with Schwann cells at 21 DPI, which is consistent with its role as a negative myelin regulator. Surprisingly, the average axon diameter size was increased in the nerves of $Sox2^{HetOE}$ compared to control mice at 21 DPI, this could possibly be due to improved guidance of regenerating large diameter axons in the presences of prolonged Sox2 overexpression. Unpublished data by Dr Xin-Peng Dun (in our group) further confirmed that axonal growth rate was significantly increased in $Sox2^{HetOE}$ mice compared to controls at 6.5 days after crush injury. Often after injury motor axons and sensory axons are misdirected, leading to the re-innervation of incorrect targets. BDNF, GDNF and Neurotrophin 3 (NT3) have been shown to be upregulated predominantly in the affected muscle following injury, and thought to drive motor neurons to regrow in the direction of the trophic cues (Fex Svennigsen and Dahlin, 2013). As the average axon diameter size is significantly increased in $Sox2^{HetOE}$ mice at 21 DPI, it would be interesting to see whether the overexpression of Sox2 in Schwann cells enhances axon maturation and increases the accuracy of motor axons being directed back to their target. In theory if these Schwann cells were then able to myelinate in the presence of Sox2, this would lead to improved motor functional recovery. It would also be interesting to see whether overexpression of Sox2 leads to an overall increase in the number of regenerative nerve fibres that reach their target by 21 DPI. Unpublished data by Dr Xin-Peng Dun revealed that Sox2 is able to regulate axonal guidance, by controlling the expression of repulsive axon guidance cues such as Robo1 and Slit 3. Nonetheless it remains unknown as to whether Sox2 regulates the expression of neurotrophins that promote axon growth. Understanding how Sox2 promotes axon growth rate would also be of great value, as the longer axons are away from their target, the more unlikely it is that successful nerve regeneration will occur.

For Schwann cells to effectively remyelinate, they must re-express Krox20, along with myelin proteins such as protein zero (P_0) and myelin basic protein (MBP). During Schwann cell development impaired/disrupted Krox20 expression is associated with Schwann cell hypomyelination (Topilko et al., 1994, Le et al., 2005a), while mutations or disruptions in P_0 expression is associated with the formation of unstable myelin, which finally degenerates leading to Schwann cell demyelination and axons becoming hypomyelinated (Giese et al., 1992) [See section 3.3.1]. True to its role as a negative myelin regulator, Sox2 was proven to impair

Schwann cell remyelination, by hindering the re-expression of Krox20, P_0 and MBP. Furthermore, Sox2 appeared to retain Schwann cells in an immature state, marked by the increased expression of cJun in the nerves of $Sox2^{HetOE}$ mice, as well as the increased number of proliferating Schwann cells (this will be discussed in Section 4.3.2). Although cJun is upregulated in the nerves of $Sox2^{HetOE}$ mice, we do not predict that Sox2 and cJun co-regulate one another as previously suggested by Parkinson et al., (2008), but rather that they are co-expressed as markers of immature Schwann cells. Experiments carried out by Dr Xin-Peng Dun confirmed that cJun protein expression in the nerves of Sox2 null mice was similar to that of controls at 3 and 7 days post cut injury [unpublished data]. Furthermore, Arthur-Farraj et al. (2012) also showed that Sox2 protein expression was upregulated normally in the injured nerves of cJun null mice.

It is clear that Sox2 is essential for nerve regeneration, as it plays a fundamental role in promoting axonal growth (Dr Xin-Peng Dun: unpublished data), as well as the guidance of regenerating axons across the nerve bridge and back to their target (Dr Xin-Peng Dun unpublished data, Parrinello et al. 2010). However, similar to the ERK1/2 signalling pathway after injury (Napoli et al., 2012), we show that Sox2 expression must be switched off in a timely manner to allow Schwann cells to effectively differentiate back into a myelinating Schwann cell, and thus remyelinated regenerating nerve fibres.

4.3.2 Sox2 regulates Schwann cell proliferation following nerve injury

After nerve injury the peripheral nervous system initiates a sequence of degenerative and molecular changes in the distal nerve segment termed Wallerian degeneration. One of the earliest events triggered by Wallerian degeneration is Schwann cell proliferation, which reaches a maximum at 2-3 days after injury and resulting in a marked increase in the number of Schwann cells in the distal nerve segment (Fex Svennigsen and Dahlin, 2013, Yang et al., 2008). It is thought that the Schwann cell proliferation event occur so that newly produced Schwann cells can replace those that have died or are dying. Schwann cells are essential for the production of neurotrophic factors that support neuronal survival following injury, promoting axon growth and the subsequent guidance of axons back to their target, it would be

expected that an abundant number of these cells would therefore be required for effective nerve repair and regeneration. Nonetheless, experiments carried out on cyclin $D1^{-/-}$ mice which lack proliferating Schwann cells, revealed that Schwann cell proliferation during Wallerian degeneration is not essential for the regeneration and functional recovery of injured nerves (Yang et al., 2008). Cyclin $D1^{-/-}$ mice regenerated normally in every respect when compared to control mice; no significant difference in mean axonal densities, remyelination (the formation of axon-Schwann cell units), myelin segment length, or motor-sensory functional recovery (assessed by static functional index and paw withdraw in response to electrical stimulation) was observed between control and cyclin $D1^{-/-}$ mice (Yang et al. 2008). Yang et al., (2008) confirmed that while there was an initial difference in Schwann numbers due to the rapid on set of proliferation in the nerves of control mice at 7 days post injury, compared to cyclin $D1^{-/-}$ nerves, Schwann cell numbers levelled out and were equivalent by 14 days post injury. The excess Schwann cells in the nerves of control mice were removed by apoptosis. Yang et al., (2008) suggested this process to be a possible mechanism that allows for the establishment of correct Schwann-axon numbers during peripheral nerve regeneration.

Although Schwann cell proliferation after nerve injury is not essential for nerve regeneration, it is possible that Schwann cell proliferation maybe required for other useful functions, such as increasing the net number of Schwann cells to compensate for those that naturally die. An inability to replace lost Schwann cells would be detrimental in the long term on nerve regeneration and functional recovery (Fex Svennigsen and Dahlin, 2013). It was noted by Yang et al. (2008) that the tests used to monitor differences in functional recovery between control and cyclin $D1^{-/-}$ mice may not have been sensitive enough to detect any delays in physiological recovery, and that nerve conduction studies would have be more informative at the electrophysiological level. It is therefore difficult to say whether the lack of Schwann cell proliferation is completely unnecessary for the complete regain of motor-sensory function.

Increased expression of Sox2 (this study, Le et al. 2005), activation of Notch signalling (Woohoo et al. 2009) and activation of the ERK 1/2 MAPK signalling pathways have been shown to enhance Schwann cell proliferation during development. Although Schwann cell proliferation has been suggested not to be

essential for nerve repair and recovery after injury, the increase in proliferation following injury may occur as an indirect effect of Sox2 being re-expressed, and the Notch and ERK 1/2 MAPK signalling pathway being reactivated. Alternatively the increase in Schwann cell proliferation may be essential for effective guidance of regenerative axons to their target, allowing for optimal functional recovery at later time-points past 3 weeks after injury. This was not previously accessed in enough detail as mentioned above (Yang et al. 2008). Furthermore, Yang et al., (2008) only analyses the difference in Schwann cell numbers between control and cyclin $D1^{-/-}$ mice up until 14 days post injury, it would be interesting to see whether the difference in Schwann cell numbers between control and cyclin $D1^{-/-}$ mice changed again at later time-points after injury. As mentioned earlier, Schwann cell proliferation may be essential for the replacement of naturally dying Schwann cells.

To address whether overexpression of Sox2 increased Schwann cell proliferation above the normal threshold following nerve injury, nerve sections taken from control and $Sox2^{HetOE}$ mice were stained with antibodies against Ki67 (a marker of Schwann cell proliferation). Whilst Schwann cell proliferation was increased at 3, 7 and 14 DPI in both control and $Sox2^{HetOE}$ mice, there did not appear to be a significant difference in the rate of Schwann cell proliferation between these animals. There are two explanations for this; firstly overexpression of Sox2 may not enhance Schwann cell proliferation above the normal proliferative threshold after injury, and therefore no significant difference is observed. Alternatively, as the protein expression of Sox2 in control and $Sox2^{HetOE}$ mice was not measured at these time-points, we cannot clearly state that Sox2 was expressed to a significantly elevated level in the nerves of $Sox2^{HetOE}$ mice compared to controls. Although we observed slight GFP re-expression in the nerves of $Sox2^{HetOE}$ by fluorescent imaging at these time-points, it is possible that the Sox2IRES-EGFP transgene was not switched back on effectively straight away. As a result Sox2 expression may not have been directly elevated above the normal level seen in controls until later time-points, such as around 18 DPI where we have observed a massive difference in Schwann cell proliferation in the nerves of $Sox2^{HetOE}$ mice compared to controls. At 21 DPI we have confirmed that Sox2 and GFP in dramatically expressed in the nerves of $Sox2^{HetOE}$ mice, and also that Sox2 protein expression (by western blot analysis) is elevated in these animals compared to controls. We were therefore able to confirm that continued Sox2

expression significantly increases Schwann cell proliferation after injury, and maintains these cells in a proliferative immature Schwann cell state. As we are unsure as to how soon the Sox2-IRES-EGFP transgene is switched back on in $Sox2^{HetOE}$ animals after nerve injury, a more effective approach to see whether overexpression of Sox2 increases Schwann cell proliferation directly after nerve injury should be used. A previous study by Napoli et al. (2012) used a tamoxifen inducible Cre recombination system which allowed for the rapid expression of their gene of interest upon tamoxifen administration. It would be useful to use the same approach to induce Sox2 overexpression directly after injury, to compare whether the overexpression of Sox2 leads to increased Schwann proliferation and faster Schwann cell demyelination and dedifferentiation directly after nerve injury compared to controls. This would enable us to further identify other functional roles of Sox2 during nerve injury, in addition to its role in regulating cell adhesion and the formation of regenerative tracts (Parrinello et al., 2010).

4.3.3 Sox2 and neuro-inflammation following nerve injury

The inflammatory response not only plays a role in removing impairs cells and pathogens from the body, but also an active role in promoting wound healing. While controlled and moderate inflammation is beneficial for promoting repair, a progressive and/or chronic inflammatory response can result in impaired tissue recovery and potentially pathology. Wallerian degeneration is a cascade of cellular and molecular events that occur in the nerve distal to the site of injury. The innate immune response is central to the process of Wallerian degeneration, as it helps to support nerve regeneration by removing inhibitory myelin and upregulating neurotrophic properties (Rotshenker, 2011).

Schwann cell myelin is composed of a range of myelin components, including myelin-associated glycoprotein (MAG) which is known to inhibit axonal outgrowth and branching (McKerracher et al., 1994, Shen et al., 1998). It is therefore essential that following Schwann cell demyelination, myelin debris is cleared by resident and recruited macrophages to allow for successful nerve regeneration. While Schwann cells are capable of clearing myelin debris in the absence of macrophages, the presence of macrophages allows for accelerated and more effective myelin clearance (Perry et al., 1995, Rotshenker, 2011). Macrophages express surface

recognition receptors such as MHC molecules and complement receptor 3 which enable them to carry out surveillance and recognise foreign microbes and myelin debris which require clearing (Gaudet et al., 2011).

Blood born macrophages are recruited to the site of injury around 2-3 days after injury via IL-1β and TNF-α cytokines and MCP-1 and MIP-1α chemokines expressed by Schwann cells. On arrival they proliferate, phagocytose axon and myelin debris, produce cytokines that activate Schwann cells and also trophic factors such as nerve growth factor (NGF) that aids axon regeneration (Barrette et al., 2008, Gaudet et al., 2011). Barrette et al. (2008) proved further that macrophages are required for axon regeneration, as depletion of CC11b-positive macrophages starting 12 hours prior to sciatic nerve crush injury in transgenic mice resulted in a significant impairment in motor-sensory functional recovery and locomotor deficits. Surprisingly macrophages were also identified to play a role in blood vessel formation/ stabilisation, as depletion of CD11b-positive macrophages resulted in a significant decrease in the number of $CD31^+$ blood vessel in the distal sciatic nerve stump (ibid). It was recently confirmed that macrophages induce blood vessel formation, by secreting VEGF-A in response to hypoxia, consequently triggering the polarized vascularisation of the nerve bridge (injury site) (Cattin et al., 2015). The newly formed blood vessels were subsequently proven to be important for Schwann cells axon guidance, as Schwann cells were shown to use these newly formed blood vessels as guidance paths across the nerve bridge, taking regrowing axons with them (Cattin et al., 2015).

While macrophages are fundamental for Wallerian degeneration and nerve regeneration, they must be cleared from the nerve following axon repair and remyelination, in order to prevent chronic inflammation. T-lymphocytes and neutrophils also infiltrate into the nerve following nerve injury. T-lymphocytes shape the later immune response by producing both pro-and anti-inflammatory cytokines which help to further activate or inhibit nearby macrophages and neutrophils (Gaudet et al., 2011). As mediators of an inflammatory environment, they must also be cleared from the nerve upon axon regeneration and remyelination to allow for complete nerve recovery. Macrophages and T-lymphocytes have been previously shown to mediate an inflammatory environment in the nerve and induce

demyelination and axonal damage (Ip et al., 2006, Kobsar et al., 2005). It is therefore possible that impaired immune cell clearance after nerve injury may lead to peripheral nerve disorders such as chronic inflammatory demyelinating polyneuropathy (CIDP) (Martini et al., 2008).

Overexpression of Sox2 in Schwann cells was previously show to result in an increased number of macrophages and T-cells within the nerves of $Sox2^{HomoOE}$ mice compared to controls (at P7 and P60) [Section 3.2.9]. We therefore wanted to determine whether Sox2 was also capable of altering the number of immune cells in the nerves of $Sox2^{HetOE}$ mice after injury. We confirm that continued expression of Sox2 resulted in a significant increase in the number of macrophages in the nerve of $Sox2^{HetOE}$ mice, compared to controls at 21DPI. $Sox2^{HetOE}$ mice also exhibited increased numbers of T-cells and neutrophils in their nerves at 21 DPI compared to controls (this was not significant). Although we have identified that continued expression of Sox2 after nerve injury increases the number of immune cells present within the nerve, the mechanism by which this is achieved remains unknown. Further experiments would need to be carried out in order to elucidate how Sox2 achieves this.

Infiltrating macrophages are known to express pro-inflammatory cytokines such as TNFα and IL-1β, which are associated neuropathic pain (Wagner and Myers, 1996). Due to the numerous macrophages present in the nerves of $Sox2^{HetOE}$ at 21 DPI, it is possible that these mice will develop neuropathic pain and hyperalgesia. In order to test for this a hot plate test could be carried out; this would require $Sox2^{HetOE}$ and control mice at various time-points after nerve injury for example at 3 and 4 weeks, to be placed on to a hot plate and their reaction to pain caused by the heat measured.

After debris clearance, axon regeneration and remyelination is complete, macrophages are no longer useful or required. Proteins on the surface of newly formed myelin signal to macrophages, causing them to emigrate away from the Schwann cell basal lamina and leave the nerve via the circulation into regional lymph nodes and spleen, any remaining macrophages are eliminated by apoptosis (Kuhlmann et al., 2001). Fry et al., (2007) identified that macrophages in the crushed sciatic nerves express Nogo receptors (NgRs) on their surface. Three members of

the NgR family have previously been identified NgR1, NgR2 and NgR3, however macrophages were shown to only express NgR1 and NgR2 (Fry et al., 2007). NgR1 and NgR2 are known to mediate the inhibitory or repulsive effect of myelin proteins: NgR1 binds to three axon growth inhibitory molecules i.e. Nogo A, MAG and oligodendrocyte-myelin glycoprotein (OMgp), whereas NgR2 binds exclusively to MAG. Using a nerve cut injury model, Fry et al. (2007) demonstrated that in the absence of newly synthesised myelin, macrophages fail to clear from the injured nerve. It was suggested that failure of macrophages to receive a repulsive signal via MAG protein-NgR receptor interaction results in macrophages not being eliminated from Schwann cell basal lamina (ibid). Further studies also showed that MAG-deficient mice exhibited impaired macrophages efflux from the Schwann cell basal lamina following Schwann cell remyelination after nerve crush (Fry et al., 2007). As continued expression of Sox2 impairs Schwann cells remyelination and therefore MAG re-expression (although we have not confirmed this), it is possible that surrounding macrophages in the nerves of $Sox2^{HetOE}$ mice do not receive the repulsive signal informing them to leave the Schwann cell basal lamina, even though axonal regeneration is complete. This may explain why $Sox2^{HetOE}$ nerves contain so many macrophages at this later time-point after injury.

Following nerve injury, Schwann cells immediately induce breakdown of the blood nerve barrier (BNB), enabling blood-borne cells and molecules to enter the endoneurium (at the damaged site of injury and along the distal nerve stump) and initiate a local inflammatory response. A previous study by Napoli et al. (2012) showed that Schwann cell activation of the ERK 1/ 2 signalling pathway causes BNB breakdown, which can occur independent of trauma. It would be interesting to see whether maintained Sox2 expression prevents the reformation of the BNB resulting in BNB dysfunction and thus the continued infiltration of immune cells into the nerve.

In addition to macrophages, Schwann cells distal to the site of injury have also been shown to actively express pro-inflammatory cytokines TNFα and IL-1β and anti-inflammatory cytokines IL-4 and IL-10 (Dubový et al., 2014). The expression of inflammatory cytokines by Schwann cells in close contact to regenerating axons (GAP43+) at 7 days after nerve crush, was shown not to alter axonal growth. Dubovy et al. (2014) suggested that the expression of pro-inflammatory and anti-inflammatory cytokines by Schwann cells may result in a balanced inflammatory

response, and thus be involved in promoting axonal growth. Sox2 has been shown to act as a pattern recognition receptor (PRR) in neutrophils, where it orchestrates the recognition of microbial double stranded DNA and elicits an immune response (Xia et al., 2015). As we have shown that continued expression of Sox2 in Schwann cells following nerve injury leads to a sustained inflammatory environment (i.e. an increased number of immune cells) in the nerve of $Sox2^{HetOE}$ mice, it would be interesting to analyse whether Sox2 mediates this effect by directly manipulating the inflammatory response. It would be interesting to see if Sox2 increases the expression of macrophages chemoattractant protein 1 (MCP-1) and shifts the cytokine expression profile of Schwann cells and macrophages towards being more pro-inflammatory, as opposed to maintaining an inflammatory balance (Dubový et al., 2014).

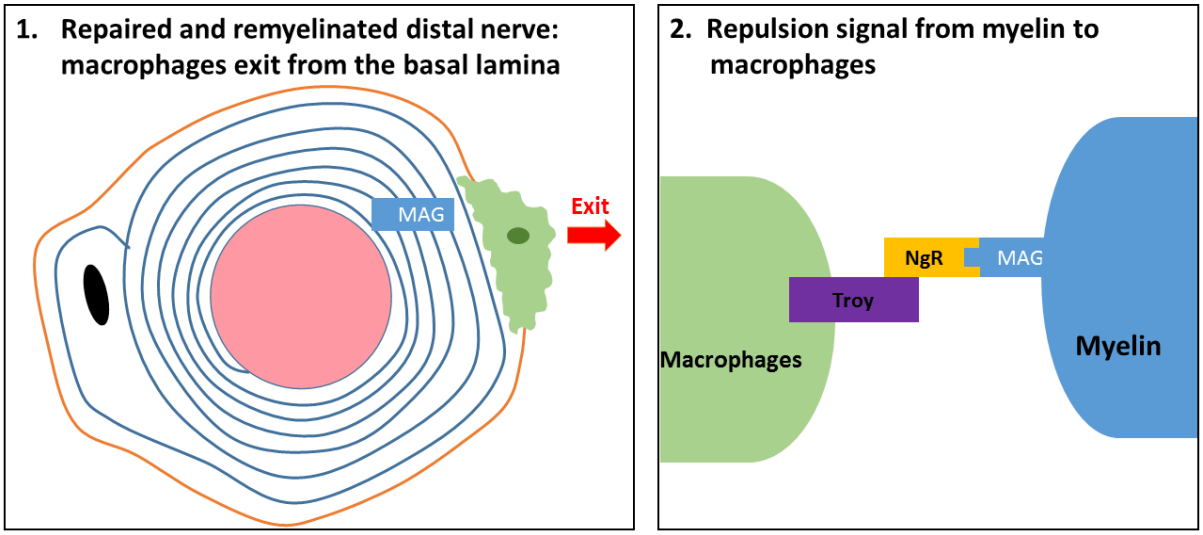

Figure 4. 12 After nerve injury and regeneration, newly formed myelin emit signals that contribute to the resolution of the inflammatory response. Single axon (pink) with myelin (blue) and basal lamina (orange), macrophages (green). (1) Following nerve regeneration and remyelination macrophages are no required within the basal lamina and therefore exit. (2) Proteins such as MAG expressed on the surface of newly formed myelin, interact with the receptor NgR and its signalling partner TROY on the macrophage membrane. Engagement of this receptor complex leads to local signalling and activation of the small GTPase RhoA, resulting in local repulsion and the moving away of macrophages from the source (myelin) (Fry et al., 2007). This causes macrophages to exit from the basal lamina. Adapted from Guadet et al. (2011).

4.3.4 Maintained Sox2 expression reduces functional recovery after nerve injury

Complete axon regeneration and remyelination after nerve injury, is usually followed by motor-sensory functional recovery in rodents between 3-4 weeks after nerve crush injury (Yang et al., 2008, Arthur-Farraj et al., 2012). Nonetheless, if Schwann cells fail to undergo cellular reprogramming after nerve injury, to support axon regeneration by providing trophic support to neurons, inducing myelin clearance and assisting with axons guidance, nerve repair and functional recovery is impaired (Arthur-Farraj et al., 2012, Fontana et al., 2012). Trans-differentiation of repair Schwann cells back to a myelinating state and the remyelination of regenerating axons is also critical for successful axon regeneration and the restoration of motor-sensory function (Fricker et al., 2013).

Studies using CAG-Cre-ER^{TM};Nrg1$^{fl/fl}$ mice, demonstrated that impaired Schwann cell remyelination after nerve, achieved through the deletion of NRG1-III in motor axons, resulted in a decrease in functional recovery (Static Functional Index) and nerve conduction velocity (NCV) (Fricker et al., 2013). In contrast, increasing the remyelination of regenerating axons following nerve crush injury, by treating mice with recombinant human Nrg1-II (rhNrg1-II) improved functional recovery (Chen et al., 1998).

Previous studies have also identified that impaired myelination during development or demyelination of axons during adulthood, results in reduced nerve conduction velocities, impaired motor-sensory function and the development of a peripheral neuropathy such as congenital hypomyelination neuropathy or Charcot-Marie-Tooth type-1 disease (Fledrich et al., 2014, Saporta et al., 2012). Promoting remyelination of adult axons through the administration of soluble Nrg1 to Schwann cells has thus been suggested as a therapy for demyelinating / neurodegenerative diseases (Syed and Kim, 2010). A particular study by Fledrich et al. (2014) showed that improving Schwann cell remyelination in mouse models of CMT-1A, by treating mice with recombinant human NRG1 (rhNRG1), strongly improved motor performance and ameliorated the disease. These studies highlight how Schwann cell myelination during development and remyelination after nerve injury is essential for normal nerve conduction velocity and motor-sensory function.

Our experiments have revealed that continued Sox2 expression after nerve crush injury, severely impairs Schwann cell remyelination of regenerating axons and increases the number of unmyelinated axons in a 1:1 relationship with Schwann cells in the nerves of $Sox2^{HetOE}$ mice at 21 DPI. We therefore wanted to determine whether impaired Schwann cell remyelination after nerve injury would affect functional recovery. Our data showed that continued Sox2 expression reduced NCV (although not significantly) and impaired motor functional recovery (confirmed by Static Sciatic Index and Toe Spread Reflex) in the nerves of $Sox2^{HetOE}$ mice at 21 DPI. Furthermore, continued Sox2 expression was shown to reduce sensory functional recovery (confirmed by Toe pinch testing and Von Frey filament withdrawal threshold testing) in the nerves of $Sox2^{HetOE}$ mice at 21 DPI. As Schwann cell myelination is fundamental for proper nerve function (motor-sensory) it thus comes to no surprised that Sox2 impairs functional recovery. It would be interesting to see if promoting Schwann cell remyelination through the administration of soluble Nrg1 improved motor-sensory functional recovery in the nerves of $Sox2^{HetOE}$ mice at 21 DPI.

Studies analysing the role of macrophages and T-lymphocytes in CMT-1A, CMT-1B and CMT-1X mouse models, have shown that the inflammatory immune response contributes to disease progression, reduced myelin thickness, NCV and impaired motor function (Klein et al., 2015). At 21 DPI the number of macrophages, T-lymphocytes and neutrophils in the nerves of $Sox2^{HetOE}$ mice is dramatic increased compared to controls. It is therefore possible that the increased number of immune cells in the $Sox2^{HetOE}$ mice further contribute to the reduced functional recovery of motor and sensory neurons.

While we might expect that continues Sox2 expression would impair motor functional recovery due to the impaired remyelination of large diameter axons, it was surprising to see that sensory functional recovery was also delayed; all small diameter axons (<0.1µm) were ensheathed and grouped into normal Remark bundle / structures. Nonetheless a subset of large diameter sensory mechanofibres such as Aδ require myelination, and thus impaired sorting and myelination of these fibres could explain the delay in sensory functional recovery. Sensory axon-derived Nrg-1 is important for axon-Schwann cell signalling and therefore normal sensory function (Fricker et al., 2009). In the absence of sensory-axon derived Nrg1, $Nrg1^{fl/fl}$;Nav1.8-Cre mice

displayed abnormal Remak bundles with numerous closely packed C-fibres, often not separated by Schwann cell cytoplasm (Fricker et al., 2009). These animals also showed an increased number of unmyelinated large diameter sensory fibres, a significant slowing of A-fibre conduction velocity and reduced sensitivity to mechanical stimuli (ibid). The requirement of Nrg1-ErbB signalling in non-myelinating Schwann cells for normal sensory function was further confirmed by Chen et al. (2003), who carried out analysis on mice that expressed a dominant negative ErbB4 receptor (DN –ErbB4) in adult non-myelinating Schwann cells. DN-ErbB4 non-myelinating Schwann cells showed significantly increased cell cycle proliferation and cell death at P30 (Chen et al., 2003). Furthermore, transgenic mice overexpressing DN-ErbB4 exhibited a distinct loss of sensory C-fibre neurons (ibid). Together these studies show that Nrg1-ErbB signalling between sensory axons and Schwann cells is necessary for Schwann cell myelination of large diameter (>1µm) sensory axons, the survival of sensory C-fibre neurons and thus normal sensory function. It would be interesting to see whether Nrg1-ErbB signalling is disrupted in Schwann cells myelinating large diameter sensory & motor axons in the nerves of $Sox2^{HetOE}$ mice. This could be achieve by carrying out protein expression analysis of ErbB2/ErbB3 and Nrg1 in the nerves of control and $Sox2^{HomoOE}$ mice at P60, and / or control and $Sox2^{HetOE}$ mice at 21 DPI, to determine whether altering Nrg1-ErbB signalling is another mechanism by which Sox2 impairs myelination and sensory-motor function.

4.4 Conclusion

This study has shown that continued Sox2 expression in Schwann cells after nerve injury severely impairs nerve repair and functional recovery. Sox2 maintains Schwann cells in a highly proliferative immature Schwann cells state, as a result Schwann cells fail to upregulate the expression of myelin proteins P_0 and Krox20 and remyelinate regenerating axons; $Sox2^{HetOE}$ mice thus demonstrate impaired motor and sensory function. Surprisingly, continued Sox2 expression also resulted in a sustained inflammatory response within the nerves of $Sox2^{HetOE}$ mice at time-points as late as 21 days post injury, when the inflammatory response is normally resolved. Our data confirms that Sox2 is a remarkable negative regulator of Schwann cell myelination, and that its expression must be reduced following the successful re-innervation of regenerating axons, to allow Schwann cell to remyelination and mice to regain functional recovery.

Chapter 5 p38α negatively regulates Schwann cell myelination

5.1 Introduction

The p38 mitogen activated protein kinase (MAPK) signalling cascade plays an essential role in governing many biological processes, including inflammation, apoptosis, proliferation, development and differentiation (Zarubin and Han, 2005). In oligodendrocytes p38 MAPK activity has been shown to drive myelin gene expression, myelination and remyelination, whilst in Schwann cells its functional role still remains unclear (Haines et al., 2008, Chung et al., 2015). Many studies have attempted to characterise the role of p38 MAPK activity in Schwann cell plasticity and development using specific p38 MAPK inhibitors and mutant mouse models, however the results have been conflicting. Whilst p38 MAPK activity has been suggested to promote Schwann cell myelination and Krox20 expression during development in some studies (Fragoso et al., 2003, Hossain et al., 2012) , others suggest that p38 MAPK activity blocks Schwann cell myelination and myelin protein expression during development (Yang et al., 2012). Furthermore, studies analysing p38 MAPK after nerve injury have shown that it is directly activated after injury and helps to initiate the injury response, by activating the expression of inflammatory cytokines and driving Schwann cell demyelination (Yang et al., 2012, Kato et al., 2013, Myers et al., 2003).

There are four isoforms of p38 MAPK; p38α, p38β, p38ɣ and p38δ, which share 60 to 70% nucleotide amino acid sequence specific homology. Of these isoforms, p38α is ubiquitously expressed and is suggested to be the most functionally relevant isoform (Nebreda and Porras, 2000, Mayor et al., 2007). p38α has been shown to play critical roles in neuron survival, inflammation and nerve regeneration, this therefore makes p38α a good target for studying the function of p38 MAPK activity (Zarubin and Han, 2005, Xing et al., 2015, Kato et al., 2013).

Previous studies have attempted to understand the functional role of p38 MAPK in Schwann cells by using pyridinyl imidazole compound inhibitors such as SB203580/ SB202190 and PD169316. These inhibitors target both p38α and p38β, without affecting p38ɣ and p38δ activity, and thus have been suggested as a good method for studying the function of p38α and β (Davies et al., 2000). Nonetheless these

inhibitors have been shown to affect other signalling pathways, such as Rip-like interacting caspase-like apoptosis-regulatory protein kinase/RIP2/CARDIAK (RICK) (Godl et al., 2003). Consequently, as mentioned earlier this has resulted in conflicting conclusions and as a result the functional role of p38 MAPK in Schwann cells remains uncertain. Given that p38α is highly expressed in Schwann cells and developing nerves, whereas p38β is undetectable (unpublished data by Dr Xin-Pen Dun in our lab, Hossain et al., 2012), we generated Schwann cell specific p38α null mice (a more specific approach than using pharmacological inhibitors) in order to study how p38 MAPK activity affects Schwann cell myelination during development and after nerve injury.

5.2 Results

5.2.1 p38 MAPK regulates Schwann cell myelination

A recent study in our laboratory by Yang et al. (2012) identified p38 MAPK as a negative regulator of Schwann cell differentiation and myelination. Yang et al. (2012) showed that p38 MAPK signalling was high at embryonic day 17 (E17), but declined at postnatal day 1, coinciding with Schwann cell myelination. Furthermore, ectopic activation of the p38 MAPK pathway, achieved through infecting Schwann cells with a lentivirus expressing MKK6-Glu, a constitutively activated form of MKK6 (a direct upstream activator of p38 MAPK) under the control of a doxycycline inducible promoter *in vitro,* and treatment with doxycycline*,* inhibited cAMP induced Schwann cell differentiation and myelin gene expression. Inhibition of the p38 MAPK pathway was further shown to enhance Schwann cell differentiation and myelin segment formation in Schwann cell-dorsal root ganglion (DRG) co-cultures (Yang et al., 2012). In contrast, Hossain et al. (2012) identified that inhibiting p38 MAPK activity in Schwann cell-DRG co-cultures, resulted in an increase in the number of unmyelinated Schwann cells, and reduced the gene expression of two core myelin regulatory transcription factors Sox10 and Krox20, as well as the gene expression of Protein zero (P_0) and Myelin basic protein (MBP). As the evidence from both of these studies are contradictory, we wanted to analyse and clarify the effect of p38 MAPK on Schwann cell myelination *in vivo*, without the use of p38 MAPK inhibitors such as SB 203580. Pharmaceutical inhibitors of p38 MAPK activity have been suggested to lead to incorrect conclusion regarding its role, due to their inhibitory effect on other signalling pathways (Godl et al., 2003). We therefore generated mice with Schwann cell specific deletion of p38α using Cre-loxP mediated gene targeting. Mice carrying conditional LoxP-flanked p38α ($p38\alpha^{fl/fl}$) alleles (Heinrichsdorff et al., 2008), were crossed with mTOTA P_0-Cre wild type/ wild type (P0 $Cre^{+\ wt/wt}$) (Schwann cell specific Cre) mice (Feltri et al., 1999); this allowed us to generate mice which were either heterozygous for the p38α flox gene and Cre^- ($p38\alpha^{fl/wt}\ Cre^-$) or heterozygous for the p38α flox gene and Cre^+ ($p38\alpha^{fl/wt}\ Cre^+$). $p38\alpha^{fl/wt}\ Cre^+$ mice were then crossed back with $p38^{fl/fl}$ mice, allowing us to generate mice that were $p38\alpha^{fl/wt}\ Cre^-$ and $p38\alpha^{fl/wt}\ Cre^+$, as well as mice that were homozygous for the p38α flox gene and Cre^- ($p38\alpha^{fl/fl}\ Cre^-$) or homozygous for the p38α flox gene and Cre^+ ($p38\alpha^{fl/fl}\ Cre^+$) [see Figure 1.13]. In this study, experiments were carried out only on homozygous $p38\alpha^{fl/fl}\ Cre^-$

mice (hereafter referred to as control mice) and homozygous p38α$^{fl/fl}$ Cre^{+} mice (hereafter referred to as conditional p38α knockout mice).

To test whether Schwann cell myelination was altered in the absence of p38 MAPK activity, the sciatic nerves from control and p38α knockout (p38α Ko) mice were removed and the ultrastructure was examined at postnatal days 2, 6, 21 and 90 using transmission electron microscopy.

At postnatal day 2 (P2), the population of axons in the sciatic nerves of p38α Ko mice were shifted towards having thicker myelin, compared to axons in the sciatic nerves of control mice; the average myelin thickness of control nerves was 0.04 ± 0.004μm, whereas the average myelin thickness in p38α Ko nerves was slightly thicker at 0.07 ± 0.02μm, nonetheless this was not significant (P=0.14, n=3 per genotype) [Figure 5.1]. Further analysis revealed however that there was a significant increase in the total percentage of myelinated axons in the sciatic nerves of p38α Ko mice (43.6 ± 5.7%), compared to control mice (22.2 ± 1.3%) (P=0.02, n=3) [Figure 5.1]. This data thus appears to confirm a role of p38α in negatively regulating myelination at the developmental stage.

We next went on to analyse myelin thickness in the sciatic nerves of control and p38α knockout mice at P6. We observed that there was a shift in axons towards having thicker myelin in the sciatic nerves of p38α Ko mice, compared to control mice; the average myelin thickness in p38α Ko nerves was higher at 0.54 ± 0.04μm, compared to control nerves, which had an average myelin thickness of 0.44 ± 0.07μm, although this change was not significant (P=0.27, n= 4 control, n=6 p38α Ko) [Figure 5.2]. Counts made on the total percentage of myelinated axons revealed that there was also no significant difference between p38α Ko mice and control mice at P6; in the nerves of p38α Ko mice the total percentage of myelinated axons was 95 ± 0.98%, whilst in the nerves of control mice, the total percentage of myelinated axons was 92 ± 1.67% (P=0.18, n= 4 control, n=6 p38α Ko) [Figure 5.2]. We next analysed axon size in the nerves of P6 animals and observed a shift in the percentage of axons toward having a larger axon diameter in the nerves of p38α Ko mice, compared to control; the average axon diameter in p38α Ko nerves was 1.11 ± 0.07μm, whereas as the average axon diameter in control nerves was slightly

smaller at 0.92 ± 0.04μm, this was however not significant (P=0.08, n= 4 control, n=6 p38α Ko) [Figure 5.3].

As we observed an increase in myelin thickness in the nerves of p38α Ko mice during the early stages of Schwann cell development (P2 and P6), we next wanted to analyse myelin thickness at later stages of Schwann cell development (P21) and during adulthood (P90). Analysis at P21 revealed that the population of axons in the nerves of p38α Ko mice remained shifted towards having thicker myelin, compared to control mice; in p38α Ko nerves the average g-ratio was 0.59 ± 0.01, whereas in the control nerves the average g-ratio was slightly higher at 0.62 ± 0.02, although this was not significant (P=0.24, n=3 per genotype) [Figure 5.4]. Analysis of the total number of myelinated axons, further revealed there was no significant difference in the total number of myelinated axons in the nerves of control and p38α Ko mice; all axons greater than 1μm in the nerves of these animals were myelinated by P21. We next analysed axon diameter size in the nerves of control and p38α Ko animals at P21. Surprisingly, again we observed an increase in the diameter size of axons in the nerves of p38α Ko mice, compared to control mice; in the nerves of p38α Ko mice the average axon diameter was 1.46 ± 0.1μm, whereas in the nerves of control mice the average axon diameter was smaller at 1.25 ± 0.1μm, however this again was not significant (P=0.24, n=3 per genotype) [Figure 5.4].

Analysis of adult P90 sciatic nerves further revealed that myelin thickness remained slightly thicker in the nerves of p38α Ko mice compared to control mice; the average g-ratio was 0.60 ± 0.07 in the nerves of p38α Ko mice, whereas the average g-ratio was 0.61 ± 0.02 in the nerves of control mice, although this change was not significant (P=0.61, n=3 control, n=4 p38α Ko). Comparisons made between axons diameter surprisingly revealed that the average axon diameter size now tended to be larger in the nerves of control mice (3.18 ± 0.61μm), compared to p38α Ko mice (2.33 ± 0.44μm) at P90, nonetheless this increase in axon diameter size was again not significant (P=0.32, n=3 control, n=4 p38α Ko) [Figure 5.5].

In summary, we observe that removal of p38α in Schwann cells leads to a marked early onset of Schwann cell myelination, as well as an increase in the total percentage of myelinated axons from as early as P2. Furthermore, there was a

tendency for myelin thickness to be slightly (although not significantly) increased in p38α Ko mice up until adulthood (P90). These results support our previous data, which suggests that the p38 MAPK signalling pathway is a negative regulator of Schwann cell myelination (Yang et al., 2012). In addition, we provide further evidence showing that p38α is the functional isoform regulating Schwann cell myelination, as depletion causes a tendency for increased myelination.

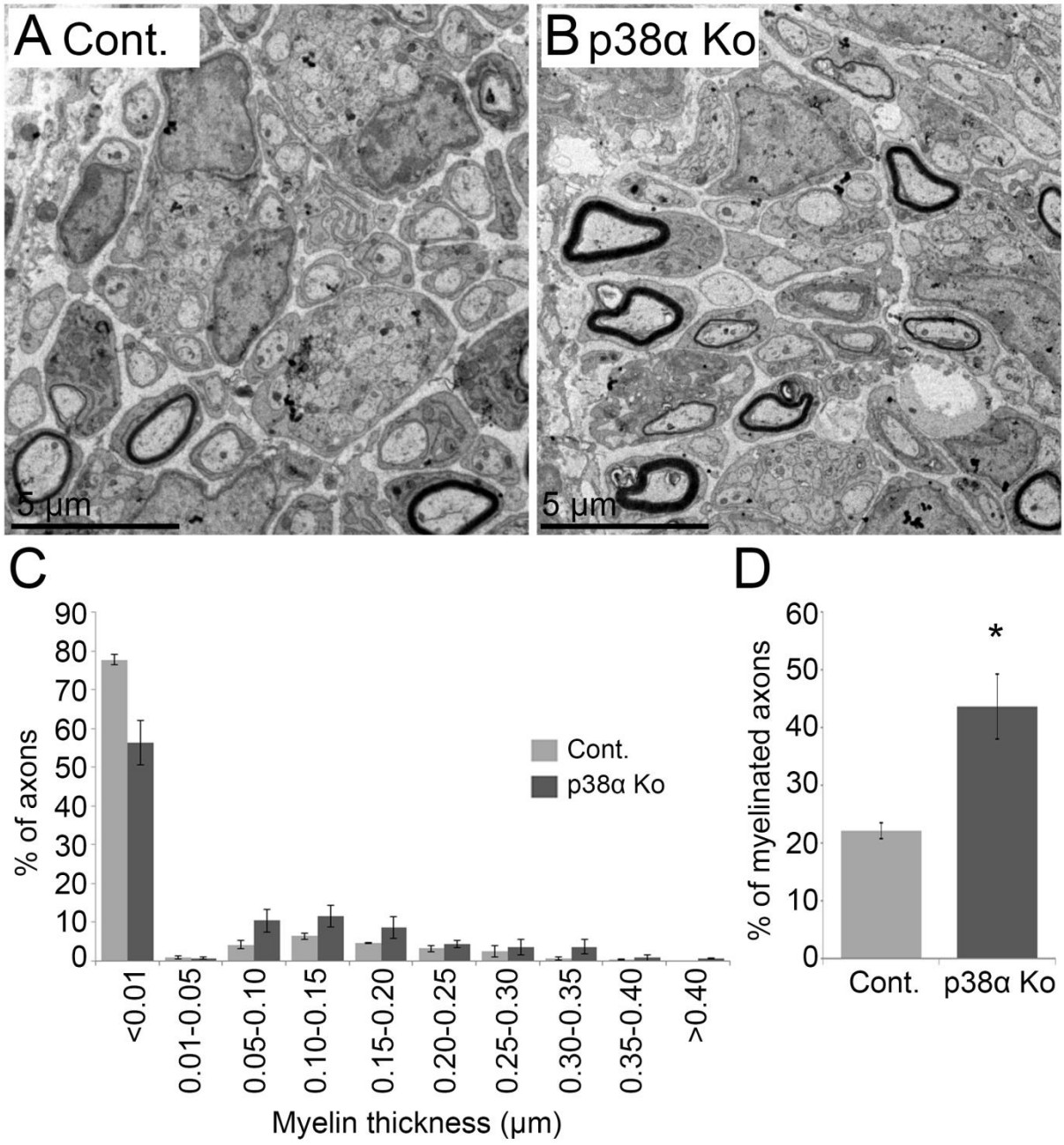

Figure 5. 1: Enhanced myelination in the nerves of p38α Ko mice at P2. Transmission electron micrographs of sciatic nerve sections taken from control (A) and p38α Ko (B) mice at P2. Graph (C) showing a shift in the total percentage of axons, towards having thicker myelin in the nerves of p38α Ko mice, compared to controls at P2. Graph (D) showing a significant average increase in the total percentage of myelinated axons in the nerves of p38α Ko mice, compared to control mice (P=0.02, n= 3 per genotype).

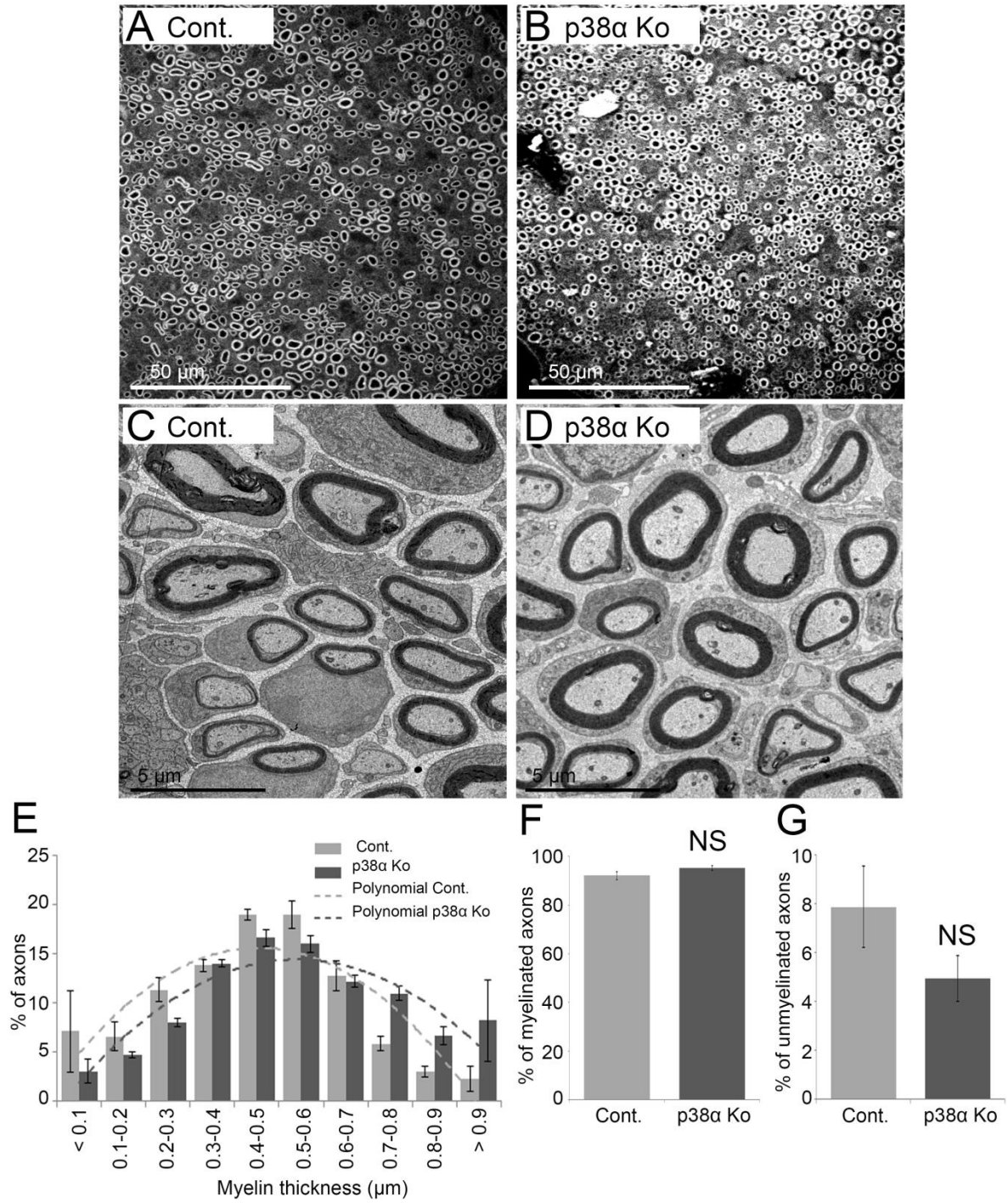

Figure 5. 2: Increased myelin thickness in the nerves of p38α Ko mice at P6. Low vacuum scanning electron micrographs of sciatic nerves taken from control (A) and p38α Ko (B) mice at P6. Transmission electron micrographs of sciatic nerves sections taken from control (C) and p38α Ko (D) mice at P6. Graph (E) showing a shift in the total percentage of axons towards having thicker myelin in the nerves of p38α Ko mice, compared to control. Graph (F) showing the percentage of myelinated axons in the nerves of control and p38α Ko mice. Graph (G) showing the percentage of unmyelinated axons in the nerves of control and p38α Ko mice (n=4 control, n=6 p38α Ko).

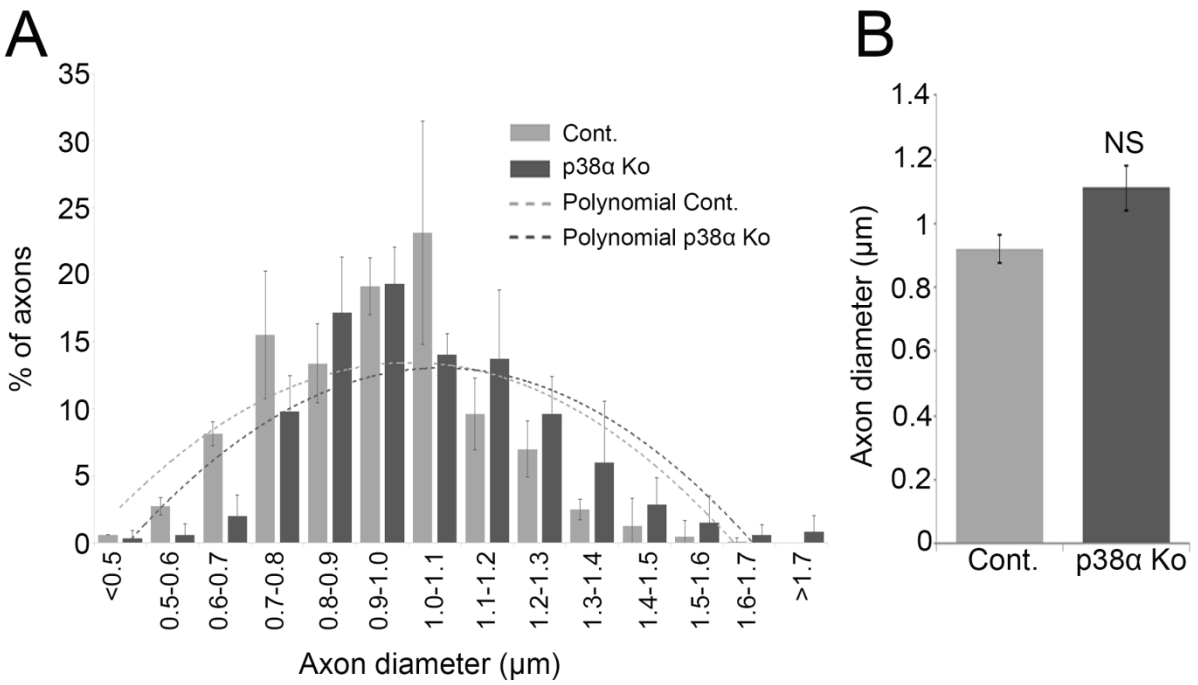

Figure 5. 3: Axon diameter is increased in p38α Ko nerves at P6. Graph (A) showing a shift in the total percentage of axons towards having a larger axon diameter the nerves of p38α Ko mice, compared to controls. Graph (B) showing an increase in the average axon diameter size in the nerves of p38α Ko mice, compared to controls (P=0.08) (n=4 control, n=6 p38α Ko).

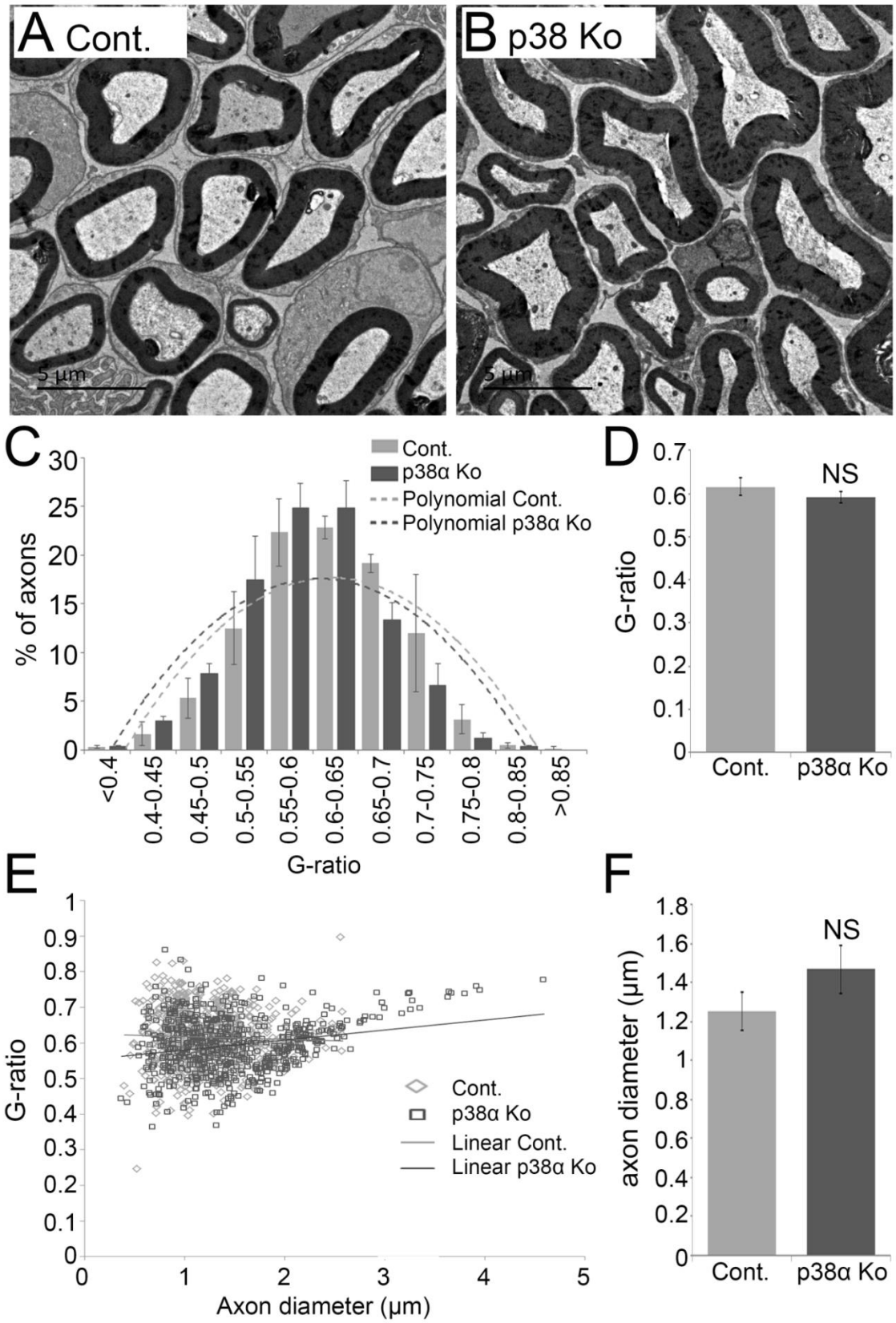

Figure 5. 4: Myelin thickness and axon diameter are both slightly increased in the nerves of p38α Ko mice at P21. Transmission electron micrographs of sciatic nerves sections taken from control (A) and p38α Ko (B) mice at P21. Graph (C) showing a shift in

the total percentage of axons towards having a lower g-ratio in the nerves of p38α Ko mice, compared to controls. Graph (D) showing the average g-ratio in the nerves of control and p38α Ko mice. Scatter plot (E) displaying the g-ratio of individual axons in relation to their axon diameter size. Graph (F) showing the average axon diameter of axons in a 1:1 with Schwann cells in the nerves of control and p38α Ko mice. (n=3 per genotype)

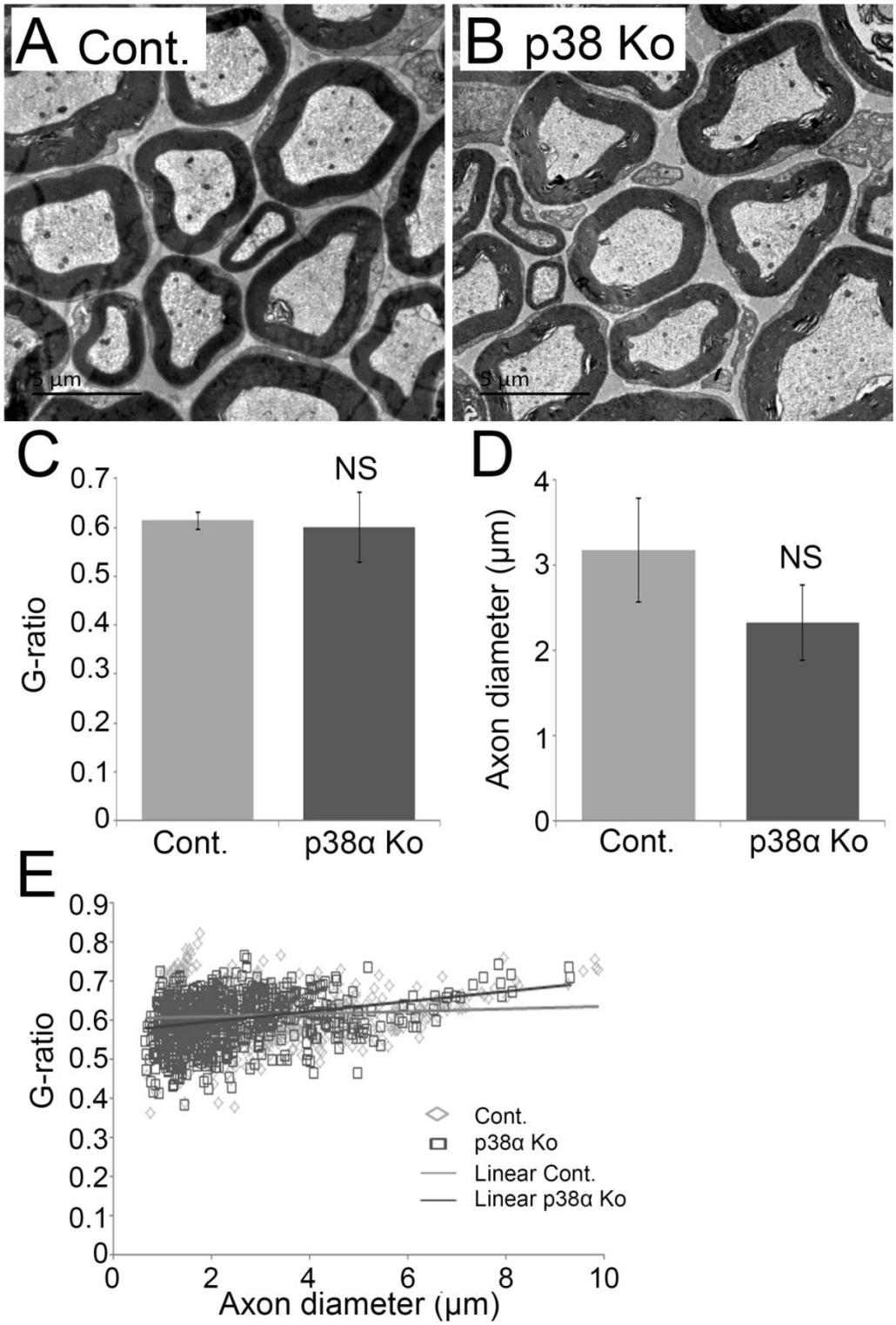

Figure 5. 5: Myelin thickness is slightly increased in the nerves of p38α Ko mice at P90. Transmission electron micrographs of sciatic nerves sections taken from control (A) and p38α Ko (B) mice at P90. Graph (C) showing the average g-ratio of control and p38α Ko sciatic nerves. Graph (D) showing the average axon diameter size of control and p38α Ko sciatic nerves. Scatter plot (E) displaying the g-ratio of individual axons in relation to their axon diameter size (n=3 control, n=4 p38α Ko).

5.2.2 p38α regulates myelin protein expression.

In order for Schwann cells to effectively myelinate large calibre axons (axons >1µm), the expression of Schwann cell myelin proteins such myelin protein zero (P_0), myelin basic protein (MBP), periaxin and myelin associated glycoprotein (MAG) must be actively upregulated by transcription factors Krox20 and Sox10. Nonetheless, as previously discussed in Chapters 3 and 4, the upregulated expression of myelin proteins can be impaired by the sustained or enhanced expression/signalling of negative myelin regulators, such as cJun, Sox2, activated Notch and ERK 1/2 MAPK signalling, leading to impaired Schwann cell differentiation and myelination. Recently Yang et al. (2012) identified that ectopic activation of the p38 MAPK signalling pathway in cultured Schwann cells blocked Schwann cell differentiation and the upregulated expression of myelin proteins Krox20 and MAG in response to cAMP, whereas inhibition of the p38 MAPK pathway enhanced Schwann cell myelin segment formation. Furthermore, blocking p38 activity with SB203580 treatment, dramatically enhanced the differentiation response of cultured Schwann cells to low doses (0.05mM) of cAMP, whereas very few differentiated cells were observed in untreated cultures (Yang et al., 2012). As we have observed an increase in myelin thickness in the nerves of p38α Ko mice compared to control mice, we therefore might expect that Schwann cells differentiate earlier and that myelin protein expression would be enhanced in the nerves of p38α Ko mice. We therefore analysed the expression of myelin proteins MBP and P_0 in the nerves of control and p38α Ko mice at P6. Western blot analysis revealed that both P_0 and MBP expression was enhanced in the nerves of p38α Ko mice compared to control nerves at P6 (n=3 per genotype) [Figure 5.6].

The results show that inactivation of p38α function in Schwann cells *in vivo,* leads to enhanced myelin protein expression at P6, further supporting our hypothesis that p38 MAPK signalling plays a true physiological role in the negative regulation of Schwann cell myelination.

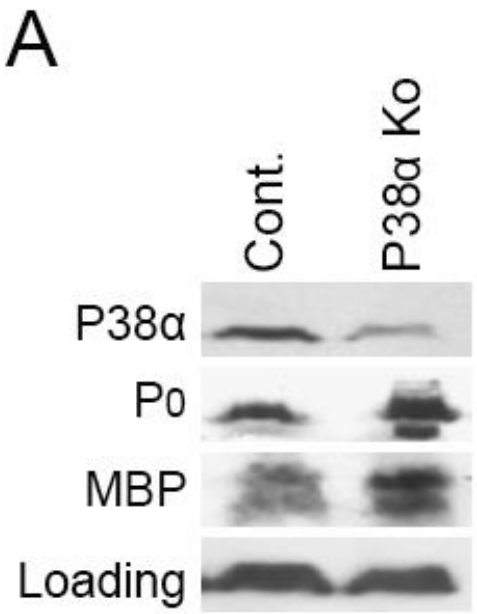

Figure 5. 6: Enhanced myelin protein expression in p38α Ko nerves at P6. Western blot (A) showing reduced expression of p38α, and enhanced expression of P_0 and MBP in the nerves of p38α Ko mice compared to control mice (n=3 per genotype).

5.2.3 Depletion of p38α reduces Schwann cell demyelination following nerve injury

p38 MAPK has been shown to be re-expressed after nerve injury and to play a role in the nerve injury response, by triggering Schwann cell demyelination and dedifferentiation. Yang et al. (2012) showed that blocking the p38 MAPK signalling pathway following nerve injury attenuated Schwann cell demyelination, leading to retained myelin regardless of axon loss. Nonetheless, this study also identified that there appeared to be a slight retention of axons in the injury nerves of mice treated with the SB203580 inhibitor, suggesting that the inhibitor may also exert non-Schwann cell dependent effects (Yang et al., 2012). We therefore wanted to follow up this study and investigate directly whether inactivation of p38α would also impair Schwann cell demyelination after nerve injury. To test this we analysed the expression levels of myelin specific proteins in the distal sciatic nerve segment, taken from control and p38α Ko mice at 3 and 7 days post cut injury (3 & 7 DPI).

Western blot analysis confirmed that p38α expression at 3 and 7 DPI and phosphorylated p38 (p-p38) expression at 3 DPI was weaker in the nerves of p38α Ko mice compared to controls (n=3 per genotype). As we expected p38α to be completely ablated from Schwann cells in the nerves of p38α Ko mice (through Cre mediated recombination), we presumed that the weakly detected p38α expression was from other cells within the nerve tissue such as macrophages and fibroblasts (Myers et al., 2003) [Figure 5.7]. The p-p38 antibody used in this experiment targets all p38 isoforms and is therefore not specific to p38α isoform. Nonetheless, as we observed a dramatic reduction in the expression of p-p38 in the nerves of p38α Ko mice compared to controls (n=3), this data further confirms that p38α is the major functional isoform responsible for activating the p38 MAPK signalling response.

Further analysis revealed that inactivation of p38α led to a delay in Schwann cell demyelination, as high levels of P_0 and MBP expression were still detectable in the nerves of p38α Ko mice, compared to control nerves; which showed reduced expression of P_0 and MBP at 3 and 7 DPI (n=3). Analysis of other MAPK signalling pathways, showed that whilst p-ERK 1/2 was not expressed in the nerves of uninjured control and p38α mice, it was highly and equally expressed within the nerves of control and p38α Ko mice at 3 DPI (n=1 control, n=2 p38α Ko) [Figure 5.7].

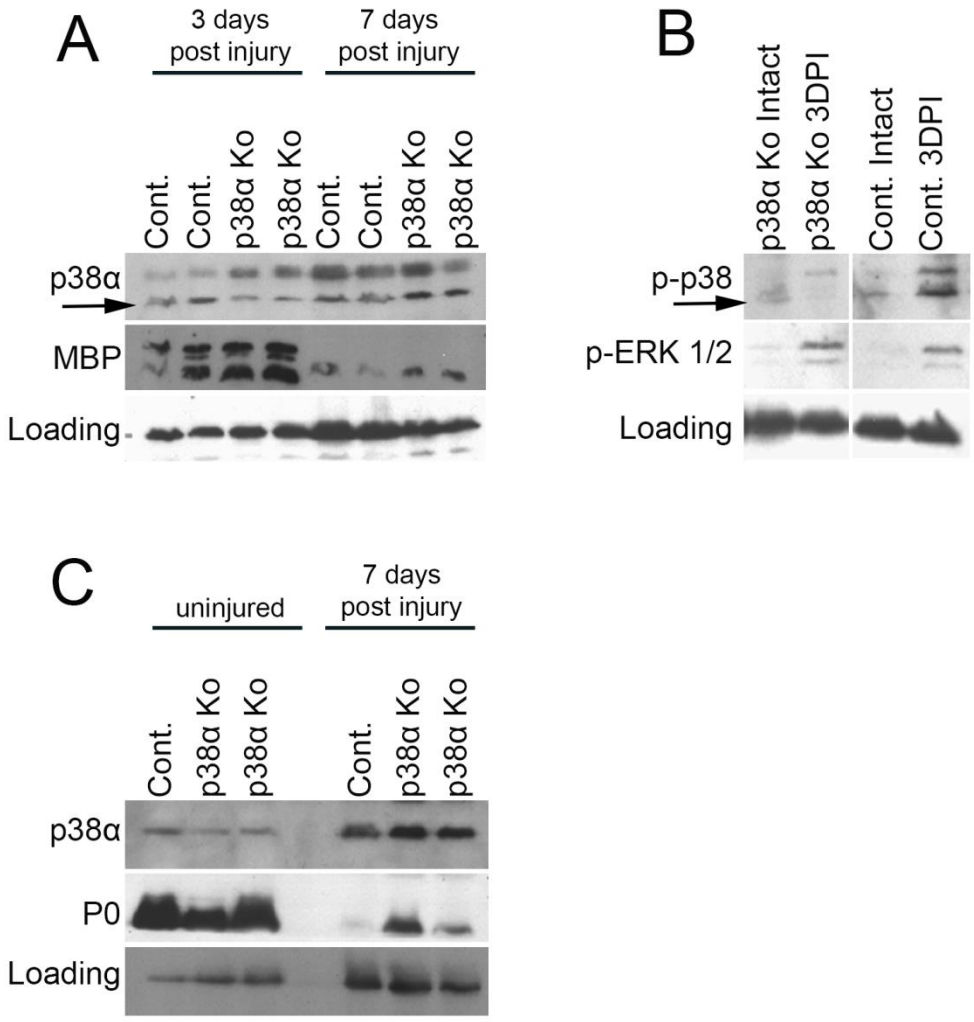

Figure 5. 7: Inactivation of p38α leads to a delayed reduction in Schwann cell myelin proteins following injury. Western blot showing (A) reduced expression of p38α and increased expression MBP in the nerves of p38α Ko mice, compared to control nerves at 3 and 7 DPI (n=3). Western blot (B) showing very weak expression of p-p38α and p-ERK 1/2 in the intact nerves of control and p38α Ko mice, as well as the weak expression of p-p38α in the nerves of 3DPI p38α Ko mice compared to controls; note, equal expression of p-ERK 1/2 in the nerves of p38α Ko and control mice at 3DPI (n=1 control, n=2 p38α Ko). Western blot (C) showing similar levels of P_0 in the uninjured nerves of control and p38α mice, however after injury P_0 expression levels are shown to be stronger in the nerves of p38α Ko mice compared to controls at 7DPI (n=3).

5.2.4 Inactivation of p38α in Schwann cells tends to increase myelin thickness at 21DPI.

Inhibition of p38 MAPK activity after nerve injury, through the use of Scios SD-169 compound; an oral inhibitor of phosphorylated p38 MAPK, has previously been shown to reduce Schwann cell TNFα production at 4 days post crush and enhance the rate of functional nerve regeneration. In addition the diameter of the regenerating axons also appeared to be thicker, with a correspondingly thicker myelin sheath at 28 day post crush injury in mice treated with SD-169 (Myers et al., 2003). However, a more recent study specifically analysed the physiological function of p38α in nerve regeneration following crush injury, by generating heterozygous p38α knock-in mutant mice (*Sevenmaker* type Mapk14). These mice contain a heterozygous point mutation (conversion of aspartate acid to asparagine) in the p38α docking site (D316N); which is responsible for regulating p38α activation and inactivation, thus resulting in the dysfunction of p38α (Kato et al., 2013, Mayor et al., 2007). The study identified that after injury, limited loss of p38α function resulted in a significant reduction in myelin thickness and axon diameter size at 4 weeks post nerve crush injury (4 WPI), a significant reduction in functional recovery at 3 and 4 WPI and also a delayed but increased expression of inflammatory cytokines, including TNFα and IL-1β at 4 WPI (Kato et al., 2013). As these studies are quite inconsistent with regards to how p38 MAPK activity affects remyelination and regeneration, and have used only heterozygous p38α mutant mice where p38α function is not completely lost, we wanted to directly analyse remyelination in the nerves of homozygous p38α Ko mice compared to controls after injury. To determine if myelination was altered, we analysed transmission electron micrographs of the distal sciatic nerve stump sections taken from control and p38α Ko mice at 21 days post crush injury (21 DPI). This time-point was chosen as full nerve repair and recovery has been shown to occur by 3-4 weeks following nerve crush injury in rodents (This study; Yang et al., 2008).

Transmission electron micrographs of distal sciatic nerves taken from control and p38α Ko mice at 21 DPI revealed that all axons in a 1:1 with a Schwann cell were remyelinated normally. Myelin thickness appeared slightly thicker and axon diameter size appeared slightly smaller in the nerves of p38α Ko mice, compared to controls

[Figure 5.8 C & D]. To determine if there was a difference in myelin thickness and axon diameter size prior to injury in the nerves of control and p38α Ko mice, we also analysed transmission electron micrographs of contralateral uninjured sciatic nerve sections taken from the same control and p38α Ko mice at 21 DPI. No obvious differences in myelin thickness or axon diameter size were observed in the contralateral uninjured nerves of control and p38α Ko, although this was not quantified (n=3) [Figure 5.8 A & B]. Nonetheless this coincides with our earlier data which showed that p38α depletion did not cause any significant chances in myelin thickness or axon diameter size in control and p38α Ko mice at P90 [Figure 5.5].

In order to determine whether myelin thickness and axon diameter were altered in the regenerating nerves of control and p38α Ko mice at 21 DPI, we quantified these two parameters. We identified that although there was no significant difference in g-ratio between control and p38α Ko mice at 21 DPI, g-ratio was lower in the nerves of p38α Ko mice (0.67 ± 0.06) compared to control mice (0.77 ± 0.02) (P=0.17, n=3). Furthermore, axon diameter was slightly reduced in the nerves of p38α Ko mice (1.57 ± 0.12um) compared to control mice (1.59 ± 0.03um) at 21 DPI, although again this was not significant (P=0.86, n=3).

In summary, there findings suggest that p38 MAPK plays a role in negatively regulating Schwann cell myelination, as inactivation of p38α leads to an increase in myelin thickness at 21 DPI. Furthermore, in contrast to the study by Kato et al. (2013), we revealed that inactivation of p38α does not significantly affect the diameter of regenerating axons.

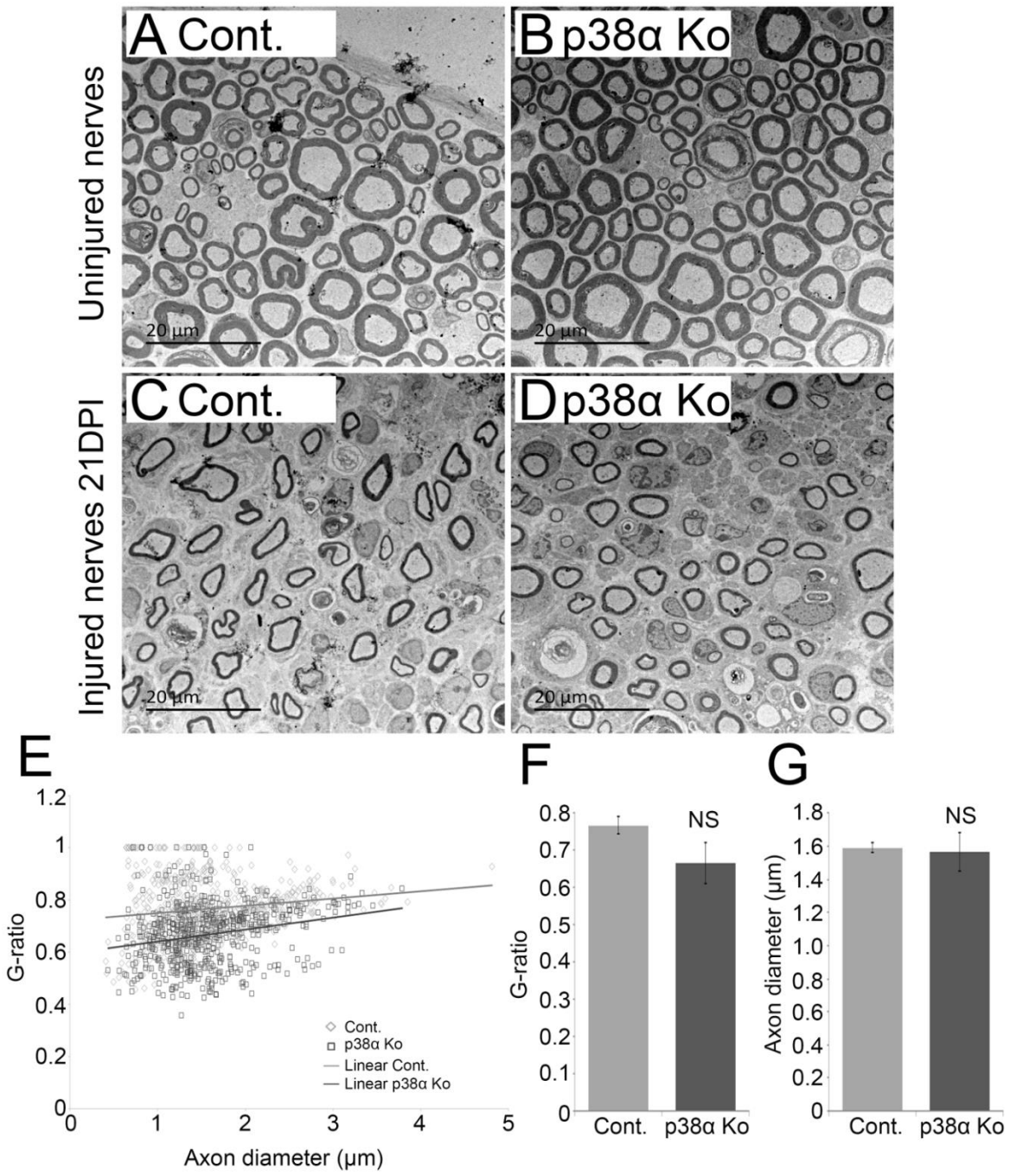

Figure 5. 8: Inactivation of p38α leads to increased myelin thickness at 21 DPI. Transmission electron micrographs of uninjured (A & B) and injured distal sciatic nerve sections (C &D) taken from control and p38α Ko mice at 21 DPI. Scatter plot (E) displaying the g-ratio of individual axons in relation to their axon diameter size: note a shift in axons toward having thicker myelin (lower g-ratio) in the nerves of p38α Ko mice (n=3). Graph (F) showing the average g-ratio of control and p38α Ko nerves at 21 DPI (n=3). Graph (G) showing the average axon diameter size of control and p38α Ko nerves at 21 DPI (n=3).

5.3 Discussion

There has been conflicting evidence from previous studies with regards to the role of p38 MAPK in regulating Schwann cell myelination. However, through analysing Schwann cell specific p38α knockout (p38 Ko) mice, our data suggests that p38 MAPK functions closely resemble those of a negative regulator of Schwann cell myelination.

5.3.1 Depletion of p38α activity in Schwann cells enhanced myelin thickness.

Schwann cell development and myelination are regulated by a variety of transcription factors and signalling pathways. The specifically timed and tightly regulated activation or expression of these cues is essential for the development of Schwann cells from Schwann cell precursors, as well as the initiation of Schwann cell myelination (Mirsky et al., 2008). It is known that activated Notch signalling, cJun and Sox2 are highly expressed in immature Schwann cells (ISC) and inhibit the early onset of myelination. Nonetheless, as negative regulators of Schwann cell myelination, their expression must be suppressed by factors such as Krox20 in order for Schwann cells to initiate myelination (Parkinson et al., 2008, Woodhoo et al., 2009).

The role of the p38 MAPK signalling pathway in Schwann cells is currently unclear, due to conflicting evidence suggesting that p38 MAPK positively and negatively controls Schwann cell myelination (Fragoso et al., 2003, Hossain et al., 2012, Yang et al., 2012). Nonetheless, increasing evidence showing that p38 MAPK activity is rapidly upregulated following nerve injury and is important for regulating Schwann cell demyelination, drives us to believe that p38 MAPK is a negative regulator of Schwann cell differentiation and myelination (Yang et al., 2012, Myers et al., 2003).

Many of the results derived from *in vivo* studies using of pharmaceutical p38 MAPK inhibitors such as SB 203580, PD169316 and SD-169, to analyse the involvement of p38 MAPK in myelination, have resulted in conflicting conclusions (Fragoso et al., 2003, Hossain et al., 2012, Myers et al., 2003, Yang et al., 2012). Off target inhibitory effects could potentially add to the variability (Davies et al., 2000): SB203580 targets p38α and β, as well as RICK (RIP-like interacting caspase-like apoptosis-regulatory

protein kinase/ RIP2/ CARDIAK) - a member of the receptor interacting kinase (RIP) family and known to promote NF-kB activity and activation of the JNK, ERK 1/2 and p38 MAP kinases (Davies et al., 2000, Godl et al., 2003, Kato et al., 2013), whilst PD169316 (an analogue of SB203580) has been shown to also block the signalling mechanisms of TGF-β and Activin (Fu et al., 2003). A compound which affects the functional activity of multiple protein kinases or proteins cannot be used to establish the specific functional role of a particular enzyme. In order to validate the existing results regarding p38 MAPK activity *in vivo*, experiments using specific p38 MAPK mutants are required (Davies et al., 2000). We therefore generated Schwann cell specific homozygous p38α depleted mice, to address the functional role of p38 MAPK activity in Schwann cells and upon myelination (Nebreda and Porras, 2000, Heinrichsdorff et al., 2008, Feltri et al., 1999a).

Similar to other negative myelin regulators, p38 MAPK activity is reported to be high within the nerves of embryonic day 17 (E17) rats, but to decline dramatically by postnatal day1 (P1); coinciding with the transition of immature Schwann cells into mature myelinating cells (Yang et al., 2012). As a negative regulator of myelination, we hypothesised that inactivation of p38 MAPK activity from E15 in Schwann cells would initiate an early onset of myelination and enhance myelin formation, similar to that observed by Yang et al. (2012). Nonetheless, if p38 MAPK activity was in fact a positive regulator of myelination, we would expect that its inactivation would result in Schwann cell hypomyelination (Fragoso et al., 2003, Hossain et al., 2012). Our data showed for the first time without the use of pharmaceutical p38 MAPK inhibitors, that complete inactivation of p38α MAPK signalling in Schwann cells results in a slight trend towards more axons being myelinated at P2 and a further shift in axons towards having thicker myelin at P6 and P21. In support of the study by Yang et al. (2012) we also observed an increase in P_0 and MBP expression in the nerves of p38α Ko mice, compared to controls at P6. As core regulators of myelination and myelin protein expression, it would have been beneficial to have also analysed the expression levels of Sox10 and Krox20 at P6, as well as at an earlier time-points such as P2; where the difference in the percentage of myelinated axons was observed to be most significant. Previous studies have highlighted that inactivation of p38 MAPK reduced the gene expression of Sox10 and Krox20, however from our data we might expect that the expression of these transcription factors would be

increased, thus enhancing myelination (Hossain et al., 2012). p38 MAPK has previously been reported to suppress the transcriptional activity of NFATc4 in adipocytes, thus preventing adipogenesis (Yang et al., 2002). It is therefore possible that p38 MAPK activation may also reduce the activity of NFATc4 in Schwann cells, thus reducing myelination though hindering its ability to synergise with Sox10 and activate Krox20 (Kao et al., 2009). It would be interesting to analyse NFATc4 expression in the sciatic nerves of early developing p38α Ko and control mice, to determine whether its localisation in the nucleus of Schwann cells is increased in the absence of p38α.

In addition to its role in regulating Schwann cell myelination, p38 MAPK has also been suggested to mediate laminin induced Schwann cell elongation and alignment along axons during the early stages of development, a process prerequisite to myelination (Fragoso et al., 2003). We therefore might expect that inactivation of p38 MAPK in Schwann cells *in vivo* would result in failure of Schwann cells to elongate and align with axons, radially sort axons and thus show signs of dysmyelination (Fragoso et al., 2003, Feltri et al., 2002, Feltri et al., 2015). Nonetheless, through observational analysis, radial sorting and myelination of axons appeared to be normal in p38 Ko mice, and we did not observed any differences between the nerves of p38 Ko and control mice at P2, P6, P21 or P90, thus suggesting that p38 MAPK is not required for Schwann cell elongation and alignment with axons. Inactivation of p38α through P_0 Cre driven recombination occurs around E13.5-E15 as revealed by lacZ “reporter” mice, however complete removal of the p38α protein from within the cell, will depend on its protein half-life. Immature Schwann cells begin to preform radial sorting of axons around E12.5 and proceed this until about P10 (Feltri et al., 2015). Previous studies have observed radial sorting defects in mice which have undergone P_0 Cre driven recombination and gene deletion around E13.5-E15 (Feltri et al., 2002), however as no radial sorting defects were observed in p38α Ko, it is possible that p38α either does not play a role in radial sorting or that it exerts its functional effects at time-points earlier than E13.5-E15. To determine the role of p38 MAPK in Schwann cell elongation, alignment and radial sorting more precisely, further analysis would need to be carried out on p38α Ko mice, where p38α activity is removed at earlier time-points such as E12, through desert hedgehog (DHH)

driven Cre recombination or E11, through periostin driven Cre recombination (Jaegle et al., 2003, Lindsley et al., 2007, Feltri et al., 1999b).

p38 MAPK is activated within the distal nerve stump very quickly after nerve injury and helps to increase the expression of neurotrophic factors and inflammatory cytokines required for Wallerian degeneration, thus enhancing Schwann cell demyelination, macrophage recruitment and nerve regeneration (Zrouri et al., 2004, Yamazaki et al., 2009, Myers et al., 2003, Yang et al., 2012). Myers et al. (2003) discovered that blocking p38 MAPK activity after nerve injury as a therapy for inflammatory induced hyperalgesia reduced TNFα production, but also significantly increased nerve regeneration rates and enhanced the number of newly formed myelinated nerve fibres; axons were larger in diameter with corresponding thicker myelin sheaths. In support of this finding Yang et al. (2012) confirmed *in vitro* that inhibition of p38 MAPK activity enhanced myelin formation, whilst activation of p38 MAPK activity triggered Schwann cell demyelination and dedifferentiation. Together these studies imply that p38 MAPK activity negatively regulates myelination and nerve regeneration and is required for the early initiation of the Schwann cell injury response.

Our findings trend towards those found in earlier studies carried out in our laboratory by Yang et al. (2012). We showed for the first time *in vivo* without the use of pharmaceutical inhibitors that p38 MAPK participates in the initiation of myelin breakdown and Schwann cell dedifferentiation following nerve injury. We show that impaired p38 MAPK activation after nerve crush injury appears to result in a delay in the downregulated expression of myelin proteins, and thus suggests that Schwann cell demyelination, which is required for nerve repair and regeneration, is postponed.

Previous studies have also confirmed that ERK 1/2 MAPK is rapidly activated following nerve injury, and drives Schwann cell demyelination and dedifferentiation (Napoli et al., 2012, Zrouri et al., 2004, Yamazaki et al., 2009). To determine whether ERK 1/2 and p38 MAPK are capable of cross signalling/regulating one another, we analysed the level of phosphorylated ERK 1/2 in the nerves of p38α Ko mice, compared to control mice following nerve injury, but observed no apparent change.

These results thus suggest that p38 MAPK does not alter ERK 1/2 MAPK activation in Schwann cells.

Our results also identified that inactivation of p38α following nerve injury, results in a trend towards remyelinated nerve fibres having thicker myelin sheaths at 21 days post crush injury (21 DPI), although this was not significant. Data from our group (G.Dee, unpublished data) also indicated through static sciatic index (SSI) analysis that nerve regeneration was slightly accelerated in the absence of p38 MAPK activity; although this was not significant. However, in agreement with Myers et al. (2003), our results suggest that inactivation of the p38 MAPK signalling pathway leads to improved nerve regeneration after injury. To determine whether depletion of p38α in Schwann cells leads to accelerated axon growth and remyelination, further analysis would need to be carried out at earlier time-points such as 14 DPI, when p38 MAPK activity is suggested to peak (Yamazaki et al., 2009), to determine whether nerve fibre regeneration is faster and whether the onset of remyelination occurs earlier in p38α Ko mice, compared to controls. This could be achieved through carrying out nerve whole mount staining to determine whether axonal growth rates are altered (Dun and Parkinson, 2015), and transmission electron microscopy to analyse remyelination in nerve fibres at 14 DPI.

A recent study by Kato et al. (2013) attempted to address the role of p38 MAPK in nerve regeneration through the use of heterozygous p38α mutant sem (*severmaker* type Mapk14) mice. This study discovered that reducing the function of p38 MAPK after nerve injury significantly reduced myelin thickness (although did not alter g-ratio), axon diameter, and nerve regeneration, whilst also leading to a delayed but increased inflammatory response at 4 weeks post crush injury. While these results contradict earlier findings, this study may not be completely reliable (Yang et al., 2012, Myers et al., 2003). Following p38α phosphorylation and activation by extracellular cues such as TNFα, p38α is normally dephosphorylated upon binding to its substrates. However, mutations in the p38α docking domain prevent it from binding to its substrate upon activation, and thus becoming dephosphorylated (auto-repressed). Kato et al. (2013) therefore suggested that this inability of p38α to be auto-repressed could be the reason for elevated TNFα expression at 4 weeks after injury, rather than a direct effect of reducing p38α activity. It is difficult to state the

functional role of p38α from this study as the results identified may be attributed to the docking domain mutation (D316N) effect i.e. the inability of p38α to be dephosporylated and thus inactivated, rather than the limited loss of p38α function. The sem mouse model used in the study by Kato et al. (2013) contains a global heterozygous p38α point mutation, thus any effects regarding nerve regeneration and inflammation cannot be attributed solely to Schwann cells, and rather all cells where p38α is expressed including fibroblasts, immune cells and neurons.

p38 MAPK is known to increase apoptosis and suggested to enhance IL-1β and TNFα production within the peripheral nerve after injury (Kato et al., 2013). While IL-1β activates the expression of neurotropic factors such as nerve growth factor (NGF) required for neuronal survival and axon growth, TNFα induces macrophage recruitment and Schwann cell demyelination. Both IL-β and TNF-α however, have been shown to be responsible for the initiation of neuropathic pain (Ellis and Bennett, 2013, Nadeau et al., 2011, Watkins and Maier, 2002). p38 MAPK activation peaks at 14 DPI, and although it begins to decline from this time-point, it remains active within the nerves at 28 DPI (Yamazaki et al., 2009). We might therefore speculate that the preserved activity of p38 MAPK within Schwann cells up to 28 DPI may result in a low grade inflammatory environment which may affect remyelination and nerve fibre regeneration, as observed in previous studies (Kato et al., 2013, Myers et al., 2003). Thus, although required for the early initiation of Schwann cell demyelination and dedifferentiation, which can also be activated by cJun, ERK1/2 and possibly Sox2, inactivation of p38 MAPK might possibly be beneficial in the long term and reduce the inflammatory response, along with apoptosis of Schwann cells. This effect leads to less tissue damage, better nerve regeneration and enhanced remyelination (Popovich et al., 1999, Myers et al., 2003). To determine if this is true, experiments analysing apoptosis and the inflammatory response, along with nerve fibre growth and remyelination, in relation to p38 MAPK activity would need to be analysed in control and p38 Ko animals from the initial time of injury up to 21/28 DPI. The inflammatory response is critical for effective nerve regeneration, as complete ablation of macrophages, IL-1β and TNFα results in severely impaired axon regeneration (Barrette et al., 2008, Nadeau et al., 2011). Thus reducing the extent of the inflammatory response through p38 MAPK inactivation at later time-points post

injury, rather than completely blocking it would be more beneficial (Ellis and Bennett, 2013, Barrette et al., 2008, Nadeau et al., 2011).

5.4 Conclusion

Using Schwann cell specific p38α knockout mice, we have shown for the first time *in vivo* that p38 MAPK plays a role in regulating Schwann cell myelination during development and after injury. In concordance with its previously published role, p38 MAPK activation shows a tendency to contribute to the initiation of Schwann cell demyelination following peripheral nerve injury. However, inactivation of p38 MAPK following injury does not appear to have any negative longer term consequences on the nerve regeneration process, and actually appears to be beneficial; we observed a tendency to slightly increased myelination at 21 days post injury, in agreement with previous studies showing improved axon growth (Myers et al., 2003). We predict that this improvement may be due to the reduced inflammatory environment as shown by Myers et al. (2003), thus enhancing the ability of axons to regrow and Schwann cells to remyelinate in the absence of negative regulatory signals.

Chapter 6 Discussion

The transcription factor Sox2, along with activation of the p38 MAPK signalling pathways in Schwann cells have been suggested to drive Schwann cell demyelination and promote an immature Schwann cell fate *in vitro* (Le at al. 2005, Yang et al. 2012). However, the direct functional effect of Sox2 on Schwann cell myelination *in vivo* has never been studied, and the functional role of p38 MAPK in Schwann cell myelination remains unclear. Using genetically modified mice (Sox2 overexpressing mice and p38α null mice) these experiments aimed to investigate the functional role of both Sox2 and activation of the p38 MAPK signalling pathways in Schwann cell myelination during development and after peripheral nerve injury.

Sox2 has been well characterised as a marker of immature Schwann cells. It is highly upregulated during embryonic Schwann cell development but is antagonised and downregulated by the increased expression of Krox20, as Schwann cells begin to mature and myelinate (Parkinson et al., 2008, Le et al., 2005a). Furthermore, Sox2 is re-expressed following peripheral nerve injury, and upon Schwann cell demyelination and dedifferentiation (Parinello et al. 2011, Bremer et al. 2011, Decker 2006). Sox2 has also been shown to exert negative effects on Schwann cell myelination; enforced Sox2 expression in Schwann cells co-cultured with dorsal root ganglion axons blocked myelination (Le et al., 2005. Parkinson et al., 2008). *In vitro* data collected by Dr R.Doddrell in our lab further expanded on the functional role of Sox2 as a negative myelin regulator. In cultured Schwann cells, Sox2 blocked the induction of myelin proteins periaxin and P_0 by the myelination regulator Krox20, as well as the upregulated expression of Oct6. While the role of Sox2 as a negative myelin regulator *in vitro* appears well defined, further experiments were needed to clarify the role of Sox2 in Schwann cells *in vivo.* Using a conditional overexpressing (Sox2-IRES-EGFP) allele of Sox2 and a Schwann cell-specific CRE line (mTOTA P_0-CRE), in the experiments presented here the role of Sox2 in Schwann cells was examined for the first time *in vivo*. We confirmed that continued Sox2 expression impairs the transition of immature/promyelinating Schwann cells into a myelinating state; this was supported by the continued expression of cJun and N-cadherin in immature Schwann cells in the nerves of Sox2 overexpressing ($Sox2^{OE}$) mice. Furthermore, continued Sox2 expression directly prevents Schwann cell myelination and impairs the expression of Krox20 and myelin proteins P_0 and MBP. Peripheral

nerves of $Sox2^{OE}$ mice therefore exhibit profound hypomyelination at all time-points during development and in adulthood. Sox2 overexpression also triggers excess Schwann cell proliferation and an influx of macrophages into intact $Sox2^{OE}$ nerves. Sox2 overexpressing mice further demonstrate reduced nerve conduction velocities and impaired motor and sensory function. Overall the continued expression of Sox2 in Schwann cells results in mice developing symptoms characteristic of a peripheral nerve disorder such as Charcot-Marie-Tooth type 1 (CMT-1). Furthermore, we identified that the phenotype observed in Sox2 overexpressing mice could be reversed following a reduction in Sox2 expression. This study thus demonstrates the direct functional effect of continued Sox2 expression in Schwann cells during development.

To further clarify the functional role of Sox2, we examined the effect of continued Sox2 expression in Schwann cells following peripheral nerve injury. Sox2 overexpression was shown to accelerate axonal growth (Dr Xin-Peng Dun, unpublished data), however its continued expression inhibited Schwann cell remyelination, myelin protein re-expression and functional recovery. Similar to what we observed during development, $Sox2^{OE}$ Schwann cells also exhibit an increased rate of cellular proliferation and an increased number of macrophages were observed in nerves with $Sox2^{OE}$ Schwann cells at 21 days post injury (21DPI).

Remarkably we found that Sox2 was able to directly modulate the expression of Sox10, a critical regulator of Schwann cell specification and myelination (Finzsch et al., 2010, Bremer et al., 2011, Britsch et al., 2001). We observed at later time-points in development that the overexpression of Sox2 results in a reduction in Sox10 expression and re-localisation of Sox10 into the Schwann cell cytoplasm. This novel finding provides an insight into a potential mechanism by which Sox2 impairs myelination and leads to a progressive worsening in the phenotype observed in $Sox2^{OE}$ mice. Further investigations of how Sox2 regulates Sox10 expression, and whether Sox2 antagonises the binding of Sox10 to the promotor regions of its downstream targets such as Oct6, Krox20 and P_0, remains essential. Further experiments would help to elucidate the exact mechanism by which Sox2 prevents Schwann cell differentiation and myelination.

Sox2 has been identified to be upregulated in mouse models of CMT-1 disease, including CMT-1A caused by mutations in PMP22 (Fledrich et al., 2014) and CMT-1B caused by mutations in P_0 (unpublished data by Dr Francesca Florio at San Raffaele University). It is possible that Sox2 expression may be upregulated in CMT-1A mouse models as a marker of immature Schwann cells and an inducer of disease progression. Nonetheless as seen in CMT-1B mouse models Sox2 may exert a protective effect, by preventing cellular stress in response to the expression of mutant myelin proteins (Dr Francesca Florio, unpublished data).

In our study we have demonstrated that overexpression of Sox2 in Schwann cells may have clinical relevance, $Sox2^{OE}$ mice show similar characteristics and symptoms to those observed in mouse models of CMT-1 disease and congenital hypomyelinating neuropathy i.e. reduced myelination and nerve conduction velocities, impaired motor-sensory function, and an increased inflammatory response in the peripheral nerves. It would be interesting to see whether Sox2 is upregulated and/or is a contributing factor to the development of demyelinating peripheral neuropathies in patients. We have observed that decreasing Sox2 expression in mice that exhibit characteristics of a peripheral neuropathy due to elevated Sox2 protein levels, can reverse the phenotype and thus allow Schwann cells to regain their myelination function. This data suggests that targeting Sox2 as a potential therapy might provide beneficial in ameliorating peripheral nerve disorders such as congenital hypomyelinating neuropathy if Sox2 is observed to be severely elevated.

As mentioned above, Sox2 induced a phenotype in Sox2 overexpressing mice similar to that of Charcot-Marie-Tooth disease. Enforced expression of Sox2 in Schwann cells *in vitro* identified that Sox2 regulates the expression of a number of genes (Dr R.Doddrell, unpublished data) which have been shown to cause forms of CMT; N-myc downstream regulated gene 1 (NDRG1), neurofilament light (Nefl) and lipopolysaccharide-induced TNF factor (LITAF) (Berger et al., 2004, Kalaydjieva et al., 2000, Okuda et al., 2004, Züchner et al., 2004, Sinkiewicz-Darol et al., 2015, Street et al., 2003). Furthermore, we identified *in vivo* that Sox2 directly reduces P_0 and Krox20 expression in Schwann cells; two proteins known to be altered in forms of CMT-1 disease. Understanding the mechanisms that regulate Schwann cell myelination is critical for designing effective treatments for demyelinating peripheral neuropathies. We show that Sox2 is a direct negative regulator of Schwann cell

myelination able to alter the expression of genes and proteins shown to cause forms of CMT-1 and also promotes a phenotype of a peripheral neuropathy when overexpressed. Sox2 might therefore be a valuable therapeutic target in peripheral nerve disorders that show aberrant expression of Sox2.

The inflammatory response is activated upon peripheral nerve injury and helps to ensure successful nerve regeneration and functional recovery when regulated correctly. Nonetheless, when the inflammatory response is not resolved following nerve repair and remyelination, this can lead to the onset of a peripheral nerve disorder and impaired functional recovery. Upon Schwann cell demyelination and dedifferentiation (marked by the re-expression of Sox2), as seen in studies where Krox20 and Sox10 have been inactivated in Schwann cells during adulthood (Decker et al., 2006, Bremer et al., 2011), macrophages begin to infiltrate into the endoneurial space and clear myelin debris. In the nerves of $Sox2^{HomoOE}$ mice, which displayed impaired myelination and numerous immature/promyelinated Schwann cells, the number of macrophages was significantly increased. From these studies there appears to be a correlation between the number of demyelinating and dedifferentiating Schwann cells, and the increased number of macrophages infiltrating the nerves. It is possible that upon Schwann cell demyelination and dedifferentiation in the absence of trauma or upon long term failure to differentiate, Schwann cells activate the ERK 1/2 signalling pathway. In mouse models of CMT-1 disease the MEK 1/2-ERK 1/2 signalling cascade is activated in mutant Schwann cells and directly mediates the expression of macrophage chemoattractant protein -1 (MCP-1), which causes macrophage recruitment (Fischer et al., 2008b, Kohl et al., 2010a). The ERK 1/2 signalling cascade is also known to induce blood nerve barrier (BNB) breakdown in the absence of trauma, leading to the infiltration of immune cells into the nerve (Napoli et al., 2012). It would be interesting to see whether the ERK 1/2 signalling pathway and the expression of MCP-1 are upregulated in Schwann cells, in response to Sox2 overexpression. Low grade inflammation involving macrophages, has been shown to substantially contribute to the pathogenesis of demyelinating neuropathies. In particular enhancing disease progression in mouse models of CMT-1 disease. Decreasing macrophage numbers in the nerves of CMT-1B and 1X mice has been show to ameliorate the disease (Martini and Willison, 2015, Martini et al., 2013, Kohl et al., 2010a, Klein et al., 2015).

As macrophage numbers are elevated in the nerves of Sox2 overexpressing mice during development and after nerve injury, it is possible that they contribute to the progressive worsening of the phenotype observed during development, and a peripheral nerve disorder after injury.

In contrast to Sox2, the role of p38 MAPK has been more widely studied in Schwann cells. Nonetheless, its functional role in regulating Schwann cell myelination remains uncertain due to conflicting results from previous studies. While studies by Fragoso et al. (2003) and Hossain et al. (2012) suggest that p38 MAPK acts as a positive driver of Schwann cell myelination, a recent study by Yang et al. (2012) identified that the p38 MAPK signalling pathway negatively regulates Schwann cell myelination. Previous studies have used pharmaceutical inhibitors of the p38 MAPK signalling pathway in order to elucidate its functional role. However, as these inhibitors also block other signalling pathways (mentioned in section 5.3.1), this could be the reason for conflicting conclusions.

The major functional isoform of p38 MAPK, has been identified as p38α (Nebreda and Porras, 2000, Zarubin and Han, 2005). We thus generated Schwann cell specific p38α null mice to be able to study the direct functional role of p38 MAPK in Schwann cell myelination, as this is a more specific method than using pharmaceutical inhibitors. Our data supported the work by Yang et al. (2012), showing that the p38 MAPK signalling pathway functions to negatively regulate Schwann cell myelination and promote demyelination following peripheral nerve injury. Nerves taken from p38α null mice showed increased myelin thickness compared to controls throughout development (although not significant), as well as an increased expression of myelin proteins P_0 and MBP (at P6). Analysis after nerve injury revealed the importance of p38 MAPK signalling in initiating Schwann demyelination, as p38α null mice failed to effectively downregulate the expression of myelin proteins P_0 and MBP at 3 and 7 DPI. Nonetheless, p38α null mice exhibited slightly accelerated nerve regeneration (G.Dee, unpublished data) and increased myelin thickness at 21 DPI, compared to control mice. These results highlighted for the first time *in vivo* that p38 MAPK acts as a negative regulator of Schwann cell myelination, and that in the absence of its activity, Schwann cell myelination is enhanced.

p38 MAPK is a stress activated protein kinase (SAPK) known to facilitate responses to cellular stresses including pathogens, cytokines and growth factors. p38 MAPK therefore plays a fundamental role in mediating the inflammatory response; the activation and recruitment of inflammatory cells, the production of pro-inflammatory cytokines (IL-1β, TNFα and IL-6) and the induction of inflammatory enzymes such as Cox2, iNOS and other inflammatory related molecules (Zarubin and Han, 2005, Herlaar and Brown, 1999, Yang et al., 2014b). Accumulating evidence has shown the p38 plays a particular role in the macrophage-mediated inflammation by regulating the production of inflammatory cytokines such as IL-1β and TNFα (Yang et al., 2014b). Reducing the activity of p38 MAPK in peripheral nerves which have undergone nerve crush injury, has been shown to reduce the expression of pro-inflammatory cytokines at early time-points post injury, decrease Schwann cell death and improve axon regeneration (Kato et al., 2013, Myers et al., 2003). We therefore speculate that in nerves where p38α has specifically been depleted from Schwann cells, improved nerve regeneration and remyelination may have been partly due to a decrease in the inflammatory response. The previous studies mentioned above have analysed nerve repair in response to a global p38 MAPK reduction (Kato et al., 2013, Myers et al., 2003), it therefore remains unknown whether specific depletion of p38 MAPK activity in Schwann cells would reduce the inflammatory response, and thus be responsible for the improved nerve regeneration. In future our group is hoping to examine whether p38α depletion in Schwann cells reduces the inflammatory response, and in particular the number of recruited macrophages to the nerves of p38α null mice after nerve injury, compared to controls.

6.1 Conclusion

This work has shown for the first time *in vivo* using Schwann cell specific Sox2 overexpressing ($Sox2^{OE}$) mice that Sox2 functions as a direct negative regulator of Schwann cell myelination. Continued Sox2 expression during development and after peripheral nerve crush injury prevents Schwann cells from differentiating into a myelinating state, upregulating the expression of Krox20 and promyelin proteins and thus impairs myelination of axons. Furthermore, we have identified that continued Sox2 expression caused an increased macrophage mediated inflammatory response within the nerves of $Sox2^{OE}$ mice, and that these mice develop a phenotype of a peripheral neuropathy. Similarly, we have indicated for the first time *in vivo* using Schwann cell specific p38α null (p38α Ko) mice, that p38 MAPK can exhibit similar functions to that of a negative myelin regulator. Schwann cells depleted of p38α, the major functional isoform of p38 MAPK, show a trend towards having an increased myelin thickness and an increased expression of myelin proteins during development. In addition, following nerve injury, depletion of p38α in Schwann cells tends to improved axon regeneration and Schwann cell remyelination.

Bibliography

ADLKOFER, K., MARTINI, R., AGUZZI, A., ZIELASEK, J., TOYKA, K. V. & SUTER, U. 1995. Hypermyelination and demyelinating peripheral neuropathy in Pmp22-deficient mice. *Nat Genet,* 11**,** 274-280.

ALEXOPOULOU, A. N., COUCHMAN, J. R. & WHITEFORD, J. R. 2008. The CMV early enhancer/chicken β actin (CAG) promoter can be used to drive transgene expression during the differentiation of murine embryonic stem cells into vascular progenitors. *BMC Cell Biology,* 9**,** 2-2.

ALIX, J. J. P. & FERN, R. 2009. Glutamate receptor-mediated ischemic injury of premyelinated central axons. *Annals of Neurology,* 66**,** 682-693.

ARNAUD, E., ZENKER, J., DE PREUX CHARLES, A.-S., STENDEL, C., ROOS, A., MÉDARD, J.-J., TRICAUD, N., KLEINE, H., LUSCHER, B., WEIS, J., SUTER, U., SENDEREK, J. & CHRAST, R. 2009. SH3TC2/KIAA1985 protein is required for proper myelination and the integrity of the node of Ranvier in the peripheral nervous system. *Proceedings of the National Academy of Sciences of the United States of America,* 106**,** 17528-17533.

ARROYO, E. J., BERMINGHAM, J. R., ROSENFELD, M. G. & SCHERER, S. S. 1998. Promyelinating Schwann Cells Express Tst-1/SCIP/Oct-6. *The Journal of Neuroscience,* 18**,** 7891-7902.

ARTHUR-FARRAJ, P., LATOUCHE, M., WILTON, D. K., QUINTES, S., CHABROL, E., BANERJEE, A., WOODHOO, A., JENKINS, B., RAHMAN, M., TURMAINE, M., WICHER, G. K., MITTER, R., GREENSMITH, L., BEHRENS, A., RAIVICH, G., MIRSKY, R. & JESSEN, K. R. 2012. c-Jun reprograms Schwann cells of injured nerves to generate a repair cell essential for regeneration. *Neuron,* 75**,** 633-47.

AYBAR, M. J., NIETO, M. A. & MAYOR, R. 2003. Snail precedes Slug in the genetic cascade required for the specification and migration of the Xenopus neural crest. *Development,* 130**,** 483-494.

BAPTISTA, A. F., GOMES, J. R., OLIVEIRA, J. T., SANTOS, S. M., VANNIER-SANTOS, M. A. & MARTINEZ, A. M. 2007. A new approach to assess function after sciatic nerve lesion in the mouse - adaptation of the sciatic static index. *J Neurosci Methods,* 161**,** 259-64.

BARRETTE, B., HÉBERT, M.-A., FILALI, M., LAFORTUNE, K., VALLIÈRES, N., GOWING, G., JULIEN, J.-P. & LACROIX, S. 2008. Requirement of Myeloid Cells for Axon Regeneration. *The Journal of Neuroscience,* 28**,** 9363-9376.

BARRIONUEVO, F. & SCHERER, G. 2010. SOX E genes: SOX9 and SOX8 in mammalian testis development. *The International Journal of Biochemistry & Cell Biology,* 42**,** 433-436.

BARTESAGHI, L., ARNAUD GOUTTENOIRE, E., PRUNOTTO, A., MÉDARD, J.-J., BERGMANN, S. & CHRAST, R. 2015. Sox4 participates in the modulation of Schwann cell myelination. *European Journal of Neuroscience,* 42**,** 1788-1796.

BASU-ROY, U., BAYIN, N. S., RATTANAKORN, K., HAN, E., PLACANTONAKIS, D. G., MANSUKHANI, A. & BASILICO, C. 2015. Sox2 antagonizes the Hippo pathway to maintain stemness in cancer cells. *Nat Commun,* 6.

BENNINGER, Y., THURNHERR, T., PEREIRA, J. A., KRAUSE, S., WU, X., CHROSTEK-GRASHOFF, A., HERZOG, D., NAVE, K.-A., FRANKLIN, R. J. M., MEIJER, D., BRAKEBUSCH, C., SUTER, U. & RELVAS, J. B. 2007. Essential and distinct roles for cdc42 and rac1 in the regulation of Schwann

cell biology during peripheral nervous system development. *The Journal of Cell Biology,* 177**,** 1051-1061.
BERGER, P., SIRKOWSKI, E. E., SCHERER, S. S. & SUTER, U. 2004. Expression analysis of the N-Myc downstream-regulated gene 1 indicates that myelinating Schwann cells are the primary disease target in hereditary motor and sensory neuropathy-Lom. *Neurobiology of Disease,* 17**,** 290-299.
BERVAR, M. 2000. Video analysis of standing — an alternative footprint analysis to assess functional loss following injury to the rat sciatic nerve. *Journal of Neuroscience Methods,* 102**,** 109-116.
BETANCUR, P., BRONNER-FRASER, M. & SAUKA-SPENGLER, T. 2010. Genomic code for Sox10 activation reveals a key regulatory enhancer for cranial neural crest. *Proceedings of the National Academy of Sciences of the United States of America,* 107**,** 3570-3575.
BHATTACHARYYA, A., FRANK, E., RATNER, N. & BRACKENBURY, R. 1991. P0 is an early marker of the schwann cell lineage in chickens. *Neuron,* 7**,** 831-844.
BIRCHMEIER, C. & NAVE, K.-A. 2008. Neuregulin-1, a key axonal signal that drives Schwann cell growth and differentiation. *Glia,* 56**,** 1491-1497.
BRAY, S. J. 2006. Notch signalling: a simple pathway becomes complex. *Nat Rev Mol Cell Biol,* 7**,** 678-689.
BREMER, M., FRÖB, F., KICHKO, T., REEH, P., TAMM, E. R., SUTER, U. & WEGNER, M. 2011. Sox10 is required for Schwann-cell homeostasis and myelin maintenance in the adult peripheral nerve. *Glia,* 59**,** 1022-1032.
BRENNAN, A., DEAN, C. H., ZHANG, A. L., CASS, D. T., MIRSKY, R. & JESSEN, K. R. 2000. Endothelins Control the Timing of Schwann Cell Generation in Vitro and in Vivo. *Developmental Biology,* 227**,** 545-557.
BRITSCH, S., GOERICH, D. E., RIETHMACHER, D., PEIRANO, R. I., ROSSNER, M., NAVE, K.-A., BIRCHMEIER, C. & WEGNER, M. 2001. The transcription factor Sox10 is a key regulator of peripheral glial development. *Genes & Development,* 15**,** 66-78.
BROCKES, J. P., FIELDS, K. L. & RAFF, M. C. 1979. Studies on cultured rat Schwann cells. I. Establishment of purified populations from cultures of peripheral nerve. *Brain Research,* 165**,** 105-118.
CARENINI, S., MÄURER, M., WERNER, A., BLAZYCA, H., TOYKA, K. V., SCHMID, C. D., RAIVICH, G. & MARTINI, R. 2001. The Role of Macrophages in Demyelinating Peripheral Nervous System of Mice Heterozygously Deficient in P0. *The Journal of Cell Biology,* 152**,** 301-308.
CARTER, G. T., JENSEN, M. P., GALER, B. S., KRAFT, G. H., CRABTREE, L. D., BEARDSLEY, R. M., ABRESCH, R. T. & BIRD, T. D. 1998. Neuropathic pain in Charcot-Marie-tooth disease. *Archives of Physical Medicine and Rehabilitation,* 79**,** 1560-1564.
CATTIN, A.-L., BURDEN, JEMIMA J., VAN EMMENIS, L., MACKENZIE, FRANCESCA E., HOVING, JULIAN J. A., GARCIA CALAVIA, N., GUO, Y., MCLAUGHLIN, M., ROSENBERG, LAURA H., QUEREDA, V., JAMECNA, D., NAPOLI, I., PARRINELLO, S., ENVER, T., RUHRBERG, C. & LLOYD, ALISON C. 2015. Macrophage-Induced Blood Vessels Guide Schwann Cell-Mediated Regeneration of Peripheral Nerves. *Cell,* 162**,** 1127-1139.
CHARLES, P., TAIT, S., FAIVRE-SARRAILH, C., BARBIN, G., GUNN-MOORE, F., DENISENKO-NEHRBASS, N., GUENNOC, A.-M., GIRAULT, J.-A., BROPHY, P. J. & LUBETZKI, C. 2002. Neurofascin Is a Glial Receptor for the

Paranodin/Caspr-Contactin Axonal Complex at the Axoglial Junction. *Current Biology,* 12**,** 217-220.

CHEN, L.-E., LIU, K., SEABER, A. V., KATRAGADDA, S., KIRK, C. & URBANIAK, J. R. 1998. Recombinant human glial growth factor 2 (rhGGF 2) improves functional recovery of crushed peripheral nerve (a double-blind study). *Neurochemistry International,* 33**,** 341-351.

CHEN, S., RIO, C., JI, R.-R., DIKKES, P., COGGESHALL, R. E., WOOLF, C. J. & CORFAS, G. 2003. Disruption of ErbB receptor signaling in adult non-myelinating Schwann cells causes progressive sensory loss. *Nat Neurosci,* 6**,** 1186-1193.

CHEN, Y., SHI, L., ZHANG, L., LI, R., LIANG, J., YU, W., SUN, L., YANG, X., WANG, Y., ZHANG, Y. & SHANG, Y. 2008. The molecular mechanism governing the oncogenic potential of SOX2 in breast cancer. *J Biol Chem,* 283**,** 17969 - 17978.

CHUNG, S. H., BISWAS, S., SELVARAJ, V., LIU, X. B., SOHN, J., JIANG, P., CHEN, C., CHMILEWSKY, F., MARZBAN, H., HORIUCHI, M., PLEASURE, D. E. & DENG, W. 2015. The p38alpha mitogen-activated protein kinase is a key regulator of myelination and remyelination in the CNS. *Cell Death Dis,* 6**,** e1748.

CINELLI, P., MADANI, R., TSUZUKI, N., VALLET, P., ARRAS, M., ZHAO, C. N., OSTERWALDER, T., RÜLICKE, T. & SONDEREGGER, P. 2001. Neuroserpin, a Neuroprotective Factor in Focal Ischemic Stroke. *Molecular and Cellular Neuroscience,* 18**,** 443-457.

COTTER, L., ÖZÇELIK, M., JACOB, C., PEREIRA, J. A., LOCHER, V., BAUMANN, R., RELVAS, J. B., SUTER, U. & TRICAUD, N. 2010. Dlg1-PTEN Interaction Regulates Myelin Thickness to Prevent Damaging Peripheral Nerve Overmyelination. *Science,* 328**,** 1415-1418.

COURT, F. A., SHERMAN, D. L., PRATT, T., GARRY, E. M., RIBCHESTER, R. R., COTTRELL, D. F., FLEETWOOD-WALKER, S. M. & BROPHY, P. J. 2004. Restricted growth of Schwann cells lacking Cajal bands slows conduction in myelinated nerves. *Nature,* 431**,** 191-195.

CRAWFORD, A. T., DESAI, D., GOKINA, P., BASAK, S. & KIM, H. A. 2008. E-cadherin expression in postnatal Schwann cells is regulated by the cAMP-dependent protein kinase A pathway. *Glia,* 56**,** 1637-1647.

CUENDA, A. & ROUSSEAU, S. 2007. p38 MAP-Kinases pathway regulation, function and role in human diseases. *Biochimica et Biophysica Acta (BBA) - Molecular Cell Research,* 1773**,** 1358-1375.

D'URSO, D., EHRHARDT, P. & MÜLLER, H. W. 1999. Peripheral Myelin Protein 22 and Protein Zero: a Novel Association in Peripheral Nervous System Myelin. *The Journal of Neuroscience,* 19**,** 3396-3403.

DAVIES, S. P., REDDY, H., CAIVANO, M. & COHEN, P. 2000. Specificity and mechanism of action of some commonly used protein kinase inhibitors. *Biochemical Journal,* 351**,** 95-105.

DAVIS, R. J. 2000. Signal Transduction by the JNK Group of MAP Kinases. *Cell,* 103**,** 239-252.

DECKER, L., DESMARQUET-TRIN-DINH, C., TAILLEBOURG, E., GHISLAIN, J., VALLAT, J.-M. & CHARNAY, P. 2006. Peripheral Myelin Maintenance Is a Dynamic Process Requiring Constant Krox20 Expression. *The Journal of Neuroscience,* 26**,** 9771-9779.

DODDRELL, R. D. S., DUN, X.-P., MOATE, R. M., JESSEN, K. R., MIRSKY, R. & PARKINSON, D. B. 2012. Regulation of Schwann cell differentiation and proliferation by the Pax-3 transcription factor. *Glia,* 60**,** 1269-1278.

DONG, Z., BRENNAN, A., LIU, N., YARDEN, Y., LEFKOWITZ, G., MIRSKY, R. & JESSEN, K. R. 1995. Neu differentiation factor is a neuron-glia signal and regulates survival, proliferation, and maturation of rat schwann cell precursors. *Neuron,* 15**,** 585-596.

DONG, Z., SINANAN, A., PARKINSON, D., PARMANTIER, E., MIRSKY, R. & JESSEN, K. R. 1999. Schwann cell development in embryonic mouse nerves. *Journal of Neuroscience Research,* 56**,** 334-348.

DUBOVÝ, P., KLUSÁKOVÁ, I. & HRADILOVÁ SVÍŽENSKÁ, I. 2014. Inflammatory Profiling of Schwann Cells in Contact with Growing Axons Distal to Nerve Injury. *BioMed Research International,* 2014**,** 691041.

DUN, X.-P. & PARKINSON, D. B. 2015. Visualizing Peripheral Nerve Regeneration by Whole Mount Staining. *PLoS ONE,* 10**,** e0119168.

ELLIS, A. & BENNETT, D. L. H. 2013. Neuroinflammation and the generation of neuropathic pain. *British Journal of Anaesthesia,* 111**,** 26-37.

EMERY, B., AGALLIU, D., CAHOY, J. D., WATKINS, T. A., DUGAS, J. C., MULINYAWE, S. B., IBRAHIM, A., LIGON, K. L., ROWITCH, D. H. & BARRES, B. A. 2009. Identification of Myelin-gene Regulatory Factor as a Critical Transcriptional Regulator Required for CNS Myelination. *Cell,* 138**,** 172-185.

FELTRI, M. L., D'ANTONIO, M., PREVITALI, S., FASOLINI, M., MESSING, A. & WRABETZ, L. 1999a. P0-Cre Transgenic Mice for Inactivation of Adhesion Molecules in Schwann Cells. *Annals of the New York Academy of Sciences,* 883**,** 116-123.

FELTRI, M. L., D'ANTONIO, M., QUATTRINI, A., NUMERATO, R., ARONA, M., PREVITALI, S., CHIU, S.-Y., MESSING, A. & WRABETZ, L. 1999b. A novel P0 glycoprotein transgene activates expression of lacZ in myelin-forming Schwann cells. *European Journal of Neuroscience,* 11**,** 1577-1586.

FELTRI, M. L., GRAUS PORTA, D., PREVITALI, S. C., NODARI, A., MIGLIAVACCA, B., CASSETTI, A., LITTLEWOOD-EVANS, A., REICHARDT, L. F., MESSING, A., QUATTRINI, A., MUELLER, U. & WRABETZ, L. 2002. Conditional disruption of beta 1 integrin in Schwann cells impedes interactions with axons. *J Cell Biol,* 156**,** 199-209.

FELTRI, M. L., POITELON, Y. & PREVITALI, S. C. 2015. How Schwann Cells Sort Axons: New Concepts. *The Neuroscientist*.

FENG, Z. & KO, C.-P. 2008. Schwann Cells Promote Synaptogenesis at the Neuromuscular Junction via Transforming Growth Factor-β1. *The Journal of Neuroscience,* 28**,** 9599-9609.

FERN, R., DAVIS, P., WAXMAN, S. G. & RANSOM, B. R. 1998. *Axon Conduction and Survival in CNS White Matter During Energy Deprivation: A Developmental Study*.

FERNER, R. E. 2007. Neurofibromatosis 1 and neurofibromatosis 2: a twenty first century perspective. *The Lancet Neurology,* 6**,** 340-351.

FEX SVENNIGSEN, Å. & DAHLIN, L. B. 2013. Repair of the Peripheral Nerve—Remyelination that Works. *Brain Sciences,* 3**,** 1182-1197.

FILBIN, M. T. 2003. Myelin-associated inhibitors of axonal regeneration in the adult mammalian CNS. *Nat Rev Neurosci,* 4**,** 703-713.

FINZSCH, M., SCHREINER, S., KICHKO, T., REEH, P., TAMM, E. R., BÖSL, M. R., MEIJER, D. & WEGNER, M. 2010. Sox10 is required for Schwann cell identity and progression beyond the immature Schwann cell stage. *The Journal of Cell Biology,* 189**,** 701-712.

FISCHER, S., KLEINSCHNITZ, C., MÜLLER, M., KOBSAR, I., IP, C. W., ROLLINS, B. J. & MARTINI, R. 2008a. Monocyte chemoattractant protein-1 is a pathogenic component in a model for a hereditary peripheral neuropathy. *Molecular and Cellular Neuroscience,* 37**,** 359-366.

FISCHER, S., WEISHAUPT, A., TROPPMAIR, J. & MARTINI, R. 2008b. Increase of MCP-1 (CCL2) in myelin mutant Schwann cells is mediated by MEK-ERK signaling pathway. *Glia,* 56**,** 836-843.

FLEDRICH, R., STASSART, R. M., KLINK, A., RASCH, L. M., PRUKOP, T., HAAG, L., CZESNIK, D., KUNGL, T., ABDELAAL, T. A. M., KERIC, N., STADELMANN, C., BRUCK, W., NAVE, K.-A. & SEREDA, M. W. 2014. Soluble neuregulin-1 modulates disease pathogenesis in rodent models of Charcot-Marie-Tooth disease 1A. *Nat Med,* 20**,** 1055-1061.

FONTANA, X., HRISTOVA, M., DA COSTA, C., PATODIA, S., THEI, L., MAKWANA, M., SPENCER-DENE, B., LATOUCHE, M., MIRSKY, R., JESSEN, K. R., KLEIN, R., RAIVICH, G. & BEHRENS, A. 2012. c-Jun in Schwann cells promotes axonal regeneration and motoneuron survival via paracrine signaling. *The Journal of Cell Biology,* 198**,** 127-141.

FRAGOSO, G., ROBERTSON, J., ATHLAN, E., TAM, E., ALMAZAN, G. & MUSHYNSKI, W. E. 2003. Inhibition of p38 mitogen-activated protein kinase interferes with cell shape changes and gene expression associated with Schwann cell myelination. *Experimental Neurology,* 183**,** 34-46.

FRATTA, P., SAVERI, P., ZAMBRONI, D., FERRI, C., TINELLI, E., MESSING, A., D'ANTONIO, M., FELTRI, M. L. & WRABETZ, L. 2011. P0S63del impedes the arrival of wild-type P0 glycoprotein to myelin in CMT1B mice. *Human Molecular Genetics,* 20**,** 2081-2090.

FRICKER, F. R., ANTUNES-MARTINS, A., GALINO, J., PARAMSOTHY, R., LA RUSSA, F., PERKINS, J., GOLDBERG, R., BRELSTAFF, J., ZHU, N., MCMAHON, S. B., ORENGO, C., GARRATT, A. N., BIRCHMEIER, C. & BENNETT, D. L. 2013. Axonal neuregulin 1 is a rate limiting but not essential factor for nerve remyelination. *Brain,* 136**,** 2279-97.

FRICKER, F. R., ZHU, N., TSANTOULAS, C., ABRAHAMSEN, B., NASSAR, M. A., THAKUR, M., GARRATT, A. N., BIRCHMEIER, C., MCMAHON, S. B., WOOD, J. N. & BENNETT, D. L. H. 2009. Sensory axon-derived Neuregulin-1 is required for axoglial signalling and normal sensory function but not for long term axon maintenance. *The Journal of neuroscience : the official journal of the Society for Neuroscience,* 29**,** 7667-7678.

FRY, E. J., HO, C. & DAVID, S. 2007. A Role for Nogo Receptor in Macrophage Clearance from Injured Peripheral Nerve. *Neuron,* 53**,** 649-662.

FU, Y., O'CONNOR, L. M., SHEPHERD, T. G. & NACHTIGAL, M. W. 2003. The p38 MAPK inhibitor, PD169316, inhibits transforming growth factor β-induced Smad signaling in human ovarian cancer cells. *Biochemical and Biophysical Research Communications,* 310**,** 391-397.

FUJIWARA, S., HOSHIKAWA, S., UENO, T., HIRATA, M., SAITO, T., IKEDA, T., KAWAGUCHI, H., NAKAMURA, K., TANAKA, S. & OGATA, T. 2014. SOX10 Transactivates S100B to Suppress Schwann Cell Proliferation and to Promote Myelination. *PLoS ONE,* 9**,** e115400.

GAO, X., DAUGHERTY, R. L. & TOURTELLOTTE, W. G. 2007. Regulation of low affinity neurotrophin receptor (p75(NTR)) by early growth response (Egr) transcriptional regulators. *Molecular and cellular neurosciences,* 36**,** 501-514.

GARBAY, B., HEAPE, A. M., SARGUEIL, F. & CASSAGNE, C. 2000. Myelin synthesis in the peripheral nervous system. *Progress in Neurobiology,* 61**,** 267-304.

GARG, S., ORAN, A. E., HON, H. & JACOB, J. 2004. The Hybrid Cytomegalovirus Enhancer/Chicken β-Actin Promoter along with Woodchuck Hepatitis Virus Posttranscriptional Regulatory Element Enhances the Protective Efficacy of DNA Vaccines. *The Journal of Immunology,* 173**,** 550-558.

GARRATT, A. N., VOICULESCU, O., TOPILKO, P., CHARNAY, P. & BIRCHMEIER, C. 2000. A Dual Role of erbB2 in Myelination and in Expansion of the Schwann Cell Precursor Pool. *The Journal of Cell Biology,* 148**,** 1035-1046.

GAUDET, A. D., POPOVICH, P. G. & RAMER, M. S. 2011. Wallerian degeneration: gaining perspective on inflammatory events after peripheral nerve injury. *Journal of Neuroinflammation,* 8**,** 110-110.

GE, B., GRAM, H., DI PADOVA, F., HUANG, B., NEW, L., ULEVITCH, R. J., LUO, Y. & HAN, J. 2002. MAPKK-Independent Activation of p38α Mediated by TAB1-Dependent Autophosphorylation of p38α. *Science,* 295**,** 1291-1294.

GEMIGNANI, F., MELLI, G., ALFIERI, S., INGLESE, C. & MARBINI, A. 2004. Sensory manifestations in Charcot-Marie-Tooth disease. *Journal of the Peripheral Nervous System,* 9**,** 7-14.

GESS, B., HALFTER, H., KLEFFNER, I., MONJE, P., ATHAUDA, G., WOOD, P. M., YOUNG, P. & WANNER, I. B. 2008. Inhibition of N-cadherin and β-catenin function reduces axon-induced Schwann cell proliferation. *Journal of Neuroscience Research,* 86**,** 797-812.

GHISLAIN, J. & CHARNAY, P. 2006. Control of myelination in Schwann cells: a Krox20 cis-regulatory element integrates Oct6, Brn2 and Sox10 activities. *EMBO Rep,* 7**,** 52-8.

GIESE, K. P., MARTINI, R., LEMKE, G., SORIANO, P. & SCHACHNER, M. 1992. Mouse P0 gene disruption leads to hypomyelination, abnormal expression of recognition molecules, and degeneration of myelin and axons. *Cell,* 71**,** 565-576.

GILLESPIE, C. S., SHERMAN, D. L., BLAIR, G. E. & BROPHY, P. J. 1994. Periaxin, a novel protein of myelinating schwann cells with a possible role in axonal ensheathment. *Neuron,* 12**,** 497-508.

GILLESPIE, C. S., SHERMAN, D. L., FLEETWOOD-WALKER, S. M., COTTRELL, D. F., TAIT, S., GARRY, E. M., WALLACE, V. C. J., URE, J., GRIFFITHS, I. R., SMITH, A. & BROPHY, P. J. 2000. Peripheral Demyelination and Neuropathic Pain Behavior in Periaxin-Deficient Mice. *Neuron,* 26**,** 523-531.

GODL, K., WISSING, J., KURTENBACH, A., HABENBERGER, P., BLENCKE, S., GUTBROD, H., SALASSIDIS, K., STEIN-GERLACH, M., MISSIO, A., COTTEN, M. & DAUB, H. 2003. An efficient proteomics method to identify the cellular targets of protein kinase inhibitors. *Proceedings of the National Academy of Sciences of the United States of America,* 100**,** 15434-15439.

GOEBBELS, S., OLTROGGE, J. H., WOLFER, S., WIESER, G. L., NIENTIEDT, T., PIEPER, A., RUHWEDEL, T., GROSZER, M., SEREDA, M. W. & NAVE, K.-A. 2012. Genetic disruption of Pten in a novel mouse model of tomaculous neuropathy. *EMBO Molecular Medicine,* 4**,** 486-499.

GOLAN, N., KARTVELISHVILY, E., SPIEGEL, I., SALOMON, D., SABANAY, H., RECHAV, K., VAINSHTEIN, A., FRECHTER, S., MAIK-RACHLINE, G., ESHED-EISENBACH, Y., MOMOI, T. & PELES, E. 2013. Genetic Deletion of Cadm4 Results in Myelin Abnormalities Resembling Charcot-Marie-Tooth Neuropathy. *The Journal of Neuroscience,* 33**,** 10950-10961.

GOMEZ-SANCHEZ, J. A., CARTY, L., IRUARRIZAGA-LEJARRETA, M., PALOMO-IRIGOYEN, M., VARELA-REY, M., GRIFFITH, M., HANTKE, J., MACIAS-CAMARA, N., AZKARGORTA, M., AURREKOETXEA, I., DE JUAN, V. G., JEFFERIES, H. B. J., ASPICHUETA, P., ELORTZA, F., ARANSAY, A. M., MARTÍNEZ-CHANTAR, M. L., BAAS, F., MATO, J. M., MIRSKY, R., WOODHOO, A. & JESSEN, K. R. 2015. Schwann cell autophagy, myelinophagy, initiates myelin clearance from injured nerves. *The Journal of Cell Biology,* 210**,** 153-168.

GOSSEN, M. & BUJARD, H. 1992. Tight control of gene expression in mammalian cells by tetracycline-responsive promoters. *Proceedings of the National Academy of Sciences,* 89**,** 5547-5551.

GROH, J., HEINL, K., KOHL, B., WESSIG, C., GREESKE, J., FISCHER, S. & MARTINI, R. 2010. Attenuation of MCP-1/CCL2 expression ameliorates neuropathy in a mouse model for Charcot–Marie–Tooth 1X. *Human Molecular Genetics,* 19**,** 3530-3543.

GROH, J., KLEIN, I., HOLLMANN, C., WETTMARSHAUSEN, J., KLEIN, D. & MARTINI, R. 2015. CSF-1-activated macrophages are target-directed and essential mediators of schwann cell dedifferentiation and dysfunction in Cx32-deficient mice. *Glia,* 63**,** 977-986.

GROH, J., WEIS, J., ZIEGER, H., STANLEY, E. R., HEUER, H. & MARTINI, R. 2012. Colony-stimulating factor-1 mediates macrophage-related neural damage in a model for Charcot–Marie–Tooth disease type 1X. *Brain,* 135**,** 88-104.

GU, R. P., FU, L. L., JIANG, C. H., XU, Y. F., WANG, X. & YU, J. 2015. Retina Is Protected by Neuroserpin from Ischemic/Reperfusion-Induced Injury Independent of Tissue-Type Plasminogen Activator. *PLoS ONE,* 10**,** e0130440.

GUO, L., MOON, C., NIEHAUS, K., ZHENG, Y. & RATNER, N. 2012. Rac1 Controls Schwann Cell Myelination through cAMP and NF2/merlin. *The Journal of Neuroscience,* 32**,** 17251-17261.

GUO, L., MOON, C., ZHENG, Y. & RATNER, N. 2013. Cdc42 Regulates Schwann Cell Radial Sorting and Myelin Sheath Folding Through NF2/Merlin-Dependent and Independent Signaling. *Glia,* 61**,** 1906-1921.

HAINES, J. D., FRAGOSO, G., HOSSAIN, S., MUSHYNSKI, W. E. & ALMAZAN, G. 2008. p38 Mitogen-activated protein kinase regulates myelination. *J Mol Neurosci,* 35**,** 23-33.

HALL, S. 2005. The response to injury in the peripheral nervous system. *Journal of Bone & Joint Surgery, British Volume,* 87-B**,** 1309-1319.

HANEMANN, C. O. 2008. Magic but treatable? Tumours due to loss of Merlin. *Brain,* 131**,** 606-615.

HANTKE, J., CARTY, L., WAGSTAFF, L. J., TURMAINE, M., WILTON, D. K., QUINTES, S., KOLTZENBURG, M., BAAS, F., MIRSKY, R. & JESSEN, K. R. 2014. c-Jun activation in Schwann cells protects against loss of sensory axons in inherited neuropathy. *Brain,* 137**,** 2922-2937.

HARRISINGH, M. C., PEREZ-NADALES, E., PARKINSON, D. B., MALCOLM, D. S., MUDGE, A. W. & LLOYD, A. C. 2004. The Ras/Raf/ERK signalling pathway drives Schwann cell dedifferentiation. *The EMBO Journal,* 23**,** 3061-3071.

HE, T.-C., ZHOU, S., DA COSTA, L. T., YU, J., KINZLER, K. W. & VOGELSTEIN, B. 1998. A simplified system for generating recombinant adenoviruses. *Proceedings of the National Academy of Sciences of the United States of America,* 95**,** 2509-2514.

HE, Y., KIM, J. Y., DUPREE, J., TEWARI, A., MELENDEZ-VASQUEZ, C., SVAREN, J. & CASACCIA, P. 2010. Yy1 as a molecular link between neuregulin and transcriptional modulation of peripheral myelination. *Nat Neurosci,* 13**,** 1472-1480.

HEINRICHSDORFF, J., LUEDDE, T., PERDIGUERO, E., NEBREDA, A. R. & PASPARAKIS, M. 2008. p38α MAPK inhibits JNK activation and collaborates with IκB kinase 2 to prevent endotoxin-induced liver failure. *EMBO Reports,* 9**,** 1048-1054.

HERLAAR, E. & BROWN, Z. 1999. p38 MAPK signalling cascades in inflammatory disease. *Molecular Medicine Today,* 5**,** 439-447.

HERREROS-VILLANUEVA, M., ZHANG, J. S., KOENIG, A., ABEL, E. V., SMYRK, T. C., BAMLET, W. R., DE NARVAJAS, A. A. M., GOMEZ, T. S., SIMEONE, D. M., BUJANDA, L. & BILLADEAU, D. D. 2013. SOX2 promotes dedifferentiation and imparts stem cell-like features to pancreatic cancer cells. *Oncogenesis,* 2**,** e61.

HILTON, D. A. & HANEMANN, C. O. 2014. Schwannomas and Their Pathogenesis. *Brain Pathology,* 24**,** 205-220.

HOFFMANN, S. A., HOS, D., KÜSPERT, M., LANG, R. A., LOVELL-BADGE, R., WEGNER, M. & REIPRICH, S. 2014. Stem cell factor Sox2 and its close relative Sox3 have differentiation functions in oligodendrocytes. *Development (Cambridge, England),* 141**,** 39-50.

HORIUCHI, K., ZHOU, H.-M., KELLY, K., MANOVA, K. & BLOBEL, C. P. 2005. Evaluation of the contributions of ADAMs 9, 12, 15, 17, and 19 to heart development and ectodomain shedding of neuregulins β1 and β2. *Developmental Biology,* 283**,** 459-471.

HOSSAIN, S., DE LA CRUZ-MORCILLO, M. A., SANCHEZ-PRIETO, R. & ALMAZAN, G. 2012. Mitogen-activated protein kinase p38 regulates Krox-20 to direct Schwann cell differentiation and peripheral myelination. *Glia,* 60**,** 1130-44.

HUANG, Y. Y., BACH, M. E., LIPP, H. P., ZHUO, M., WOLFER, D. P., HAWKINS, R. D., SCHOONJANS, L., KANDEL, E. R., GODFRAIND, J. M., MULLIGAN, R., COLLEN, D. & CARMELIET, P. 1996. Mice lacking the gene encoding tissue-type plasminogen activator show a selective interference with late-phase long-term potentiation in both Schaffer collateral and mossy fiber pathways. *Proceedings of the National Academy of Sciences of the United States of America,* 93**,** 8699-8704.

HUEBNER, E. A. & STRITTMATTER, S. M. 2009. Axon Regeneration in the Peripheral and Central Nervous Systems. *Results and problems in cell differentiation,* 48**,** 339-351.

HUNTINGTON, J. A., READ, R. J. & CARRELL, R. W. 2000. Structure of a serpin-protease complex shows inhibition by deformation. *Nature,* 407**,** 923-926.

HUTTON, E. J., CARTY, L., LAURÁ, M., HOULDEN, H., LUNN, M. P. T., BRANDNER, S., MIRSKY, R., JESSEN, K. & REILLY, M. M. 2011. c-Jun

expression in human neuropathies: a pilot study. *Journal of the Peripheral Nervous System,* 16**,** 295-303.

IP, C. W., KRONER, A., BENDSZUS, M., LEDER, C., KOBSAR, I., FISCHER, S., WIENDL, H., NAVE, K.-A. & MARTINI, R. 2006. Immune Cells Contribute to Myelin Degeneration and Axonopathic Changes in Mice Overexpressing Proteolipid Protein in Oligodendrocytes. *The Journal of Neuroscience,* 26**,** 8206-8216.

ITO, Y., WIESE, S., FUNK, N., CHITTKA, A., ROSSOLL, W., BÖMMEL, H., WATABE, K., WEGNER, M. & SENDTNER, M. 2006. Sox10 regulates ciliary neurotrophic factor gene expression in Schwann cells. *Proceedings of the National Academy of Sciences of the United States of America,* 103**,** 7871-7876.

IVANOV, D. B., PHILIPPOVA, M. P. & TKACHUK, V. A. 2001. Structure and Functions of Classical Cadherins. *Biochemistry (Moscow),* 66**,** 1174-1186.

JACOB, C. 2015. Transcriptional control of neural crest specification into peripheral glia. *Glia,* 63**,** 1883-1896.

JACOB, C., LÖTSCHER, P., ENGLER, S., BAGGIOLINI, A., VARUM TAVARES, S., BRÜGGER, V., JOHN, N., BÜCHMANN-MØLLER, S., SNIDER, P. L., CONWAY, S. J., YAMAGUCHI, T., MATTHIAS, P., SOMMER, L., MANTEI, N. & SUTER, U. 2014. HDAC1 and HDAC2 Control the Specification of Neural Crest Cells into Peripheral Glia. *The Journal of Neuroscience,* 34**,** 6112-6122.

JAEGLE, M., GHAZVINI, M., MANDEMAKERS, W., PIIRSOO, M., DRIEGEN, S., LEVAVASSEUR, F., RAGHOENATH, S., GROSVELD, F. & MEIJER, D. 2003. The POU proteins Brn-2 and Oct-6 share important functions in Schwann cell development. *Genes & Development,* 17**,** 1380-1391.

JAEGLE, M., MANDEMAKERS, W., BROOS, L., ZWART, R., KARIS, A., VISSER, P., GROSVELD, F. & MEIJER, D. 1996. The POU Factor Oct-6 and Schwann Cell Differentiation. *Science,* 273**,** 507-510.

JAGALUR, N. B., GHAZVINI, M., MANDEMAKERS, W., DRIEGEN, S., MAAS, A., JONES, E. A., JAEGLE, M., GROSVELD, F., SVAREN, J. & MEIJER, D. 2011. Functional dissection of the Oct6 Schwann cell enhancer reveals an essential role for dimeric Sox10 binding. *J Neurosci,* 31**,** 8585-94.

JANG, S.-W., LEBLANC, S. E., ROOPRA, A., WRABETZ, L. & SVAREN, J. 2006. In vivo detection of Egr2 binding to target genes during peripheral nerve myelination. *Journal of Neurochemistry,* 98**,** 1678-1687.

JANI-ACSADI, A., KRAJEWSKI, K. & SHY, M. E. 2008. Charcot-Marie-Tooth Neuropathies: Diagnosis and Management. *Semin Neurol,* 28**,** 185-194.

JESSEN, K., MIRSKY, R. & ARTHUR-FARRAJ, P. 2015. The Role of Cell Plasticity in Tissue Repair: Adaptive Cellular Reprogramming. *Developmental Cell,* 34**,** 613-620.

JESSEN, K. R. 2004. Glial cells. *The International Journal of Biochemistry & Cell Biology,* 36**,** 1861-1867.

JESSEN, K. R., BRENNAN, A., MORGAN, L., MIRSKY, R., KENT, A., HASHIMOTO, Y. & GAVRILOVIC, J. 1994. The schwann cell precursor and its fate: A study of cell death and differentiation during gliogenesis in rat embryonic nerves. *Neuron,* 12**,** 509-527.

JESSEN, K. R. & MIRSKY, R. 2005. The origin and development of glial cells in peripheral nerves. *Nat Rev Neurosci,* 6**,** 671-682.

JESSEN, K. R. & MIRSKY, R. 2008. Negative regulation of myelination: Relevance for development, injury, and demyelinating disease. *Glia,* 56**,** 1552-1565.

JONES, E. A., LOPEZ-ANIDO, C., SRINIVASAN, R., KRUEGER, C., CHANG, L.-W., NAGARAJAN, R. & SVAREN, J. 2011. Regulation of the PMP22 gene through an intronic enhancer. *The Journal of neuroscience : the official journal of the Society for Neuroscience,* 31**,** 4242-4250.

JOUHILAHTI, E.-M., PELTONEN, S., HEAPE, A. M. & PELTONEN, J. 2011. The Pathoetiology of Neurofibromatosis 1. *The American Journal of Pathology,* 178**,** 1932-1939.

JUN-ICHI, M., SATOSHI, T., KIMI, A., FUMI, T., AKIRA, T., KIYOSHI, T. & KEN-ICHI, Y. 1989. Expression vector system based on the chicken β-actin promoter directs efficient production of interleukin-5. *Gene,* 79**,** 269-277.

KALAYDJIEVA, L., GRESHAM, D., GOODING, R., HEATHER, L., BAAS, F., DE JONGE, R., BLECHSCHMIDT, K., ANGELICHEVA, D., CHANDLER, D., WORSLEY, P., ROSENTHAL, A., KING, R. H. M. & THOMAS, P. K. 2000. N-myc Downstream-Regulated Gene 1 Is Mutated in Hereditary Motor and Sensory Neuropathy–Lom. *American Journal of Human Genetics,* 67**,** 47-58.

KAMACHI, Y. & KONDOH, H. 2013. Sox proteins: regulators of cell fate specification and differentiation. *Development,* 140**,** 4129-4144.

KAO, S.-C., WU, H., XIE, J., CHANG, C.-P., RANISH, J. A., GRAEF, I. A. & CRABTREE, G. R. 2009. Calcineurin/NFAT Signaling Is Required for Neuregulin-Regulated Schwann Cell Differentiation. *Science (New York, N.Y.),* 323**,** 651-654.

KATO, N., MATSUMOTO, M., KOGAWA, M., ATKINS, G. J., FINDLAY, D. M., FUJIKAWA, T., ODA, H. & OGATA, M. 2013. Critical role of p38 MAPK for regeneration of the sciatic nerve following crush injury in vivo. *Journal of Neuroinflammation,* 10**,** 1-1.

KAUR, J., ZHAO, Z., KLEIN, G. M., LO, E. H. & BUCHAN, A. M. 2004. The Neurotoxicity of Tissue Plasminogen Activator[quest]. *J Cereb Blood Flow Metab,* 24**,** 945-963.

KIEFER, R., KIESEIER, B. C., STOLL, G. & HARTUNG, H.-P. 2001. The role of macrophages in immune-mediated damage to the peripheral nervous system. *Progress in Neurobiology,* 64**,** 109-127.

KINTER, J., LAZZATI, T., SCHMID, D., ZEIS, T., ERNE, B., LÜTZELSCHWAB, R., STECK, A. J., PAREYSON, D., PELES, E. & SCHAEREN-WIEMERS, N. 2013. An essential role of MAG in mediating axon-myelin attachment in Charcot-Marie-Tooth 1A disease. *Neurobiology of disease,* 0**,** 221-231.

KIOUSSI, C., GROSS, M. K. & GRUSS, P. 1995. Pax3: A paired domain gene as a regulator in PNS myelination. *Neuron,* 15**,** 553-562.

KIPANYULA, M. J., WOODHOO, A., RAHMAN, M., PAYNE, D., JESSEN, K. R. & MIRSKY, R. 2013. Calcineurin–nuclear factor of activated t cells regulation of Krox-20 expression in Schwann cells requires elevation of intracellular cyclic AMP. *Journal of Neuroscience Research,* 91**,** 105-115.

KLEIN, D., PATZKÓ, Á., SCHREIBER, D., VAN HAUWERMEIREN, A., BAIER, M., GROH, J., WEST, B. L. & MARTINI, R. 2015. Targeting the colony stimulating factor 1 receptor alleviates two forms of Charcot–Marie–Tooth disease in mice. *Brain*.

KOBSAR, I., BERGHOFF, M., SAMSAM, M., WESSIG, C., MÄURER, M., TOYKA, K. V. & MARTINI, R. 2003. Preserved myelin integrity and reduced axonopathy in connexin32-deficient mice lacking the recombination activating gene-1. *Brain,* 126**,** 804-813.

KOBSAR, I., HASENPUSCH-THEIL, K., WESSIG, C., MÜLLER, H. W. & MARTINI, R. 2005. Evidence for macrophage-mediated myelin disruption in an animal model for Charcot-Marie-Tooth neuropathy type 1A. *Journal of Neuroscience Research,* 81**,** 857-864.

KOHL, B., FISCHER, S., GROH, J., WESSIG, C. & MARTINI, R. 2010a. MCP-1/CCL2 Modifies Axon Properties in a PMP22-Overexpressing Mouse Model for Charcot-Marie-Tooth 1A Neuropathy. *The American Journal of Pathology,* 176**,** 1390-1399.

KOHL, B., GROH, J., WESSIG, C., WIENDL, H., KRONER, A. & MARTINI, R. 2010b. Lack of evidence for a pathogenic role of T-lymphocytes in an animal model for Charcot-Marie-Tooth disease 1A. *Neurobiology of Disease,* 38**,** 78-84.

KONDO, T. & RAFF, M. 2004. Chromatin remodeling and histone modification in the conversion of oligodendrocyte precursors to neural stem cells. *Genes & Development,* 18**,** 2963-2972.

KRISHNAN, A. 2013. Neuregulin-1 Type I: A Hidden Power Within Schwann Cells for Triggering Peripheral Nerve Remyelination. *Science Signaling,* 6**,** jc1-jc1.

KRUEGER, S. R., GHISU, G.-P., CINELLI, P., GSCHWEND, T. P., OSTERWALDER, T., WOLFER, D. P. & SONDEREGGER, P. 1997. Expression of Neuroserpin, an Inhibitor of Tissue Plasminogen Activator, in the Developing and Adult Nervous System of the Mouse. *The Journal of Neuroscience,* 17**,** 8984-8996.

KUHLBRODT, K., HERBARTH, B., SOCK, E., HERMANS-BORGMEYER, I. & WEGNER, M. 1998. Sox10, a Novel Transcriptional Modulator in Glial Cells. *The Journal of Neuroscience,* 18**,** 237-250.

KUHLMANN, T., BITSCH, A., STADELMANN, C., SIEBERT, H. & BRÜCK, W. 2001. Macrophages Are Eliminated from the Injured Peripheral Nerve via Local Apoptosis and Circulation to Regional Lymph Nodes and the Spleen. *The Journal of Neuroscience,* 21**,** 3401-3408.

KÜSPERT, M., WEIDER, M., MÜLLER, J., HERMANS-BORGMEYER, I., MEIJER, D. & WEGNER, M. 2012. Desert Hedgehog Links Transcription Factor Sox10 to Perineurial Development. *The Journal of Neuroscience,* 32**,** 5472-5480.

LE, N., NAGARAJAN, R., WANG, J. Y. T., ARAKI, T., SCHMIDT, R. E. & MILBRANDT, J. 2005a. Analysis of congenital hypomyelinating Egr2(Lo/Lo) nerves identifies Sox2 as an inhibitor of Schwann cell differentiation and myelination. *Proceedings of the National Academy of Sciences of the United States of America,* 102**,** 2596-2601.

LE, N., NAGARAJAN, R., WANG, J. Y. T., SVAREN, J., LAPASH, C., ARAKI, T., SCHMIDT, R. E. & MILBRANDT, J. 2005b. Nab proteins are essential for peripheral nervous system myelination. *Nat Neurosci,* 8**,** 932-940.

LEBLANC, S. E., JANG, S.-W., WARD, R. M., WRABETZ, L. & SVAREN, J. 2006. Direct Regulation of Myelin Protein Zero Expression by the Egr2 Transactivator. *Journal of Biological Chemistry,* 281**,** 5453-5460.

LEBLANC, S. E., SRINIVASAN, R., FERRI, C., MAGER, G. M., GILLIAN-DANIEL, A. L., WRABETZ, L. & SVAREN, J. 2005. Regulation of cholesterol/lipid biosynthetic genes by Egr2/Krox20 during peripheral nerve myelination. *Journal of Neurochemistry,* 93**,** 737-748.

LEE, M. J., BRENNAN, A., BLANCHARD, A., ZOIDL, G., DONG, Z., TABERNERO, A., ZOIDL, C., DENT, M. A. R., JESSEN, K. R. & MIRSKY, R. 1997. P0Is Constitutively Expressed in the Rat Neural Crest and Embryonic Nerves and

Is Negatively and Positively Regulated by Axons to Generate Non-Myelin-Forming and Myelin-Forming Schwann Cells, Respectively. *Molecular and Cellular Neuroscience,* 8**,** 336-350.

LEE, T. W., COATES, L. C. & BIRCH, N. P. 2008. Neuroserpin regulates N-cadherin-mediated cell adhesion independently of its activity as an inhibitor of tissue plasminogen activator. *Journal of Neuroscience Research,* 86**,** 1243-1253.

LEWALLEN, K. A., SHEN, Y.-A. A., DE LA TORRE, A. R., NG, B. K., MEIJER, D. & CHAN, J. R. 2011. Assessing the Role of the Cadherin/Catenin Complex at the Schwann Cell–Axon Interface and in the Initiation of Myelination. *The Journal of Neuroscience,* 31**,** 3032-3043.

LI, C., TROPAK, M. B., GERLAI, R., CLAPOFF, S., ABRAMOW-NEWERLY, W., TRAPP, B., PETERSON, A. & RODER, J. 1994. Myelination in the absence of myelin-associated glycoprotein. *Nature,* 369**,** 747-750.

LI, H., COLLADO, M., VILLASANTE, A., MATHEU, A., LYNCH, C. J., CANAMERO, M., RIZZOTI, K., CARNEIRO, C., MARTINEZ, G., VIDAL, A., LOVELL-BADGE, R. & SERRANO, M. 2012. p27(Kip1) directly represses Sox2 during embryonic stem cell differentiation. *Cell Stem Cell,* 11**,** 845-52.

LINDEBOOM, F., GILLEMANS, N., KARIS, A., JAEGLE, M., MEIJER, D., GROSVELD, F. & PHILIPSEN, S. 2003. A tissue-specific knockout reveals that Gata1 is not essential for Sertoli cell function in the mouse. *Nucleic Acids Research,* 31**,** 5405-5412.

LINDSLEY, A., SNIDER, P., ZHOU, H., ROGERS, R., WANG, J., OLAOPA, M., KRUZYNSKA-FREJTAG, A., KOUSHIK, S. V., LILLY, B., BURCH, J. B. E., FIRULLI, A. B. & CONWAY, S. J. 2007. Identification and characterization of a novel Schwann and outflow tract endocardial cushion lineage-restricted periostin enhancer. *Developmental biology,* 307**,** 340-355.

LITTLEWOOD, T. D., HANCOCK, D. C., DANIELIAN, P. S., PARKER, M. G. & EVAN, G. I. 1995. A modified oestrogen receptor ligand-binding domain as an improved switch for the regulation of heterologous proteins. *Nucleic Acids Research,* 23**,** 1686-1690.

LIU, T., VAN ROOIJEN, N. & TRACEY, D. J. 2000. Depletion of macrophages reduces axonal degeneration and hyperalgesia following nerve injury. *Pain,* 86**,** 25-32.

LU, Y., FUTTNER, C., ROCK, J. R., XU, X., WHITWORTH, W., HOGAN, B. L. & ONAITIS, M. W. 2010a. Evidence that SOX2 overexpression is oncogenic in the lung. *PLoS One,* 5**,** e11022.

LU, Y., FUTTNER, C., ROCK, J. R., XU, X., WHITWORTH, W., HOGAN, B. L. M. & ONAITIS, M. W. 2010b. Evidence That SOX2 Overexpression Is Oncogenic in the Lung. *PLoS ONE,* 5**,** e11022.

MAGER, G. M., WARD, R. M., SRINIVASAN, R., JANG, S.-W., WRABETZ, L. & SVAREN, J. 2008. Active Gene Repression by the Egr2·NAB Complex during Peripheral Nerve Myelination. *The Journal of Biological Chemistry,* 283**,** 18187-18197.

MAGYAR, J. P., MARTINI, R., RUELICKE, T., AGUZZI, A., ADLKOFER, K., DEMBIC, Z., ZIELASEK, J., TOYKA, K. V. & SUTER, U. 1996. Impaired Differentiation of Schwann Cells in Transgenic Mice with Increased PMP22 Gene Dosage. *The Journal of Neuroscience,* 16**,** 5351-5360.

MARTINI, R., FISCHER, S., LÓPEZ-VALES, R. & DAVID, S. 2008. Interactions between Schwann cells and macrophages in injury and inherited demyelinating disease. *Glia,* 56**,** 1566-1577.

MARTINI, R., KLEIN, D. & GROH, J. 2013. Similarities between Inherited Demyelinating Neuropathies and Wallerian Degeneration: An Old Repair Program May Cause Myelin and Axon Perturbation under Nonlesion Conditions. *The American Journal of Pathology,* 183**,** 655-660.

MARTINI, R., MOHAJERI, M., KASPER, S., GIESE, K. & SCHACHNER, M. 1995. Mice doubly deficient in the genes for P0 and myelin basic protein show that both proteins contribute to the formation of the major dense line in peripheral nerve myelin. *The Journal of Neuroscience,* 15**,** 4488-4495.

MARTINI, R. & WILLISON, H. 2015. Neuroinflammation in the peripheral nerve: Cause, modulator, or bystander in peripheral neuropathies? *Glia***,** n/a-n/a.

MAUREL, P., EINHEBER, S., GALINSKA, J., THAKER, P., LAM, I., RUBIN, M. B., SCHERER, S. S., MURAKAMI, Y., GUTMANN, D. H. & SALZER, J. L. 2007. Nectin-like proteins mediate axon–Schwann cell interactions along the internode and are essential for myelination. *The Journal of Cell Biology,* 178**,** 861-874.

MAUREL, P. & SALZER, J. L. 2000. Axonal Regulation of Schwann Cell Proliferation and Survival and the Initial Events of Myelination Requires PI 3-Kinase Activity. *The Journal of Neuroscience,* 20**,** 4635-4645.

MÄURER, M., KOBSAR, I., BERGHOFF, M., SCHMID, C. D., CARENINI, S. & MARTINI, R. 2002. Role of immune cells in animal models for inherited neuropathies: facts and visions. *Journal of Anatomy,* 200**,** 405-414.

MAYOR, J. F., JURADO-PUEYO, M., CAMPOS, P. M. & MURGA, C. 2007. Interfering with MAP Kinase Docking Interactions: Implications and Perspectives for the p38 Route. *Cell Cycle,* 6**,** 528-533.

MCKERRACHER, L., DAVID, S., JACKSON, D. L., KOTTIS, V., DUNN, R. J. & BRAUN, P. E. 1994. Identification of myelin-associated glycoprotein as a major myelin-derived inhibitor of neurite growth. *Neuron,* 13**,** 805-811.

MEIER, C., PARMANTIER, E., BRENNAN, A., MIRSKY, R. & JESSEN, K. R. 1999. Developing Schwann Cells Acquire the Ability to Survive without Axons by Establishing an Autocrine Circuit Involving Insulin-Like Growth Factor, Neurotrophin-3, and Platelet-Derived Growth Factor-BB. *The Journal of Neuroscience,* 19**,** 3847-3859.

MEIRI, N., MASOS, T., ROSENBLUM, K., MISKIN, R. & DUDAI, Y. 1994. Overexpression of urokinase-type plasminogen activator in transgenic mice is correlated with impaired learning. *Proceedings of the National Academy of Sciences of the United States of America,* 91**,** 3196-3200.

MENG, W. & TAKEICHI, M. 2009. Adherens Junction: Molecular Architecture and Regulation. *Cold Spring Harbor Perspectives in Biology,* 1**,** a002899.

MERTIN, S., MCDOWALL, S. G. & HARLEY, V. R. 1999. The DNA-binding specificity of SOX9 and other SOX proteins. *Nucleic Acids Research,* 27**,** 1359-1364.

MICHAILOV, G. V., SEREDA, M. W., BRINKMANN, B. G., FISCHER, T. M., HAUG, B., BIRCHMEIER, C., ROLE, L., LAI, C., SCHWAB, M. H. & NAVE, K.-A. 2004. Axonal Neuregulin-1 Regulates Myelin Sheath Thickness. *Science,* 304**,** 700-703.

MIRSKY, R. & JESSEN, K. R. 1999. The Neurobiology of Schwann Cells. *Brain Pathology,* 9**,** 293-311.

MIRSKY, R., JESSEN, K. R., BRENNAN, A., PARKINSON, D., DONG, Z., MEIER, C., PARMANTIER, E. & LAWSON, D. 2002. Schwann cells as regulators of nerve development. *Journal of Physiology-Paris,* 96**,** 17-24.

MIRSKY, R., WOODHOO, A., PARKINSON, D. B., ARTHUR-FARRAJ, P., BHASKARAN, A. & JESSEN, K. R. 2008. Novel signals controlling embryonic Schwann cell development, myelination and dedifferentiation. *Journal of the Peripheral Nervous System,* 13**,** 122-135.

MOGHA, A., BENESH, A. E., PATRA, C., ENGEL, F. B., SCHÖNEBERG, T., LIEBSCHER, I. & MONK, K. R. 2013. Gpr126 Functions in Schwann Cells to Control Differentiation and Myelination via G-Protein Activation. *The Journal of Neuroscience,* 33**,** 17976-17985.

MONK, K. R., FELTRI, M. L. & TAVEGGIA, C. 2015. New insights on schwann cell development. *Glia*, 63**,** 1376-93

MONK, K. R., NAYLOR, S. G., GLENN, T. D., MERCURIO, S., PERLIN, J. R., DOMINGUEZ, C., MOENS, C. B. & TALBOT, W. S. 2009. A G Protein-Coupled Receptor is Essential for Schwann Cells to Initiate Myelination. *Science (New York, N.Y.),* 325**,** 1402-1405.

MONK, K. R., OSHIMA, K., JÖRS, S., HELLER, S. & TALBOT, W. S. 2011. Gpr126 is essential for peripheral nerve development and myelination in mammals. *Development (Cambridge, England),* 138**,** 2673-2680.

MONTAG, D., GIESE, K. P., BARTSCH, U., MARTINI, R., LANG, Y., BLÜTHMANN, H., KARTHIGASAN, J., KIRSCHNER, D. A., WINTERGERST, E. S., NAVE, K.-A., ZIELASEK, J., TOYKA, K. V., LIPP, H.-P. & SCHACHNER, M. 1994. Mice deficient for the glycoprotein show subtle abnormalities in myelin. *Neuron,* 13**,** 229-246.

MYERS, R. R., SEKIGUCHI, Y., KIKUCHI, S., SCOTT, B., MEDICHERLA, S., PROTTER, A. & CAMPANA, W. M. 2003. Inhibition of p38 MAP kinase activity enhances axonal regeneration. *Experimental Neurology,* 184**,** 606-614.

NADEAU, S., FILALI, M., ZHANG, J., KERR, B. J., RIVEST, S., SOULET, D., IWAKURA, Y., DE RIVERO VACCARI, J. P., KEANE, R. W. & LACROIX, S. 2011. Functional recovery after peripheral nerve injury is dependent on the pro-inflammatory cytokines IL-1beta and TNF: implications for neuropathic pain. *J Neurosci,* 31**,** 12533-42.

NADRA, K., DE PREUX CHARLES, A.-S., MÉDARD, J.-J., HENDRIKS, W. T., HAN, G.-S., GRÈS, S., CARMAN, G. M., SAULNIER-BLACHE, J.-S., VERHEIJEN, M. H. G. & CHRAST, R. 2008. Phosphatidic acid mediates demyelination in Lpin1 mutant mice. *Genes & Development,* 22**,** 1647-1661.

NAGARAJAN, R., SVAREN, J., LE, N., ARAKI, T., WATSON, M. & MILBRANDT, J. 2001. EGR2 Mutations in Inherited Neuropathies Dominant-Negatively Inhibit Myelin Gene Expression. *Neuron,* 30**,** 355-368.

NAPOLI, I., NOON, LUKE A., RIBEIRO, S., KERAI, AJAY P., PARRINELLO, S., ROSENBERG, LAURA H., COLLINS, MELISSA J., HARRISINGH, MARIE C., WHITE, IAN J., WOODHOO, A. & LLOYD, ALISON C. 2012. A Central Role for the ERK-Signaling Pathway in Controlling Schwann Cell Plasticity and Peripheral Nerve Regeneration In Vivo. *Neuron,* 73**,** 729-742.

NAVARRO, X., VIVÓ, M. & VALERO-CABRÉ, A. 2007. Neural plasticity after peripheral nerve injury and regeneration. *Progress in Neurobiology,* 82**,** 163-201.

NAVE, K.-A. & SALZER, J. L. 2006. Axonal regulation of myelination by neuregulin 1. *Current Opinion in Neurobiology,* 16**,** 492-500.

NEBREDA, A. R. & PORRAS, A. 2000. p38 MAP kinases: beyond the stress response. *Trends in Biochemical Sciences,* 25**,** 257-260.

NEWBERN, J. M., LI, X., SHOEMAKER, S. E., ZHOU, J., ZHONG, J., WU, Y., BONDER, D., HOLLENBACK, S., COPPOLA, G., GESCHWIND, D. H., LANDRETH, G. E. & SNIDER, W. D. 2011. Specific functions for ERK/MAPK signaling during PNS development. *Neuron,* 69**,** 91-105.

NODARI, A., ZAMBRONI, D., QUATTRINI, A., COURT, F. A., D'URSO, A., RECCHIA, A., TYBULEWICZ, V. L. J., WRABETZ, L. & FELTRI, M. L. 2007. β1 integrin activates Rac1 in Schwann cells to generate radial lamellae during axonal sorting and myelination. *The Journal of Cell Biology,* 177**,** 1063-1075.

NOTTERPEK, L., SNIPES, G. J. & SHOOTER, E. M. 1999. Temporal expression pattern of peripheral myelin protein 22 during in vivo and in vitro myelination. *Glia,* 25**,** 358-369.

O'DONNELL, M., HONG, C.-S., HUANG, X., DELNICKI, R. J. & SAINT-JEANNET, J.-P. 2006. Functional analysis of Sox8 during neural crest development in Xenopus. *Development,* 133**,** 3817-3826.

O'SHAUGHNESSY, J. & BUSSIÈRES, A. 2006. Subtle clinical signs of a spinal cord ependymoma at the cervicothoracic level in an adult: a case report. *The Journal of the Canadian Chiropractic Association,* 50**,** 244-248.

OGATA, T., IIJIMA, S., HOSHIKAWA, S., MIURA, T., YAMAMOTO, S.-I., ODA, H., NAKAMURA, K. & TANAKA, S. 2004. Opposing Extracellular Signal-Regulated Kinase and Akt Pathways Control Schwann Cell Myelination. *The Journal of Neuroscience,* 24**,** 6724-6732.

OKUDA, T., HIGASHI, Y., KOKAME, K., TANAKA, C., KONDOH, H. & MIYATA, T. 2004. Ndrg1-Deficient Mice Exhibit a Progressive Demyelinating Disorder of Peripheral Nerves. *Molecular and Cellular Biology,* 24**,** 3949-3956.

OSTERWALDER, T., CONTARTESE, J., STOECKLI, E. T., KUHN, T. B. & SONDEREGGER, P. 1996. Neuroserpin, an axonally secreted serine protease inhibitor. *The EMBO Journal,* 15**,** 2944-2953.

PAAVOLA, K. J., SIDIK, H., ZUCHERO, J. B., ECKART, M. & TALBOT, W. S. 2014. Type IV collagen is an activating ligand for the adhesion G protein-coupled receptor GPR126. *Science signaling,* 7**,** ra76-ra76.

PARKINSON, D. B., BHASKARAN, A., ARTHUR-FARRAJ, P., NOON, L. A., WOODHOO, A., LLOYD, A. C., FELTRI, M. L., WRABETZ, L., BEHRENS, A., MIRSKY, R. & JESSEN, K. R. 2008. c-Jun is a negative regulator of myelination. *J Cell Biol,* 181**,** 625-37.

PARKINSON, D. B., BHASKARAN, A., DROGGITI, A., DICKINSON, S., D'ANTONIO, M., MIRSKY, R. & JESSEN, K. R. 2004. Krox-20 inhibits Jun-NH(2)-terminal kinase/c-Jun to control Schwann cell proliferation and death. *The Journal of Cell Biology,* 164**,** 385-394.

PARKINSON, D. B., DONG, Z., BUNTING, H., WHITFIELD, J., MEIER, C., MARIE, H., MIRSKY, R. & JESSEN, K. R. 2001. Transforming growth factor beta (TGFbeta) mediates Schwann cell death in vitro and in vivo: examination of c-Jun activation, interactions with survival signals, and the relationship of TGFbeta-mediated death to Schwann cell differentiation. *The Journal of neuroscience : the official journal of the Society for Neuroscience,* 21**,** 8572-8585.

PARRINELLO, S., NAPOLI, I., RIBEIRO, S., DIGBY, P. W., FEDOROVA, M., PARKINSON, D. B., DODDRELL, R. D. S., NAKAYAMA, M., ADAMS, R. H. & LLOYD, A. C. 2010. EphB Signaling Directs Peripheral Nerve Regeneration through Sox2-Dependent Schwann Cell Sorting. *Cell,* 143**,** 145-155.

PATZKÓ, Á. & SHY, M. E. 2011. Update on Charcot-Marie-Tooth Disease. *Current neurology and neuroscience reports,* 11**,** 78-88.

PEIRANO, R. I., GOERICH, D. E., RIETHMACHER, D. & WEGNER, M. 2000. Protein Zero Gene Expression Is Regulated by the Glial Transcription Factor Sox10. *Molecular and Cellular Biology,* 2**0,** 3198-3209.

PEREIRA, J. A., BAUMANN, R., NORRMÉN, C., SOMANDIN, C., MIEHE, M., JACOB, C., LÜHMANN, T., HALL-BOZIC, H., MANTEI, N., MEIJER, D. & SUTER, U. 2010. Dicer in Schwann Cells Is Required for Myelination and Axonal Integrity. *The Journal of Neuroscience,* 30**,** 6763-6775.

PEREIRA, J. A., LEBRUN-JULIEN, F. & SUTER, U. 2012. Molecular mechanisms regulating myelination in the peripheral nervous system. *Trends in Neurosciences,* 35**,** 123-134.

PERRY, V. H., TSAO, J. W., FEAM, S. & BROWN, M. C. 1995. Radiation-induced Reductions in Macrophage Recruitment Have Only Slight Effects on Myelin Degeneration in Sectioned Peripheral Nerves of Mice. *European Journal of Neuroscience,* 7**,** 271-280.

PETERSEN, SARAH C., LUO, R., LIEBSCHER, I., GIERA, S., JEONG, S.-J., MOGHA, A., GHIDINELLI, M., FELTRI, M. L., SCHÖNEBERG, T., PIAO, X. & MONK, KELLY R. 2015. The Adhesion GPCR GPR126 Has Distinct, Domain-Dependent Functions in Schwann Cell Development Mediated by Interaction with Laminin-211. *Neuron,* 85**,** 755-769.

PODUSLO, J. F., BERG, C. T., ROSS, S. M. & SPENCER, P. S. 1985. Regulation of myelination: Axons not required for the biosynthesis of basal levels of the major myelin glycoprotein by schwann cells in denervated distal segments of the adult cat sciatic nerve. *Journal of Neuroscience Research,* 14**,** 177-185.

PODUSLO, J. F., WALIKONIS, R. S., DOMEC, M.-C., BERG, C. T. & HOLTZ-HEPPELMANN, C. J. 1995. The Second Messenger, Cyclic AMP, Is Not Sufficient for Myelin Gene Induction in the Peripheral Nervous System. *Journal of Neurochemistry,* 65**,** 149-159.

POITELON, Y., BOGNI, S., MATAFORA, V., DELLA-FLORA NUNES, G., HURLEY, E., GHIDINELLI, M., KATZENELLENBOGEN, B. S., TAVEGGIA, C., SILVESTRI, N., BACHI, A., SANNINO, A., WRABETZ, L. & FELTRI, M. L. 2015. Spatial mapping of juxtacrine axo-glial interactions identifies novel molecules in peripheral myelination. *Nat Commun,* 6.

POPOVICH, P. G., GUAN, Z., WEI, P., HUITINGA, I., VAN ROOIJEN, N. & STOKES, B. T. 1999. Depletion of Hematogenous Macrophages Promotes Partial Hindlimb Recovery and Neuroanatomical Repair after Experimental Spinal Cord Injury. *Experimental Neurology,* 158**,** 351-365.

PRASAD, M. K., REED, X., GORKIN, D. U., CRONIN, J. C., MCADOW, A. R., CHAIN, K., HODONSKY, C. J., JONES, E. A., SVAREN, J., ANTONELLIS, A., JOHNSON, S. L., LOFTUS, S. K., PAVAN, W. J. & MCCALLION, A. S. 2011. SOX10 directly modulates ERBB3 transcription via an intronic neural crest enhancer. *BMC Developmental Biology,* 11**,** 40-40.

PRIVAT, A., JACQUE, C., BOURRE, J. M., DUPOUEY, P. & BAUMANN, N. 1979. Absence of the major dense line in myelin of the mutant mouse 'shiverer'. *Neuroscience Letters,* 12**,** 107-112.

QUARLES, R. H. 2007. Myelin-associated glycoprotein (MAG): past, present and beyond. *Journal of Neurochemistry,* 100**,** 1431-1448.

QUARLES, R. H., MACKLIN, W. B. & MORELL, P. 2005. Myelin Formation, Structure and Biochemistry. *In:* BRADY, S., SIEGEL, G., ALBERS, R. W. & PRICE, D. (eds.) *Basic Neurochemistry: Molecular, Cellular and Medical Aspects.* Seventh ed. Academic Press: Elsevier.

RASBAND, M. N. & TRIMMER, J. S. 2001. Developmental Clustering of Ion Channels at and near the Node of Ranvier. *Developmental Biology,* 236**,** 5-16.

RASHID, Q., KAPIL, C., SINGH, P., KUMARI, V. & JAIRAJPURI, M. A. 2014. Understanding the specificity of serpin–protease complexes through interface analysis. *Journal of Biomolecular Structure and Dynamics,* 33**,** 1352-1362.

READHEAD, C. & HOOD, L. 1990. The dysmyelinating mouse mutations shiverer (shi) and myelin deficient (shi mld). *Behavior Genetics,* 20**,** 213-234.

REILLY, M. 2001. Charcot-Marie-Tooth disease. A practical guide. *Journal of Neurology, Neurosurgery & Psychiatry,* 71**,** 566.

REILLY, M. M. & SHY, M. E. 2009. Diagnosis and new treatments in genetic neuropathies. *Journal of Neurology, Neurosurgery & Psychiatry,* 80**,** 1304-1314.

REIPRICH, S., KRIESCH, J., SCHREINER, S. & WEGNER, M. 2010. Activation of Krox20 gene expression by Sox10 in myelinating Schwann cells. *J Neurochem,* 112**,** 744-54.

RESSOT, C. & BRUZZONE, R. 2000. Connexin channels in Schwann cells and the development of the X-linked form of Charcot-Marie-Tooth disease. *Brain Research Reviews,* 32**,** 192-202.

RIBEIRO, S., NAPOLI, I., WHITE, IAN J., PARRINELLO, S., FLANAGAN, ADRIENNE M., SUTER, U., PARADA, LUIS F. & LLOYD, ALISON C. 2013. Injury Signals Cooperate with Nf1 Loss to Relieve the Tumor-Suppressive Environment of Adult Peripheral Nerve. *Cell Reports,* 5**,** 126-136.

RISTOIU, V. 2013. Contribution of macrophages to peripheral neuropathic pain pathogenesis. *Life Sciences,* 93**,** 870-881.

ROACH, A., TAKAHASHI, N., PRAVTCHEVA, D., RUDDLE, F. & HOOD, L. 1985. Chromosomal mapping of mouse myelin basic protein gene and structure and transcription of the partially deleted gene in shiverer mutant mice. *Cell,* 42**,** 149-155.

ROCKHILL, J., MRUGALA, M. & CHAMBERLAIN, M. C. 2007. Intracranial meningiomas: an overview of diagnosis and treatment. *Neurosurgical Focus,* 23**,** E1.

ROTSHENKER, S. 2011. Wallerian degeneration: the innate-immune response to traumatic nerve injury. *Journal of Neuroinflammation,* 8**,** 109-109.

ROULEAU, G. A., MEREL, P., LUTCHMAN, M., SANSON, M., ZUCMAN, J., MARINEAU, C., HOANG-XUAN, K., DEMCZUK, S., DESMAZE, C., PLOUGASTEL, B., PULST, S. M., LENOIR, G., BIJLSMA, E., FASHOLD, R., DUMANSKI, J., JONG, P. D., PARRY, D., ELDRIGE, R., AURIAS, A., DELATTRE, O. & THOMAS, G. 1993. Alteration in a new gene encoding a putative membrane-organizing protein causes neuro-fibromatosis type 2. *Nature,* 363**,** 515-521.

ROUSSEL, B. D., IRVING, J. A., EKEOWA, U. I., BELORGEY, D., HAQ, I., ORDÓÑEZ, A., KRUPPA, A. J., DUVOIX, A., RASHID, S. T., CROWTHER, D. C., MARCINIAK, S. J. & LOMAS, D. A. 2011. Unravelling the twists and turns of the serpinopathies. *FEBS Journal,* 278**,** 3859-3867.

RUSNAK, F. & MERTZ, P. 2000. Calcineurin: Form and Function. *Physiological Reviews,* 80**,** 1483-1521.

RYU, E. J., WANG, J. Y. T., LE, N., BALOH, R. H., GUSTIN, J. A., SCHMIDT, R. E. & MILBRANDT, J. 2007. Misexpression of Pou3f1 Results in Peripheral Nerve Hypomyelination and Axonal Loss. *The Journal of Neuroscience,* 27**,** 11552-11559.

SALZER, J. L. 2008. Switching myelination on and off. *J Cell Biol,* 181**,** 575-7.

SALZER, J. L. 2012. Axonal regulation of Schwann cell ensheathment and myelination. *Journal of the peripheral nervous system : JPNS,* 17**,** 14-19.

SALZER, J. L., BROPHY, P. J. & PELES, E. 2008. Molecular domains of myelinated axons in the peripheral nervous system. *Glia,* 56**,** 1532-1540.

SAMANTA, J. & SALZER, J. L. 2015. Myelination: Actin Disassembly Leads the Way. *Developmental Cell,* 34**,** 129-130.

SAPORTA, M. A. C., SHY, B. R., PATZKO, A., BAI, Y., PENNUTO, M., FERRI, C., TINELLI, E., SAVERI, P., KIRSCHNER, D., CROWTHER, M., SOUTHWOOD, C., WU, X., GOW, A., FELTRI, M. L., WRABETZ, L. & SHY, M. E. 2012. MpzR98C arrests Schwann cell development in a mouse model of early-onset Charcot–Marie–Tooth disease type 1B. *Brain,* 135**,** 2032-2047.

SAUER, B. 1998. Inducible Gene Targeting in Mice Using the Cre/loxSystem. *Methods,* 14**,** 381-392.

SCHAFER, D. P. & RASBAND, M. N. 2006. Glial regulation of the axonal membrane at nodes of Ranvier. *Current Opinion in Neurobiology,* 16**,** 508-514.

SCHERER, S., DESCHENES, S., XU, Y., GRINSPAN, J., FISCHBECK, K. & PAUL, D. 1995a. Connexin32 is a myelin-related protein in the PNS and CNS. *The Journal of Neuroscience,* 15**,** 8281-8294.

SCHERER, S. S., XU, Y. T., BANNERMAN, P. G., SHERMAN, D. L. & BROPHY, P. J. 1995b. Periaxin expression in myelinating Schwann cells: modulation by axon-glial interactions and polarized localization during development. *Development,* 121**,** 4265-4273.

SCHREINER, S., COSSAIS, F., FISCHER, K., SCHOLZ, S., BOSL, M. R., HOLTMANN, B., SENDTNER, M. & WEGNER, M. 2007. Hypomorphic Sox10 alleles reveal novel protein functions and unravel developmental differences in glial lineages. *Development,* 134**,** 3271-81.

SEREDA, M., GRIFFITHS, I., PÜHLHOFER, A., STEWART, H., ROSSNER, M. J., ZIMMERMANN, F., MAGYAR, J. P., SCHNEIDER, A., HUND, E., MEINCK, H.-M., SUTER, U. & NAVE, K.-A. 1996. A Transgenic Rat Model of Charcot-Marie-Tooth Disease. *Neuron,* 16**,** 1049-1060.

SEREDA, M. W. & NAVE, K. A. 2006. Animal models of Charcot-Marie-Tooth disease type 1A. *NeuroMolecular Medicine,* 8**,** 205-215.

SHAH, N. M., MARCHIONNI, M. A., ISAACS, I., STROOBANT, P. & ANDERSON, D. J. 1994. Glial growth factor restricts mammalian neural crest stem cells to a glial fate. *Cell,* 77**,** 349-360.

SHEN, Y. J., DEBELLARD, M. E., SALZER, J. L., RODER, J. & FILBIN, M. T. 1998. Myelin-Associated Glycoprotein in Myelin and Expressed by Schwann Cells Inhibits Axonal Regeneration and Branching. *Molecular and Cellular Neuroscience,* 12**,** 79-91.

SHINE, H. D. & SIDMAN, R. L. 1984. Immunoreactive myelin basic proteins are not detected when shiverer mutant Schwann cells and fibroblasts are co-cultured with normal neurons. *The Journal of Cell Biology,* 98**,** 1291-1295.

SHIVANE, A., PARKINSON, D. B., AMMOUN, S. & HANEMANN, C. O. 2013. Expression of c-Jun and Sox-2 in human schwannomas and traumatic neuromas. *Histopathology,* 62**,** 651-656.

SICONOLFI, L. B. & SEEDS, N. W. 2001. Mice Lacking tPA, uPA, or Plasminogen Genes Showed Delayed Functional Recovery after Sciatic Nerve Crush. *The Journal of Neuroscience,* 21**,** 4348-4355.

SIKORSKA, M., SANDHU, J. K., DEB-RINKER, P., JEZIERSKI, A., LEBLANC, J., CHARLEBOIS, C., RIBECCO-LUTKIEWICZ, M., BANI-YAGHOUB, M. & WALKER, P. R. 2008. Epigenetic modifications of SOX2 enhancers, SRR1 and SRR2, correlate with in vitro neural differentiation. *Journal of Neuroscience Research,* 86**,** 1680-1693.

SIMONS, M. & NAVE, K.-A. 2015. Oligodendrocytes: Myelination and Axonal Support. *Cold Spring Harbor Perspectives in Biology*.

SIMONS, M. & TRAJKOVIC, K. 2006. Neuron-glia communication in the control of oligodendrocyte function and myelin biogenesis. *Journal of Cell Science,* 119**,** 4381-4389.

SINKIEWICZ-DAROL, E., LACERDA, A., KOSTERA-PRUSZCZYK, A., POTULSKA-CHROMIK, A., SOKOŁOWSKA, B., KABZIŃSKA, D., BRUNETTI, C., HAUSMANOWA-PETRUSEWICZ, I. & KOCHAŃSKI, A. 2015. The LITAF/SIMPLE I92V sequence variant results in an earlier age of onset of CMT1A/HNPP diseases. *neurogenetics,* 16**,** 27-32.

SPIEGEL, I., ADAMSKY, K., ESHED, Y., MILO, R., SARIG–NADIR, O., HORRESH, I., SCHERER, S. S., RASBAND, M. N. & PELES, E. 2007. A central role for Necl4 (SynCAM4) in Schwann cell–axon interaction and myelination. *Nature neuroscience,* 10**,** 861-869.

SRINIVASAN, R., SUN, G., KELES, S., JONES, E. A., JANG, S.-W., KRUEGER, C., MORAN, J. J. & SVAREN, J. 2012. Genome-wide analysis of EGR2/SOX10 binding in myelinating peripheral nerve. *Nucleic Acids Research,* 40**,** 6449-6460.

STASSART, R. M., FLEDRICH, R., VELANAC, V., BRINKMANN, B. G., SCHWAB, M. H., MEIJER, D., SEREDA, M. W. & NAVE, K.-A. 2013. A role for Schwann cell-derived neuregulin-1 in remyelination. *Nat Neurosci,* 16**,** 48-54.

STEWART, H. J. S., BRENNAN, A., RAHMAN, M., ZOIDL, G., MITCHELL, P. J., JESSEN, K. R. & MIRSKY, R. 2001. Developmental regulation and overexpression of the transcription factor AP-2, a potential regulator of the timing of Schwann cell generation. *European Journal of Neuroscience,* 14**,** 363-372.

STOLL, G., JANDER, S. & MYERS, R. R. 2002. Degeneration and regeneration of the peripheral nervous system: From Augustus Waller's observations to neuroinflammation. *Journal of the Peripheral Nervous System,* 7**,** 13-27.

STREET, V. A., BENNETT, C. L., GOLDY, J. D., SHIRK, A. J., KLEOPA, K. A., TEMPEL, B. L., LIPE, H. P., SCHERER, S. S., BIRD, T. D. & CHANCE, P. F. 2003. Mutation of a putative protein degradation gene LITAF/SIMPLE in Charcot-Marie-Tooth disease 1C. *Neurology,* 60**,** 22-26.

SUTER, U. & SCHERER, S. S. 2003. Disease mechanisms in inherited neuropathies. *Nat Rev Neurosci,* 4**,** 714-26.

SVAREN, J. & MEIJER, D. 2008. The molecular machinery of myelin gene transcription in Schwann cells. *Glia,* 56**,** 1541-1551.

SVENNIGSEN, Å. & DAHLIN, L. B. 2013. Repair of the Peripheral Nerve—Remyelination that Works. *Brain Sciences,* 3**,** 1182-1197.

SYED, N. & KIM, H. A. 2010. Soluble Neuregulin and Schwann Cell Myelination: a Therapeutic Potential for Improving Remyelination of Adult Axons. *Molecular and cellular pharmacology,* 2**,** 161-167.

TAKAHASHI, K. & YAMANAKA, S. 2006. Induction of Pluripotent Stem Cells from Mouse Embryonic and Adult Fibroblast Cultures by Defined Factors. *Cell,* 126**,** 663-676.

TAKAHASHI, M. & OSUMI, N. 2005. Identification of a novel type II classical cadherin: Rat cadherin19 is expressed in the cranial ganglia and Schwann cell precursors during development. *Developmental Dynamics,* 232**,** 200-208.

TANAKA, Y. & HIROKAWA, N. 2002. Mouse models of Charcot-Marie-Tooth disease. *Trends in Genetics,* 18**,** S39-S44.

TAVEGGIA, C., FELTRI, M. L. & WRABETZ, L. 2010. Signals to promote myelin formation and repair. *Nature reviews. Neurology,* 6**,** 276-287.

TAVEGGIA, C., ZANAZZI, G., PETRYLAK, A., YANO, H., ROSENBLUTH, J., EINHEBER, S., XU, X., ESPER, R. M., LOEB, J. A., SHRAGER, P., CHAO, M. V., FALLS, D. L., ROLE, L. & SALZER, J. L. 2005. Neuregulin-1 Type III Determines the Ensheathment Fate of Axons. *Neuron,* 47**,** 681-694.

THORNTON, M. R., MANTOVANI, C., BIRCHALL, M. A. & TERENGHI, G. 2005. Quantification of N-CAM and N-cadherin expression in axotomized and crushed rat sciatic nerve. *Journal of Anatomy,* 206**,** 69-78.

TIMMERMAN, V., DE JONGHE, P., CEUTERICK, C., DE VRIENDT, E., LÖFGREN, A., NELIS, E., WARNER, L. E., LUPSKI, J. R., MARTIN, J.-J. & VAN BROECKHOVEN, C. 1999. Novel missense mutation in the early growth response 2 gene associated with Dejerine–Sottas syndrome phenotype. *Neurology,* 52**,** 1827.

TOFARIS, G. K., PATTERSON, P. H., JESSEN, K. R. & MIRSKY, R. 2002. Denervated Schwann Cells Attract Macrophages by Secretion of Leukemia Inhibitory Factor (LIF) and Monocyte Chemoattractant Protein-1 in a Process Regulated by Interleukin-6 and LIF. *The Journal of Neuroscience,* 22**,** 6696-6703.

TOPILKO, P., LEVI, G., MERLO, G., MANTERO, S., DESMARQUET, C., MANCARDI, G. & CHARNAY, P. 1997. Differential regulation of the zinc finger genes Krox-20 and Krox-24 (Egr-1) suggests antagonistic roles in Schwann cells. *Journal of Neuroscience Research,* 50**,** 702-712.

TOPILKO, P., SCHNEIDER-MAUNOURY, S., LEVI, G., BARON-VAN, EVERCOOREN, A., CHENNOUFI, A. B. Y., SEITANIDOU, T., BABINET, C. & CHARNAY, P. 1994. Krox-20 controls myelination in the peripheral nervous system. *Nature,* 371**,** 796-799.

TRUETT, G. E., HEEGER, P., MYNATT, R. L., TRUETT, A. A., WALKER, J. A. & WARMAN, M. L. 2000. Preparation of PCR-quality mouse genomic DNA with hot sodium hydroxide and tris (HotSHOT). *Biotechniques,* 29**,** 52, 54.

VELANAC, V., UNTERBARNSCHEIDT, T., HINRICHS, W., GUMMERT, M. N., FISCHER, T. M., ROSSNER, M. J., TRIMARCO, A., BRIVIO, V., TAVEGGIA, C., WILLEM, M., HAASS, C., MÖBIUS, W., NAVE, K.-A. & SCHWAB, M. H. 2012. BACE1 Processing of NRG1 Type III Produces a Myelin-Inducing Signal but Is Not Essential for the Stimulation of Myelination. *Glia,* 60**,** 203-217.

VERRIER, J. D., SEMPLE-ROWLAND, S., MADORSKY, I., PAPIN, J. E. & NOTTERPEK, L. 2010. Reduction of Dicer Impairs Schwann Cell

Differentiation and Myelination. *Journal of neuroscience research,* 88**,** 2558-2568.
VERRIJZER, C. P. & VAN DER VLIET, P. C. 1993. POU domain transcription factors. *Biochimica et Biophysica Acta (BBA) - Gene Structure and Expression,* 1173**,** 1-21.
VOGELAAR, C. F., VRINTEN, D. H., HOEKMAN, M. F. M., BRAKKEE, J. H., BURBACH, J. P. H. & HAMERS, F. P. T. 2004. Sciatic nerve regeneration in mice and rats: recovery of sensory innervation is followed by a slowly retreating neuropathic pain-like syndrome. *Brain Research,* 1027**,** 67-72.
VOGL, M. R., REIPRICH, S., KÜSPERT, M., KOSIAN, T., SCHREWE, H., NAVE, K.-A. & WEGNER, M. 2013. Sox10 Cooperates with the Mediator Subunit 12 during Terminal Differentiation of Myelinating Glia. *The Journal of Neuroscience,* 33**,** 6679-6690.
WAGNER, R. & MYERS, R. R. 1996. Endoneurial injection of TNF-[alpha] produces neuropathic pain behaviors. *NeuroReport,* 7**,** 2897-2902.
WAKAMATSU, Y., ENDO, Y., OSUMI, N. & WESTON, J. A. 2004. Multiple roles of Sox2, an HMG-box transcription factor in avian neural crest development. *Dev Dyn,* 229**,** 74-86.
WAKAMATSU, Y., MAYNARD, T. M. & WESTON, J. A. 2000. Fate determination of neural crest cells by NOTCH-mediated lateral inhibition and asymmetrical cell division during gangliogenesis. *Development,* 127**,** 2811-2821.
WANNER, I. B., GUERRA, N. K., MAHONEY, J., KUMAR, A., WOOD, P. M., MIRSKY, R. & JESSEN, K. R. 2006. Role of N-cadherin in Schwann cell precursors of growing nerves. *Glia,* 54**,** 439-459.
WARNER, L. E., MANCIAS, P., BUTLER, I. J., MCDONALD, C. M., KEPPEN, L., KOOB, K. G. & LUPSKI, J. R. 1998. Mutations in the early growth response 2 (EGR2) gene are associated with hereditary myelinopathies. *Nat Genet,* 18**,** 382-384.
WATKINS, L. R. & MAIER, S. F. 2002. Beyond Neurons: Evidence That Immune and Glial Cells Contribute to Pathological Pain States. *Physiological Reviews,* 82**,** 981-1011.
WEBSTER, H. D., MARTIN, J. R. & O'CONNELL, M. F. 1973. The relationships between interphase Schwann cells and axons before myelination: A quantitative electron microscopic study. *Developmental Biology,* 32**,** 401-416.
WEGNER, M. 2010. All purpose Sox: The many roles of Sox proteins in gene expression. *Int J Biochem Cell Biol,* 42**,** 381-90.
WEINA, K. & UTIKAL, J. 2014. SOX2 and cancer: current research and its implications in the clinic. *Clinical and Translational Medicine,* 3**,** 19-19.
WEISS, M. D., LUCIANO, C. A. & QUARLES, R. H. 2001. Nerve conduction abnormalities in aging mice deficient for myelin-associated glycoprotein. *Muscle & Nerve,* 24**,** 1380-1387.
WOODHOO, A., ALONSO, M. B. D., DROGGITI, A., TURMAINE, M., D'ANTONIO, M., PARKINSON, D. B., WILTON, D. K., AL-SHAWI, R., SIMONS, P., SHEN, J., GUILLEMOT, F., RADTKE, F., MEIJER, D., FELTRI, M. L., WRABETZ, L., MIRSKY, R. & JESSEN, K. R. 2009. Notch controls embryonic Schwann cell differentiation, postnatal myelination and adult plasticity. *Nat Neurosci,* 12**,** 839-847.
WRABETZ, L., D'ANTONIO, M., PENNUTO, M., DATI, G., TINELLI, E., FRATTA, P., PREVITALI, S., IMPERIALE, D., ZIELASEK, J., TOYKA, K., AVILA, R. L., KIRSCHNER, D. A., MESSING, A., FELTRI, M. L. & QUATTRINI, A. 2006.

Different Intracellular Pathomechanisms Produce Diverse Myelin Protein Zero Neuropathies in Transgenic Mice. *The Journal of Neuroscience,* 26**,** 2358-2368.

XIA, P., WANG, S., YE, B., DU, Y., HUANG, G., ZHU, P. & FAN, Z. 2015. Sox2 functions as a sequence-specific DNA sensor in neutrophils to initiate innate immunity against microbial infection. *Nat Immunol,* 16**,** 366-375.

XING, B., BACHSTETTER, A. D. & VAN ELDIK, L. J. 2015. Inhibition of neuronal p38alpha, but not p38beta MAPK, provides neuroprotection against three different neurotoxic insults. *J Mol Neurosci,* 55**,** 509-18.

YAMAZAKI, T., SABIT, H., OYA, T., ISHII, Y., HAMASHIMA, T., TOKUNAGA, A., ISHIZAWA, S., JIE, S., KURASHIGE, Y., MATSUSHIMA, T., FURUTA, I., NOGUCHI, M. & SASAHARA, M. 2009. Activation of MAP kinases, Akt and PDGF receptors in injured peripheral nerves. *Journal of the Peripheral Nervous System,* 14**,** 165-176.

YANG, D. P., KIM, J., SYED, N., TUNG, Y.-J., BHASKARAN, A., MINDOS, T., MIRSKY, R., JESSEN, K. R., MAUREL, P., PARKINSON, D. B. & KIM, H. A. 2012. p38 MAPK activation promotes denervated Schwann cell phenotype and functions as a negative regulator of Schwann cell differentiation and myelination. *The Journal of neuroscience,* 32**,** 7158-7168.

YANG, D. P., ZHANG, D. P., MAK, K. S., BONDER, D. E., POMEROY, S. L. & KIM, H. A. 2008. Schwann cell proliferation during Wallerian degeneration is not necessary for regeneration and remyelination of the peripheral nerves: axon-dependent removal of newly generated Schwann cells by apoptosis. *Molecular and cellular neurosciences,* 38**,** 80-88.

YANG, N., HUI, L., WANG, Y., YANG, H. & JIANG, X. 2014a. Overexpression of SOX2 promotes migration, invasion, and epithelial-mesenchymal transition through the Wnt/β-catenin pathway in laryngeal cancer Hep-2 cells. *Tumor Biology,* 35**,** 7965-7973.

YANG, T. T. C., XIONG, Q., ENSLEN, H., DAVIS, R. J. & CHOW, C.-W. 2002. Phosphorylation of NFATc4 by p38 Mitogen-Activated Protein Kinases. *Molecular and Cellular Biology,* 22**,** 3892-3904.

YANG, Y., KIM, S. C., YU, T., YI, Y.-S., RHEE, M. H., SUNG, G.-H., YOO, B. C. & CHO, J. Y. 2014b. Functional Roles of p38 Mitogen-Activated Protein Kinase in Macrophage-Mediated Inflammatory Responses. *Mediators of Inflammation,* 2014**,** 13.

YEPES, M. & LAWRENCE, D. A. 2004. Neuroserpin: a selective inhibitor of tissue-type plasminogen activator in the central nervous system. *Thrombosis and Haemostasis,* 91**,** 457-464.

YIN, X., CRAWFORD, T. O., GRIFFIN, J. W., TU, P.-H., LEE, V. M.-Y., LI, C., RODER, J. & TRAPP, B. D. 1998. Myelin-Associated Glycoprotein Is a Myelin Signal that Modulates the Caliber of Myelinated Axons. *The Journal of Neuroscience,* 18**,** 1953-1962.

ZAMBROWICZ, B. P., IMAMOTO, A., FIERING, S., HERZENBERG, L. A., KERR, W. G. & SORIANO, P. 1997. Disruption of overlapping transcripts in the ROSA βgeo 26 gene trap strain leads to widespread expression of β-galactosidase in mouse embryos and hematopoietic cells. *Proceedings of the National Academy of Sciences of the United States of America,* 94**,** 3789-3794.

ZARELLI, V. E. & DAWID, I. B. 2013. Inhibition of neural crest formation by Kctd15 involves regulation of transcription factor AP-2. *Proceedings of the National Academy of Sciences,* 110**,** 2870-2875.

ZARUBIN, T. & HAN, J. 2005. Activation and signaling of the p38 MAP kinase pathway. *Cell Res,* 15**,** 11-18.

ZHANG, S. M., MARSH, R., RATNER, N. & BRACKENBURY, R. 1995. Myelin glycoprotein P0 is expressed at early stages of chicken and rat embryogenesis. *Journal of Neuroscience Research,* 40**,** 241-250.

ZHAO, C., MA, D., ZAWADZKA, M., FANCY, S. P. J., ELIS-WILLIAMS, L., BOUVIER, G., STOCKLEY, J. H., DE CASTRO, G. M., WANG, B., JACOBS, S., CASACCIA, P. & FRANKLIN, R. J. M. 2015. Sox2 Sustains Recruitment of Oligodendrocyte Progenitor Cells following CNS Demyelination and Primes Them for Differentiation during Remyelination. *The Journal of Neuroscience,* 35**,** 11482-11499.

ZHU, Y., GHOSH, P., CHARNAY, P., BURNS, D. K. & PARADA, L. F. 2002. Neurofibromas in NF1: Schwann Cell Origin and Role of Tumor Environment. *Science,* 296**,** 920-922.

ZROURI, H., LE GOASCOGNE, C., LI, W. W., PIERRE, M. & COURTIN, F. 2004. The role of MAP kinases in rapid gene induction after lesioning of the rat sciatic nerve. *European Journal of Neuroscience,* 20**,** 1811-1818.

ZÜCHNER, S., VORGERD, M., SINDERN, E. & SCHRÖDER, J. M. 2004. The novel neurofilament light (NEFL) mutation Glu397Lys is associated with a clinically and morphologically heterogeneous type of Charcot-Marie-Tooth neuropathy. *Neuromuscular Disorders,* 14**,** 147-157.